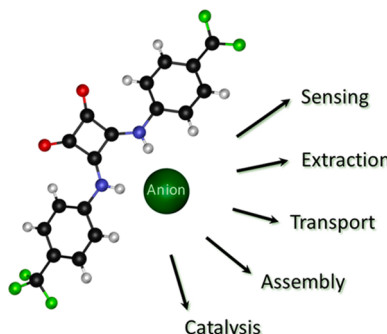


Applications of Supramolecular Anion Recognition

Nathalie Busschaert,^{†,§} Claudia Caltagirone,[‡] Wim Van Rossom,[†] and Philip A. Gale*,[†]

[†]Chemistry, University of Southampton, Southampton SO17 1BJ, United Kingdom

[‡]Dipartimento di Scienze Chimiche e Geologiche, Università degli Studi di Cagliari, S.S. 554 Bivio per Sestu, 09042 Monserrato, Cagliari, Italy



CONTENTS

1. Introduction	8038
2. Anion Sensing	8039
2.1. Discrete Colorimetric and Fluorescence (Optical) Anion Sensors	8039
2.1.1. Discrete Optical Sensors for Fluoride Anions	8039
2.1.2. Discrete Optical Sensors for Cyanide Anions	8046
2.1.3. Discrete Optical Sensors for Phosphates	8050
2.1.4. Discrete Optical Sensors for Other Anions	8057
2.2. Assemblies for Optical Sensing of Anions	8063
2.2.1. Dye Displacement Assays for Anion Sensing	8063
2.2.2. Microarrays and Artificial Tongues for Anion Sensing	8066
2.2.3. Vesicular- and Micellar-Based Assemblies for Anion Sensing	8068
2.2.4. Other Assemblies for Anion Sensing	8071
2.3. Electrochemical Anion Sensing	8073
2.4. Anion-Responsive Gels	8076
2.5. Dual- and Triple-Channel Anion Sensors	8079
2.6. Conclusions and Outlook on Anion Sensing	8081
3. Extraction and Separation of Anions	8082
3.1. Liquid–Liquid Extraction	8083
3.1.1. Extraction of Halide Anions	8083
3.1.2. Extraction of Oxoanions	8086
3.1.3. Extraction of Metalates	8089
3.2. Liquid–Solid Extraction	8090
3.2.1. Using Metal–Organic Frameworks (MOFs) or Other Anion Receptors in the Solid State	8090
3.2.2. Using Modified Solid Supports and Membranes	8096
3.2.3. Using Selective Crystallization and Precipitation	8098
3.3. Conclusions and Outlook on Anion Extraction	8100
4. Transmembrane Anion Transport	8101
4.1. Anion Transport via Synthetic Anion Channels	8101
4.2. Anion Transport via Synthetic Mobile Carriers	8106
4.3. Anion Transport via Other Mechanisms	8111
4.4. Conclusions and Outlook on Transmembrane Anion Transport	8113
5. Anion-Driven Supramolecular Architectonics	8113
5.1. Anion-Templated Topologies	8113
5.2. Anion-Controlled Gelation	8119
5.3. Conclusions and Outlook on Anion-Driven Assemblies	8122
6. Anion-Driven Organocatalysis	8122
6.1. Organocatalysis Based on Interactions with Halide Anions	8122
6.2. Organocatalysis Based on Interactions with Cyanide Anions	8125
6.3. Organocatalysis Based on Interactions with Carboxylate Anions	8126
6.4. Organocatalysis Based on Interactions with Nitronate Anions	8130
6.5. Organocatalysis Based on Interactions with Other Oxoanions	8131
6.6. Conclusions and Outlook on Anion-Driven Organocatalysis	8133
7. Conclusions	8134
Author Information	8134
Corresponding Author	8134
Present Address	8134
Author Contributions	8134
Notes	8134
Biographies	8134
Acknowledgments	8135
Abbreviations	8135
References	8136

1. INTRODUCTION

The study of the complexation of anions, from its beginnings in the late 1960s and 1970s,^{1–3} has moved on from being an area solely of academic interest to a fundamental pillar of supramolecular chemistry with applications in many areas. Over recent years^{4,5} we have seen the development of a plethora of anion

Special Issue: 2015 Supramolecular Chemistry

Received: February 18, 2015

Published: May 21, 2015

sensors, anion-responsive materials, organocatalytic processes involving anion complexation, as well as development of new systems to selectively extract anions from mixtures and compounds designed to mediate the transport of anions across cell membranes. It therefore seems appropriate that this review on anion complexation focuses on the applications of this area of research over the past decade.⁶ These span a wide range of areas but for the purposes of this review are divided into sensing, extraction, transport through lipid bilayers, the roles anions can play in the formation of molecular assemblies, and finally organocatalysis.

2. ANION SENSING

Anion sensing by discrete molecular receptors relies on the fact that the recognition of a given anion by a receptor can induce a response, be it an optical (color change or fluorescence), an electrochemical, or a sol–gel transition, that can be used to monitor the presence and in some cases the concentration of an anionic guest.⁷ This is particularly useful for the detection of potentially toxic anions (e.g., cyanide), for the detection of environmentally deleterious anions (e.g., phosphate, nitrate), or in medical diagnostics. Consequently, anion sensing has become one of the most active areas of supramolecular chemistry. In this review we provide an overview of different classes of anion sensor, illustrated with selected examples, to highlight the different strategies used to sense anionic species.

2.1. Discrete Colorimetric and Fluorescence (Optical) Anion Sensors

Optical anion sensors, where the interaction with an anion leads to a change in the absorbance (color) or fluorescence properties of the receptor, are the most widely studied class of anion sensor. This is due to the high sensitivity of many of these systems which allows low concentrations of anions to be detected, and their potential for monitoring anions in biological systems (bioimaging) coupled to straightforward detection techniques—absorbance and fluorescence changes—can be detected either spectroscopically or with the naked eye. There are a number of ways in which optical anion sensing can be achieved. Discrete sensors usually consist of an anion binding site covalently linked to a signaling unit (e.g., fluorophore or other dye). The signaling unit can be attached to the receptor directly, so that the receptor is part of the conjugated π system of the chromophore (Figure 1a) or can be separated from the receptor through a short covalent linker (Figure 1b).⁸ “Chemodosimeters” are another type of discrete optical sensors. In this case anion sensing does not occur by noncovalent interactions and the formation of a supramolecular anion–receptor complex, but instead the anion reacts with the sensor (or catalyzes a reaction) to create a new molecule with different optical properties (Figure 1c).⁹ In recent years, more elaborate ways of optical sensing have emerged that employ “molecular ensembles”, such as dye displacement assays, microarrays, and other assemblies, rather than discrete single-molecule-based sensors. This type of anion sensing will be discussed later in the review (see sections 2.2 and 2.6). For simple anion sensors to be useful in real-life applications it is important that the sensor is selective and thus that the optical response only occurs upon the interaction with one particular anion. As this review focuses on the applications of anion recognition, only selective sensors will be discussed in the following section. Readers are referred to other reviews for more examples of anion sensing.^{8,10–14}

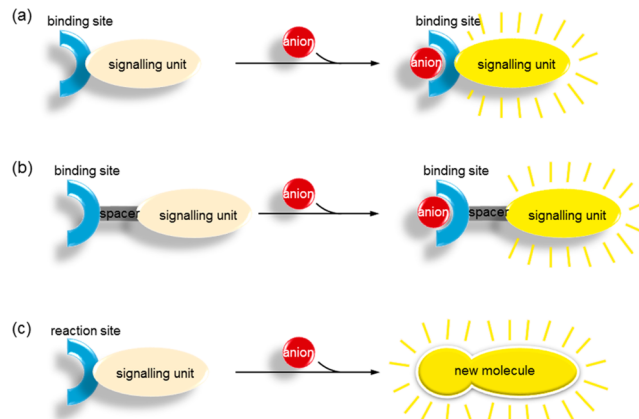


Figure 1. Schematic overview of the various types of single-molecule-based optical anion sensors. All sensors are shown as “switch on” fluorescent sensor, but “switch off” fluorescence sensors or colorimetric sensors are also possible. (a) Binding site is an integral part of the signaling unit. (b) The anion binding site is covalently linked to the signaling unit through a short spacer. (c) Chemodosimeter approach where the anion induces an irreversible reaction in the signaling unit.

2.1.1. Discrete Optical Sensors for Fluoride Anions.

Fluoride anions are an important target in supramolecular chemistry due to the importance of fluoride in biological and medical processes. The positive role of fluoride in dental health is well known (e.g., fluoride containing toothpaste), but overexposure to fluoride (fluorosis) can have detrimental effects such as kidney failure and debilitating skeletal defects.¹⁵ Furthermore, a number of chemical warfare agents, such as Sarin (used during the terrorist attack by the Aum Shinrikyo cult in Tokyo in 1995), release fluoride during hydrolysis, and the detection of fluoride anions could thus be used as a means of detecting whether nerve agents have been used during terrorist attacks or in war zones.^{16,17} However, the popularity of fluoride in the field of anion sensing is also partially due to some of the characteristics of fluoride that render the selective detection of this anion more feasible. The reactivity of fluoride toward Lewis acids such as boron has resulted in a plethora of boron-containing fluoride sensors. Additionally, the high basicity of fluoride in organic solvents, combined with the formation of the stable self-complex $[\text{HF}_2]^-$, can lead to deprotonation of the hydrogen-bond donors in the anion receptor which often results in dramatic color changes. Cametti and Rissanen as well as Yoon and colleagues have recently (2009 and 2014, respectively) written comprehensive reviews about fluoride sensing to which the reader is directed for more information.^{18,19}

The small ionic radius of fluoride gives this anion a high charge density, and therefore, hydrogen bonds with this ion are often very strong. It must be noted however, that fluoride anions also have a very high hydration energy ($\Delta G_{\text{hydr}} = -465 \text{ kJ/mol}$),²⁰ and therefore, recognition of fluoride anions in water, especially by hydrogen bonding, is challenging. On the other hand, the high basicity of fluoride anions in organic solvents helps in the development of hydrogen-bond-based fluoride sensors, especially as deprotonation of the hydrogen-bond donor can occur in these solvents. The use of deprotonation by fluoride anions for developing optical sensors was first studied independently by the groups of Gale^{21,22} and Gunnlaugsson.^{23,24} The latter group initially investigated the sensing properties of thiourea **1** appended with the highly colored fluorescent dye 4-amino-1,8-naphthalimide (see Figure 2). Titration studies in DMSO

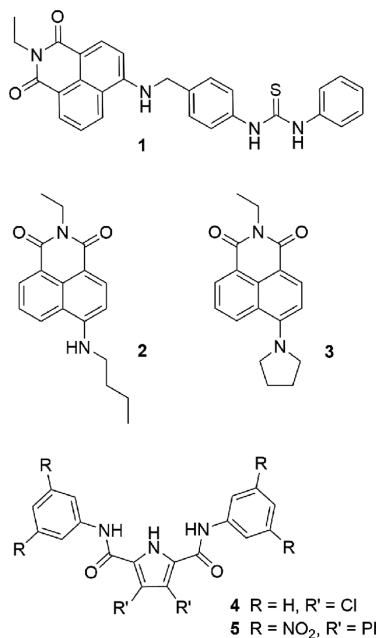


Figure 2. Structures of compounds 1–5.

showed that the addition of small amounts of fluoride anions leads to quenching of the emission of **1** without concomitant changes in absorbance, and similar effects were seen for OAc^- and H_2PO_4^- but not for Cl^- or Br^- . However, when excess fluoride was added (≥ 2 equiv), a dramatic change in absorbance occurred resulting in a color change from light yellow to deep purple. This was attributed to deprotonation of the amino NH as the same color change was seen upon the addition of tetrabutylammonium (TBA) hydroxide. To test this hypothesis, Gunnlaugsson and co-workers prepared reference compounds **2** and **3**, which lack the thiourea anion binding site but still possess an amino NH in the case of **2** (see Figure 2). A similar color change from yellow to red/purple was observed upon the addition of excess fluoride to a DMSO solution of **2** but not of **3**, indicating that the color changes observed for both **1** and **2** are due to the presence of the amino group. Proton NMR titrations of **2** with TBA fluoride in $\text{DMSO}-d_6$ showed the disappearance of the amino NH signal and the appearance of the signal corresponding to $[\text{HF}_2]^-$, providing further evidence that the changes in absorbance are due to deprotonation of the amino group by fluoride anions. It must be noted that the color change only occurred in the presence of fluoride (and strong bases such as TBAOH, NaH, and LDA) but not in the presence of other anions such as AcO^- , H_2PO_4^- , Cl^- , and Br^- , suggesting that **1** and **2** can function as fluoride sensors in organic solvents. Contemporaneously, Gale and co-workers reported that the pyrrole NH present in receptor **4** is sufficiently acidic due to the presence of the electron-withdrawing chlorine substituents that it can be easily deprotonated by fluoride, benzoate, and dihydrogen phosphate in dichloromethane, as shown by NMR titrations and X-ray crystallography. More selective deprotonation was seen for analogous receptor **5** (see Figure 2), for which a color change from colorless to deep blue was only observed upon the addition of excess tetrabutylammonium fluoride (and hydroxide) in acetonitrile.

Fabbrizzi and colleagues conducted in-depth studies of the deprotonation of hydrogen-bonding-based receptors by fluoride.^{25–29} Fabbriizi demonstrated that simple monoureas such as **6–8** (see Figure 3) undergo color changes upon deprotonation

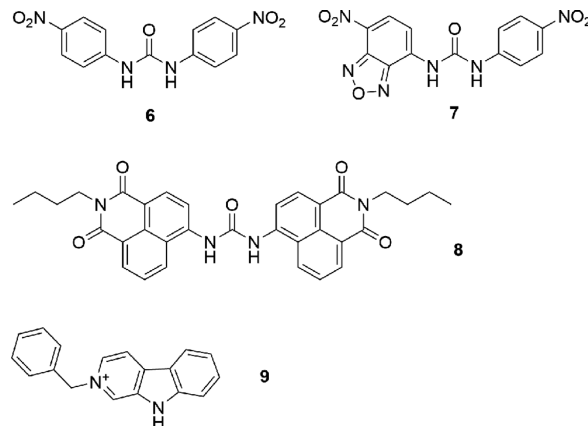


Figure 3. Structures of compounds 6–9.

by certain anions. UV-vis experiments in acetonitrile and ^1H NMR titrations in $\text{DMSO}-d_6$ showed that the addition of fluoride to **6** results in the formation of a hydrogen-bonded anion complex, followed by the deprotonation of **6** and the formation of $[\text{HF}_2]^-$ at higher fluoride concentrations.²⁵ Deprotonation by fluoride was also signaled by a pale yellow to red color change, an event not observed upon the addition of the other anions tested (OAc^- , OBz^- , H_2PO_4^- , NO_2^- , HSO_4^- , and NO_3^-) which form hydrogen-bonded complexes. On the other hand, the similar but more acidic receptor **7** was deprotonated in acetonitrile by OAc^- and H_2PO_4^- as well as F^- .²⁶ Furthermore, Fabbriizi and co-workers showed that the tendency for deprotonation is related to the acidity of the receptor and the stability of the $[\text{HX}_2]^-$ anion. Similarly, bisnaphthalimide urea **8** in DMSO could be doubly deprotonated by F^- and OH^- (resulting in a blue color) but only monodeprotonated by OAc^- and excess H_2PO_4^- (resulting in a red color) and could not be deprotonated by less basic anions such as NO_2^- , NO_3^- , HSO_4^- , Cl^- , and Br^- (solution remains yellow).²⁷ The same group also showed that positively charged carbazole receptor **9** (Figure 3) can be deprotonated in acetonitrile by 2 equiv of fluoride and 1 equiv of hydroxide, resulting in the appearance of a bright yellow color.²⁸

Since the initial studies by Gale, Gunnlaugsson, and Fabbriizi, many other fluoride sensors based on deprotonation of hydrogen-bond donors have been reported. In addition to the sensors based on amines (**1–3**), pyrroles (**4** and **5**), ureas (**6–8**), and carbazoles (**9**), deprotonation-based fluoride sensors have been developed using almost every known hydrogen-bond-donating moiety, including amide NHs, phenol OHs, and triazolium CHs (see Figure 4). In this respect, a number of fluoride sensors analogous to Fabbriizi's ureas have been reported. Taylor and co-workers, for example, showed that squaramide **10** is sufficiently acidic that it exists in its monodeprotonated state in DMSO. Upon the addition of fluoride anions **10** becomes doubly deprotonated, resulting in the formation of a blue color, which is not observed for other basic anions such as OAc^- and H_2PO_4^- .³⁰ Similarly, Pfeffer, Gunnlaugsson, and Kruger reported that sufficiently acidic thioureas such as **11** function as a colorimetric fluoride sensor in DMSO, as deprotonation results in a color change from yellow to red.³¹ Acylthioureas, such as **12**,³² and thiosemicarbazones/thiocarbonohydrzones, such as **13**,^{33,34} are more acidic analogues of thioureas and unsurprisingly have been used by a number of research groups to develop colorimetric fluoride sensors.^{35–39} Bose and Ghosh showed that **13**, as well as urea and guanidine analogues **14** and **15**, can selectively detect fluoride

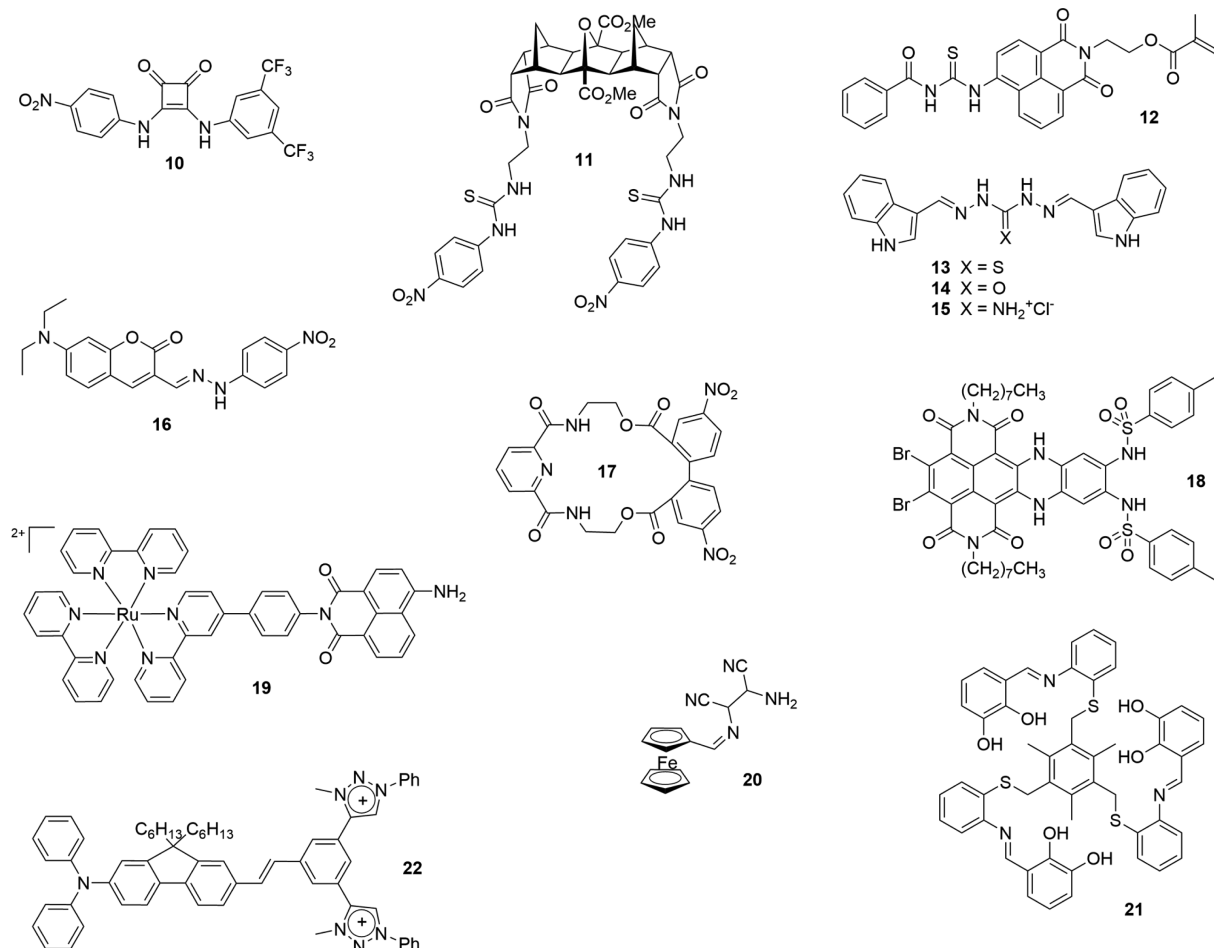


Figure 4. Structures of various fluoride sensors (**10–22**) where the sensing is based on deprotonation of the hydrogen-bond donor.

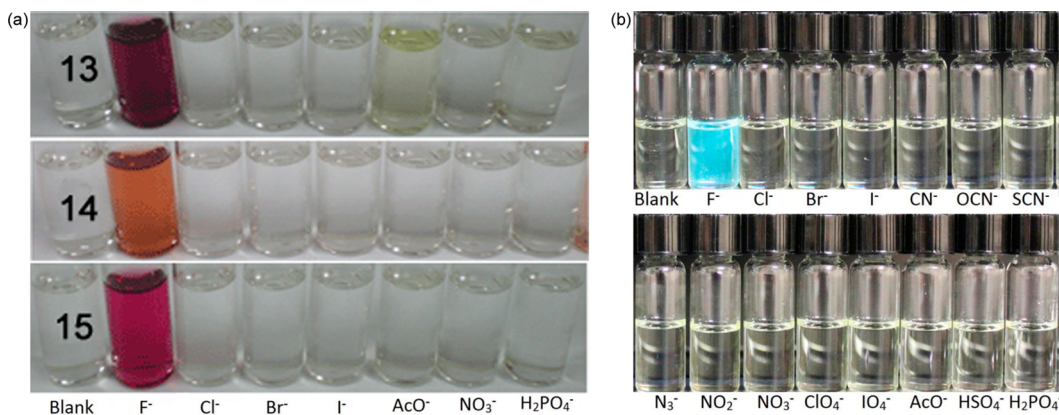


Figure 5. (a) Color changes observed upon addition of 30 equiv of various TBA salts to a 96:4 MeCN:DMF solution of **13–15**. Reprinted with permission from ref 34. Copyright 2011 Royal Society of Chemistry. (b) Fluorescence response of **22** in DMSO after excitation at 365 nm upon addition of 20 equiv of various TBA salts. Reprinted with permission from ref 48. Copyright 2013 American Chemical Society.

anions over other anions by a dramatic color change with a near-infrared signature that was attributed to the fact that fluoride-induced deprotonation leads to enhanced conjugation and delocalization of the negative charge over the entire molecule (see Figure 5a).^{33,34} Hydrazones in their own right have also been shown to function as fluoride sensors. Zhuang et al. developed chemosensor **16**, which displays a color change from yellow to blue upon the addition of excess fluoride in acetonitrile but not upon the addition of Cl⁻, Br⁻, I⁻, NO₃⁻, H₂PO₄⁻,

HSO₄⁻, and AcO⁻.⁴⁰ The appearance of the [HF₂]⁻ triplet at ~16 ppm during proton NMR experiments in DMSO-d₆ suggests that this is due to deprotonation of the hydrazone NH.

Apart from the ureas and isosteres, functional groups containing only a single nitrogen-based hydrogen-bond donor, such as amides, indoles, and anilines, are also prone to deprotonation in organic media and have thus been used in the design of fluoride sensors. Costero and colleagues found that bis-amide macrocycle **17** can function as an optical sensor for F⁻

in acetonitrile due to a colorless-to-orange color change ascribed to a deprotonation event in the presence of this anion.⁴⁰ An example of sulfonamide deprotonation can be found in the work of Bhosale, Langford, and co-workers, who reported that bis-sulfonamide **18** displays a green-to-blue color change and quenching of fluorescence in CHCl₃ upon the addition of fluoride but not upon the addition of other anions (H₂PO₄⁻, AcO⁻, Cl⁻, Br⁻, I⁻, HSO₄⁻).⁴¹ Indoles, carbazoles, and (benz)imidazoles have comparable properties to pyrroles (e.g., **4** and **5**) and have subsequently also been used for deprotonation-based fluoride sensors.⁴²⁻⁴⁴ Other hydrogen-bond donors include the —NH₂ functionalities in receptors **19** (by Elmes and Gunnlaugsson)⁴⁵ and **20** (by Kumar et al.),⁴⁶ which were both shown to be selective colorimetric fluoride sensors due to deprotonation. In addition to the nitrogen-based hydrogen-bond receptors, hydroxyl groups also form highly acidic hydrogen-bond donors that can be easily deprotonated. For example, Hundal and co-workers developed tripodal catechol-based receptor **21** that showed a strong color change in DMSO from colorless to bright yellow in the presence of TBA fluoride.⁴⁷ This was attributed to deprotonation of the hydroxyl groups based on ¹H NMR studies and the fact that a similar optical response was seen for the strong base TBA hydroxide. Recently, CH-based hydrogen-bond donors have become increasingly employed in anion recognition, but the CH bond is usually considered too weakly acidic to be easily deprotonated. However, a strongly polarized CH bond may be acidic enough to allow C—H deprotonation by anions. Belfield and co-workers have shown that this can be the case for cationic triazolium-containing receptors, such as **22**.⁴⁸ It was shown that **22** is nonfluorescent in DMSO, but the fluorescence can be selectively switched on in the presence of fluoride anions but not in the presence of other common anions (see Figure 5b). Proton and ¹³C NMR titrations provided evidence that this was due to the double deprotonation of the two triazolium moieties of **22** in DMSO. Interestingly, test strips of **22** loaded onto filter paper were capable of sensing fluoride in water.

While the above examples clearly show that deprotonation might be a useful method for achieving fluoride sensing, there are still a number of issues related with this approach. When the hydrogen-bond donor is too acidic, deprotonation is often also observed for other basic anions such as OAc⁻ and H₂PO₄⁻, and so selectivity is reduced. Furthermore, nearly all deprotonation-based fluoride sensors only function in aprotic organic solvents, and the sensing ability is lost in the presence of protic solvents such as water or MeOH due to reprotonation (this was observed in the case of, e.g., **1**, **2**, **16**, **17**, **18**, and **19**). This implies that for real-life applications this approach is not ideal, unless it is combined with fluoride extraction into the correct medium or by loading the sensors onto test strips (e.g., **22**).

There have also been a large number of fluoride sensors that function through hydrogen bonding to the fluoride anion rather than via deprotonation (see Figure 6). However, the possibility that fluoride sensing by hydrogen-bond donors is due to deprotonation is not always investigated, and therefore, we will focus on examples where deprotonation has been specifically excluded as a sensing mechanism. Gunnlaugsson and co-workers reported thiourea analogue **23** that presumably can sense anions through hydrogen bonding.⁴⁹ In DMSO this receptor undergoes a color change from yellow to purple upon the addition of F⁻ and OAc⁻, and in the presence of excess F⁻ additional absorbance changes (purple to orange) were observed due to deprotonation of the thiourea NH group. Interestingly, when the receptor was

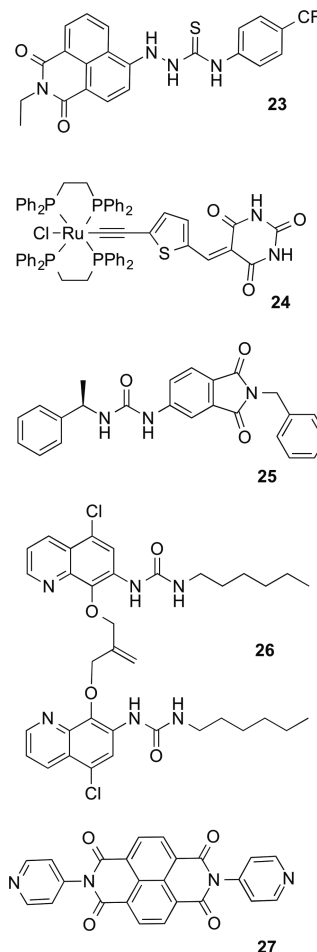


Figure 6. Structures of **23**–**27**.

used as a solution in EtOH or 1:1 EtOH:water a color change of yellow to purple was still observed upon the addition of F⁻ and OAc⁻, but no deprotonation occurred at high anion concentrations. Although **23** is not a selective sensor for fluoride, it demonstrates that anion sensing in aqueous solutions through hydrogen bonding can be achieved. Fillaut et al. found that barbiturate-based receptor **24** displays a color change in dichloromethane from blue to pink in the presence of fluoride (4 equiv) but not in the presence of other anions (AcO⁻, H₂PO₄⁻, HSO₄⁻, Cl⁻, and Br⁻).⁵⁰ A different color change (from blue to pale yellow) was observed in the presence of strong bases such as KO^tBu, piperidine, or tetramethylammonium (TMA) hydroxide, and the authors therefore attributed the fluoride sensing ability of **24** to hydrogen bonding to the barbiturate NHs and not to deprotonation of the NHs. Griesbeck and colleagues showed that urea **25** displays a small red shift in absorbance and a large fluorescence quenching in acetonitrile upon the addition of fluoride but not upon the addition of other halides.⁵¹ Comparison of the optical response with a strong base (DBU), as well as ¹H NMR titrations with TBA fluoride and DFT calculations, provided evidence that led the authors to suggest that this effect might be due to hydrogen bonding rather than deprotonation. Similar results were obtained by Cho and co-workers for bis-urea **26**, which showed a small red shift and a large fluorescence increase in acetonitrile upon the addition of F⁻, attributed to hydrogen bonding rather than deprotonation based on ¹H and ¹⁹F NMR experiments.⁵²

Anion– π interactions could in theory also be used for the development of fluoride sensors, as many of the electron deficient aromatic systems that are required for this type of interaction are also chromophores. This was demonstrated by Guha and Saha, who found that naphthalenediimide **27** (see Figure 6) can selectively sense fluoride anions over the other anions tested (Cl^- , Br^- , I^- , NO_2^- , NO_3^- , N_3^- , PF_6^- , AcO^- , and H_2PO_4^-).⁵³ Color changes from colorless to orange to pink were observed upon the gradual addition of F^- to **27** in aqueous DMSO, DMF, DMAc, MeCN, Me_2CO , and THF. ESI-MS experiments showed the presence of $[\text{27}^\bullet\text{F}^-]$ and $[\text{27}^\bullet\text{F}^-\cdot\text{27}]$ complexes, while ^1H NMR titration experiments did not show any evidence of $\text{CH}\cdots\text{F}$ hydrogen bonding, suggesting that complex formation is due to anion– π interactions. The authors attribute the observed color change to efficient electron transfer processes from F^- to **27**, resulting in the initial formation of the orange **27** $^{\bullet-}$ radical anion (as confirmed by EPR), followed by further reduction to pink **27** $^{2-}$ dianion in the presence of excess fluoride anions (as confirmed by ESI-MS).

Fluoride is also a hard Lewis base, and many fluoride sensors have been synthesized that employ the interaction of fluoride anions with (hard) Lewis acids such as boron- and silicon-containing species. Furthermore, fluoride is a very reactive anion, and a number of anion sensors exist that use fluoride-mediated reactions to achieve sensing (chemodosimeter approach). The advantage of this type of interaction over hydrogen-bond-based fluoride sensors is that it can sometimes persist in aqueous solution, and so, the development of receptors that can sense fluoride in water is possible, despite the high hydration energy of fluoride anions. The affinity of fluoride anions for boron to form fluoroborate species is well known and has been reviewed by a number of authors.^{54–56} Early boron-based anion receptors focused on pure organoboranes^{57–61} or boronic acids (and esters)^{62,63} for the recognition of fluoride ions, and while most of them do not function in water they are still the most popular building blocks for Lewis-acid-based fluoride sensors (see Figure 7). Liu et al., for example, reported organoborane **28** as a colorimetric and two-photon fluorescent fluoride sensor.⁶⁴ It was reported that a THF solution of **28** changed from green-yellow to colorless upon the addition of tetrabutylammonium fluoride, with a concomitant ratiometric change in the single-photon excited fluorescence spectra and a complete quenching of the two-photon excited fluorescence emission. Organoboron species **28** was also found to be highly selective, as other halides, OAc^- , NO_2^- , NO_3^- , H_2PO_4^- , and ClO_4^- , did not induce any spectral changes. The use of boronic acids and esters as sensors has been extensively studied by the groups of James, Yoon, and others. James and co-workers reported calix[4]arene-based boronic ester **29** as a selective fluorescent fluoride sensor in chloroform, attributed to bidentate “endo” binding of F^- by the two boron units.⁶⁵ This group also reported boronic acid **30**, which shows a colorimetric response in chloroform from colorless to yellow due to deboronation of **30** followed by deprotonation of the resulting phenol moiety, suggesting that this process can be a competing equilibrium in boronic acid-based sensors.⁶⁶ More recently, Yoon and co-workers reported boronic acids appended with an imidazolium unit for additional C–H hydrogen bonding (e.g., **31**) that can selectively sense fluoride ions over other anions in 95:5 MeCN:HEPES buffer by means of a ratiometric fluorescent response.^{67,68} Unfortunately, the sensor does not work in the presence of >5% water. Another interesting addition to the boron-based fluoride sensors is the subphthalocyanines, such as **32**, which were shown by Tian and co-workers to function as

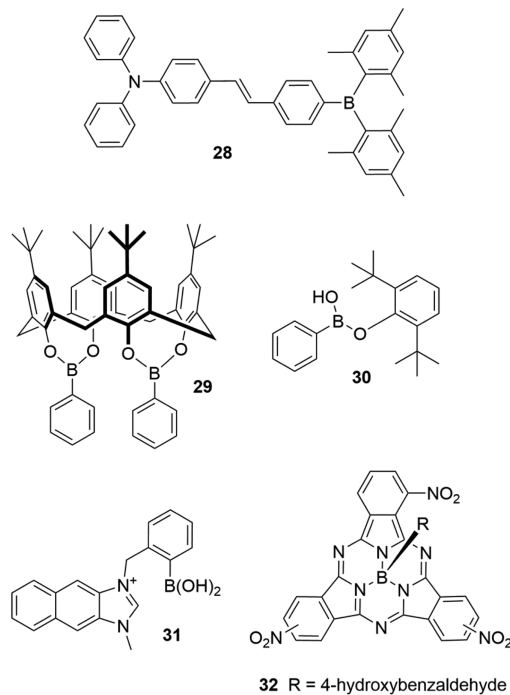


Figure 7. Structures of **28**–**32**.

powerful colorimetric (magenta to colorless) and fluorescent (quenching of red-orange emission) sensors for fluoride anions in THF.

In an effort to create more water-stable boron-based receptors that can sense fluoride in aqueous environments, Gabbaï and others reported a number of bidentate receptors, such as **33**–**37** (Figure 8). In their earlier work Gabbaï and co-workers reported

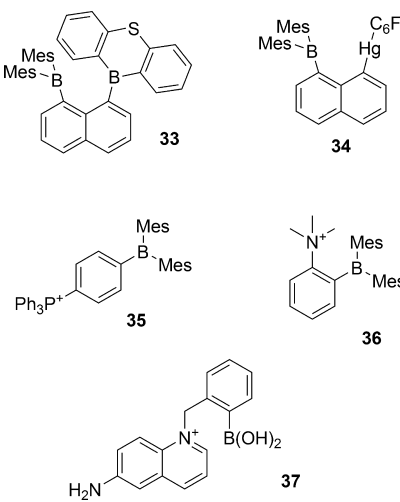


Figure 8. Structures of **33**–**37**.

diborane **33**, which reacts with fluoride anions in THF, resulting in a color change from yellow to colorless.⁶⁹ NMR experiments, as well as single-crystal X-ray diffraction, revealed that the fluoride anion forms a bridge between both boron atoms. Interestingly, the addition of water to the formed fluoride chelate does not lead to decomplexation of the fluoride anion. Later, the same group studied the properties of heteronuclear receptor **34**, which contains both a boron and a mercury Lewis-acidic center for anion complexation.⁷⁰ In THF and THF:water (9:1, v/v) this

receptor shows a decrease in the 361 nm absorption band upon the addition of fluoride anions but not upon the addition of other anions (Cl^- , Br^- , I^- , CN^- , OAc^- , NO_3^- , SO_4^{2-} , H_2PO_4^-). Once again, ^{11}B , ^{19}F , and ^{199}Hg NMR experiments and X-ray diffraction showed that the bound fluoride anions bridge both Lewis-acid centers. In an unusual experiment, Gabbaï and co-workers also showed that **34** and its fluoride complex display different phosphorescent behavior in the solid state (neat crystals or frozen THF solutions), allowing naked eye fluoride detection upon irradiation with a hand-held UV lamp. More recently, this group reported the synthesis of cationic boranes such as mixed-phosphonium-appended borane **35**.^{71–73} It was shown that the addition of KF to a solution of **35** in 9:1 $\text{H}_2\text{O}:\text{MeOH}$ leads to a decrease in the absorbance at 325 nm with this property being used for the detection of fluoride ions in pure water. Similar results were obtained with cationic ammonium borane **36**, which can selectively sense F^- over Cl^- , Br^- , I^- , NO_3^- , HSO_4^- , OAc^- , and CN^- in aqueous solutions (60:40 $\text{H}_2\text{O:DMSO}$).⁷⁴ Interestingly, the selectivity is reversed in the case of an analog of **36** where both substituents are located in the para position, which is able to sense CN^- over F^- due to a mix of steric and electronic factors that influence the anion binding in both receptors. Geddes and co-workers also reported a mixed-ammonium/boronic acid receptor (**37**), which shows a ratiometric absorbance and fluorescence response to fluoride anions in pure water and can even sense fluoride anions in the presence of sugars (fructose and glucose) and other halides.⁷⁵ These examples suggest that mixed receptors containing both boron-based species and cationic moieties could represent one of the most potent sensors for fluoride in water.

Boron is not the only Lewis acid that can coordinate anions, and fluoride sensors based on the interaction of the hard Lewis base F^- with other Lewis acids and metal cations have also been reported (see Figure 9). Gabbaï and co-workers, for example,

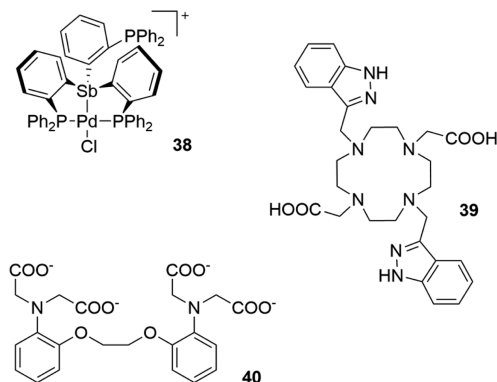


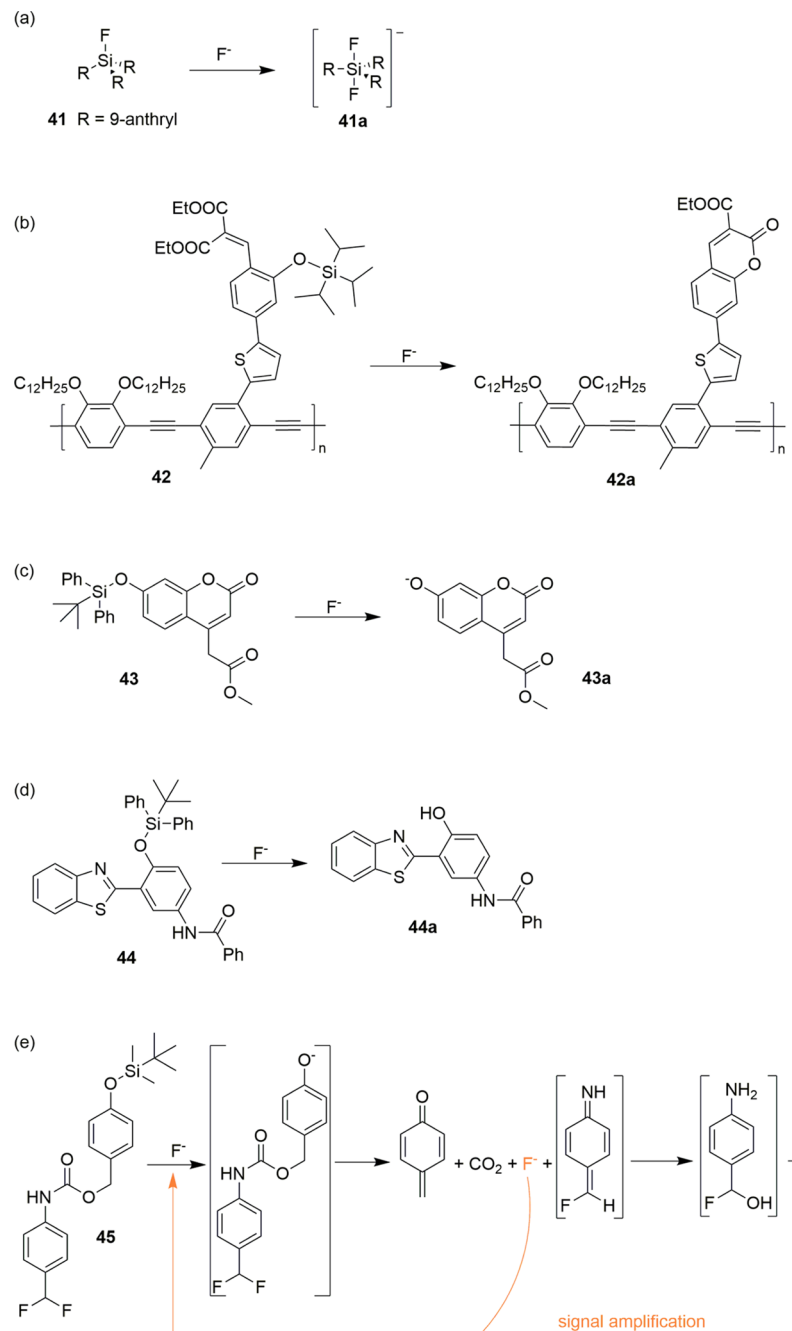
Figure 9. Structures of compounds **38–40**.

reported that antimony–palladium complex **38** undergoes a selective color change in dichloromethane from pale yellow to orange upon the addition of tetrabutylammonium fluoride.⁷⁶ NMR experiments and single-crystal structure determinations revealed that this color change is due to the binding of the fluoride anion to antimony, which induces a change in the palladium coordination geometry from square planar to trigonal bipyramidal (with all phosphines coordinated). Furthermore, the authors showed that this receptor can be used for the detection of fluoride in water by using a biphasic system where the aqueous fluoride solution is layered on top of a dichloromethane solution of **38**, which produces a color change in the organic layer after

shaking. Tripier, Platas-Iglesias, Charbonnière, and colleagues focused on the sensing ability of lanthanide complexes of DOTA derivatives such as **39**.^{77–79} A large increase in the emission of an aqueous solution of the europium complex of **39** was observed upon the addition of fluoride anions but not upon the addition of other anions (Cl^- , Br^- , HCO_3^- , AcO^- , HPO_4^{2-}). NMR, ES-MS, and X-ray diffraction suggest that this is due to the formation of a dimeric europium capsule around the fluoride anion, stabilized by a Eu–F–Eu bridge, π – π interactions between the indazole groups, and hydrogen bonding involving the indazole and carboxylate moieties. Rochat and Severin employed the Lewis basicity of fluoride anions in a different way.⁸⁰ They developed an assay where an aqueous F^- solution was spiked with a known amount of CaCl_2 and CaF_2 to induce the precipitation of CaF_2 . After filtration of the precipitate, the concentration of remaining Ca^{2+} ions was determined using the calcium sensor **40**, and this could subsequently be used to back-calculate the fluoride concentration in the original sample. The system was found to be selective for fluoride over other common anions, except phosphates, which also induce Ca^{2+} precipitation. Nonetheless, the authors showed that this setup could be used to determine the fluoride concentrations in commercial products such as mouthwashes and toothpaste.

Silicon is another Lewis-acidic center with high fluorophilicity that deserves special attention when it comes to the development of fluoride sensors. There have been a number of early sensors that involve the direct addition of F^- to silicon, including tri(9-anthryl)fluorosilane **41** developed by Yamaguchi, Akiyama, and Tamao which can selectively react with F^- in THF to create a hypervalent silicon center where the change in geometry leads to different through-space interactions between the anthryl groups and hence to a large increase in the fluorescence intensity of the receptor (Scheme 1a).^{81,82} The most common silicon-bearing receptors, however, are the reaction-based sensors (chemodosimeters) where fluoride anions trigger the cleavage of Si–O or Si–C bonds in favor of the formation of the highly stable Si–F bonds. This approach was first developed independently by the groups of Martínez-Máñez⁸³ and Swager.⁸⁴ Kim and Swager synthesized polymeric receptor **42** that can undergo desilylation reactions followed by a cyclization reactions to create coumarin polymer **42a** upon the addition of tetrabutylammonium fluoride in dichloromethane (Scheme 1b). This coumarin dye formation leads to a red shift in both the absorbance and the emission spectra of the polymer and a visible change in emission color from blue to blue-green, indicating that this reaction can be used to sense fluoride anions. Since then a number of sensors have been developed that employ fluoride-mediated desilylation reactions, but many of them still have a slow reaction time or only function in organic solvents (see the review by Yoon and co-workers¹⁹ for an overview of the many silicon-based fluoride sensors).^{85–89} Exceptions include the coumarin-derived sensor **43** by Hong and colleagues that was shown to function as a fluorescent switch on sensor for fluoride anions in aqueous HEPES buffer due to a desilylation reaction that can only be induced by F^- but not by Cl^- , Br^- , I^- , AcO^- , NO_3^- , N_3^- , and H_2PO_4^- (Scheme 1c).^{90,91} Interestingly, the authors were able to show that **43** can be used to quantify the fluoride concentration in cells (A549 human lung carcinoma cells). Hu et al. also created a fluoride sensing system based on receptor **44** that can function in water.⁹² Sensor **44** is not soluble in water by itself but can be solubilized by a micellar CTAB solution. It was observed that this assembly displays a ratiometric fluorescent response toward fluoride anions and not toward other anions (Cl^- , Br^- , OAc^- ,

Scheme 1. Fluoride Sensors Based on the Desilylation Reactions of Receptors 41–45



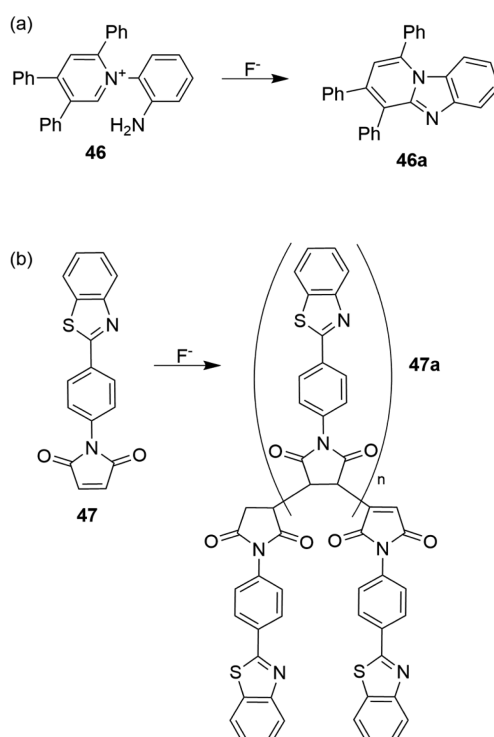
NO_3^- , H_2PO_4^- , and HSO_4^-), which was ascribed to the selective desilylation of **44** (Scheme 1d). Filter paper loaded with **44** could also be used to sense fluoride anions in water with high sensitivity and selectivity.

Baker and Scott reported another interesting desilylation-based fluoride sensor (**45**).⁹³ When an aqueous fluoride solution (CsF) was added to a $\text{MeOH}:\text{pyridine}$ or $\text{isopropanol}:\text{pyridine}$ solution of **45**, a visible yellow color developed over time. The yellow color change was attributed to the desilylation of **45** that causes a cascade of reactions ultimately leading to yellow compound **45a** (Scheme 1e). Interestingly, during these reactions, additional F^- anions are released that can induce the cascade in other molecules **45**, and hence, the signal is amplified. As a consequence, the detection limit for fluoride anions is significantly lower than without amplification. A similar cascade-

based signal amplification system for fluoride detection has also been reported by Shabat and co-workers.⁹⁴

Desilylation reactions are not the only reactions that can be triggered by fluoride anions, and a number of sensors based on other types of reactions have been developed. Gong, Ning, and co-workers developed receptor **46** as a novel chemodosimeter for fluoride.⁹⁵ It was found that the addition of F⁻ to an acetonitrile solution of **46** leads to a large increase in fluorescence, which was not observed in the presence of Cl⁻, Br⁻, NO₃⁻, H₂PO₄⁻, or OAc⁻. Proton NMR experiments suggested that this was due to an intramolecular cyclization reaction leading to **46a** (Scheme 2a). The role of fluoride in this reaction is presumably to increase the basicity of the amino group (through hydrogen bonding or deprotonation) so that it can attack the α position of the pyridinium ring. Padié and Zeitler

Scheme 2. Reactions Responsible for the Chemodosimetric Fluoride Response of 46 and 47



employed the reactivity of fluoride to develop maleimide-based sensor **47**.⁹⁶ It was observed that the addition of tetrabutylammonium fluoride to a solution of **47** in DMSO leads to the appearance of a dark red color, the formation of a precipitate, and an increase in fluorescence. It was suggested that these optical changes are due to a nucleophilic attack of fluoride on the α,β -unsaturated systems that initiates an anionic polymerization to create **47a** (Scheme 2b). A similar increase in fluorescence was also observed in the presence of OH^- and CN^- , but the fluorescence maximum was different for OH^- compared to F^- , while CN^- did not lead to the dark red color observed with F^- and OH^- . This implies that this sensing system could be used to differentiate between these three anions and can be considered as an effective sensor.

2.1.2. Discrete Optical Sensors for Cyanide Anions.

Cyanide salts have been known for centuries to be potent toxic substances, and there has thus been great interest in developing methods for the detection of this anion. In recent years, a number of reviews about cyanide sensing have emerged, and the reader is referred to these manuscripts for additional examples.^{97–100} This section will be limited to an overview of the common strategies employed to achieve selective cyanide sensing. Cyanide shares a number of characteristics with fluoride which can provide a starting point in the design of sensors for this anion, such as high basicity (leading to deprotonation) and high affinity for Lewis acids (e.g., boron). This therefore can result in low selectivity between cyanide and fluoride, and it can sometimes be difficult to discriminate between these two anions. The majority of cyanide sensors are therefore usually based upon other properties that distinguish cyanide anions from other anions, such as a high affinity for Cu^{2+} and a high nucleophilic character that allows reaction-based cyanide sensing (chemodosimeters). However, due to the similar basicity of fluoride and cyanide some examples have been reported in the literature in which the detection of

both F^- and CN^- can be achieved by the same system. Bhattacharya and co-workers, for example, described receptor **48** (Figure 10) as a colorimetric probe for both cyanide and

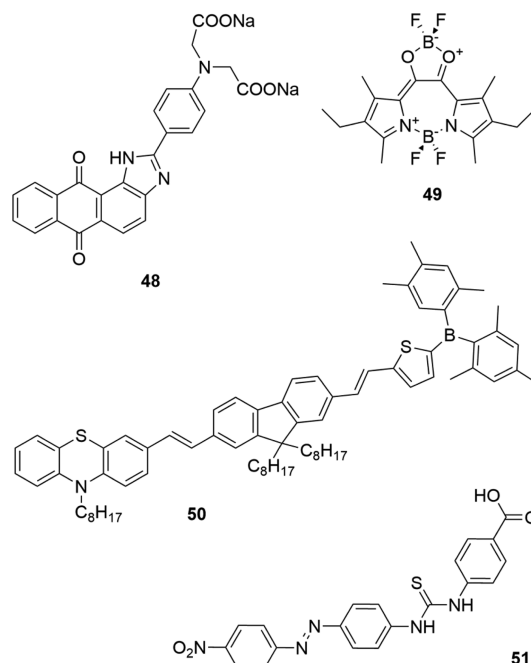


Figure 10. Structures of compounds **48–51**.

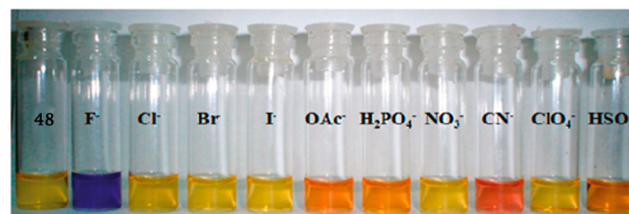


Figure 11. Color change of **48** in $\text{CH}_3\text{CN}/5\%$ DMSO upon addition of 50 equiv of various anions. Reprinted with permission from ref 101. Copyright 2011 American Chemical Society.

fluoride.¹⁰¹ As shown in Figure 11, the addition of F^- or CN^- to a solution of **48** in $\text{CH}_3\text{CN}/5\%$ DMSO leads to a color change from yellow to, respectively, blue or red due to an intramolecular charge-transfer (ICT) process. More interestingly, in the presence of water the same receptor only shows a selective optical response in the presence of CN^- because the higher degree of hydration of F^- ($\Delta H_{\text{hyd}} = -505 \text{ kJ/mol}$) with respect to CN^- ($\Delta H_{\text{hyd}} = -67 \text{ kJ/mol}$) results in a diminution of the fluoride sensing ability of **48** in water.¹⁰² Another example of a double-response colorimetric sensor was reported by Akkaya and collaborators, who showed that expanded BODIPY dye **49** (Figure 10) is able to produce a different color change upon the addition of both F^- and CN^- in chloroform as shown in Figure 12.¹⁰³

A fluorescent sensor for the dual recognition of F^- and CN^- based on a dimesitylboron derivative with a terminal phenothiazine bridged by fluorenevinyl (**50**, Figure 10) was recently reported by Lu and co-workers.¹⁰⁴ This D–π–A (Donor–π–Acceptor) receptor shows a blue shift in both the

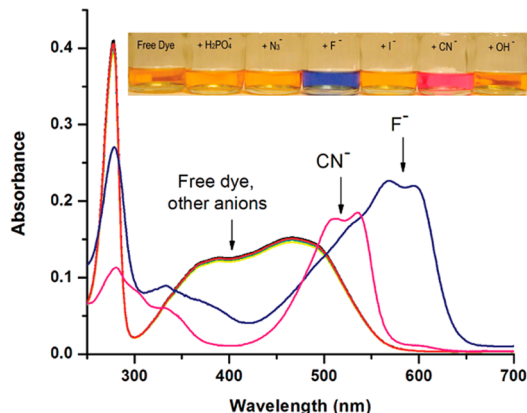


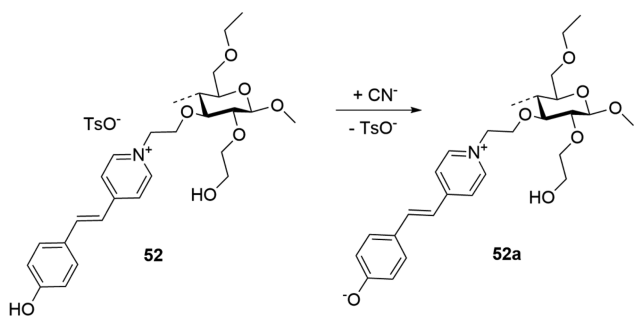
Figure 12. Changes in the UV–vis spectrum of **49** upon addition of CN^- and F^- in chloroform. (Inset) Photograph taken at ambient light of free **49** in the presence of different anions. Reprinted with permission from ref 103. Copyright 2012 American Chemical Society.

absorbance and the emission of the free receptor in dichloromethane upon addition of F^- and CN^- .

Similarly to fluoride (see section 2.1.1), cyanide can also cause deprotonation of the receptors, often accompanied by a color change. Vilar and co-workers reported the anion binding properties and the colorimetric response of thiourea **51** (Figure 10).¹⁰⁵ In protic solvents such as MeOH, **51** changes its color only upon the addition of CN^- with a detection limit of 8 ppm, while in DMSO a colorimetric response is observed not only in the presence of CN^- but also upon the addition of F^- , CH_3COO^- , and H_2PO_4^- due to the deprotonation of the thiourea NHs. Furthermore, dye **51** can also be supported onto Al_2O_3 nanostructured films resulting in a material that can selectively detect cyanide in water down to a concentration of 2.6 ppm.

Another recent example of an analytical device able to detect the presence of CN^- in water due to deprotonation has been reported by the group of Machado.¹⁰⁶ 1-Methyl-4-[(1-oxocyclohexa-2,5-dienylidene)ethylidene]-1,4-dihdropyridine (Brooker's merocyanine, BM), a solvatochromic dye, was covalently linked to ethyl(hydroxyethyl)-cellulose (EHEC) to afford **52**. As shown in Scheme 3, the addition of CN^- in water

Scheme 3. Cyanide Sensor **52** Is Deprotonated by Cyanide



leads to deprotonation of the OH group of the dye (**52a**) with a concomitant change in the emission and absorption properties of the system. The functionalized polymer can also be easily transformed into a film able to sense cyanide in water as well as in cassava (*Manihot esculenta* Crantz) roots, which are a well-known source of endogenous biological cyanide.

It is well known that triarylboranes interact with cyanide to form the corresponding cyanoborate complexes. One of the most elegant examples of ammonium boranes that can sense cyanide in water have been reported by the group of Gabbaï (see section 2.1.1).¹⁰⁷ Additionally, Gabbaï has shown that sulfonium boranes can also benefit from attractive Coulombic effects similar to those occurring in ammonium boranes.¹⁰⁸ Receptor **53**, for example, can sense CN^- in water at pH 7 at the subparts per million level in water (see Figure 13). The use of phosphonium boranes has also resulted effectively in CN^- sensing.¹⁰⁹

Another interesting example of a boron-containing receptor has been reported by Fallis and Aldridge.¹¹⁰ They described the logic-gate behavior of boron-functionalized ferrocene compound **55** (Scheme 4). In acetonitrile/MeOH (>100:1) solvent mixture, **55** changes color from pink to intense purple in the presence of cyanide anions and an oxidant (tetrazolium violet). As the free receptor **55** and the cyanide adduct **55a** have a different redox potential, the tetrazolium violet oxidant is able to oxidize adduct **55a** but not free **55**, and the ensemble can thus be used as a colorimetric cyanide sensor.

Among the various systems designed to detect cyanide, sensors that employ the affinity of this anion for copper (due to the ability of cyanide to react with copper ions to form stable $[\text{Cu}(\text{CN})_x]^{n-}$ species) have attracted specific attention. Park and Yoon described the behavior of compound **56** as a fluorescent sensor in aqueous solutions at pH 7.4.¹¹¹ Receptor **56** is a derivative of fluorescein which is in an “on” state at pH 7.4 with an emission maximum at 522 nm. As shown in Scheme 5a, upon the addition of 1 equiv of Cu^{2+} , quenching of the fluorescence is observed due to the formation of complex **56a**. When cyanide is added to the solution the formation of $[\text{Cu}(\text{CN})_2]$ results in the restoration of the emission of **56**. This system also gives a colorimetric response with a color change from yellow (**56**) to pink (**56a**) and back to yellow. Furthermore, the authors demonstrated that **56** can be used as a cyanide sensor for in vivo imaging. The same authors also reported the first example of a NIR (near-infrared) emitting dye for cyanide, **57** (Scheme 5b), a derivative of the dye IR-780.¹¹² In this case a quenching of the fluorescence of the receptor at 748 nm is observed upon the addition of 1 equiv of Cu^{2+} , which can subsequently be selectively restored in the presence of CN^- . This system is able to sense cyanide in the pH range 2.7–10.4 with a detection limit of 5 μM . The authors also employed **57** for in vivo bioimaging and used it to investigate whether cyanide is present in the nematode *Caenorhabditis elegans* infected with a *Pseudomonas aeruginosa* strain (PA14). PA is the most important pathogen causing chronic infections in cystic fibrosis patients and is able to synthesize HCN, a potent inhibitor of cellular respiration. To confirm bacterial infection in the intestine of the nematodes, *C. elegans* were fed on a PA14 strain labeled with GFP (green fluorescent protein) before imaging. As shown in Figure 14b–d, both green and NIR fluorescence were observed in the nematodes fed on PA14 and exposed to the copper complex of **57**, indicating that the system is able to sense the cyanide produced by the *P. aeruginosa* in *C. elegans*.

Das and collaborators used an Ir(III)-based cyclometalated complex (**58**, Scheme 5c) with a pendant Cu(II) moiety (**58a**, Scheme 5c) for the recognition of CN^- in 10 mM aqueous HEPES buffer– CH_3CN (99.6:0.4, v/v) at pH 7.6 via a “turn on” phosphorescence response.¹¹³ This reagent could also be used as an imaging reagent for the detection of the cellular uptake of CN^- ions in HeLa cells from aqueous buffer (pH 7.6), which can be used to develop an assay for probing the in-situ release of

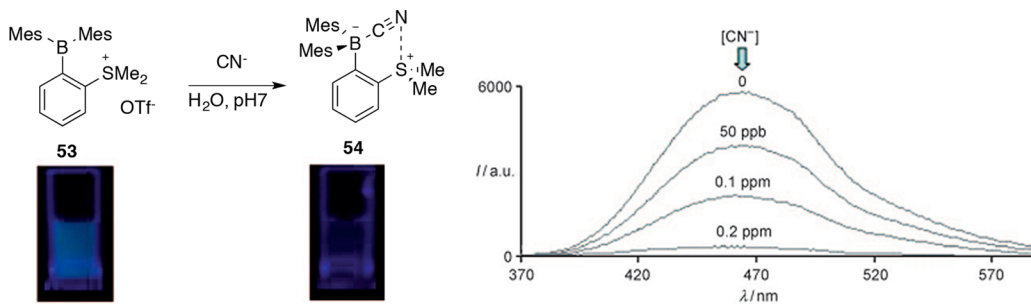
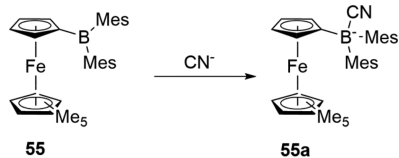


Figure 13. Visible fluorescence changes caused by the formation of **54**, and spectral fluorescence changes of **53** upon addition of CN^- . Reprinted with permission from ref 108. Copyright 2009 Wiley-VCH.

Scheme 4. Binding Mechanism of Cyanide to Compound **55**



cyanide from a cyanohydrin by the HNL (hydroxynitrile lyase) enzyme under physiological conditions.

Copper complexes are also able to sense cyanide anions by simple ligand exchange reactions. The first example of this type of sensor was reported by Caltagirone and Lippolis.¹¹⁴ The copper complex of receptor **59** (Scheme 5d) is coordinatively unsaturated and therefore suitable for anion complexation. In MeCN, **59** acts as a colorimetric sensor for both I^- and CN^- with different colors observed for the formation of the 1:1 and 2:1 complex with cyanide (Figure 15a), while in water only CN^- causes a color change (Figure 15b).

Receptor **60**, reported by Jang and collaborators, also works by a ligand exchange mechanism on the copper center, and as shown in Scheme 5e, a demetalation reaction occurs in the presence of excess CN^- that completely restores the fluorescent emission of compound **60**.¹¹⁵

Porphyrins containing receptors are another type of metal-containing compounds that can be used to sense cyanide. Examples include ditopic receptors in which a Zn-porphyrin can be conjugated to a crown ether for NaCN sensing^{116,117} or triarylboration-decorated Zn-porphyrins.¹¹⁸

Various types of chemodosimeters have been developed for cyanide sensing based on different reactions. Carbonyl compounds, for example, react with CN^- to form the corresponding cyanohydrins. Sun and co-workers described the colorimetric sensing by **61** of cyanide over other common inorganic anions in $\text{CH}_3\text{CN}/\text{H}_2\text{O}$ (9:1, v/v).¹¹⁹ In this case, the addition of CN^- to the amide carbonyl group (**61a**) is stabilized by the formation of intramolecular hydrogen bonds, as shown in Scheme 6a. The two amide protons and the two pyrrole protons form a hydrogen-bonding pocket that can bring CN^- in the vicinity of the amide carbonyl groups. The addition of CN^- causes a color change in the solution of **61** (from colorless to yellow). The affinity of the carbonyl groups toward cyanide may be further enhanced by attaching electron-withdrawing groups such as CF_3 to the carbonyl group. For example, BODIPY derivative **62** can undergo an addition reaction of cyanide (Scheme 6b) with a concomitant change of both its absorption and its emission properties.¹²⁰ Another way of increasing the reactivity of the carbonyl groups toward cyanide is through intramolecular hydrogen bonding. The simple coumarin-based

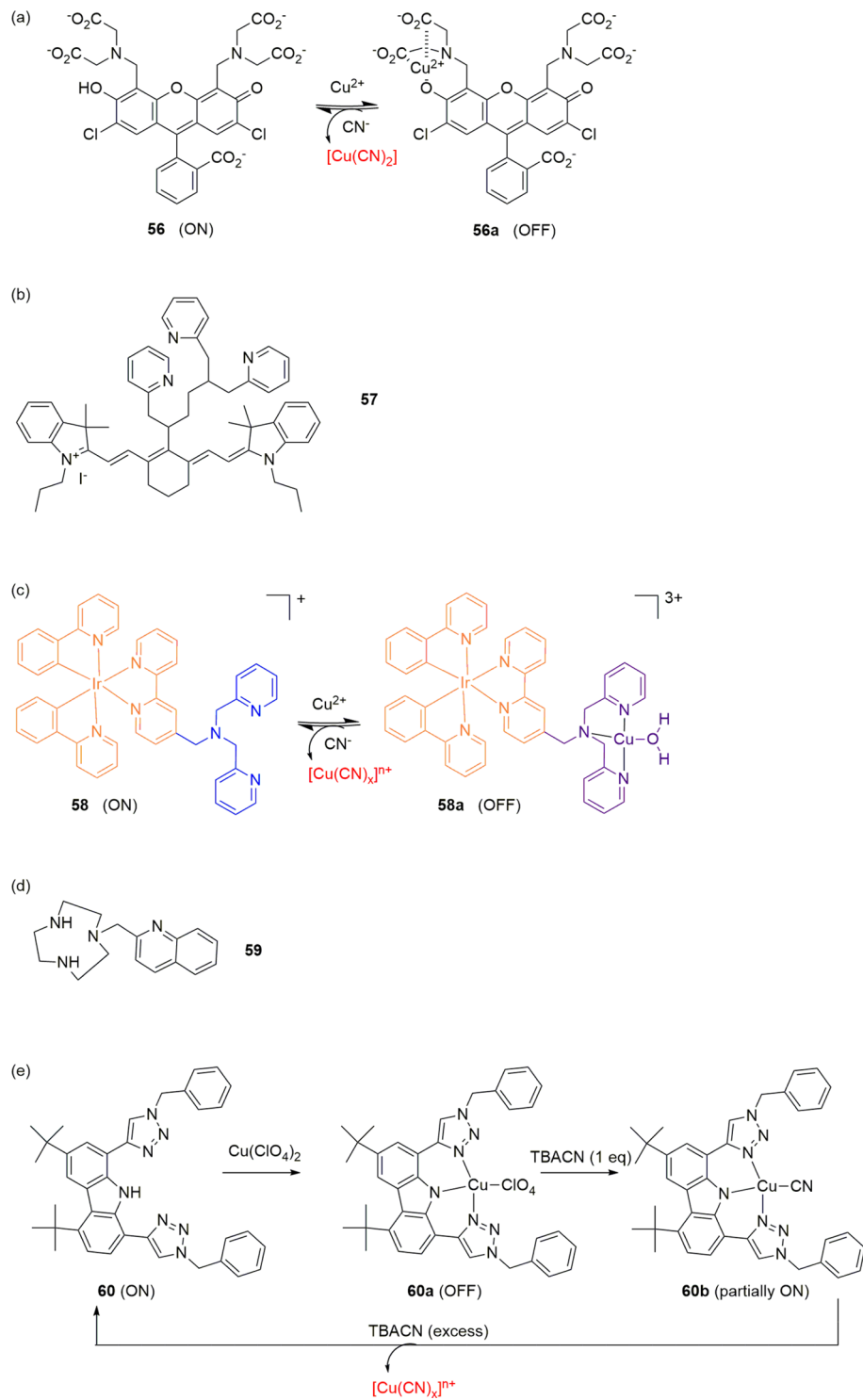
fluorescent chemodosimeter **63** containing a salicylaldehyde functionality as binding site has been developed by Kim, Hong, and co-workers.¹²¹ Cyanide acts as a nucleophile toward the carbonyl group activated by the formation of an intramolecular hydrogen bond with the phenol group, inducing the formation of cyanohydrin **63a**, which leads to an enhancement in fluorescence (see Scheme 6c).

Another strategy to design chemodosimeters for cyanide sensing is to exploit Michael addition reactions. Kim et al. described α,β -unsaturated sensor **64** (Scheme 7a) that can undergo a Michael addition with CN^- .¹²² In MeCN **64** is in an off state due to the presence of conjugated dimethylamino and carbonyl groups. When CN^- is added to a solution of **64**, however, fluorescent compound **64b** is obtained in which this intramolecular PET (photoinduced electron transfer) process is blocked.

Martínez-Mañez and co-workers also developed a Michael addition-based system with the ability to colorimetrically sense cyanide in water (borax buffer, pH 10.6, 1% acetonitrile) and HCN in the gas phase.¹²³ Upon addition of CN^- the *p*-quinomethane derivative **65** undergoes a color change from pink to colorless owing to the conjugated addition reaction (see Scheme 7b). When absorbed on an aminated basic silica support, **65** can be used to detect HCN at concentrations as low as 2 ppm.

An interesting example of sequential recognition of two anions (F^- and CN^-) has been recently reported by Wang and co-workers.¹²⁴ Receptor **66** (Scheme 7c) is based on the 1,10-binaphthyl scaffold and displays blue fluorescence at 480 nm in THF due to the formation of an intermolecular excimer (emission of the monomer at 360 nm is also observed). Addition of F^- causes quenching of the band of the monomer and the formation of a new band at 460 nm ascribed to the formation of the monomeric coumarin derivative **66a**. When CN^- is added to the solution of **66a**, a Michael addition occurs and fluorescence emission bands with intensity enhancement are observed at 470 and 550 nm, deriving from the formation of the cyano-coumarin derivative **66b**.

The 1,1-dicyanovinyl groups have also been employed as a selectively reactive moiety for CN^- recognition. Cyanide can add to the 1,1-dicyanovinyl group to form a stabilized anionic adduct, causing a change in the absorption and emission properties of the sensors. Jang and co-workers, for example, synthesized and studied the switch on fluorescent sensor **67** (Scheme 8a) in which the dicyanovinyl group is conjugated to a BODIPY structure.¹²⁵ The sensor exhibits weak fluorescence at around 520 nm in a 1% $\text{THF}/\text{H}_2\text{O}$ solvent mixture due to ICT (intramolecular charge transfer) quenching. The formation of adduct **67a** in the presence of CN^- leads to a dramatic increase in fluorescence because this ICT process is no longer possible.

Scheme 5. Proposed Mechanisms of CN^- Sensing for Receptors 56, 58, and 60, and Structures of 57 and 59

Xie et al. introduced a dicyanovinyl group at a sterically demanding position of a large π framework.¹²⁶ Receptors 68–68b (Scheme 8b), with a dicyanovinyl group in the 9 position of an anthracene ring with an electron-donating group attached to the 10 position, show a weak fluorescent emission deriving from the nonplanarity of the molecules which increases up to 242-fold upon the addition of CN^- in dichloromethane. In contrast, in receptor 69 the dicyanovinyl group is in a less sterically demanding position on the anthracene (in the 2 position), resulting in an almost planar conformation where the

fluorescence is more intense and can be switched off by CN^- as the addition of cyanide can disrupt the large planar conjugated system. Finally, receptor 70 contains a porphyrin framework, which is distorted by the steric hindrance associated with the dicyanovinyl group, so that weak fluorescence is observed. Addition of CN^- disrupts the dicyanovinyl group, leading to recovery of the planarity of the porphyrin macrocycle. The increase in the fluorescence emission suggests that the porphyrin aromaticity is enhanced as the porphyrin approaches planarity,

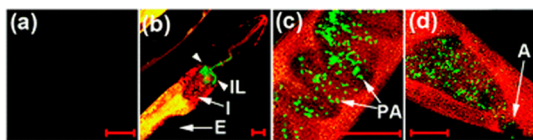


Figure 14. NIR imaging of cyanide in *C. elegans* infected with a *P. aeruginosa* strain (PA14) labeled with green fluorescent protein (GFP): (a) control (nematodes fed on GFP-labeled noninfectious *E. coli* OPS0), (b–d) nematodes fed on GFP-labeled PA14 for 2 days ((b) anterior end, (c) medial part, (d) posterior end of *C. elegans*). Scale bars represent 20 mm (IL = intestinal lumen; I = intestine; E = eggs; PA = PA14-GFP; A = anus). Reprinted with permission from ref 112. Copyright 2010 Royal Society of Chemistry.

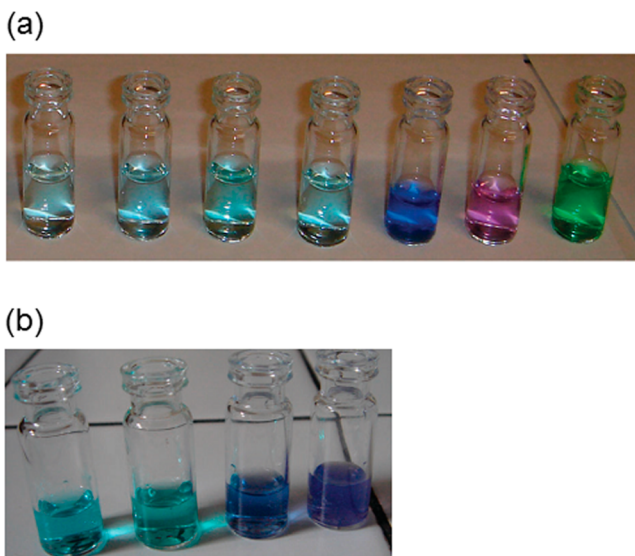


Figure 15. (a) Color change of $[\text{Cu}(60)](\text{BF}_4)_2$ in MeCN (1.00×10^{-3} M) upon addition of different anions in MeCN. (From left to right) Free complex; +1 equiv of F^- ; +1 equiv of Cl^- ; +1 equiv of Br^- ; +1 equiv of CN^- ; +2 equiv of CN^- ; +1 equiv of I^- . (b) Color change of $[\text{Cu}(59)](\text{BF}_4)_2$ in H_2O (1.72×10^{-3} M) upon addition of different anions in H_2O . (From left to right) Free complex; +1 equiv of I^- ; +1 equiv of CN^- ; +2 equiv of CN^- . Reprinted with permission from ref 114. Copyright 2011 Royal Chemical Society.

although the conjugation is reduced after disruption of the dicyanovinyl group.

Several probes for cyanide sensing containing positively charged nitrogen atoms, such as indolium or pyridinium moieties, have been developed because positively charged nitrogens can enhance the electrophilicity of a sp^2 carbon atom toward CN^- . A good example can be found in the work of Tae and co-workers, who developed acridinium salt 71 (Scheme 9a) as a fluorescent and colorimetric sensor for CN^- in $\text{DMSO-H}_2\text{O}$ (95:5, v/v).¹²⁷ Upon addition of CN^- at 50 °C, the adduct 71a is initially formed which rapidly reacts with oxygen to produce acridinone 71b. The reaction with CN^- causes a quenching of the emission of 71 at 481 nm and a color change from orange to blue.

Aprahamian and collaborators developed another positively charged cyanide sensor based on the triazolopyridinium salt 72.¹²⁸ In $\text{DMSO-H}_2\text{O}$ (99:1, v/v) the perchlorate salt of 72 is in an off state because the presence of the *p*-OMe group enhances the charge transfer from the phenyl ring to the triazolopyridinium subunit. As shown in Scheme 9b, the addition of CN^- causes a ring-opening reaction on the bridgehead nitrogen via a

pseudopericyclic pathway leading to the formation of intermediate 72a and then 72b, which shows an emission band at 504 nm.

Kim et al. developed the positively charged indolium-conjugated coumarin chemodosimeter 73 (Scheme 9c) as a cyanide sensor.¹²⁹ Free 73 is characterized by two absorption bands at 398 and 610 nm in $\text{H}_2\text{O}/\text{MeCN}$ (5:95, v/v). Addition of CN^- causes a red shift of the band from 398 to 409 nm with a concomitant disappearance of the band at 610 nm, causing a color change from blue to yellow. Moreover, the fluorescence of 73 is switched on when compound 73a is formed, as the nucleophilic addition of cyanide disrupts the conjugation between the indole group and the coumarin, i.e., ICT does not occur.

A similar strategy for cyanide sensing in water has been developed by Zhang and co-workers, who reported that the addition of CN^- to the indolium-containing receptor 74 causes the formation of 74a, which forms aggregates that display an emission maximum at 466 nm.¹³⁰ The formation of the aggregates was demonstrated by dynamic light scattering (DLS) and confocal laser scanning microscopy (CLSM).

Raymo, Sortino, and collaborators designed chromogenic oxazine 75 for the colorimetric recognition of cyanide in acetonitrile.¹³¹ As shown in Scheme 10a, the addition of cyanide causes the opening of the oxazine ring in 75 to afford 4-nitrophenylazophenolate 75a. This reaction causes a decrease of the absorption band at 381 nm and the formation of a new band at 581 nm with a concomitant color change of the solution from pale yellow to red.

The ring-opening reaction on the oxazine caused by the presence of cyanide was used also by Tian and co-workers to develop the chemodosimeters 76 and 77 (Scheme 10b) that are able to colorimetrically detect CN^- due to the formation of 76a and 77a, respectively, in $\text{MeCN}/\text{H}_2\text{O}$ (19:1, v/v) at pH 7.6.¹³²

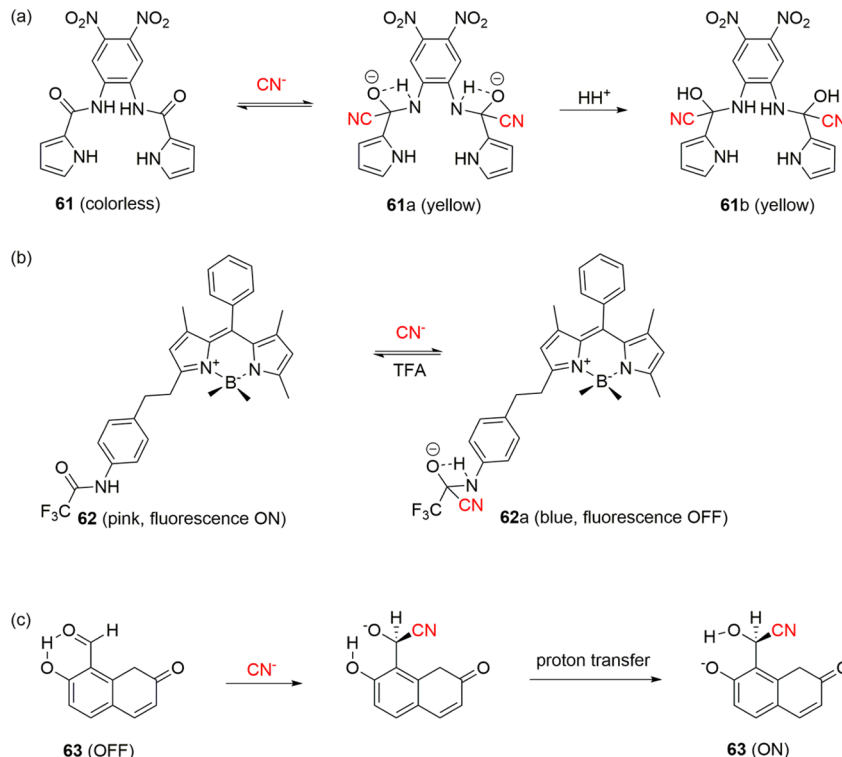
Apart from the above-mentioned chemodosimeters based on carbonyl chemistry, Michael additions, dicyanovinyl reactivity, and ring-opening reactions, other types of reactions can also be used to design chemodosimeters for cyanide detection, e.g., C–C bond formation utilizing croconium¹³³ or triarylmethane^{134,135} dyes and C–S bond formation induced by cyanide.¹³⁶ The reader is referred to more specialized reviews for additional examples of these types of chemodosimeters.¹⁰⁰

2.1.3. Discrete Optical Sensors for Phosphates.

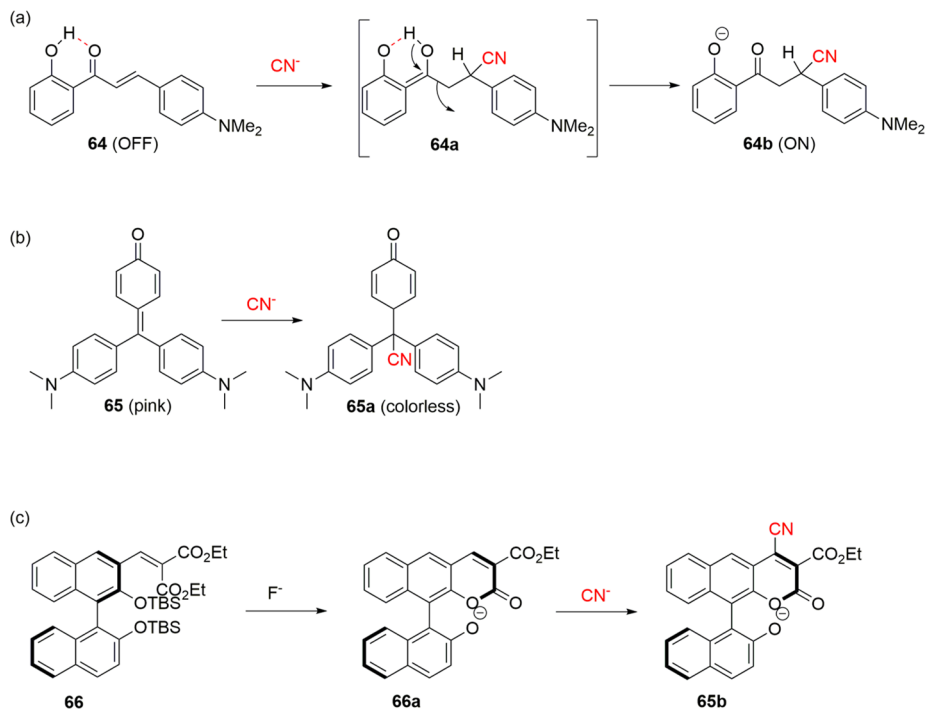
Phosphates play a central role in the building of two of the most fundamental molecules in living systems, DNA and RNA; they are constituents of membrane lipids (in the form of phospholipids) and are involved in many biological processes such as energy storage, gene regulation, muscle contraction, and signal transduction.^{137,138} Moreover, phosphates are important components of medicinal drugs and fertilizers. Eutrophication in the aquatic ecosystem is often related to pollution from phosphates and phosphorylated compounds.^{139,140} Due to their importance in both biological and environmental fields a great effort have been made in order to develop systems to selectively sense phosphate and phosphorylated compounds. Recently, very comprehensive reviews for the recognition of phosphorylated molecules by artificial receptors have been published.^{141,142}

One of the main difficulties of binding phosphate arises from the high hydration energy for this anion (−2765 kJ/mol) that places it near the bottom of the Hofmeister selectivity series.¹⁴³ Moreover, phosphate-type anions exist in water, at neutral pH, in different protonated states bearing different negative charges. For

Scheme 6. Cyanide Sensing by Receptors 61–63 via Formation of Cyanohydrins



Scheme 7. Cyanide Sensing by Receptors 64–66 via Michael Additions

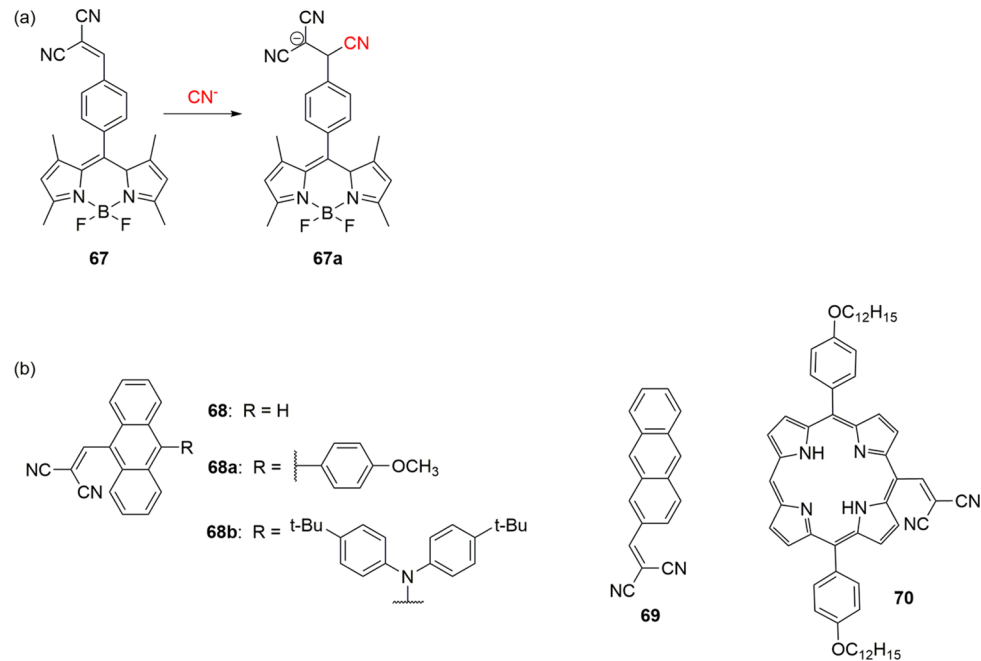


these reasons the binding of the inorganic phosphate-based anions PO_4^{3-} (orthophosphate), $\text{P}_2\text{O}_7^{4-}$ (pyrophosphate), and $\text{P}_3\text{O}_{10}^{5-}$ (triprophosphate) by artificial receptors requires the optimization of both electrostatic and hydrogen-bond interactions through topological complementarity. One of the strategies adopted in the design of receptors for phosphate anions is to use receptors bearing groups which can be easily protonated, such as polyammonium, imidazolium, and guanidinium moieties.

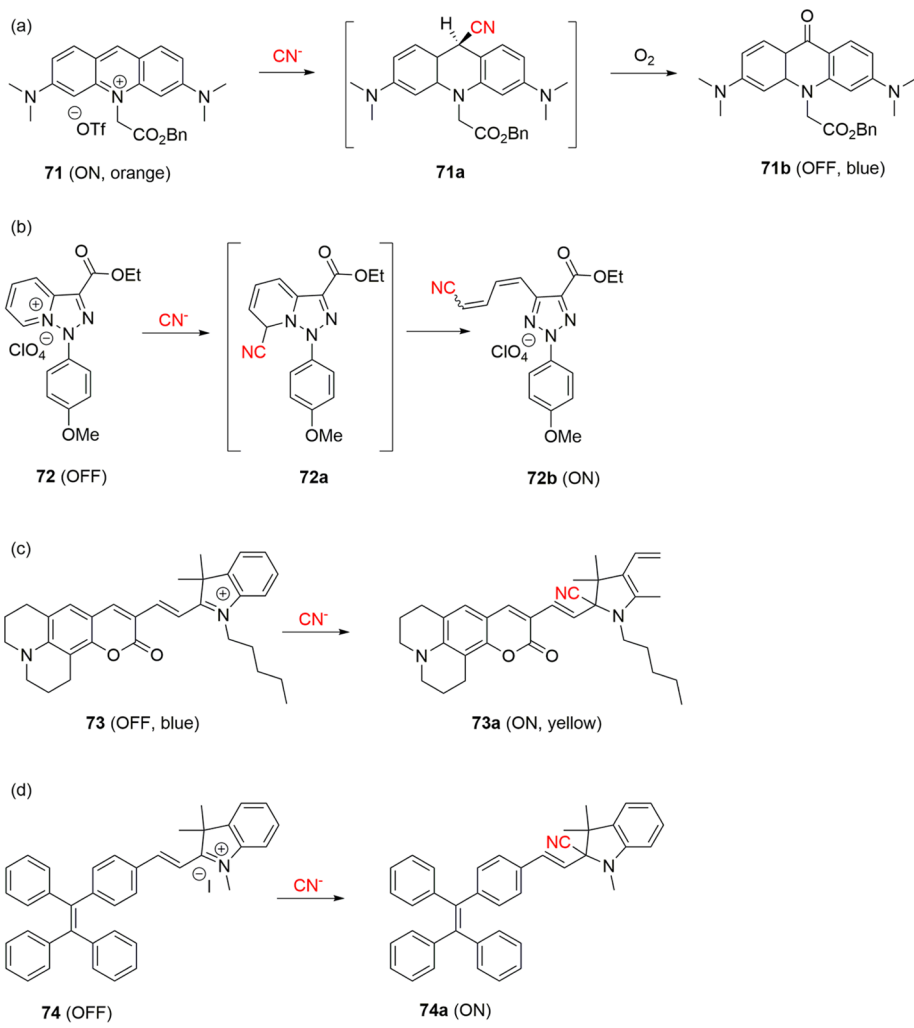
One of the early pioneers in this area was Czarnik, who designed and synthesized fluorescent chemosensors for phosphate and other anions.¹⁴⁴ Bencini and Lippolis recently reviewed the most significant achievements in the design of cyclic receptors containing mainly aliphatic amine groups as metal-free hosts for phosphate-based guests in aqueous environment.¹⁴⁵

The phenanthroline-containing polyammonium receptor **78** (Figure 16) described by Bencini and co-workers is able to sense

Scheme 8. Cyanide Sensing by Receptors 67–70 Containing a Dicyanovinyl Group



Scheme 9. Cyanide Sensing by Receptors 71–74 Containing Positively Charged Nitrogen Atoms



Scheme 10. Cyanide Sensing by Receptors 75–77 Based on Oxazine Ring-Opening Reaction

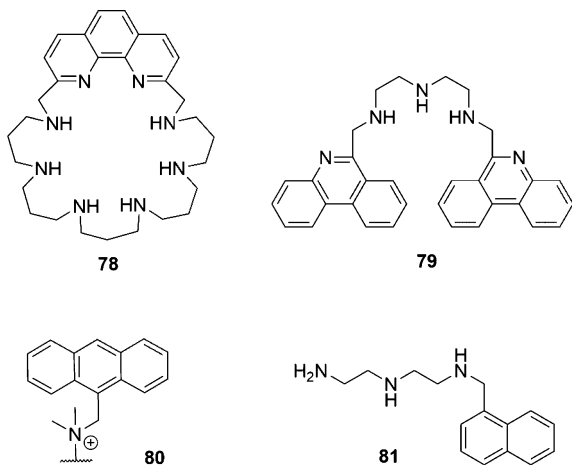
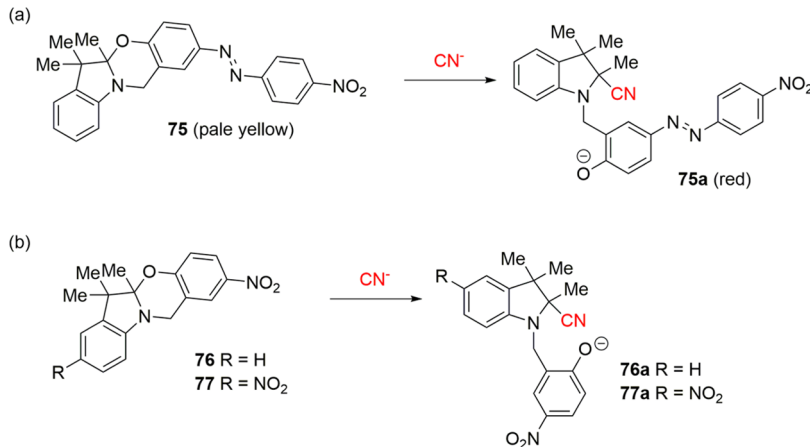


Figure 16. Structures of 78–81.

ATP over other triphosphate nucleotides (CTP, GTP, TTP) in aqueous environment at pH 6 via a selective quenching of the fluorescence.¹⁴⁶ When excited at 270 nm, the fluorescent emission of **78** (which is fully protonated at pH 6) at 365 nm dramatically decreases due to the formation of a 1:1 complex with ATP. The authors suggest that the phenanthroline moiety not only acts as the signaling unit of the sensor but also takes part in the interaction with ATP thanks to its ability to give strong $\pi-\pi$ interaction with the nucleobase.

Piantanida and co-workers reported strong nucleotide binding by the phenanthridine-containing receptor 79 (Figure 16) in aqueous media.¹⁴⁷ Binding constants were determined through fluorescence titrations performed at pH 5 and 7 in a 0.05 M sodium cacodylate buffer. Stronger binding was observed with the purine nucleotides at both pH values, with higher selectivity at pH 7 when the phenanthridine unit is unprotonated and $\pi-\pi$ stacking can occur. The stability trend follows the order AMP < ADP < ATP, i.e., the greater the phosphorylation of the nucleotide the greater the stabilization, supporting the contribution of electrostatic interactions to the binding affinity.

Martínez-Mañez et al. demonstrated that anthrylmethylamine **80** (Figure 16) can be anchored in mesoporous solids to permit fluorescent sensing of ATP in aqueous media.¹⁴⁸ Addition of ATP to suspensions of the solids at pH 2.8 caused a quenching of the anthracene emission. These solids showed a cooperative effect that resulted in a remarkable improvement in ATP

response with respect to the free anthrylmethylamine probe in solution.

In 2007 García-España and Alcarón reported bohemite nanoparticles with covalently linked polyammonium naphthalene receptor **81** (Figure 16) as potential materials for the preparation of chemosensors for ATP recognition.¹⁴⁹ Fluorescence emission studies showed that when the receptor is not linked to the nanoparticles quenching of the naphthalene fluorescence is only observed below pH 5. This pH dependence is attributed to a PET process from the naphthalene excited state to the protonated adenine ring. On the other hand, ATP-dependent quenching was achieved over a broad pH range (2–12) by supporting **81** on the bohemite matrix.

Imidazolium-based receptors have also been employed in the design of phosphate sensors, in particular, by the groups of Kim and Yoon. This group described the behavior of anthracene dimer **82** (Figure 17) connected by two imidazolium moieties. In MeCN/DMSO (9:1, v/v) the emission of **82** is selectively switched off via a PET mechanism due to the binding of H_2PO_4^- and $\text{HP}_2\text{O}_7^{3-}$ over other anions (HSO_4^- , I^- , Br^- , Cl^- , F^-).^{150,151} Ab initio calculations demonstrated that the binding selectivity toward H_2PO_4^- is related to the rigidity of the framework of the receptor.

Another example of a bis-imidazolium receptor functionalized with a quinoxaline group (**83**, Figure 17) able to sense pyrophosphate has been reported by Kim and co-workers. In the presence of anions compound **83** shows an emission band at 430 nm in MeCN ascribed to the formation of intermolecular $\pi-\pi$ stacking between two antiparallel quinoxaline rings (excimer). Interestingly, upon addition of pyrophosphate the formation of the excimer is not observed, and an intense charge-transfer band at 500 nm is formed instead.¹⁵²

The dissociation of an excimer (intramolecular, in this case) is responsible for the recognition of ATP over other nucleoside triphosphates by receptor 84 (Figure 17) in HEPES buffer at pH 7.4.¹⁵³ The authors postulate that the selectivity of 84 toward ATP over GTP, CTP, and UTP depends on the fact that guanine, cytosine, thymine, or uracil interacts with the exterior of the already stabilized stacked pyrene-pyrene dimer, which quenches the excimer fluorescence due to the large dipole moments. On the other hand, adenine can insert in between the two pyrene moieties, thereby separating them and allowing pyrene monomer fluorescence. High selectivity for ATP is also observed in comparison with ADP and AMP, which is ascribed to the difference in electrostatic interaction due to their anionic charges.

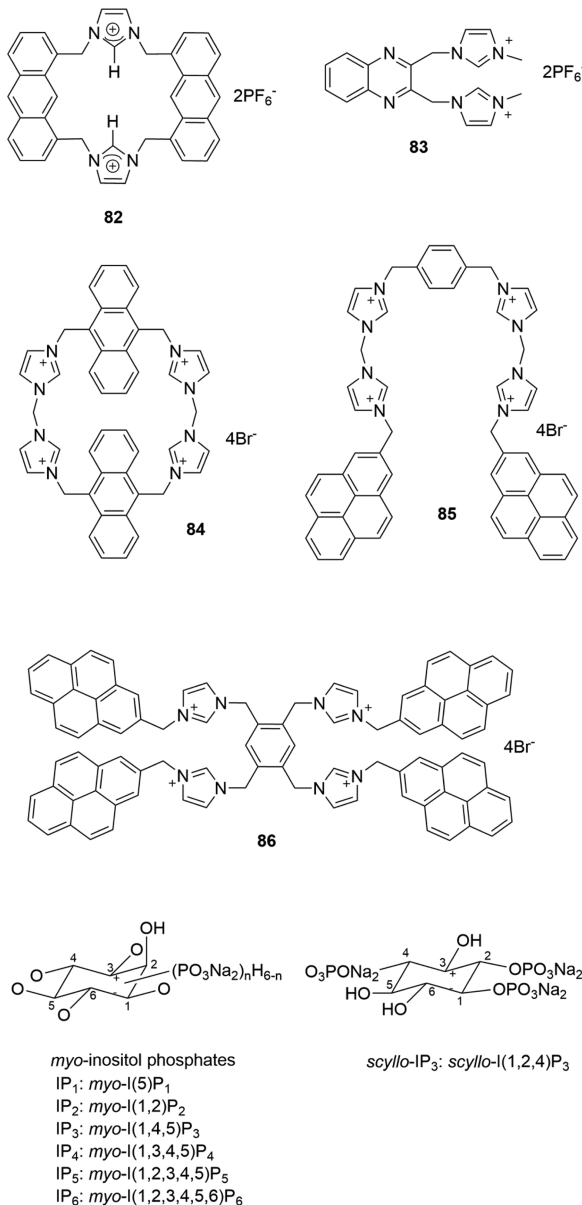


Figure 17. Structures of **82–86** and inositol phosphates (IP_x).

and the difference in the adenine ring stacking between the two pyrene moieties. A ratiometric fluorescence assay based on **84** for ATP-relevant enzyme activity, such as apyrase, was also studied.

The imidazolium–anthracene cyclophane **85** (Figure 17) effectively recognizes the biologically important GTP and I^- anions over other anions in a 100% aqueous solution of pH 7.4 via fluorescence quenching.¹⁵⁴ These affinities can be attributed to the strong $(\text{C}-\text{H})^+ \cdots \text{A}^-$ ionic hydrogen bonding.

Recently, Yoon and co-workers described the first example of an imidazolium-based fluorescent receptor (**86**, Figure 17) for d-myo-inositol 1,4,5-trisphosphate (IP_3).¹⁵⁵ IP_3 plays a pivotal role as a secondary messenger in intracellular signal transduction events. Receptor **86** contains four imidazolium and four pyrene groups. The emission of the excimer of **86** at 486 nm in DMSO–HEPES buffer (1:9, v/v) is dramatically quenched upon the formation of a 1:1 complex between **86** and IP_3 . Other phosphorylated species such as pyrophosphate, ATP, and other IP compounds (Figure 17) did not induce a significant change in the emission.

In the design of neutral receptors for phosphate anions recognition the use of functional groups such as ureas, thioureas, amides, and pyrrole moieties has been widely explored. Gunnlaugsson and co-workers described the ability of the pyridyl-based bis-amidothiourea **87** (Figure 18) bearing two nitro groups to colorimetrically sense AMP and ADP over ATP in DMSO/water (4:1, v/v).¹⁵⁶ Upon addition of AMP and ADP but also $\text{HP}_2\text{O}_7^{3-}$, the formation of an absorption band at 425 nm is observed with a concomitant color change of the solution from colorless to yellow. The authors suggested that both hydrogen bonding and deprotonation are involved in the recognition process. The same authors have shown that a similar receptor (**88**, Figure 18) tailored with a glycol chain in order to improve its solubility in aqueous medium is able to sense AMP in EtOH/ H_2O (1:1, v/v).¹⁵⁷ Similarly, Gale and co-workers reported that the fluorescence of bis-urea acridinone **89** (Figure 18) is selectively switched off upon addition of H_2PO_4^- in MeCN/DMSO (96:4, v/v) with respect to other anions (chloride, benzoate, and acetate).¹⁵⁸

Espinosa and Molina recently described two new chemosensors for $\text{HP}_2\text{O}_7^{3-}$ (**90** and **91**, Figure 18) that are able to work in a competitive mixed MeCN/ H_2O medium.¹⁵⁹ Receptor **90**, in which the two urea-functionalized arms are decorated with *p*-nitrophenyl rings, behaves as a highly selective chromogenic molecular probe for hydrogenpyrophosphate anions. Upon the addition of this anion in MeCN/ H_2O (70:30, v/v), a modest increase of the absorption bands of **90** in the region 370–400 nm was observed, resulting in a color change from colorless to yellow. Receptor **91**, bearing two photoactive pyrenyl rings, acts as a highly selective fluorescent molecular probe for hydrogen pyrophosphate anions in both acetonitrile and in MeCN/ H_2O (85:15, v/v). This receptor exhibits three emission bands: two due to monomer and the other due to excimer emission at 394, 416, and 496 nm, respectively. Upon the addition of $\text{HP}_2\text{O}_7^{3-}$ in MeCN, the excimer band disappears, whereas the monomer band is slightly increased and a 1:1 complex is formed. Interestingly, in MeCN/ H_2O (85:15, v/v) a strong increase of the excimer emission band is observed, while the monomer emission bands remain almost unaffected, and the stoichiometry of the complex changes to 1:2 (**91**:anion).

Other examples of bis-ureas functioning as optical chemosensors selective for $\text{HP}_2\text{O}_7^{3-}$ bearing two nitrophenyl groups (**92** and **92a**, Figure 18) or two naphthalene groups (**93** and **93a**, Figure 18) have been reported by Caltagirone and co-workers.¹⁶⁰ Among all the anions investigated (AcO^- , BzO^- , H_2PO_4^- , glutarate, and malonate) only $\text{HP}_2\text{O}_7^{3-}$ causes a change in the spectroscopic properties of the four receptors in DMSO. In particular, in the case of **92** and **92a** the formation of a complex with $\text{HP}_2\text{O}_7^{3-}$ is accompanied by a color change of the solution from yellow to orange. When this anion is added to a solution of **93** and **93a**, quenching of the emission band attributed to a single urea–naphthalene fragment at 380 nm is observed with the concomitant formation of a new fluorescence band at approximately 500 nm that can be attributed to the formation of an excimer.

Sessler and collaborators described a dipyrrolyl-functionalized bipyridine-based receptor (**94**, Figure 18) as fluorescent chemosensor for H_2PO_4^- recognition in DMSO.¹⁶¹ The bipyridine fragment is used to coordinate Ru^{2+} , which acts as the fluorogenic unit. Upon addition of H_2PO_4^- a decrease in the intensity of the band of free **94** at 630 nm is observed. Job plot analysis revealed a 1:1 host to dihydrogen phosphate stoichiometry.

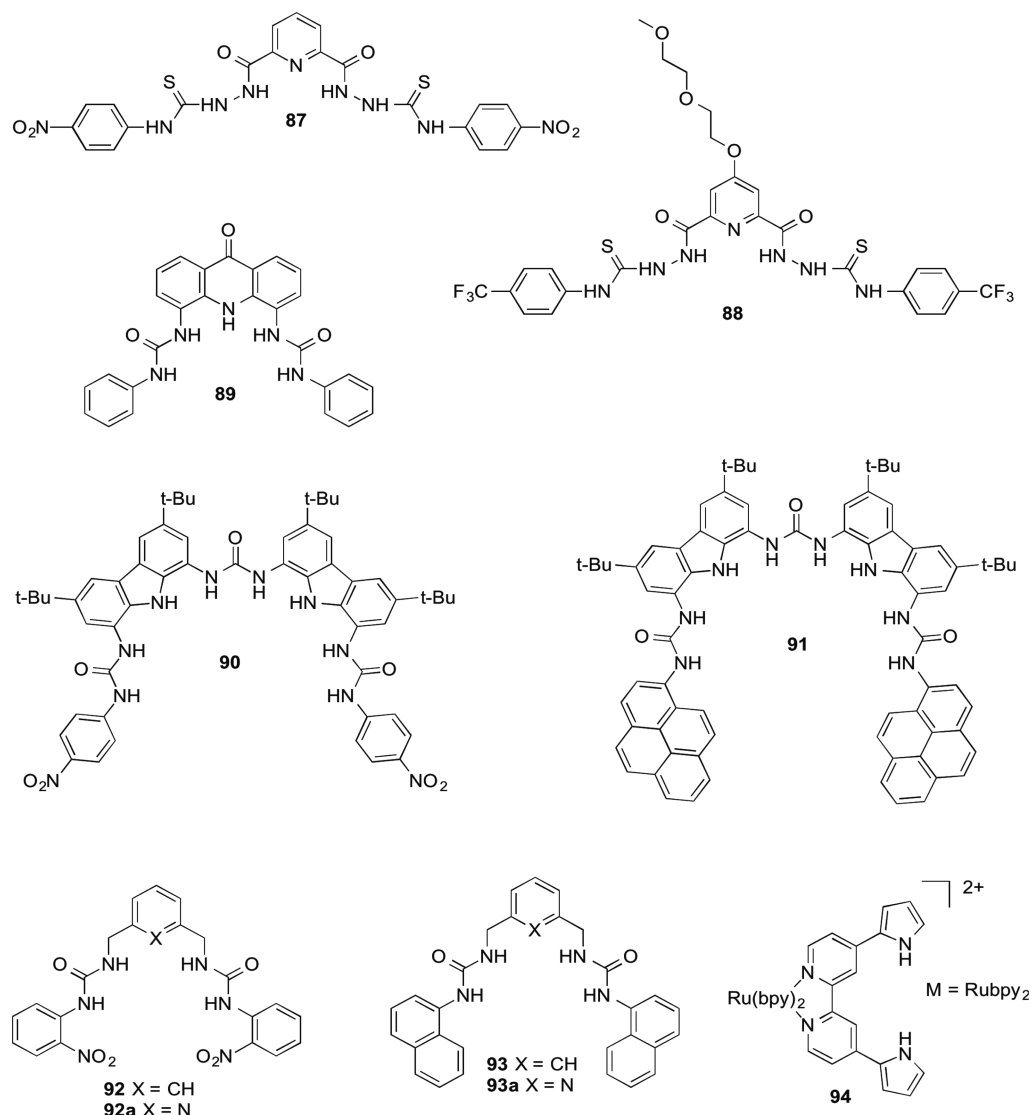


Figure 18. Structures of 87–94.

Zinc is present in the binding site of various metalloenzymes for which phosphate anions are substrates or inhibitors because of their tendency to reversibly bind to one or more Zn ions located in the prosthetic group of the enzyme. Examples include alkaline phosphatases in which two zinc(II) ions are located in close proximity to bind and cleave the phosphate ester bond in phosphate monoesters and P1 nucleases which cleave the phosphodiester bond in RNA or single-stranded DNA and contain three zinc ions in their active site, which act cooperatively in the process of substrate binding and hydrolysis.¹⁴¹ For this reason synthetic zinc(II) complexes are commonly used as receptors and optical dyes for phosphate anions. Readers are referred to specific reviews on the subject for additional examples.¹⁶²⁻¹⁶⁴ Here, only the most recent examples of Zn(II)-based sensors for phosphate will be discussed.

The dipicolylamino (DPA) ligand is one of the most commonly employed ligands in such systems, providing a tridentate ligand with three nitrogen donors that affords good selectivity for Zn^{2+} over biologically relevant metals such as Na^+ , K^+ , Mg^{2+} , and Ca^{2+} and leaves coordination sites free for anion binding.¹⁶⁵ The group of Hamachi has been very active in this area and reported many examples of DPA-Zn(II)-based artificial

receptors for phosphate recognition.^{164,166–169} For example, Hamachi and co-workers designed dual-emission chemosensors **95** and **96** (Figure 19) for nucleoside polyphosphates that are based on a new mechanism involving binding-induced recovery of FRET.¹⁷⁰ These chemosensors possess a coumarin unit (the FRET donor) that is connected to a xanthene ring (the FRET acceptor) through a short, rigid linker unit. In the nonbinding state, the xanthene part of the chemosensors adopts a nonconjugated form, so the chemosensors predominantly show blue emission from the coumarin unit (Figure 19). The binding of a nucleoside polyphosphate induces the recovery of the conjugated structure of the xanthene ring. This structural change brings about a large spectral overlap between the two fluorophores, causing the chemosensors to exhibit strong green emission from the xanthene due to the significant enhancement of the FRET efficiency. The significant ratiometric change observed using these chemosensors permits the ratiometric visualization of the ATP level inside living cells as well as the precise monitoring of two enzyme reactions involving nucleoside polyphosphates.

Along with DPA-Zn(II)-based sensors, another strategy adopted to design phosphate sensors is to use macrocyclic Zn(II)

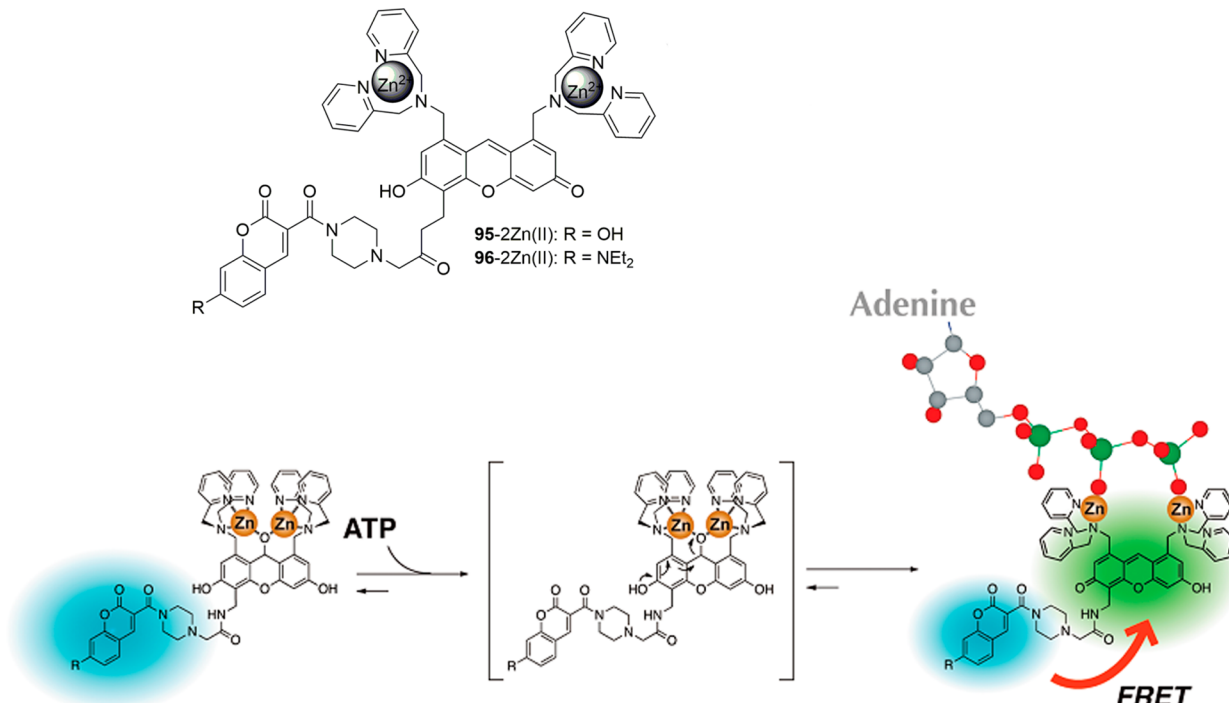


Figure 19. Structures of **95–96**, and schematic illustration of the dual-emission sensing of ATP with the two chemosensors. Reprinted with permission from ref 170. Copyright 2010 American Chemical Society.

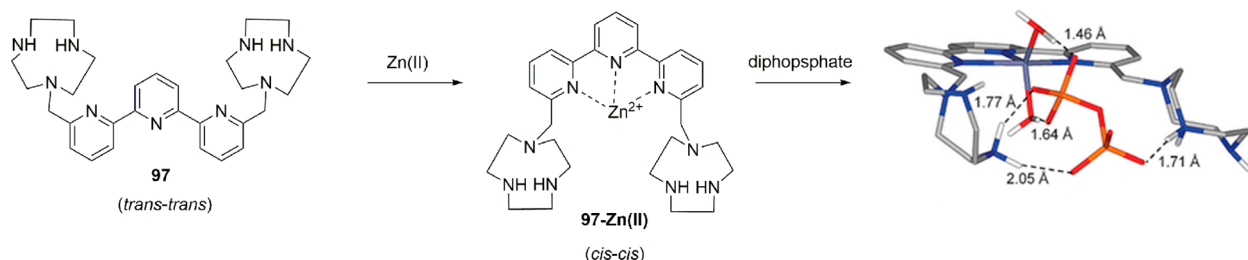


Figure 20. Diphosphate sensing by receptor **97**, showing the DFT-minimized structure of the adduct $[\text{Zn}97\text{H}_2(\text{H}_2\text{O})_2(\text{P}_2\text{O}_7)]$. Reprinted with permission from ref 171. Copyright 2012 Royal Society of Chemistry.

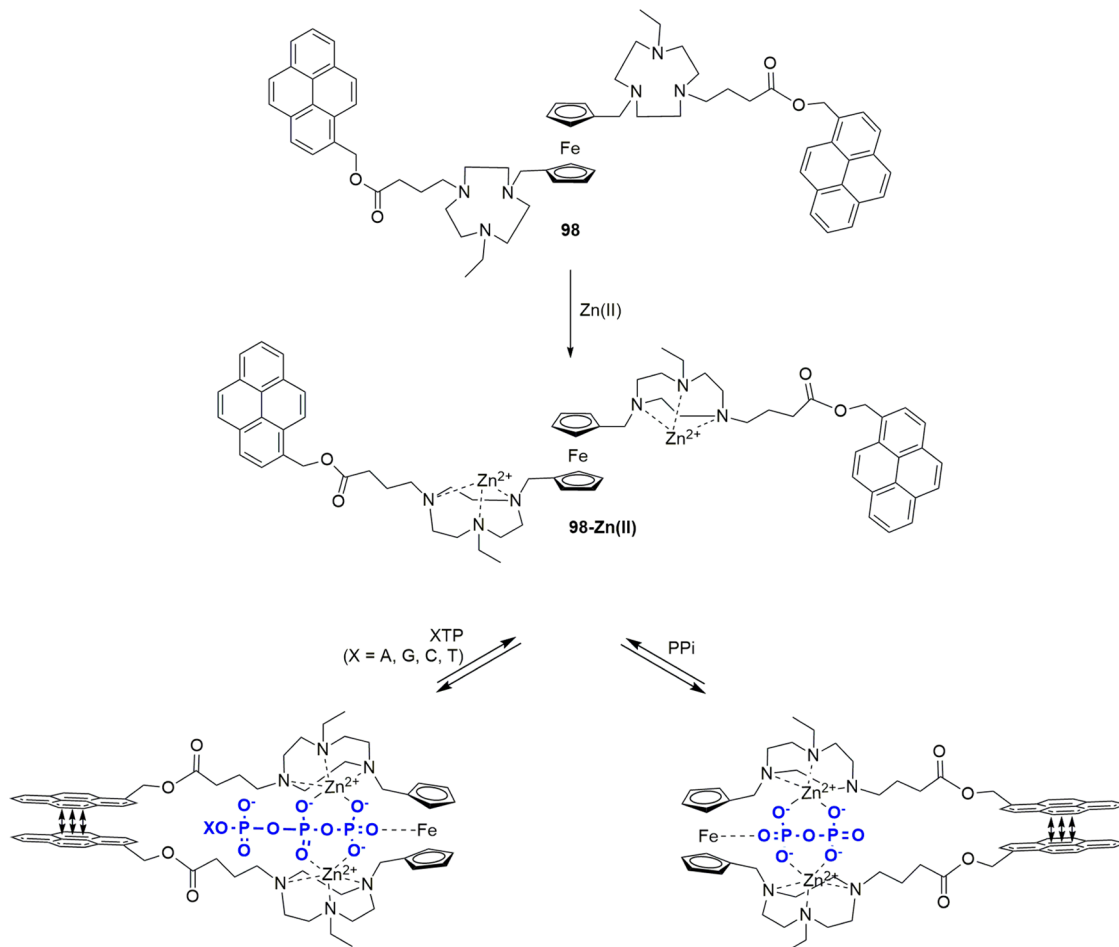
complexes. Bencini, Lippolis, and co-workers, for example, described the selective binding and sensing of diphosphate over mono- and triphosphate by a Zn(II) complex with a terpyridine-based receptor featuring two [9]aneN₃ units (**97**, Figure 20).¹⁷¹ Upon addition of 1 equiv of Zn(II) in water a significant enhancement of the fluorescence of **97** at 355 nm is observed. This luminescent Zn(II) complex is capable of sensing diphosphate in water at pH 7, as the anion causes a selective quenching of the fluorescence (Figure 20). This selectivity can be ascribed to the optimal spacial fit of this anion within the cleft between the two [9]aneN₃ units, generated by the ligand conformational change (from a trans-trans to a cis-cis conformation) upon Zn(II) coordination (Figure 20).

Another example of bis-[9]aneN₃-Zn(II) complex (**98**-Zn(II), Scheme 11) for polyphosphate nucleotide sensing has been proposed by Bond and Spiccia.¹⁷² In receptor **98** the two macrocyclic units are functionalized with fluorescent pyrene chromophores and are linked together by a ferrocene unit. In MeCN/Tris-HCl (1:9, v/v) in the absence of polyphosphate guest molecules, very weak excimer emission is observed, indicating that the two pyrene-bearing **98**-Zn(II) units are arranged in a trans-like configuration with respect to the

ferrocene bridging unit. Binding of a variety of polyphosphate anionic guests (PPi and nucleotide di- and triphosphates) promotes the interaction between pyrene units and results in an enhancement in excimer emission (Scheme 11).

An example of a Zn(II) complex with a pyridyl-based triazole-linked calix[4]arene for pyrophosphate over phosphate and ATP over ADP, AMP, and NP (β -naphthylphosphate) has been recently reported by Rao and co-workers.¹⁷³ Recently, Lu and collaborators demonstrated high selectivity achieved by the dinuclear Zn(II) complex of macrocycle **99** toward ATP and ADP.¹⁷⁴ Upon addition of ATP (or ADP) to a solution of the **99**-Zn₂(II) complex in water buffered at pH 7.4 an increase in the emission intensity at around 434 nm can be easily observed (Figure 21). DFT calculations suggest that the complex **99**-Zn₂(II) possesses recognition sites for both phosphate and adenine groups in ATP and ADP (Figure 21). Moreover, the sandwich-like binding mode between the two anthracene moieties of **99**-Zn₂(II) and a pair of adenine groups in ATP/ADP enhances the selectivity and affinity of the complex toward ATP/ADP. The authors demonstrated that the complex **99**-Zn₂(II) also allows the visualization of the ATP and ADP in living cells.

Scheme 11. Mechanism of Polyphosphate Sensing by 98



Zinc complexes with simple open-chain receptors have also been employed for phosphates recognition.¹⁷⁵ For example, Kuxami and co-workers have shown that the mononuclear Zn(II) complex of receptor **100** (Scheme 12) can selectively change its photophysical properties upon interaction with pyrophosphate in the presence of inorganic phosphates, halides, acetate, ATP, and other nucleotides in neutral aqueous solutions.¹⁷⁶ On gradual addition of Zn(II) ions to an aqueous solution of **100**, the absorbance of the free receptor at 408 nm decreases in intensity with a concomitant increase in absorbance intensity at 528 nm due to the formation of a 1:1 complex. The fluorescence of **100** is also switched on when the Zn(II) complex is formed in solution with an emission band at 475 nm. When a solution of **100**-Zn(II) is titrated with pyrophosphate the absorption intensity at 528 nm decreases along with formation of a new band at 630 nm associated with visible color change from pink to blue. Moreover, the emission band at 475 nm blue shifts to 428 nm, and an obvious fluorescence quenching at 475 nm occurs. Receptor **100** can be used to develop a molecule-based JK-latch function using Zn(II) and pyrophosphate ions as chemical inputs.

Other types of metal have been employed in the literature for phosphate recognition including Cu(II),^{155,177} Mn(II),¹⁷⁸ Mg(II),¹⁷⁹ or lanthanide complexes.¹⁸⁰ In particular Albrecht, Subramanian, and Mishra very recently described the phenanthroline-based chiral receptor **101** and its Eu(III) and Tb(III) complexes (Figure 22).¹⁸¹ The complexes show a red and green emission, respectively, in water buffered at pH 7.4. Upon the

addition of various anions (Figure 22) a selective quenching of the luminescence in the presence of dihydrogen phosphate is observed. Furthermore, the Tb(III) complex shows a very similar quenching behavior in the presence of the different nucleoside phosphates and can act as a “universal” luminescent probe for the total determination of the three nucleosides ATP, ADP, and AMP. When microalgal cells (*Chlorella vulgaris* CCNM 1017) are treated with the complexes **101**-Eu(III) or **101**-Tb(II) it is possible to monitor phosphate in the cell membranes.

Pope, Skabara, Faulkner, and co-workers combined lanthanide DO3A complexes and chromophores bound to the metal via carboxylate or phosphonate groups.¹⁸² Phosphate was found to displace carboxylate-bound chromophores from the metal, switching off the lanthanide centered emission.

2.1.4. Discrete Optical Sensors for Other Anions.

Although, as described in section 2.1.1, many examples of sensors for the selective recognition of fluoride have been reported in the literature, the number of sensors for the other halides is not so extensive. An example can be found in the work of Steed, Prodi, and co-workers, who reported an interesting receptor (**102**, Figure 23) which is able to sense chloride in MeCN, even though the system is not selective for this anion from a thermodynamic point of view.¹⁸³ Receptor **102** binds anions in a 2:1 anion:receptor stoichiometry, with stability constants much higher for dicarboxylates (such as malonate) than for chloride. However, only chloride causes significant changes in the emission properties of the receptor. The emission spectrum of **102** shows an emission band at ca. 400 nm attributed

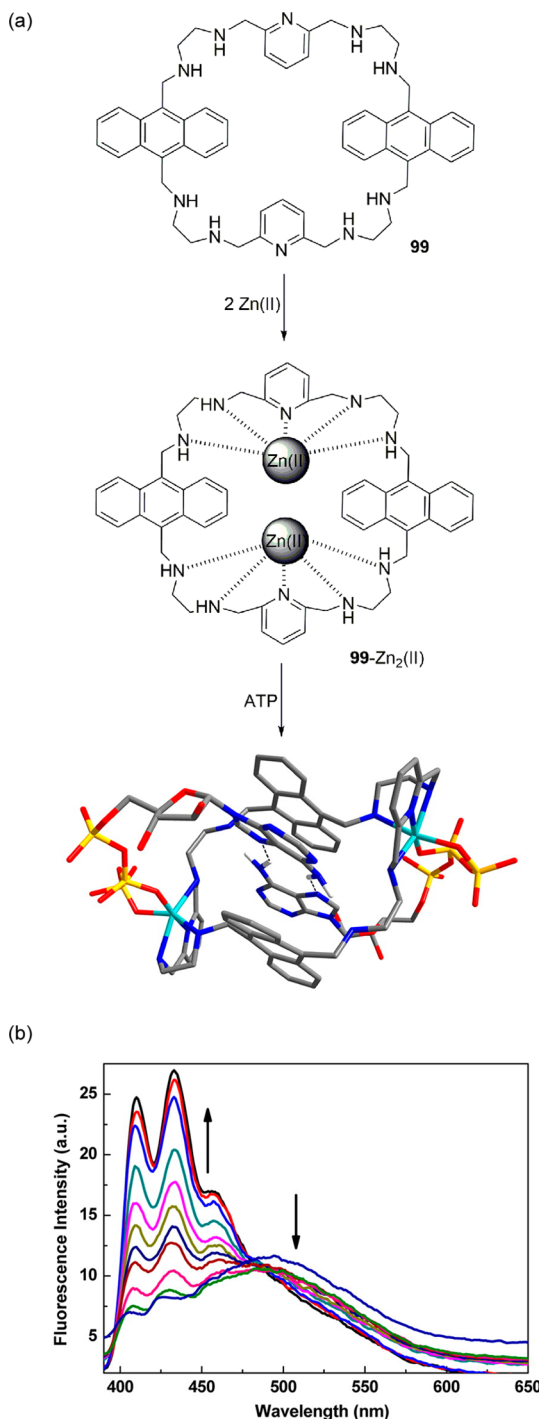


Figure 21. (a) Mechanism of ATP sensing by **99**, including the DFT energy-minimized structure of the ATP complex. (b) Fluorescence changes of **99** ($5 \mu\text{M}$) with the addition of various amounts of ATP ($0\text{--}5 \mu\text{M}$) in HEPES buffer. Reprinted with permission from ref 174. Copyright 2013 American Chemical Society.

to the pyrene monomer and an additional very weak and unstructured band in the $500\text{--}620 \text{ nm}$ region. As shown in Figure 23, an increase of the emission intensity of both the monomer and the excimer bands is observed upon the addition of chloride. In particular, on addition of fewer than 20 equiv of the anion, the spectrum shows an increase in intensity and a significant blue shift of the nonstructured, low-energy band. Upon addition of more equivalents of chloride, a further modest

increase of the intensity of this band occurs, concomitant with a red shift and an increase of the fluorescence of the monomeric form of pyrene. On the basis of DFT calculations, the authors suggest that only the binding of chloride anions in the cleft between the two pyridinium arms leads to a conformational change that brings the pyrenyl groups into close enough proximity to induce an increase in excimer emission. The other anions tested (acetate, malonate, succinate, Br^- , F^- , and HPO_4^{2-}) do not lead to a similar conformation, and no significant change in fluorescence is observed.

Another example of a chloride-selective fluorescent sensor has been reported by Johnson and Haley.¹⁸⁴ They demonstrated that the 2,6-ethynylpyridine bisphenylurea **103** containing electron-withdrawing pentafluorophenyl substituents is not emissive in MeCN in its unbound state, but in the presence of 1 equiv of chloride the fluorescence is switched on (Figure 24). On the other hand, compound **104** bearing a nitrophenyl substituent is not able to sense chloride.

Chifotides, Dunbar, and co-workers recently reported the first study of a neutral π -electron-deficient aromatic unit (**105**, Figure 25) that can exhibit both CT and anion- π interactions in solution and the solid state able to sense halides.¹⁸⁵ In the UV-vis solution studies, addition of a colorless solution of TBA X ($X^- = \text{I}^-, \text{Br}^-, \text{Cl}^-$) to a yellow solution of **105** in THF induces the spontaneous appearance of new intense absorption bands at 630, 419, or 408 nm, respectively, for I^- , Br^- , or Cl^- that progressively grow with increasing concentration of salt. These bands correspond to the electronic transitions from the HOMO of the electron donors to the low-lying LUMO of acceptor **105**.

Maeda and co-workers reported that compound **106** can function as a sensor for chloride.¹⁸⁶ Conformational changes by flipping of two pyrrole rings as a result of anion binding can control the chiroptical properties of the receptors. In particular, as shown in Figure 26, changes in the UV-vis, CD (circular dichroism), emission, and CPL (circular polarized luminescence) spectra of **106** can be observed in the presence of chloride in dichloromethane. The presence of chloride can also be detected by the naked eye.

Various examples have been reported in the literature for iodide recognition.^{187–189} Iodide plays an important role in several biological processes such as neurological activity and thyroid function. Very recently, Mahulikar, Patil, and co-workers synthesized an Imatinib (a derivative of 2-phenylamino-pyrimidine used as an anticancer drug and tyrosine kinase inhibitor) intermediate **107** (Figure 27) for iodide recognition in MeCN/H₂O (4:6, v/v). Addition of iodide to a solution of **107** resulted in a remarkable spectroscopic response in the form of a new intense peak in the absorption spectrum at 232 nm with a detection limit of $0.22 \mu\text{M}$.¹⁹⁰

Alkyl halides are extremely useful reagents for organic synthesis but, due to their high reactivity, can be potentially toxic/mutagenic as they can react with numerous biological nucleophiles present in living organisms. Bull, Fossey, and co-workers recently reported that N-alkylation with MeI, for example, of the pyridine sensor **108** causes the formation of a pyridinium salt such as **108a**.¹⁹¹ Compound **108a** is stabilized by cation- π interactions that cause the formation of an emission band at 400 nm upon excitation at 260 nm in dichloromethane, as shown in Figure 28. Interestingly, the fluorescent response of the *N*-alkylpyridinium triflate salt was 2.3 times greater than the corresponding iodide salt **108a**, probably because of the known heavy atom quenching effect of the iodide counterion.¹⁹² The response in terms of increase of the fluorescence is immediate for

Scheme 12. Pyrophosphate Sensing by Mononuclear Complex 100–Zn(II)

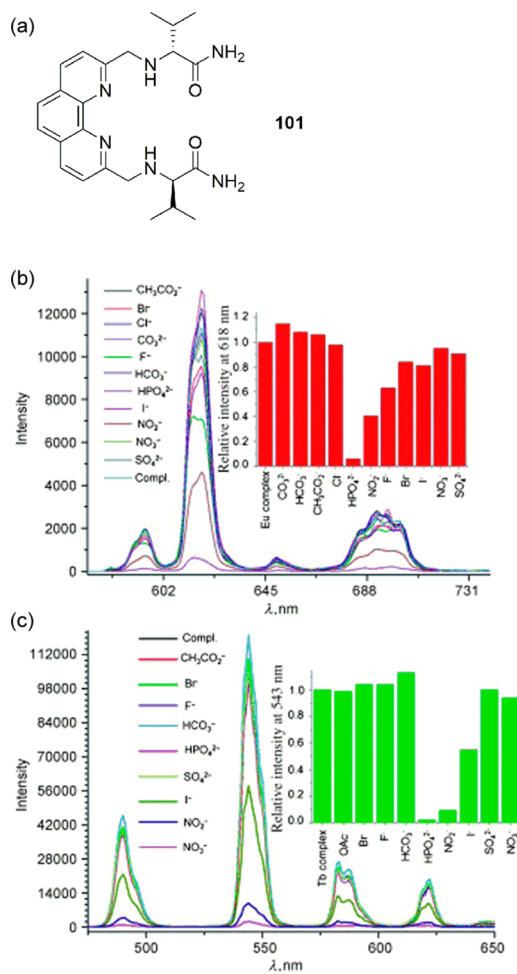
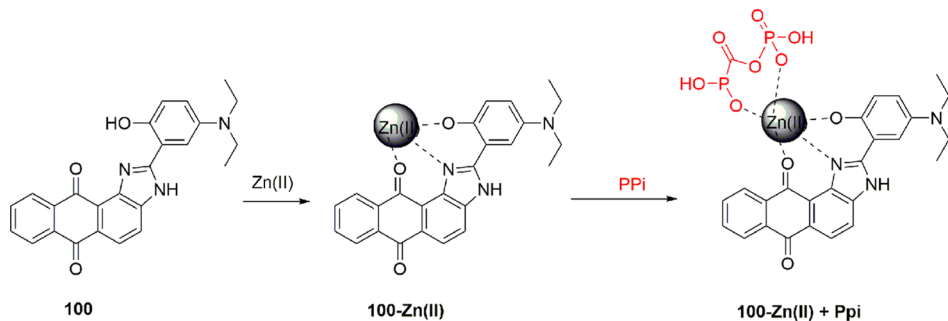


Figure 22. Sensing of H_2PO_4^- and nucleosides by Eu(III) and Tb(III) complexes of 101. (a) Structure of 101. (b) Emission spectra ($\lambda_{\text{exc}} = 276 \text{ nm}$) of 101–Eu(II) ($2 \times 10^{-5} \text{ M}$), and bar diagram (inset) showing relative intensities of the emission peak at $\lambda = 614 \text{ nm}$. (c) Emission spectra ($\lambda_{\text{exc}} = 278 \text{ nm}$) of 101–Tb(III) ($5 \times 10^{-6} \text{ M}$), and bar diagram (inset) showing relative intensities of the emission peak at $\lambda = 544 \text{ nm}$. Reprinted with permission from ref 181. Copyright 2014 Wiley-VCH.

alkyl triflates or alkyl iodides, while it is longer (hours) for bromide compounds.

Carboxylates also form a large class of anions with various functions and uses, and a number of examples of carboxylate sensors will therefore be briefly discussed, from simple mono- and bis-carboxylates to more complex higher order carboxylates. Beer and co-workers reported that simple preorganized indolo-[2,3-*a*]carbazole derivative 109 (Figure 29a) is able to bind

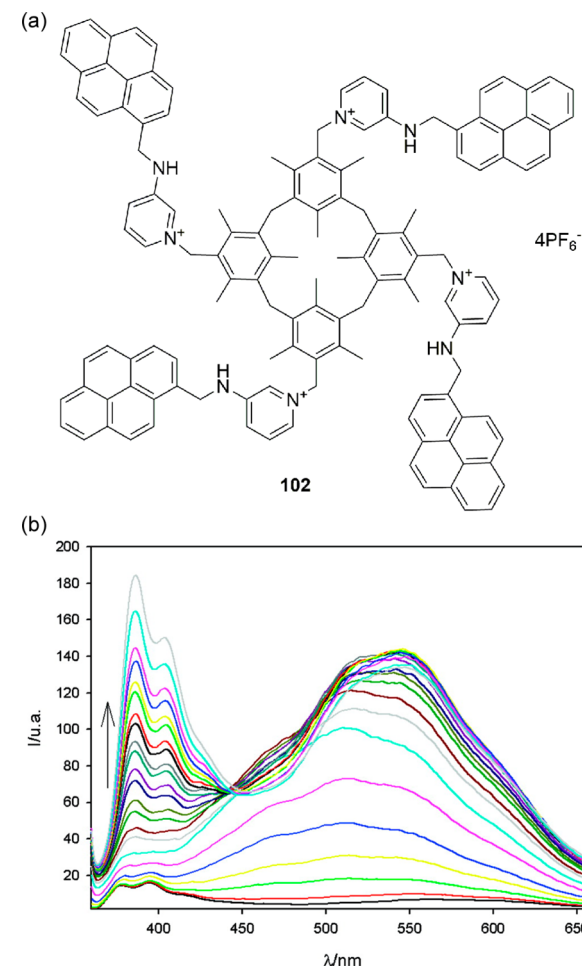
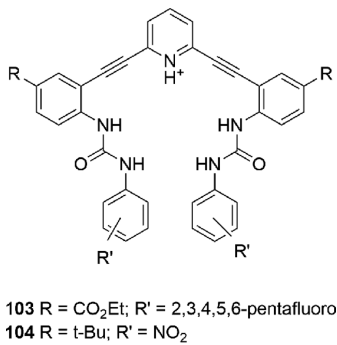
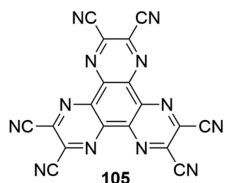
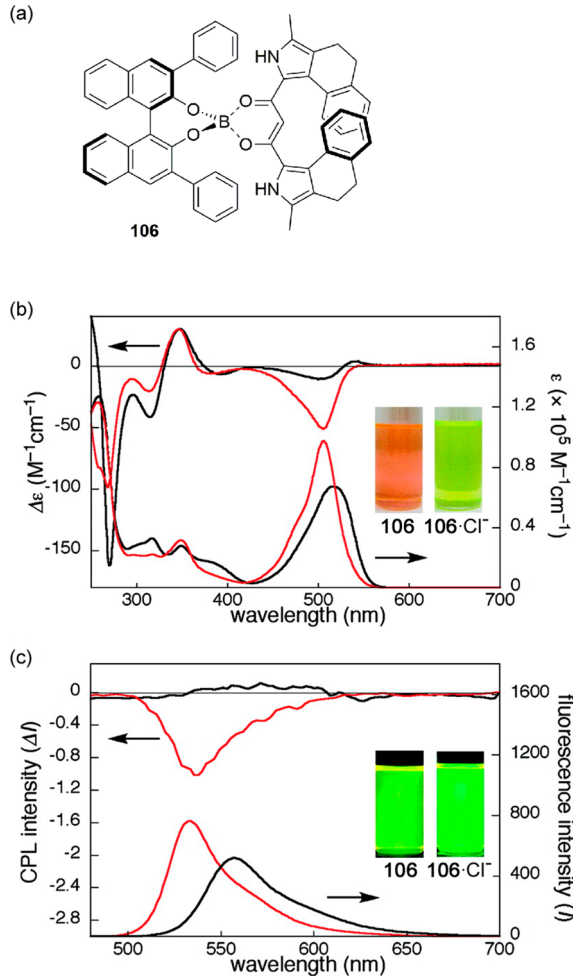
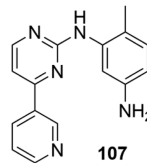
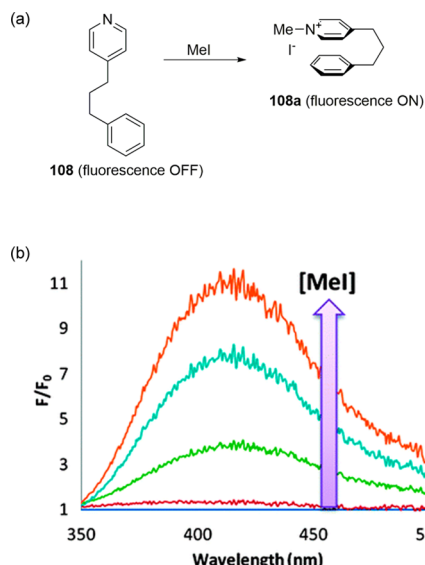
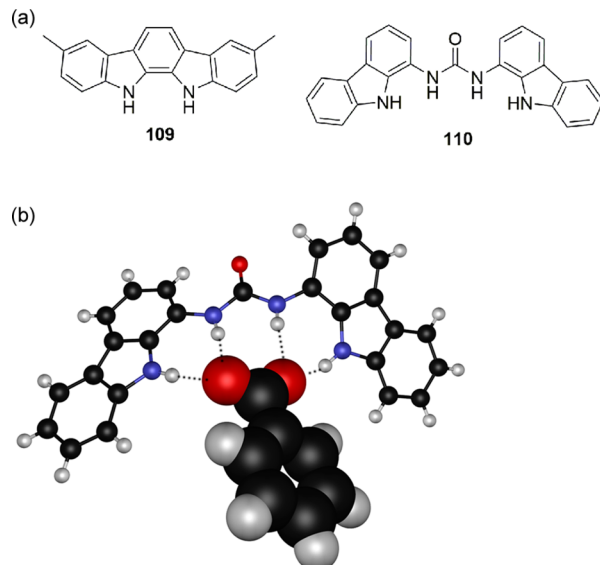


Figure 23. (a) Structure of 102 and (b) changes in its emission properties ($\lambda_{\text{exc}} = 343 \text{ nm}$) upon the addition of chloride in MeCN. Reprinted with permission from ref 183. Copyright 2008 American Chemical Society.

benzoate with a stability constant of $\log K_a = 5.4$ in acetone.¹⁹³ The binding event causes a quenching in the fluorescence of 109, while fluoride and chloride cause a significant enhancement in the emission of the receptor. Similarly, Gale and co-workers have shown that the dicarbazolyl urea 110 (Figure 29a) can sense BzO^- in DMSO/0.5% H_2O via fluorescence quenching.¹⁹⁴ The authors also reported the crystal structure of the 1:1 complex between 110 and this anion in which each anion is bound to the four hydrogen bonds (Figure 29b).

A calix[4]arene-based amide receptor (111) with anthracene as fluorophore that functions as a fluorescence sensor for acetate

**Figure 24.** Structures of **103** and **104**.**Figure 25.** Structure of **105**.**Figure 26.** (a) Structure of **106**; (b) changes in the UV-vis (bottom) or CD (top) spectra of **106** in dichloromethane in the presence of an excess of chloride; (c) changes in the emission (bottom) and CPL (top) spectra of **106** in dichloromethane in the presence of an excess of chloride. Reprinted with permission from ref 186. Copyright 2011 American Chemical Society.**Figure 27.** Structure of iodide sensor **107**.**Figure 28.** (a) Mechanism of MeI sensing by **108**. (b) Changes in the fluorescence of **108** upon addition of MeI in CH₂Cl₂ ($\lambda_{\text{ex}} = 260 \text{ nm}$). Reprinted with permission from ref 191. Copyright 2011 Royal Society of Chemistry.**Figure 29.** (a) Structures of benzoate sensors **109** and **110**. (b) X-ray crystal structure of **110** with BzO⁻. TBA counterions are omitted for clarity. The sensor is shown in ball-and-stick representation with the bound anion in space fill (0.6 times the van der Waals radius), and the atoms are color coded as follows: C (black), N (blue), O (red), H (white).

via a PET mechanism in MeCN has been reported by Chen, Wang, and co-workers (Figure 30).¹⁹⁵ The authors proposed that coordination with acetate involves the amide NHs and the 9-H of anthracene.

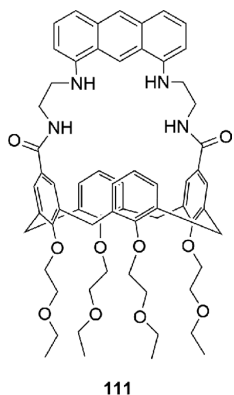


Figure 30. Structure of 111.

A very interesting example of a fluorescent sensor for the dicarboxylate anion maleate over fumarate has been reported by Costero and co-workers.¹⁹⁶ The interest in selective sensors able to distinguish maleate vs fumarate is not only related to *p*-diastereomer recognition but also due to the different biological behavior of these anions. In fact, whereas fumarate is generated in the Krebs cycle, maleate is an inhibitor of this cycle and involved in a number of kidney diseases.¹⁹⁷ As shown in Figure 31a, compound 112 is a thiourea derivative of cyclohexane functionalized with two naphthyl moieties. Fluorescence studies showed that 112 presents an emission band at 410 nm ($\lambda_{\text{ex}} = 290 \text{ nm}$) in DMSO. Upon addition of increasing amounts of fumarate (113, Figure 31b) only a small amount of quenching is observed. Interestingly, when maleate (114, Figure 31c) is added to a solution of 112, a new band at 495 nm is observed. The authors ascribed this new band to the formation of an excimer between the two naphthalene moieties. Indeed, the cis disposition of maleate induces a change in the conformation of the receptor, bringing the two naphthalene groups in close proximity and in an almost parallel disposition so that excimer emission is possible. On the other hand, fumarate with a trans disposition of the carboxylate moieties is unable to form the 1:1 complex, and two molecules are bound to the ligand, one in each thiourea group, and thus, the naphthalene moieties are not able to interact.

Among biologically relevant dicarboxylates, mandelate plays an important role. L-Mandelic acid is a metabolite of phenylalanine in mammalian cells. When the hydroxylation of phenylalanine to tyrosine is defective, for example, in phenylketonuria (PKU), L-mandelic acid is metabolized by alternative pathways in which mandelate is produced. Therefore, the synthesis of enantioselective receptors for the mandelate anion has attracted considerable interest. In particular, Chan and co-workers reported a chiral fluorescent receptor based on cholic acid bearing two pyrene moieties as signaling units (115, Figure 32).¹⁹⁸ Compound 115 shows two bands ascribable to monomer and excimer emission in MeCN. Upon addition of increasing amounts of S-mandelate a decrease in intensity of both bands is observed (quenching of 20% and 30% for the monomer and the excimer, respectively), while the enantiomer D-mandalate causes a quenching of only 5%. The same authors also reported a similar system able to sense long-chain carboxylates.¹⁹⁹

Tartaric acid is a dicarboxylic acid that is a common natural product present in wines and other grape-derived beverages. The structure of tartaric acid (116, Figure 33a) makes it quite attractive for complexation by synthetic sensors since it is relatively small while still possessing several functional groups for

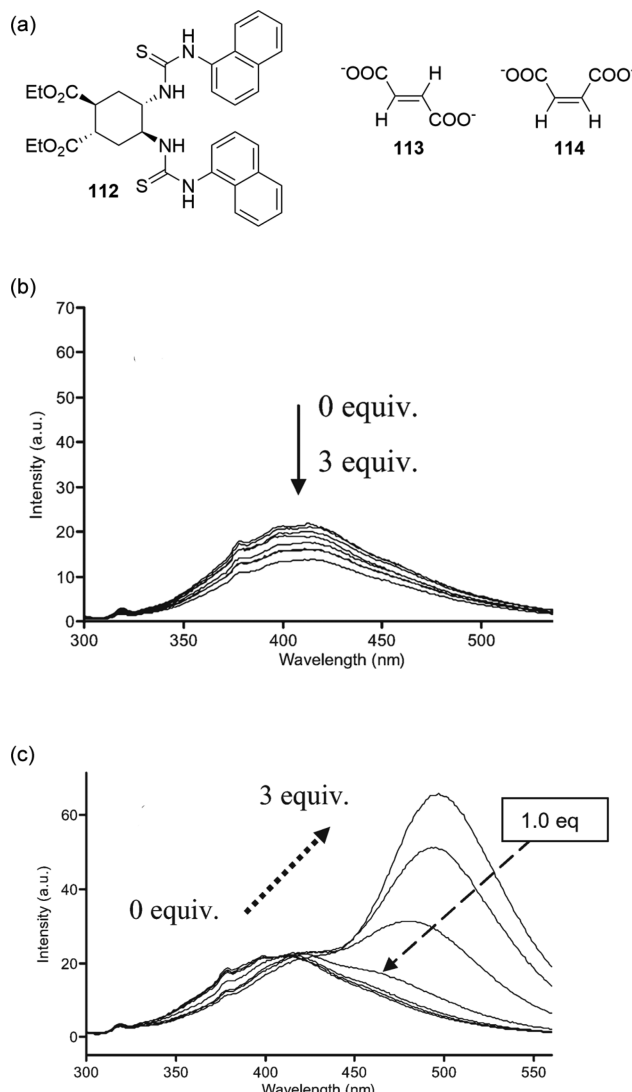


Figure 31. (a) Structure of compound 112, and (b and c) changes in its emission upon addition of fumarate (b) or maleate (c) in DMSO. Reprinted with permission from ref 196. Copyright 2006 Royal Society of Chemistry.

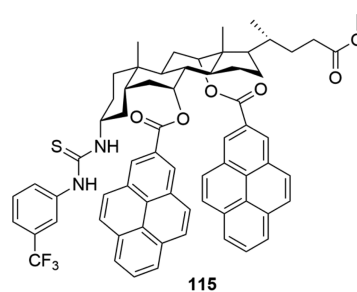


Figure 32. Structure of 115.

binding interaction.²⁰⁰ Bencini, Lippolis, Pasini, and collaborators recently reported that the chiral ditopic polyammonium receptor (117, Figure 33a), featuring two [9]aneN₃ moieties separated by a (S)-BINOL linker, is able to selectively bind and sense (S,S)-tartaric acid over its (R,R)/mesoforms and also over (S)/(R)-malate, succinate, maleate, fumarate, and (S)/(R)-lactate in water (Figure 33b).²⁰¹ Addition of increasing amounts of this anion to a solution of 117 at pH 7 (TRIS buffer) leads to a

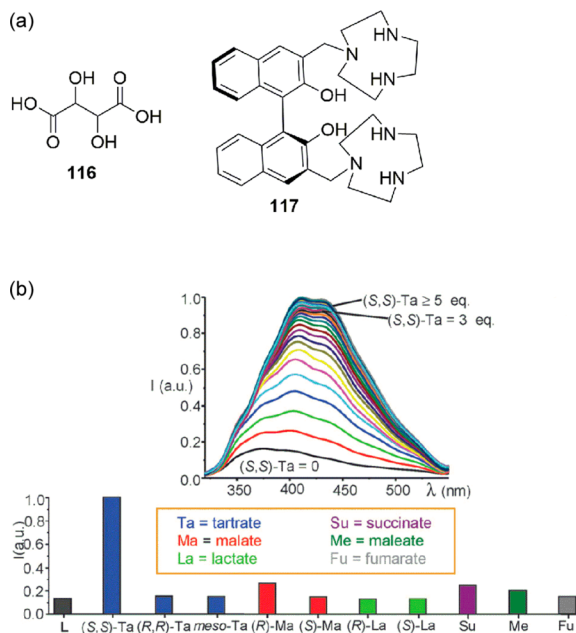


Figure 33. (a) Structures of **116** and **117**. (b) Changes in the emission of **117** at pH 7 upon the addition of (*S,S*)-tartrate (top) and selectivity over other carboxylates (bottom, 10 equiv of each anion added). Reprinted with permission from ref 201. Copyright 2012 Royal Society of Chemistry.

progressive red shift of the typical band of BINOL at 370 nm, accompanied by a marked increase in the emission intensity at 420 nm (Figure 33b), accounting for deprotonation of the $-\text{OH}$ groups in the BINOL unit.

Sensors for the recognition of long-chain carboxylates/multicarboxylates^{202,203} or amino acids^{204–207} have also been reported. Wolfbeis and co-workers, for example, reported on the selective sensing in water of the tris-carboxylate citrate by a europium(III)–tetracycline complex.²⁰⁸ The authors postulate that the citrate anions function as a polydentate ligand for europium and displace the water molecules that occupy the eight to nine coordination sites of the Eu^{3+} ion, thereby leading to an increase in fluorescence intensity. Interestingly, a number of common interferents, including some of the other intermediates of the citric acid cycle (isocitrate, α -ketoglutarate, succinate, fumarate, L-malate, and oxaloacetate), were also investigated and found not to induce as large an increase in fluorescence as citrate.

Parker and co-workers developed a series of luminescent europium(III) complexes for the detection of lactate and citrate in biological fluids.²⁰⁹ Complexation of these carboxylates leads to reversible displacement of water molecules bound to the europium center which modulates the luminescence of the metal (in terms of lifetime and spectral form of the luminescence). This approach was used to measure citrate in prostate fluid as a test for prostate adenocarcinoma.

Developing effective probes for nitrate recognition and sensing is highly desirable because of its multiple sources of contamination from nuclear waste, industrial sewage, acid rain, fertilizers, and chemicals disposals. However, nitrate sensing is particularly challenging due to the low basicity of this anion and its high hydration energy. One of the few examples of a fluorescent sensor for nitrate recognition is the tripododal receptor **118** (Figure 34) functionalized with three dansyl moieties.²¹⁰ Upon protonation, **118** adopts in situ a cone-shaped conformation through hydrogen-bonding and C–H \cdots π inter-

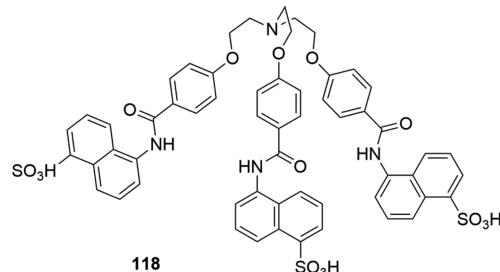


Figure 34. Structure of **118**.

actions. The protonation-induced interior preorganized cavity is capable of entrapping nitrate anions through the amide N–H bonds to form discrete nitrate complexes. Moreover, the presence of the dansyl groups which can be easily deprotonated permits the formation of a zwitterionic species. Nitrate sensing is achieved in $\text{DMSO}/\text{H}_2\text{O}$ (80:20, v/v) by the quenching of the fluorescent emission of **118**.

The sulfide anion is a toxic pollutant that is widespread in the environment due to various industrial processes and biological metabolism, but few examples of sulfide sensors have been reported in the literature.^{211–213} One example has been reported by Li, Yu, and co-workers, who exploited the reaction of formation of CuS and demonstrated that the luminescence of the copper complex of receptor **119** (Figure 35) can be switched on by sulfide anions in water at pH 7.4.

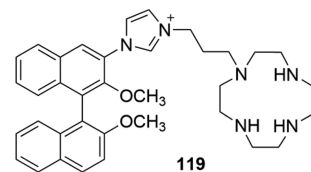
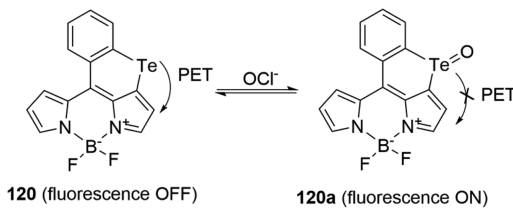


Figure 35. Structure of **119**.

Molecular probes are currently also essential in efforts to understand the presence and concentration of analytes such as reactive oxygen species (ROS) in biological systems. These species are thought to play an important role in various diseases such as diabetes, cancer, and neurodegenerative diseases. Among ROS, hypochlorous acid (HOCl) is a potential antimicrobial agent that plays a significant role in the immune system. However, its excess production can also lead to diseases such as lung injury, atherosclerosis, rheumatoid arthritis, and cardiovascular diseases. Very recently, Churchill and co-workers reported the new BODIPY telluride sensor **120** which is able to sense hypochlorite in water through an oxidation mechanism (Scheme 13).²¹⁴ Compound **120** is highly sensitive and selective (detection limit 3.7 μM) for hypochlorite over other ROS

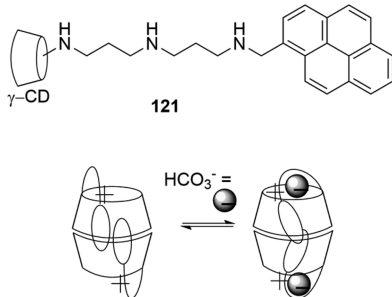
Scheme 13. Mechanism of Sensing of Hypochlorite in Sensor **120**



under physiologically relevant conditions ($\text{H}_2\text{O}/\text{EtOH}$ (99:1, v/v), 0.1 M PBS, pH 7.5).

Among oxo anions bicarbonate plays a crucial role in biological systems. Suzuki and co-workers synthesized a γ -cyclodextrin (CD) derivative **121** in which a triamine linker connects a pyrene residue to a γ -CD (Scheme 13).²¹⁵ At pH 8.6 **121** exhibits the typical fluorescence emission of pyrene around 370–400 nm with a strong excimer emission at 475 nm due to the formation of a dimer of two units of **121** causing a π – π interaction with two pyrene moieties in a parallel conformation (Scheme 14). In the

Scheme 14. Proposed Mechanism of Bicarbonate Sensing by Compound **121**



presence of bicarbonate a new fluorescence band centered at 425 nm appears. The changes observed in the fluorescence properties of the association dimer of **121** were ascribed by the authors to a change in the relative position of the pyrene rings of the dimer that pass from a parallel conformation to a twisted and imperfectly stacked conformation as bicarbonate binds to the protonated ammonium strap between the cyclodextrin and the pyrene unit (Scheme 13).

Glutathione (GSH) is the most abundant cellular thiol and plays an important role in maintaining the appropriate redox status of biological systems along with cysteine (Cys) and homocysteine (Hcy). Discrimination between GSH, Cys and Hcy is therefore an important challenge. A ratiometric fluorescent sensor for highly selective detection of GSH over Cys and Hcy based on monochlorinated BODIPY derivative (**122**) has been described by Yang and co-workers.²¹⁶ As shown in Figure 36, thiols such as GSH, Cys, and Hcy displace the chlorine by thiol–halogen nucleophilic substitution resulting in a significant red shift of the fluorescence emission of the receptor (Figure 36). The amino groups of Cys/Hcy, but not GSH, further displace the sulfur to form an amino-substituted BODIPY, which exhibits relatively weak, blue-shifted fluorescence. This allows GSH to be distinguished from Cys/Hcy. Interestingly, the same authors reported a similar BODIPY derivative able to sense Cys over GSH and Hcy.²⁰⁵

In the past decade, sensors for the recognition of other anions, such as sulfate²¹⁷ and heparin,^{218–221} have been developed. Readers can refer to more specialized reviews to find examples of sensors for other anions (e.g., David K. Smith and co-workers recently reviewed heparin sensing).²²²

2.2. Assemblies for Optical Sensing of Anions

The selective recognition of anions in protic solvents is more challenging than in aprotic solvents and therefore often requires the construction of more elaborate sensors, including the development of multicomponent systems, three-dimensional receptors, and nanoassemblies. In the next section various examples of these systems will be described.

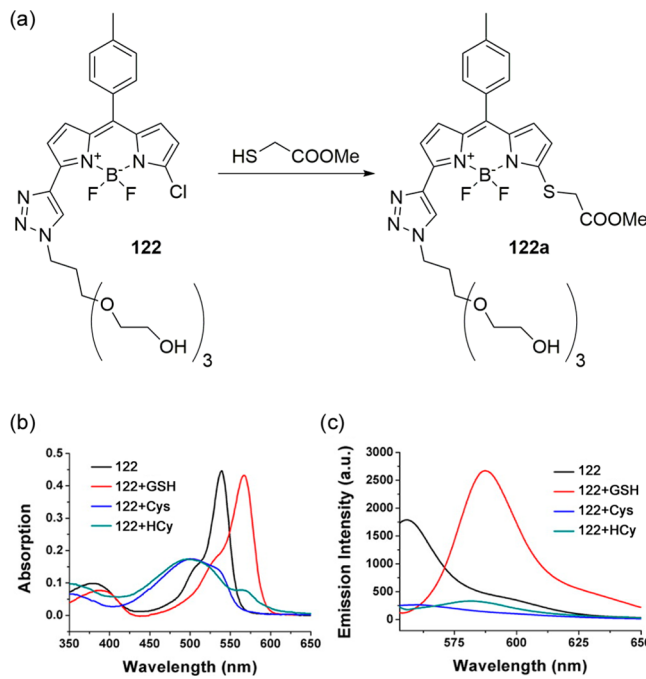


Figure 36. (a) Mechanism of thiol sensing by **122**, and changes in the absorption (b) and emission (c) spectra of **122** upon addition of GSH, Cys, and Hcy. Reprinted with permission from ref 216. Copyright 2012 American Chemical Society.

2.2.1. Dye Displacement Assays for Anion Sensing. The dye displacement assay or indicator displacement assay (IDA) has become a common approach for the development of anion sensors. As shown in Figure 37, the receptor (or binding site) is

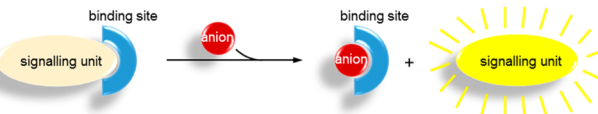
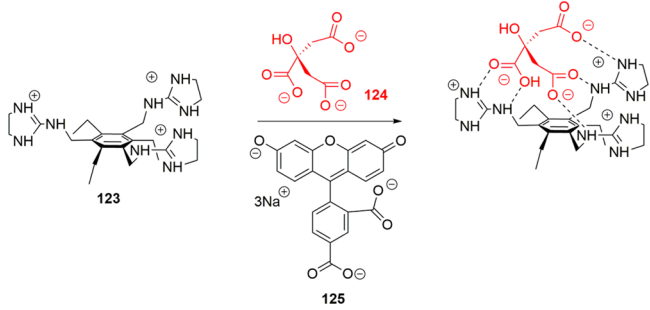


Figure 37. Schematic representation of the dye displacement assay mechanism.

able to bind an anionic guest or a signaling unit (a fluorescent or colored dye). The photophysical properties of the bound dye should be different from those of the free dye. When the signaling unit is displaced from the receptor (the coordination complex between the two is called a molecular ensemble) by the presence of the anionic substrate and released in solution, the anion–receptor binding event is sensed by the changes in the fluorescence or in the color of the dye in free solution. To design an efficient sensing system, the stability constant for the formation of the complex between the binding site and the signalling unit should be lower than that between the anionic analyte and the binding site. This approach provides advantages, for example it is possible to use a great variety of signalling units, as they are non-covalently attached to the binding site so obviating the need for further functionalization. This approach works well in both organic and aqueous solvent regimes allowing the possibility of tuning the solvent medium in order to obtain optimum K_a values for the signalling subunit and the analyte with the receptor.²²³

This approach to anion sensing was pioneered by Anslyn and co-workers, who developed an assay for citrate (**124**, Scheme 15), employing an ensemble of receptor **123** as binding site and

Scheme 15. Dye Displacement Assay Reported by Anslyn for Citrate Recognition



5-carboxyfluorescein (**125**) as signaling unit.²²⁴ Receptor **123** features three guanidinium groups preorganized on the same face of the phenyl ring due to steric interaction with the ethyl groups in the 2, 4, and 6 positions of the central ring and provides a network of hydrogen-bond donor groups and ionic sites for interaction with the substrate. In H₂O/MeOH (25:75, v/v) buffered at pH 7.4 the binding constant of the ensemble **123**–**125** is 4.7×10^3 M, while the binding constant of **123** and **124** is 2.9×10^5 M. This ensures that addition of citrate causes a displacement of the dye and hence an increase in emission. The assay can be used to determine citrate in soft drinks and sport drinks.

Another example of dye displacement assay reported by Anslyn and collaborators consists of a colorimetric boronic-acid-based sensing ensemble for carboxy- and phosphosugars.²²⁵ The cadmium-centered tris-boronic acid receptor (**126**, Figure 38) is

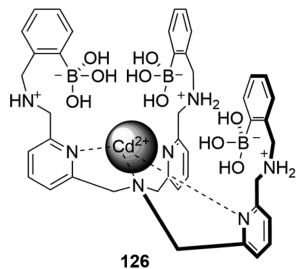


Figure 38. Structure of Cd²⁺ complex **126** used in the IDA for carboxy- and phosphosugar sensing.

able to bind to various carboxy- and phosphosugars in aqueous solution (MeOH/H₂O 3:1, v/v). Using an indicator displacement assay, a color change of pyrocatechol violet was observed upon addition of anionic sugars. This colorimetric test was used as a facile screening technique to qualitatively analyze guest affinities.

Costa and collaborators described an IDA based on squaramide receptor **127** (Figure 39) and two acid–base indicators, i.e., Red Cresol (RC) and Bromocresol Green (BG). Upon addition of various anions (F[−], Cl[−], Br[−], I[−], NO₃[−], NO₂[−], HCO₃[−]) in EtOH/H₂O (9:1, v/v) only phosphate and sulfate (**127**-RC) or only sulfate (**127**-BG) causes a color change in solution, enabling the sensing of these two anions (Figure 39).²²⁶

More recently Sessler, Lee, and co-workers reported an interesting IDA for the selective fluorescent sensing of hydrogenpyrophosphate in acetonitrile. This system consists of bis-pyridinium calix[4]pyrrole derivative **128** as a binding unit and tetrabutylammonium-2-oxo-4-(trifluoromethyl)-2H-chro-

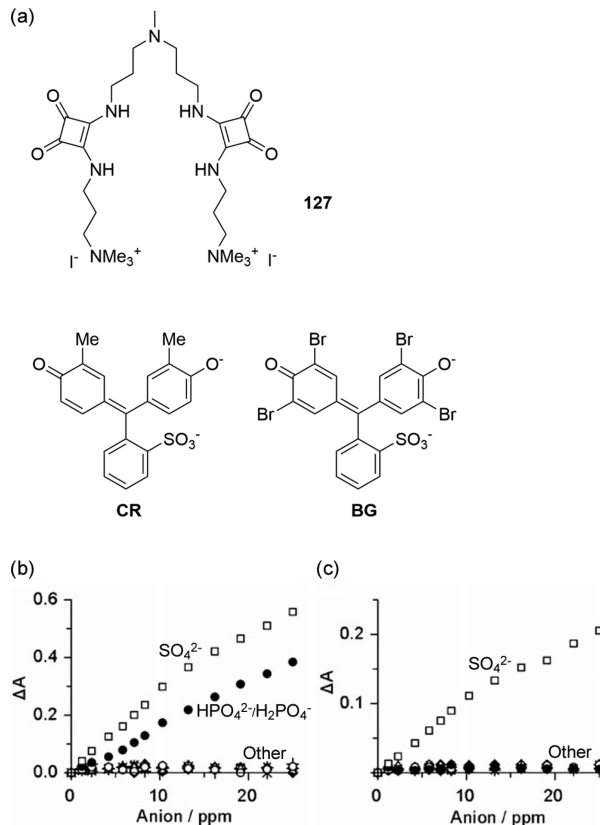


Figure 39. (a) Structures of **127**, Red Cresol (RC), and Bromocresol Green (BG). (b and c) Changes in the absorbance at 580 nm of the **127**-CR (b) and **127**-BG (c) ensembles upon addition of various anions in EtOH/H₂O (9:1, v/v). Reprinted with permission from ref 226. Copyright 2008 Royal Society of Chemistry.

men-7-olate (**129**) as a fluorescent signaling unit.²²⁷ As shown in Scheme 16, upon addition of hydrogen pyrophosphate displacement of the dye occurs and an increase in the fluorescence emission at 410 nm can be observed. The presence of the anion can also be detected by the naked eye (Scheme 16).

Another example of pyrophosphate sensing based on the same principle which is able to sense this anion in aqueous solution has been reported by Jolliffe and co-workers. The bis[zinc(II)-dipicolylamine]-functionalized linear peptide **130** can bind to pyrocatechol violet **131**.²²⁸ By monitoring the decrease in the absorbance of the **130**–**131** ensemble at 646 nm (Figure 40) the sensing of pyrophosphate over other anions (ATP, ADP, AMP, cAMP, p-threonine, citrate, sulfate, and hydrogen phosphate) in buffered saline solution (pH 7.4, 5 mM HEPES, 145 mM NaCl) was achieved.

Very recently, Mateus, Delgado, and co-workers reported that the hexaaza cryptand **132** can sense sulfate in H₂O/MeOH (50:50, v/v) at pH 4 via an IDA strategy.²²⁹ As shown in Scheme 17, **132** can form a chemosensing ensemble with alizarin red S (AR). At pH 4 AR is protonated and exhibits a yellow color. In the presence of **132** the pK_a of AR is lowered and the dye is deprotonated, binds to the receptor, and changes color with the maximum absorption shifting from 420 nm for AR in the free state to 510 nm for AR in the bound state. Upon addition of sulfate AR is displaced, the absorption band at 510 nm decreases, and the color of the solution turns orange (not completely yellow because under the conditions used the indicator is not fully displaced).

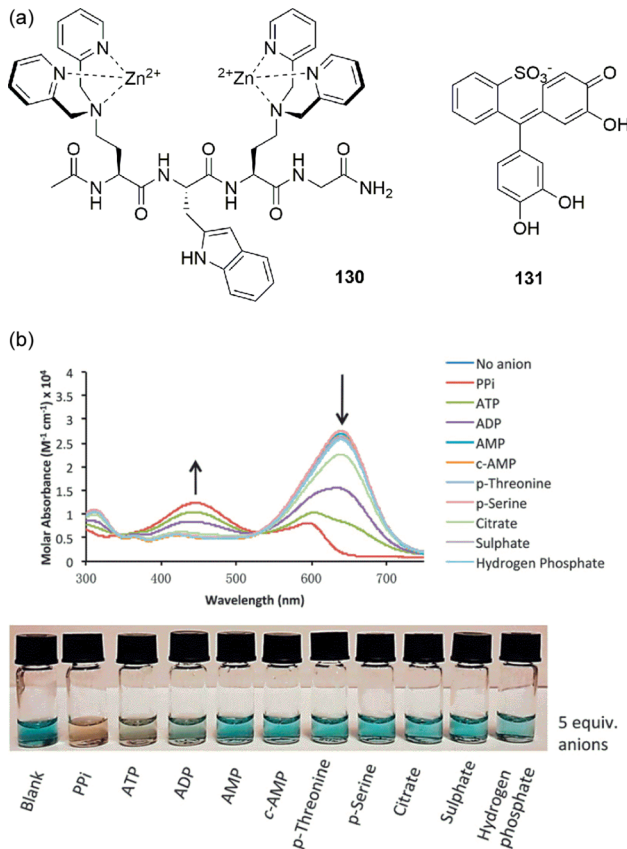
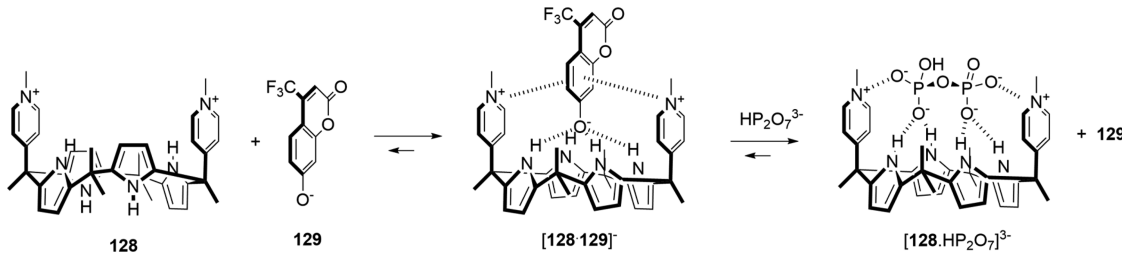
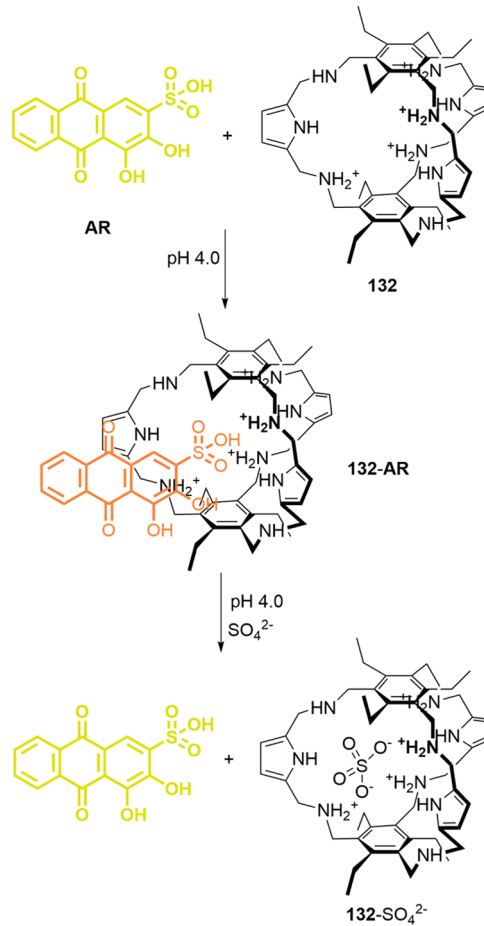
Scheme 16. IDA for $\text{HP}_2\text{O}_7^{3-}$ Based on Bis-pyridinium Calix[4]pyrrole Derivative 128 and Fluorophore 129

Figure 40. (a) Structures of receptor 130 and pyrocatechol violet 131. (b) Changes in absorbance and color of the 130–131 ensemble upon the addition of 5 equiv of anion. Reprinted with permission from ref 228. Copyright 2013 Royal Society of Chemistry.

Recently, taking inspiration from the original principle of Anslyn's IDA, new approaches to the design of displacement assays have been reported. For example, Schiller and co-workers reported an example of an allosteric indicator displacement assay (AIDA) for cyanide in water at pH 7.20.²³⁰ The system consists of the enzyme β -glucosidase and a boronic-acid-appended viologen (133) together with a fluorescent reporter dye (HPTS). As shown in Figure 41a, β -glucosidase degrades the cyanogenic glycoside amygdalin into hydrogen cyanide, glucose, and benzaldehyde. The released cyanide binds at the allosteric site of the receptor (boronic acid) and induces a change in the affinity of a formerly bound fluorescent indicator dye at the other side of the receptor. The generation of an anionic boronate displaces the HPTS molecule, which is responsible for the fluorescence enhancement (Figure 41b).

One of the disadvantages of the IDA is the low sensitivity due to the excess of the dye used. To overcome this drawback,

Scheme 17. IDA for SO_4^{2-} Based on the Hexaaza Cryptand 132 and the Dye Alizarin Red S (AR)

Anzenbacher and co-workers developed an intramolecular indicator displacement assay (IIDA).²³¹ As shown in Figure 42, the sensor comprises a receptor and a spacer with an attached anionic chromophore (dye). In the resting state, the anionic dye is bound by the receptor, and then the anionic analyte can compete for binding into the receptor. The photophysical properties of the dye change when it is displaced by the anionic analyte. The sensor may be regenerated by washing away the analyte to re-establish the dye–receptor complex. In this way a 1:1 ratio between the receptor and the indicator is enough, which endows the assay with high sensitivity and an instant reversibility.

The IIDA developed by Anzenbacher is based on receptor 134 (Figure 43), which features thiourea and amide groups as anion recognition moieties, naphthyl carboxylate as an anionic chromophore, and two naphthalimide moieties to generate bright fluorescence.²³¹ In DMSO/H₂O (95:5, v/v) the

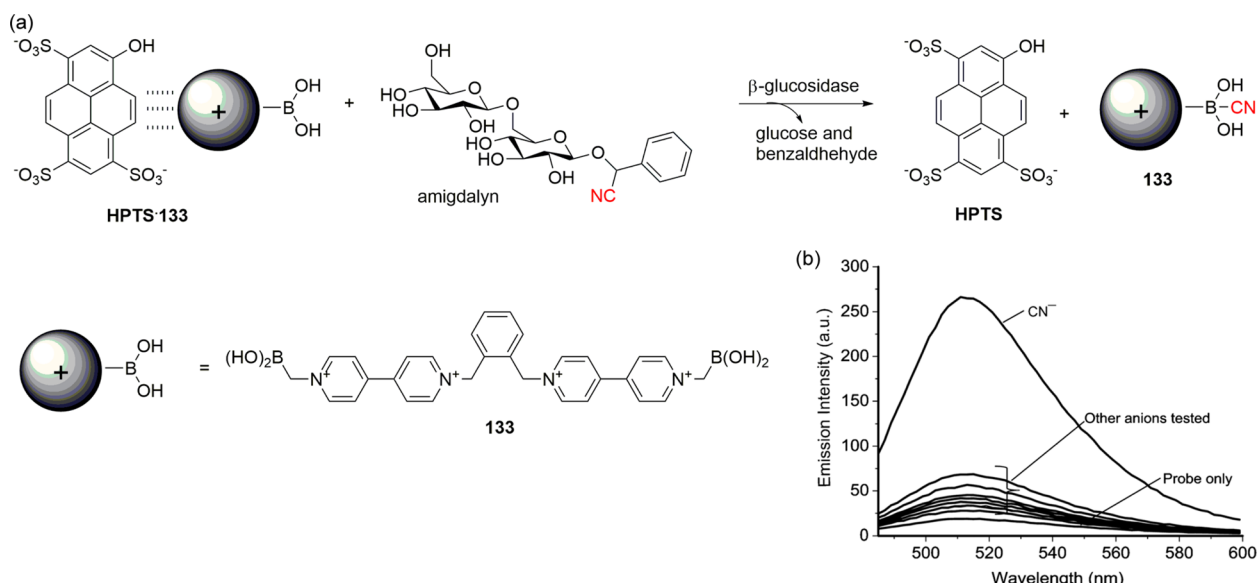


Figure 41. (a) Working principle of cyanide detection from amygdalin by an allosteric indicator displacement enzyme assay (AIDA) based on 133 and fluorophore HPTS. (b) Changes in the emission of the AIDA upon addition of cyanide in water at pH 7.20. Reprinted with permission from ref 230. Copyright 2013 Wiley-VCH.

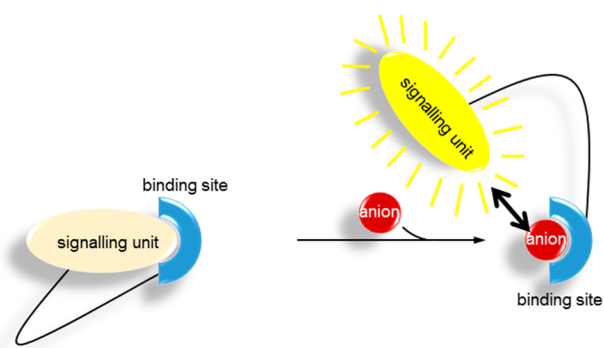


Figure 42. Schematic representation of the intramolecular indicator displacement assay mechanism.

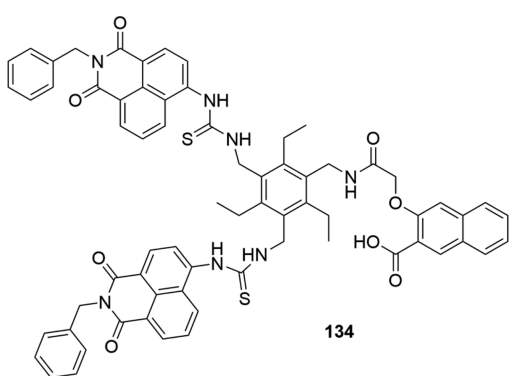


Figure 43. Structure of 134 designed as an intramolecular indicator displacement assay (IIIDA).

fluorescence arising from the naphthalimide groups of 134 increases with increasing anion concentration. The authors attributed this behavior to complex formation with suitable guests that causes an increase in the rigidity of the receptor and limits the rotational/vibrational modes that would otherwise cause nonradiative decay. Moreover, fluorescence could be quenched by the formation of an excited charge-transfer complex

between the naphthalene and the naphthalimide moieties. Once a guest displaces the naphthalene from the cavity, the charge-transfer complex ceases to exist, inducing an increase in fluorescence. Receptor **134** is able to sense phosphate anions.

Martínez-Máñez, Rurack, and collaborators proposed another modification of the conventional displacement assay concept describing a QDA (quencher displacement assay) using terpyridine (135) and sulforhodamine B (136) anchored onto the surface of silica nanoparticles.²³² In this assay a mediator, which is at the same time a good binder for the anion and a quencher for the fluorophore (i.e., a metal ion), is included in the system. When a cation is bound to the terpyridine quenching of the fluorescence of the fluorophore occurs. Upon addition of anions, however, the fluorescence is restored as the metal cations have higher affinity for the anionic guest than for terpyridine (Figure 44). In particular, when Pb^{2+} is added to the system, only $H_2PO_4^-$ is able to revive the sulforhodamine fluorescence in MeCN, allowing the detection of this anion in concentrations as low as 5 ppm.

Leonard, Gunnlaugsson, and co-workers employed a cyclen-based europium complex bound to a β -diketonate which functions as a sensitizing antenna.²³³ Addition of sodium tartarate, lactic acid, fluoride, acetate, or potassium bicarbonate at pH 7.4 reduced the luminescence of the complex as the anion displaced the antenna from the europium–cyclen complex.

2.2.2. Microarrays and Artificial Tongues for Anion

Sensing. An alternative to the “lock-and-key” approach to chemosensing is differential sensing.^{234,235} Traditionally, much effort is directed to the design and synthesis of highly selective receptor–indicator sensors for a given analyte (Figure 45). Differential sensing, on the other hand, takes inspiration from the process of the human olfaction and gustation, which uses cross-reactive receptors that interact differentially with odors and tastes. As shown in Figure 45 an array built from a combinatorial library of sensors is needed, but the sensors do not need to be highly selective or specific for target analytes. In particular, in the case of multianalyte recognition most of the individual sensors in the array respond to each analyte, but this response must have a level of variance that allows discrimination of the analytes. With

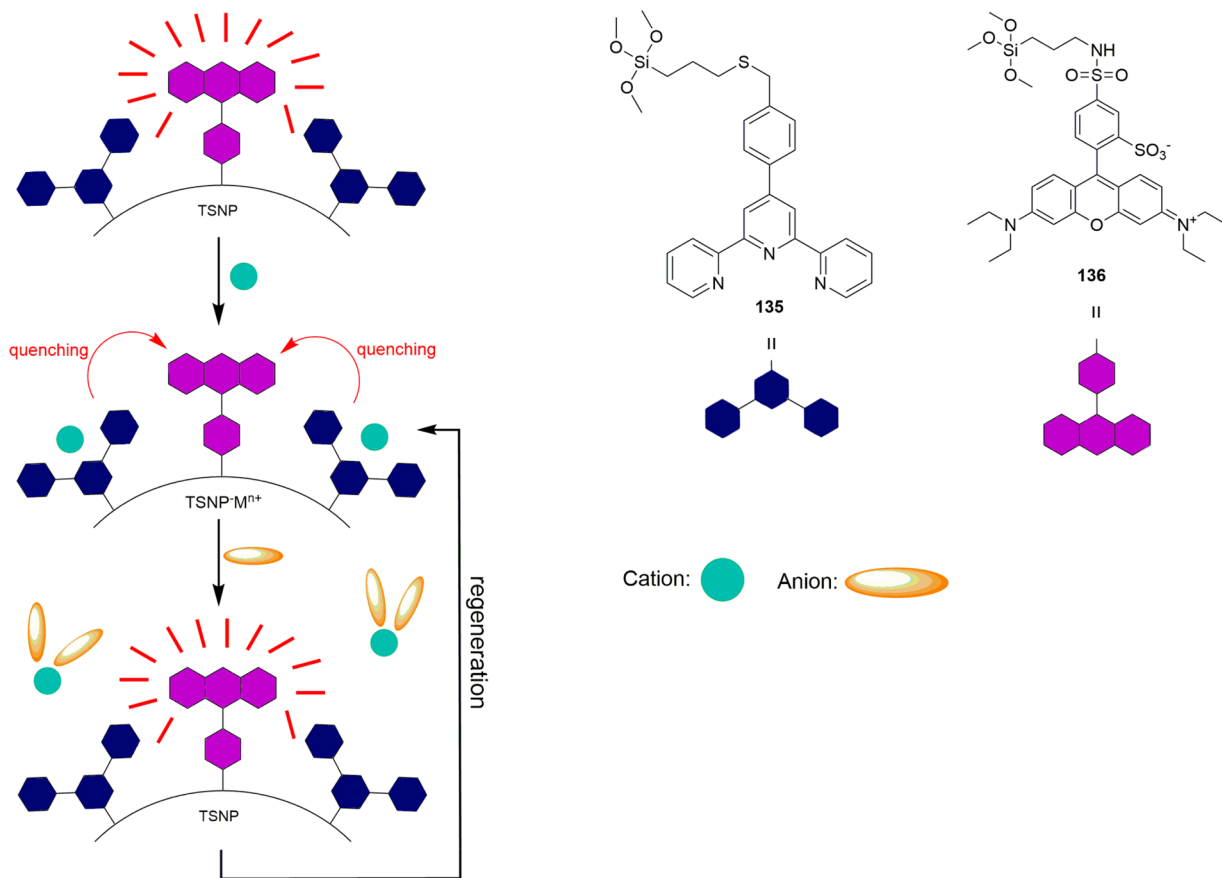


Figure 44. Representation of the quencher displacement assay (QDA) based on terpyridine (**135**) and sulforhodamine (**136**).

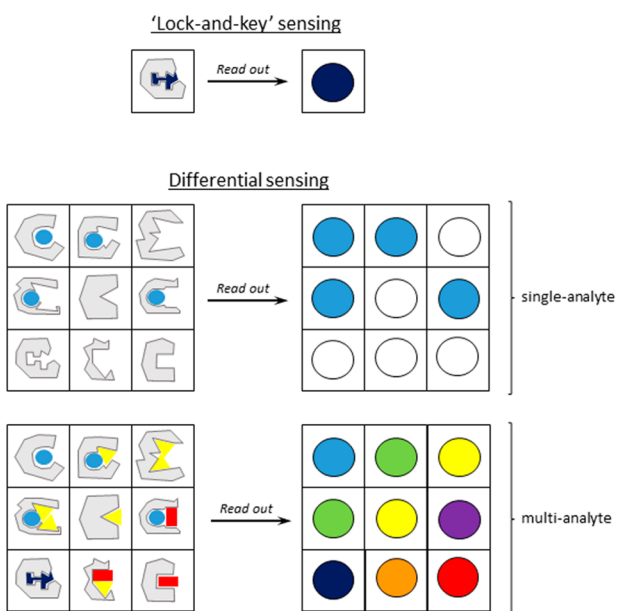


Figure 45. Schematic representation of the classic lock-and-key approach and the differential approach for single-analyte and multi-analyte recognition.

differential sensing the evaluation of the response is achieved using chemometric analysis such as principal component analysis (PCA), linear discriminant analysis (LDA), artificial neural networks (ANN), and hierarchical cluster analysis (HCA).^{236,237}

Ansglyn's group reported various examples of microarrays for anion recognition. For example, they recently described an array sensing approach for the *in vitro* differentiation of mitogen-activated protein (MAP) kinases and their phosphorylated counterparts.²³⁸ This family of kinases triggers key cell-signaling pathways, thus regulating a variety of cellular responses, such as mitosis, cell differentiation, the cell cycle, and apoptosis. Their malfunction is related to many diseases such as cancer, hematologic malignancies, and inflammatory states. The authors used a library of differential receptors created *in situ* containing peptides known for affinity to MAP kinases and a family of Zn(II)-dipicolylamine complexes that bind phosphate groups on proteins. An indicator-displacement assay signals the binding of the individual receptors to the kinases. The results, analyzed by LDA, demonstrate that this sensing system is capable of fingerprinting different classes of MAP kinases and cell lysates *in vitro* under neutral aqueous conditions. The same group also reported a system able to discriminate different plasticizers contained in plastic explosives using the same cross-reactive arrays approach.²³⁹

Anzenbacher and co-workers also reported several examples of microarrays for anion sensing. Using eight sensors (Figure 46) based on *N*-confused calix[4]pyrrole (**137**), regular calix[4]pyrrole (**138–143**), and receptor **144** they prepared an array for multianion sensing in water.²⁴⁰ In a solution of DMSO/0.5% water (MeCN for **144**) the eight sensors do not show any particular affinity for anions. The sensors were used to fabricate an array by embedding them in a polyurethane hydrogel, and a qualitative and quantitative response toward different anions in aqueous solution was evaluated. As shown in Figure 46, the

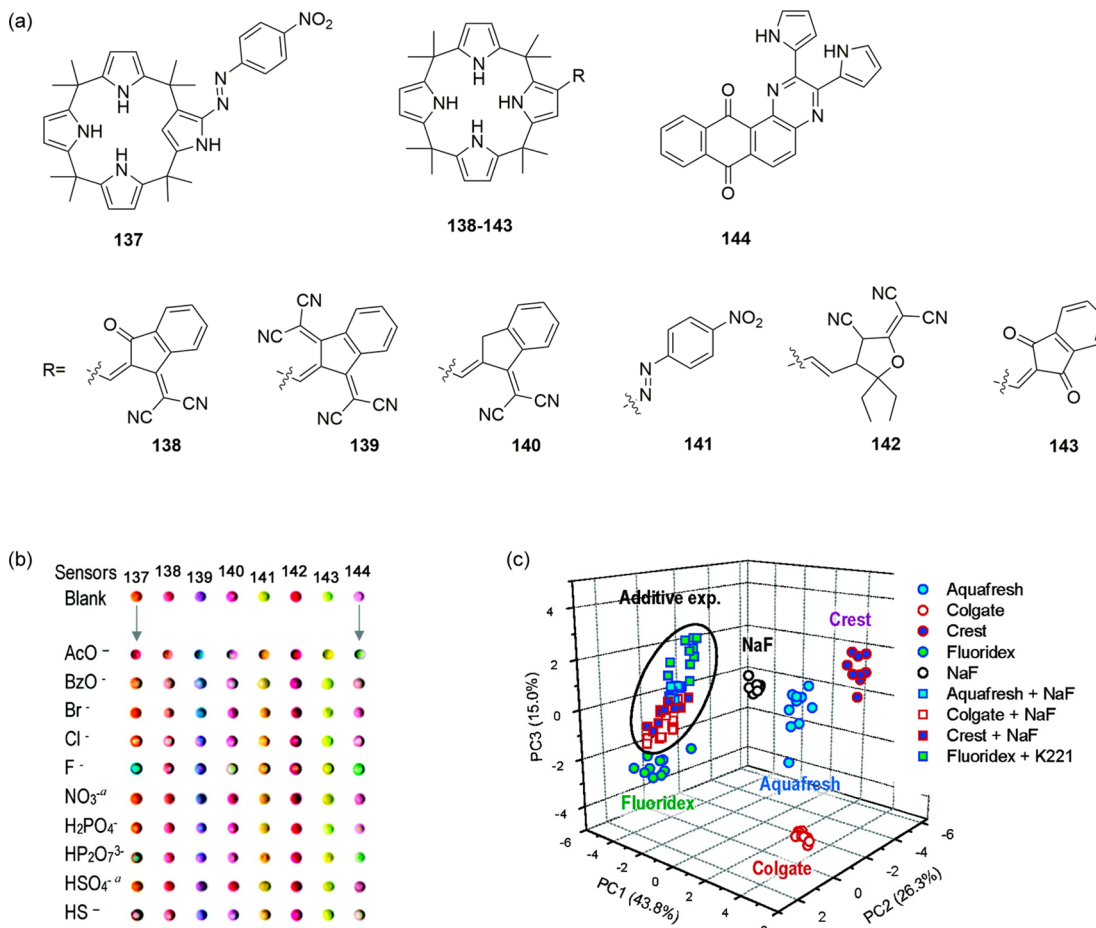


Figure 46. (a) Structures of **137–144**. (b) Eight-sensor array responses to aqueous anion solutions. (c) PCA score plot for four toothpaste brands. Reprinted with permission from ref 240. Copyright 2007 American Chemical Society.

colorimetric response given by the array for each anion allows discrimination. The system can be used for the identification of toothpaste samples. PCA permits discrimination between different brands as shown in Figure 46. The fluoride-selective, yet cross-reactive, array proposed uses the F⁻ content of the toothpastes as the main discriminatory factor with the other anionic components further differentiating the different samples.

The same authors also described an array for the detection of phosphate in blood serum using simple fluorescent tripodal receptors.²⁴¹ As shown in Figure 47, blood serum behaves as a unique buffer containing phosphates and carboxylates and causes a response in the array. When phosphates are added to the serum a unique response is generated in the array for each anion as demonstrated by PCA.

More recently, Anzenbacher and co-workers reported the first example of phosphonate anion sensing using a fluorescent microarray.²⁴² Phosphonates, in particular isopropylmethyl phosphonate (IMP) and methyl phosphonate (MP), are the hydrolysis products of the nerve gas Sarin. Seven tripodal sensors similar to **145–150** were dissolved in DMSO and found to give a fingerprinted response for IMP and MP over other common anions, as demonstrated by LDA (Figure 48).

2.2.3. Vesicular- and Micellar-Based Assemblies for Anion Sensing. One of the major drawbacks of anion sensing in water is the high affinity of the substrates to this solvent. Additionally, as shown in the examples reported in the previous paragraphs, the receptors used to preferentially bind anions are

poorly soluble in water. In order to overcome these problems the use of micellar and vesicular microenvironments have been developed.

The salophen–UO₂ complex **151** (Figure 49) has been reported by the group of Dalla Cort as a very efficient ditopic receptor toward tetraalkylammonium halides in organic solvents and in the solid state.²⁴³ Compound **151** can be solubilized in water in the presence of cationic surfactant cetyltrimethylammonium (CTAB) micelles.²⁴⁴ In this environment a stability constant of $10\ 800 \pm 800\ M^{-1}$ for the 1:1 complex of **151** with fluoride can be measured by UV–vis spectroscopy. Interestingly, this value is much higher than that observed in MeOH ($360 \pm 800\ M^{-1}$). Authors have assessed by NOE experiments that the preferential location and orientation of **151** is at the micelle–water interface, where fluoride can easily interact with the receptor.

Martínez-Máñez and Sancenón also used a micellar system for the chromogenic cyanide recognition in water.²⁴⁵ Receptor **152** contains a thiopyrylium moiety whose electrophilic character facilitates the attack of the nucleophilic cyanide anion on the aromatic thiopyrylium ring in acetonitrile, resulting in the disruption of electronic delocalization. This event is reported as a bleaching of the solution. A derivative of **152**, **153**, which is very insoluble in water, can be dissolved in aqueous Triton X-100 micellar solutions at pH 9.5. As shown in Figure 50 only cyanide causes a decrease in the intensity of the band of **153** in the micellar solution, while all other anions tested, F⁻, Cl⁻, Br⁻, I⁻,

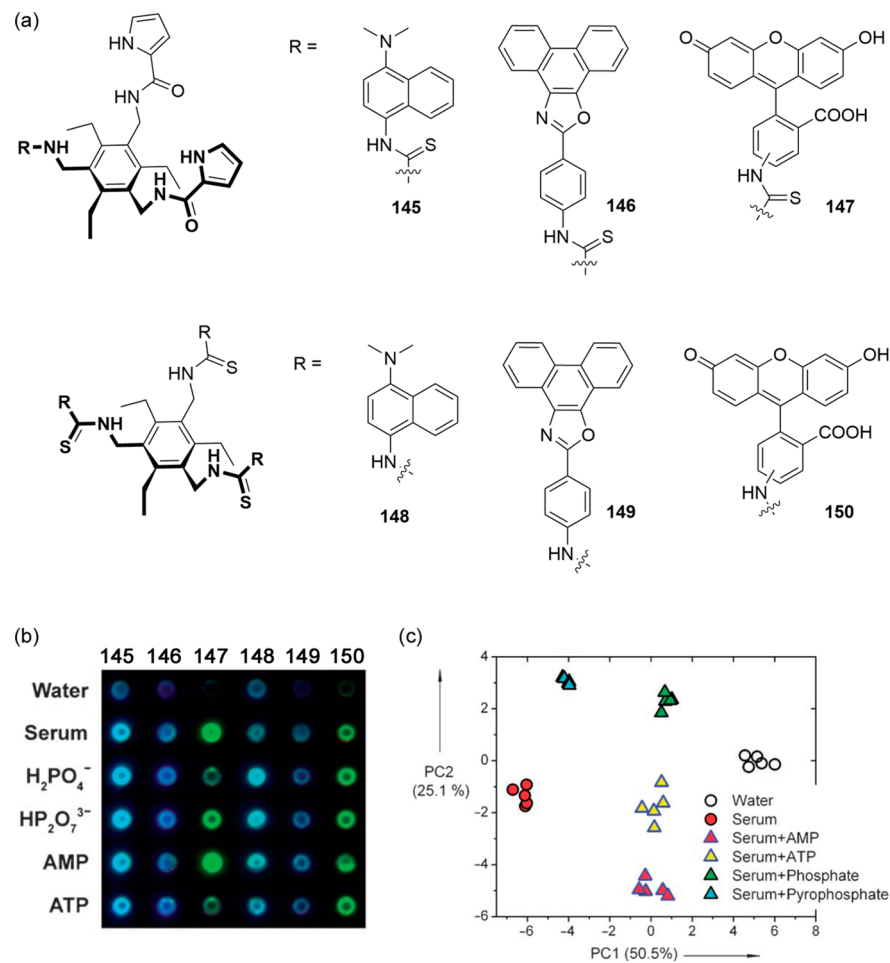


Figure 47. (a) Structure of sensor 145–150. (b) Qualitative changes in the fluorescence of the sensor–polyurethane films after addition of human blood serum and serum with added anions. (c) PCA score plot. Reprinted with permission from ref 241. Copyright 2007 Wiley-VCH.

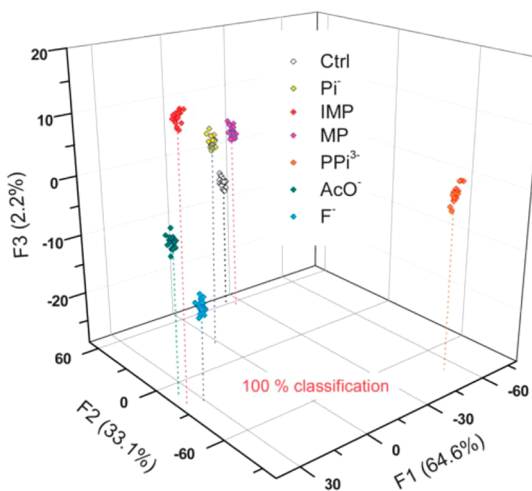


Figure 48. LDA graphical output of a qualitative assay which shows canonical score plots for the first three canonical factors. Reprinted with permission from ref 242. Copyright 2013 Royal Society of Chemistry.

AcO⁻, NO₃⁻, NCS⁻, H₂PO₄⁻, and HSO₄⁻, do not cause any change in the absorption spectrum of the system.

In an interesting paper, König and co-workers described the use of self-assembled vesicular polydiacetylene (PDA) particles for colorimetric and fluorimetric anion sensing.²⁴⁶ Starting from two cyclen-Zn(II) complexes 154 and 155 and iminodiaceta-

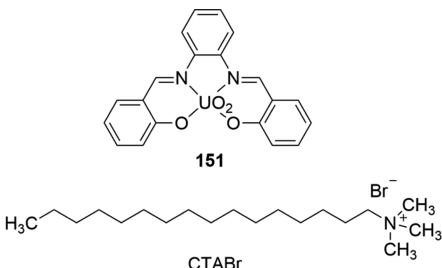


Figure 49. Structure of 151 and CTABr.

to–Cu(II) complex 156, three different types of liposomes (**LP-154**, **LP-155**, and **LP-156**) are obtained after irradiation at 254 nm of the complexes in the presence of diacetylene monomers (Figure 51b). The average dimensions of the liposomes was between 160 and 180 nm as determined by dynamic light scattering. Interestingly, the self-assembly of the liposomes causes a color change in the solution from colorless to blue, depending on the extended conjugation of the p orbitals in the main chain of the polydiacetylene polymers. In water buffered at pH 7.2, the color of the liposomes gradually shifts from blue to red upon the addition of certain anions, in particular, ATP, pyrophosphate, and cyanide (**LP-154**, **LP-155**) or only pyrophosphate (**LP-156**). This color change can be ascribed to the partial twist of the conjugated p orbitals which undergo distortion upon analyte binding to the embedded receptor sites.

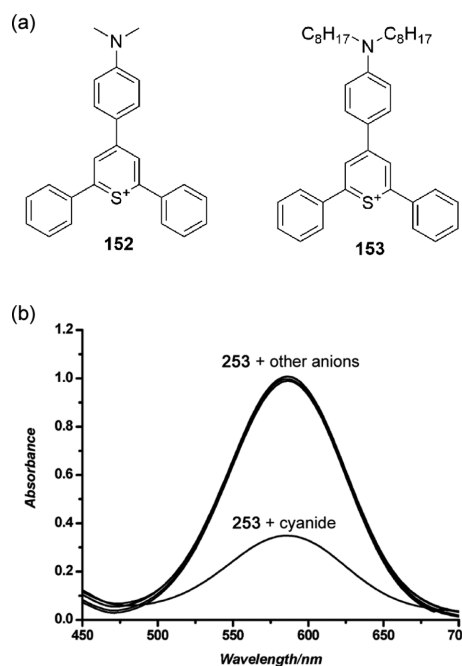


Figure 50. (a) Structures of **152** and **153**. (b) Changes in the visible band of **153** upon the addition of various anions in aqueous Triton X-100 micellar solutions at pH 9.5. Reprinted with permission from ref 245. Copyright 2009 Royal Society of Chemistry.

Additionally, the liposomes also show a weak emission band centered at 625 nm, and upon addition of ATP and pyrophosphate an increase in the fluorescence emission is observed.

More recently, König and co-workers described a modular design of a vesicular chemosensor for the detection of different phosphate analytes by coembedding a Tb(III) complex (157), functioning as a phosphorescent reporter, with a phosphate receptor (the Zn(II) complex 158) in phospholipid vesicles (~100 nm) (Figure 52).²⁴⁷ When phosphate analytes such as

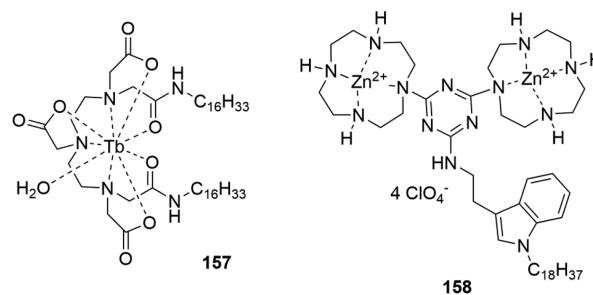


Figure 52. Structures of 157 and 158.

UTP, GTP, ATP, PP_i, pSer, ADP, and AMP are added to the **158/157(1:1)** coembedded vesicles, a gradual decrease in Tb(III) luminescence intensity is observed. Presumably, the two coembedded complexes initially form self-assembled mixed patches, bringing the Tb(III) ions in close proximity to the

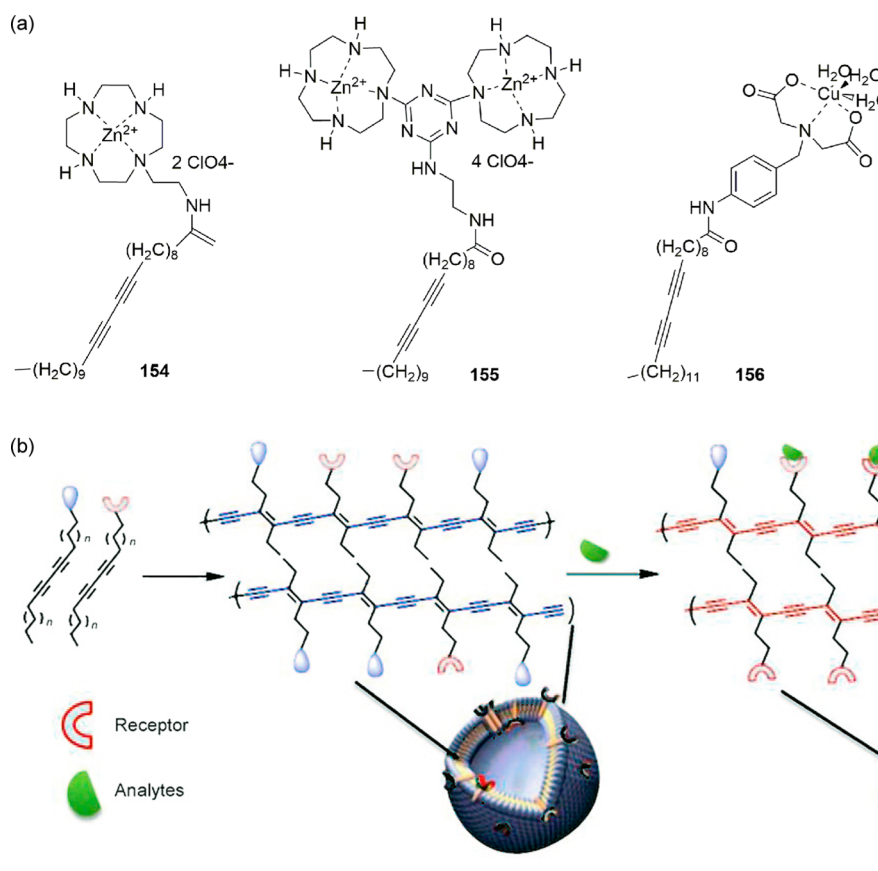


Figure 51. (a) Structures of **154–156**. (b) Schematic representation of the preparation and the analyte response of self-assembled polydiacetylene vesicles with embedded metal complex binding sites for anions. Reprinted with permission from ref 246. Copyright 2009 Wiley-VCH.

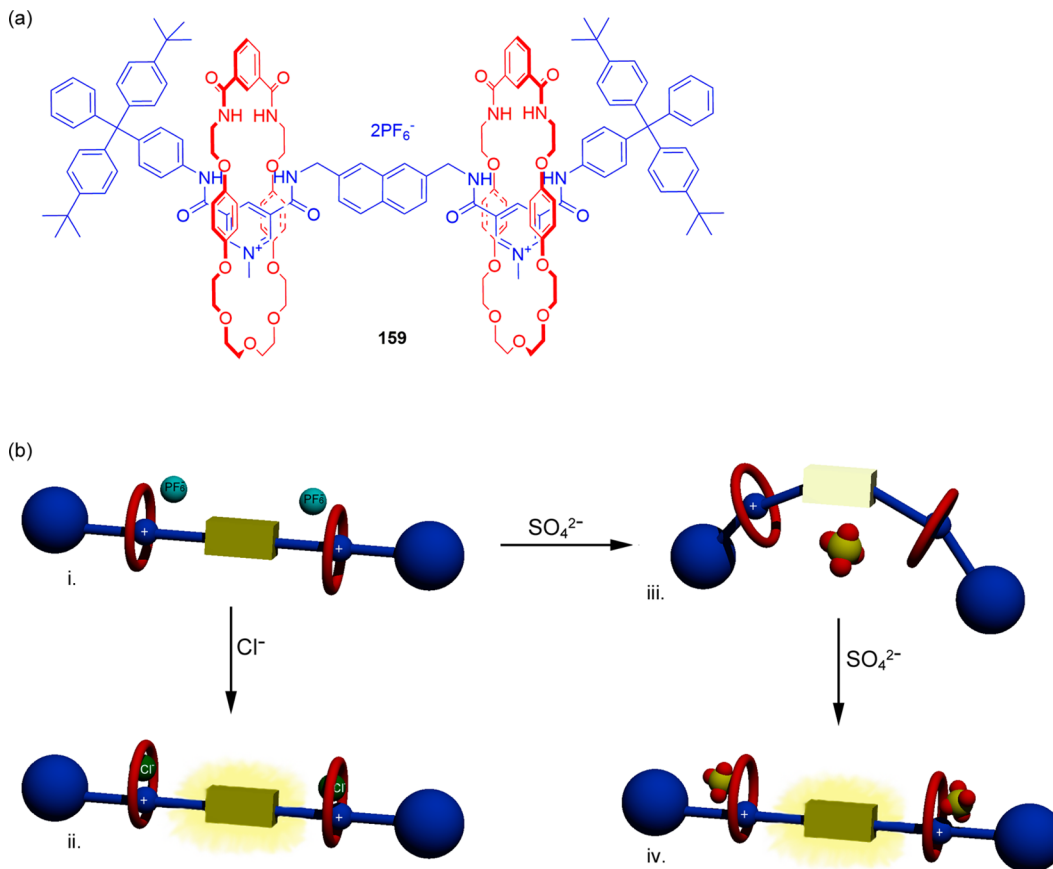


Figure 53. (a) Structure of rotaxane 159. (b) Schematic representation of anion binding: (i) emissive unbound host; (ii) enhanced emission in the 2:1 stoichiometric anion–host complex with chloride; (iii) quenched emission in the 1:1 stoichiometric sandwich complex with sulfate; (iv) enhanced emission in the 2:1 stoichiometric complex with sulfate.

sensitizer. After analyte addition, however, the patches are disrupted, causing an increase in their mutual separation and a concomitant decrease in Tb(III) emission. Interestingly, the addition of other monovalent and divalent anions, such as Cl⁻, Br⁻, OAc⁻, CO₃²⁻, and SO₄²⁻, result in only minor changes in the Tb(III) emission.

2.2.4. Other Assemblies for Anion Sensing. Various examples of anion sensing via interlocked systems, and in particular rotaxanes, have been reported in the literature. Recent reviews by Beer and co-workers deal specifically with this topic, describing examples of redox-active or photoactive sensors.^{248,249}

Beer's group has been a pioneer in this area and reported many examples of anion chemosensors based on interlocked systems. For example, they described the ability of the fluorescent [3]rotaxane 159 to sense sulfate. In chloroform the rotaxane selectively recognizes sulfate.²⁵⁰ As shown in Figure 53, a 1:1 stoichiometric sandwich complex with sulfate is initially formed, in which the anion is bridged between the two macrocycles and held in proximity to the naphthalene unit, leading to quenching of the fluorescence. Further addition of sulfate results in the rotaxane changing conformation in order to bind a second anion. As a consequence, sulfate is no longer bound in close vicinity to the naphthalene moiety and the fluorescence is restored. A fluorescence enhancement is also observed for the 2:1 complexes of chloride, bromide, and acetate. The authors attributed this behavior to the increased rigidity of the system, which reduces the efficiency of the vibrational relaxation pathway of the naphthalene excited state.

Beer also reported the first catenane (160) which can selectively recognize chloride and bromide anions solely by halogen bonding (through the cooperative action of two bromine halogen-bond-donor atoms) and which can optically sense anions using fluorescence spectroscopy.²⁵¹ Catenane 160 exhibits one broad and structureless emission band at $\lambda = 309$ nm in CH₃CN ($\lambda_{\text{ex}} = 280$ nm). The addition of increasing amounts of Cl⁻ and Br⁻ causes a progressive decrease in the intensity of the emission band located at $\lambda = 309$ nm with a concomitant appearance and increase of a new broad band at $\lambda = 445$ nm, characteristic of the excimer emission of naphthalene (Figure 54).

Smith and co-workers studied a number of squaraine rotaxanes for NIR anion sensing.²⁵² In particular, they reported an interesting example of squaraine rotaxane shuttle (161) as a ratiometric chloride sensor.²⁵³ Rotaxane 161 shows a color change from green to blue in the presence of chloride in acetone. Additionally, the fluorescence emission band of free rotaxane at 698 nm decreases and a new band at 665 nm appears in the presence of chloride. These optical changes were ascribed to anion-induced displacement of the macrocycle of the rotaxane away from the squaraine core. A chloride sensing dipstick was also fabricated by adsorbing 161 onto C18-coated silica gel TLC plates. As shown in Figure 55, upon immersion of the dipstick into an aqueous solution of chloride a change both in the color and in the emission of the system is observed. The observed changes are reversible.

Designing functional hybrid nanomaterials and supramolecular systems is of great current interest, particularly for molecular

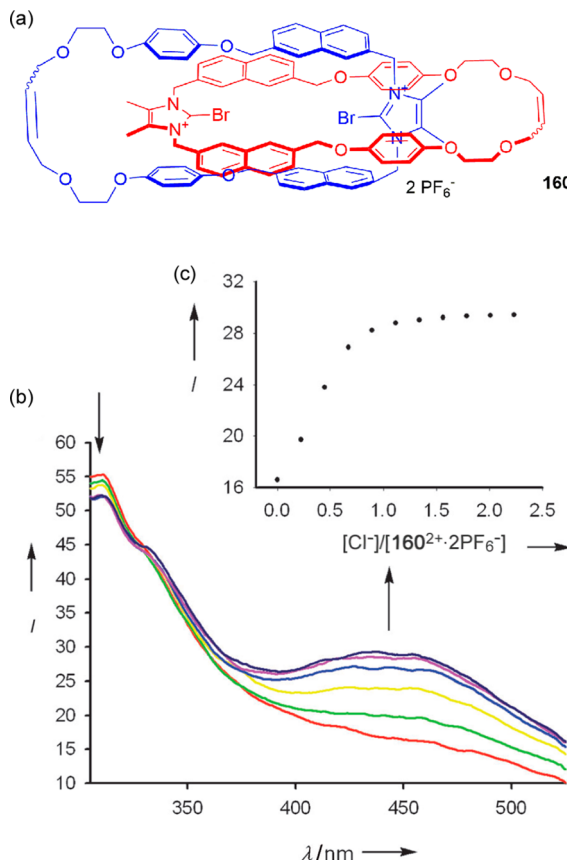


Figure 54. (a) Structure of catenane 160. (b) Changes in the emission spectra of 160 upon addition of chloride. (c) Plot of the emission vs the $[\text{Cl}^-]/[160]$ ratio at 445 nm in CH_3CN . Reprinted with permission from ref 251. Copyright 2012 Wiley-VCH.

recognition and sensing. Gold nanoparticles (AuNPs) have attracted much attention for this purpose, because of their biocompatibility, unique size and shape dependence, and optoelectronic properties. Gunnlaugsson and co-workers reported the first example of a system that combines the peculiar properties of AuNPs with those of lanthanide complexes for anion sensing purposes.²⁵⁴ The Eu(III) complex 162 bearing a thiol moiety is adsorbed onto the surface of the nanoparticle, forming the water-soluble system AuNP-162. The formation of ternary complexes between 162-AuNP and the β -diketone antenna 163 causes an intense luminescence of the solution. The system can be used for the sensing of biologically relevant phosphates such as flavin monophosphate (164) through the displacement of the antenna by the analyte, as shown schematically in Figure 56.

AuNPs have also been used for the detection of cyanide.²⁵⁵ The positively charged Rhodamine-B dye can be easily adsorbed onto the surface of citrate-stabilized AuNPs. The NPs show very weak fluorescence due to an efficient energy transfer process between the dye and the AuNPs. In the presence of cyanide, due to the well-known property of this anion to dissolve metals such as Au and Ag in the presence of oxygen through the formation of soluble metal-cyanide complexes, the AuNPs are gradually dissolved, releasing the fluorophore and thereby causing an increase in emission.

Gold nanoclusters have also been employed in the detection of anions. Xia, Zhu, and collaborators described the photophysical properties of NIR-emitting gold nanoclusters (AuNCs).²⁵⁶ As

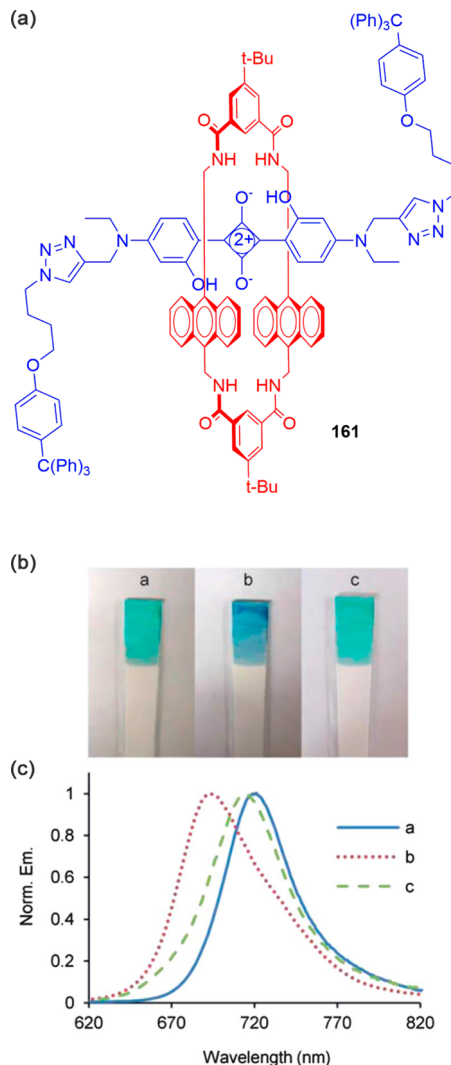


Figure 55. (a) Structure of rotaxane 161. (b) Photographs of the same dipstick treated with 161 during the following sequence: (a) before immersion, (b) after immersion in aqueous chloride (1 M), (c) after aqueous washing. (c) Fluorescence spectra ($\lambda_{\text{ex}} = 600$ nm) of the dipstick surface at the same time points, showing a blue shift of emission maxima induced by Cl^- , which is subsequently reversed after washing. Reprinted with permission from ref 253. Copyright 2013 Royal Society of Chemistry.

shown in Figure 57, an almost complete quenching of the NIR emission is observed upon the addition of Hg(II) due to the interaction between Hg(II) and Au(I) on the surface of the AuNCs. Upon addition of GSH to the AuNCs-Hg(II) system, an enhancement of the fluorescence occurs because of the displacement of the Hg(II) from the AuNCs to form a complex with GSH. The AuNCs-Hg(II) system can also be used to monitor GSH in living cells. After AuNCs-Hg(II) are added and incubated for 15 min, an intense red fluorescence can be observed in the cytosol of the cells under an inverted fluorescent microscope with green excitation light (Figure 57).

Apart from AuNP, other types of nanoparticles, ionic liquid polymers,²⁵⁷ quantum dots,^{258,259} and graphene oxide materials²⁶⁰ have also been used for the development of optical anion sensing. Pandey and co-workers, for example, synthesized bile-acid-based polymers which can be used for stabilizing silver

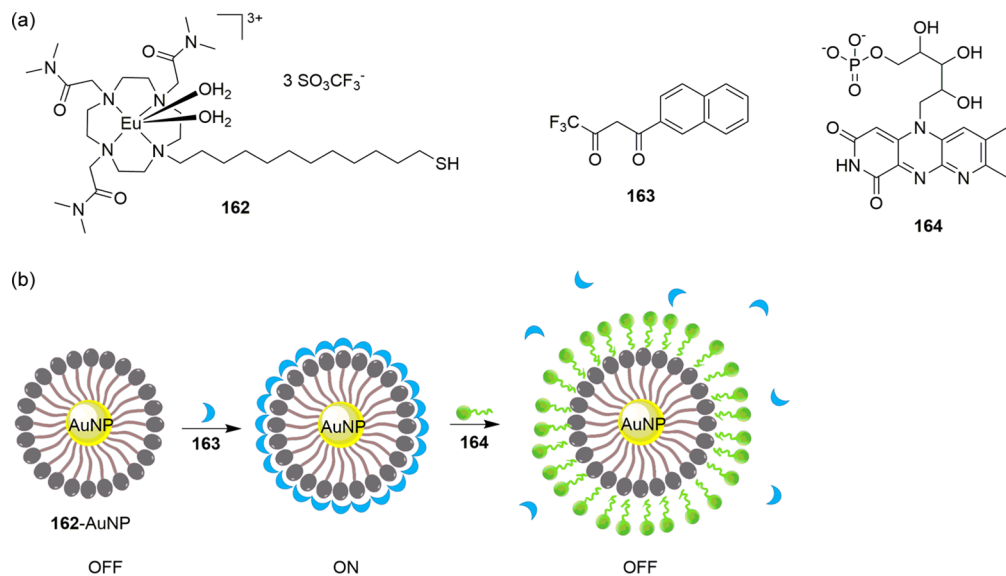


Figure 56. (a) Structure of **162–164**. (b) Schematic representation of the sensing of flavin monophosphate **164** by the displacement of **163** from the **162–AuNP** system.

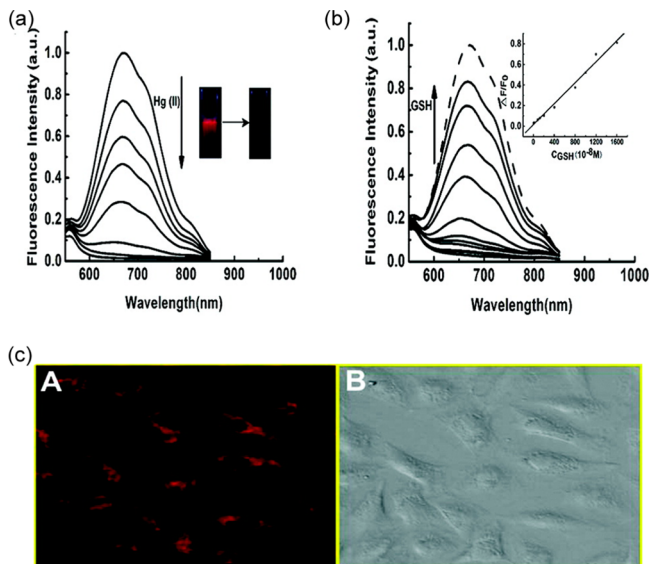


Figure 57. (a) Changes in the fluorescence spectra of AuNCs with increasing Hg(II) concentration, with photographs under UV light (354 nm) of AuNCs without and with Hg(II). (b) Changes in the fluorescence spectra ($\lambda_{\text{ex}} = 530 \text{ nm}$) of AuNCs–Hg(II) with increasing GSH. (c) Fluorescence microscopic images of living BEL-7402 cell supplemented with the AuNCs–Hg(II) system for 15 min under green light (A) and under visible light (B). Reprinted with permission from ref 256. Copyright 2012 American Chemical Society.

nano particles (AgNPs) that show colorimetric sensing properties toward iodide.²⁶¹

Mesoporous silica supports also provide ideal scaffolds for hosting functional guest molecules due to their distinctive characteristics, i.e., high homogeneous porosity, inertness, thermal stability, the presence of tunable pore sizes with a diameter in the region of 2–10 nm, and the possibility of easily functionalizing their external (or internal) surface.²⁶² As an example of this application, Martínez-Máñez and co-workers showed that mesoporous solids functionalized with anion binding groups can be suitable anion hosts and used in selective colorimetric displacement assays.²⁶³ Similarly, Costa, Alarcón,

García-España, and co-workers grafted squaramides on the surface of bohemite or silica-coated bohemite nanoparticles to achieve sulfate sensing in water using an IDA approach with Bromocresol Green as the dye.²⁶⁴

Polyacrylamide nanoparticles with diameters from 40 to 120 nm have been used by Sun and co-workers to embed fluorescent inorganic phosphate binding proteins (phosphate binding protein (PiBP) fused between two different fluorescent reporter proteins, namely, cyan fluorescent protein (CFP) and yellow fluorescent protein (YFP)) for the sensing of phosphate (Pi).²⁶⁵ The FRET efficiency between the two reporter proteins changes as a result of the relative conformational movement of the two lobes on PiBP when the substrate is bound (Figure 58). Quantification of the analyte is obtained through analysis of the ratio between YFP and CFP fluorescence emission intensity.

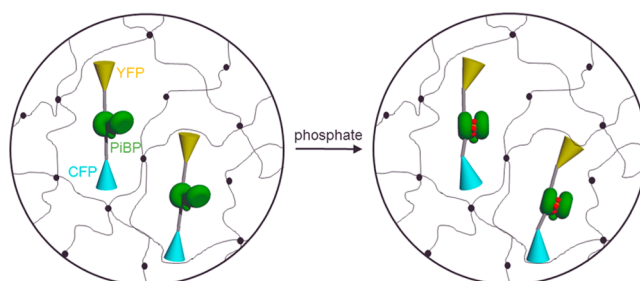


Figure 58. Schematic representation of the sensing mechanism of polyacrylamide nanoparticles embedded with a fluorescent phosphate binding protein.

2.3. Electrochemical Anion Sensing

Anions can also be sensed electrochemically, and there are a number of ways in which this goal can be achieved. The most important strategies include the synthesis of redox-active molecules that are able to change their electrochemical properties when the binding event occurs or the immobilization of anion receptors into membranes to produce ion-selective electrodes (ISEs).

In redox-active sensors the signaling unit is a redox-active group which must be coupled to the binding unit in order to detect a change in the redox properties of the system. Beer and co-workers have been pioneers in redox sensing, and they identified four major mechanisms for the coupling between the active unit and the binding unit: (1) *through-space coupling*, in which the binding site and the active unit are in close proximity so that the electrostatic effect of the guest perturbs the redox properties of the active unit; (2) *through-bond coupling*, in which there is a conjugated chemical bond pathway between the active unit and the binding unit; (3) additional direct coordination between the active unit and the anionic guest; (4) conformationally induced perturbations of the active unit caused by the presence of the guest.²⁶⁶

Numerous examples of redox-active sensors for anion recognition have been reported so far in the literature, and only a few recent examples will be described in this section. As already stated above, the group of Beer has been very active in this field. Their recent work has focused on ferrocene-functionalized rotaxanes for anion recognition.^{267–270} In particular, they recently reported the first example of a redox-active interlocked system (**165**).²⁶⁸ Rotaxane **165** (Figure 59) is the redox-active analogue of **159** bearing a ferrocene moiety instead of a naphthalene. In order to evaluate the electrochemical sensory properties of **165** cyclic voltammograms were recorded in 0.1 M TBAPF₆ CH₃CN electrolyte solutions. The rotaxane **165** exhibits a quasi-reversible oxidation for the Fc/Fc⁺ redox couple at $E_{1/2} = +125$ mV (compared to $E_{1/2}$ (ferrocene) = 0 V).

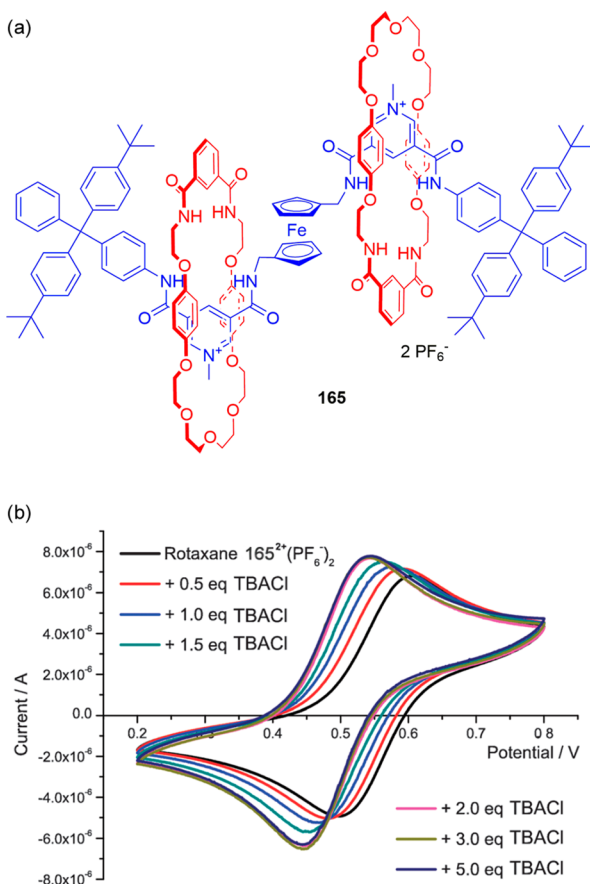


Figure 59. (a) Structure of rotaxane **165**. (b) CV of **165** upon the addition of TBACl. Reprinted with permission from ref 268. Copyright 2011 Royal Society of Chemistry.

Upon addition of increasing amounts of TBACl, a stepwise cathodic perturbation of the redox wave is observed, which is attributed to the stabilization of the oxidized form of the axle ferrocene motif by halide anion guest binding (Figure 59). The observed shift of -55 mV upon the addition of two equivalents, with negligible further shift (<5 mV) thereafter, suggests that chloride is bound within each of the two interlocked cavities. Upon addition of (TBA)₂SO₄ the electrochemical response is more complicated because of slow kinetics of the binding behavior. A much larger cathodic shift of $\Delta E_{1/2} = -265$ mV is observed after 5 equiv of sulfate addition which may be attributed at least in part to the oxoanion possessing twice the charge of chloride.

Rotaxane **166** (Figure 60) is another receptor reported by the Beer group that is able to sense chloride.²⁶⁷ A cathodic shift of 20

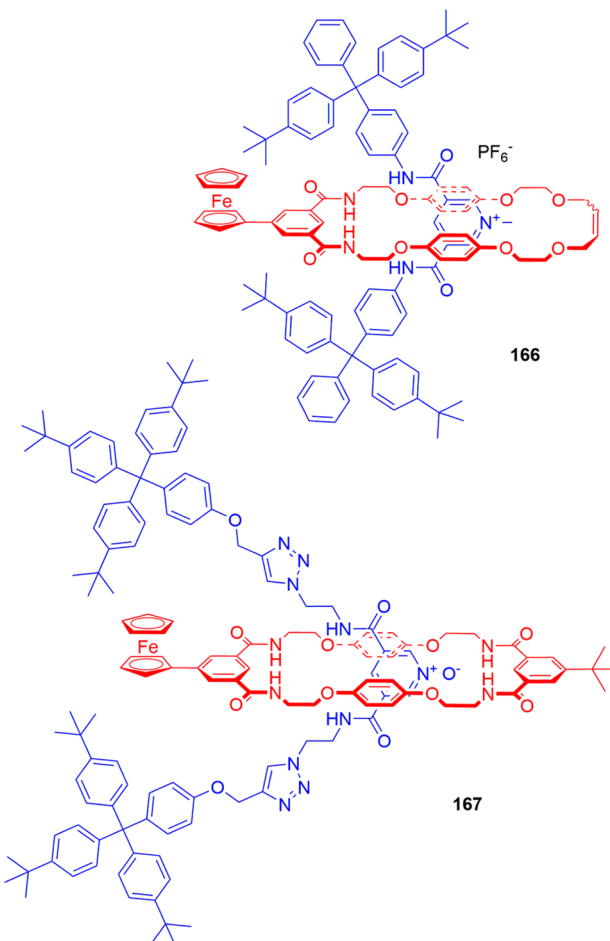


Figure 60. Structure of rotaxanes **166** and **167**.

mV of the Fc/Fc⁺ redox couple was observed upon the addition of chloride in MeCN at a 1:1 **166**:Cl⁻ molar ratio with a negligible further shift on addition of further aliquots of chloride. On the other hand, the addition of oxoanions causes a continuous shift in the ferrocene/ferrocenium redox couple. Very recently, Beer and co-workers also described the first example of redox-active chloride sensing by a neutral ferrocene-functionalized [2]rotaxane (**167**, Figure 60).²⁷⁰ Electrochemical voltammetry experiments demonstrated that the rotaxane can sense chloride via cathodic perturbations of the ferrocene–ferrocenium redox couple upon anion addition in CH₂Cl₂/MeCN (1:1, v/v).

The same authors also reported ferrocenylimidazoliophanes **168**.²⁷¹ The electrochemical halide sensing in MeCN has been performed by means of Osteryoung squarewave voltammetry (OSWV). As shown in Figure 61, the addition of iodide to a

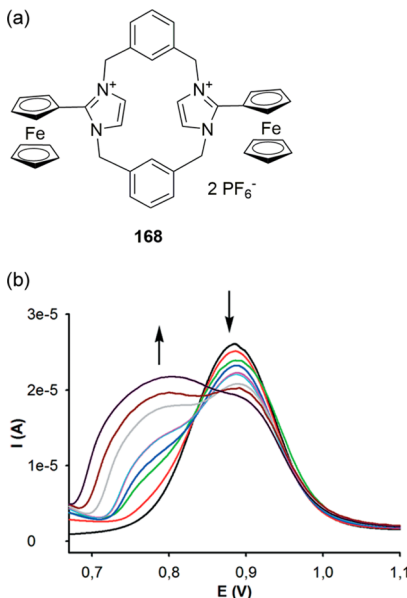


Figure 61. (a) Structure of ferrocenylimidazoliophane **168**. (b) Evolution of the OSWV of **168** upon addition of iodide up to one equivalent. Arrows indicate current intensities that increase or decrease during the titration. Reprinted with permission from ref 271. Copyright 2014 Royal Society of Chemistry.

solution of **168** results in typical “two-wave behavior” with the appearance of a new wave at more negative potentials ($\Delta E = -100$ mV) with a concomitant disappearance of the wave corresponding to the free receptor. The addition of Cl^- and Br^- causes similar two-wave behavior with a smaller cathodic shift ($\Delta E = -50$ mV), while F^- does not cause any perturbation of the system.

Other types of anions can be detected using electrochemical sensing. Moody, Tucker, and co-workers reported a series of chiral ureas containing the redox-active ferrocene group for chiral carboxylate recognition.²⁷² The authors reported that in MeCN the enantioselectivity with receptor **169** improves to such an extent that the (*S*)-enantiomer of the protected amino acid *N*-benzenesulfonyl proline (**170**) is bound approximately 1.7 times more strongly than its (*R*)-enantiomer. By plotting the observed ΔE_{obs} value (where $\Delta E_{\text{obs}} = E_{\text{obs}} - E_{\text{host}}^\circ$) for receptor **169** against molar equivalents of **170** (Figure 62) a discernible difference in the electrochemical response to the binding of opposite enantiomers is seen in the region around equimolar amounts of host and guest. With other chiral guests (e.g., 2-phenylbutyric acid **171**) no differentiation between the two enantiomers was observed.

Sargent, Siebert, and co-workers described two simple Wurster-type ureas (**172** and **173**, Figure 63) for the electrochemical recognition of oxo anions in MeCN.²⁷³ Wurster's reagent, *N,N'*-tetramethyl-*p*-phenylenediamine (*p*-TMPD), has two reversible one-electron oxidations. Free receptor **172** undergoes two oxidations (107 and 241 mV relative to Fc/Fc^+) that, by analogy to *p*-TMPD, are ascribed to the one-electron oxidation of each phenylenediamine subunit. Free **173**, containing only one phenylenediamine unit, only undergoes a

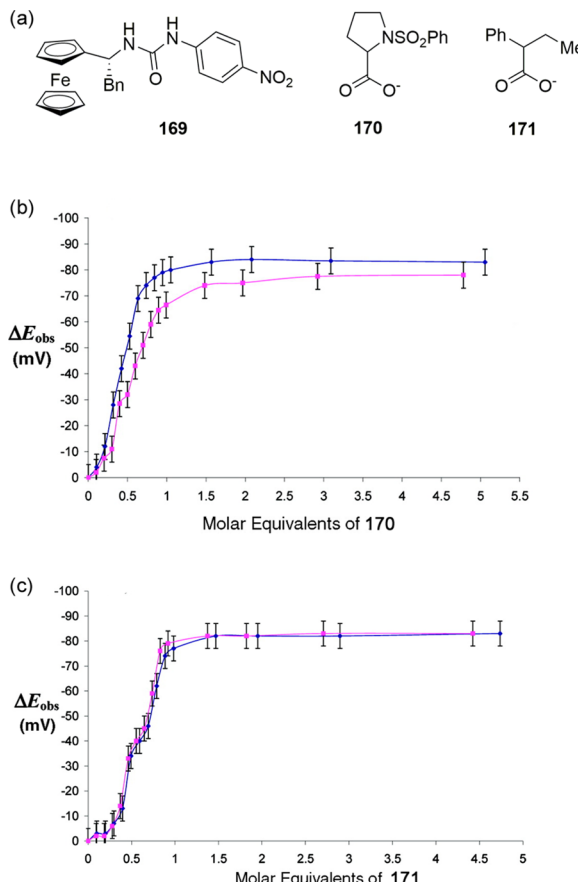


Figure 62. (a) Structures of receptor **169** and chiral guests **170** and **171**. (b) Titration of the ΔE_{obs} value in MeCN of the redox wave of **169** against molar equivalents of (*S*)-**170** (blue diamonds) and (*R*)-**170** (pink squares). (c) Titration of the ΔE_{obs} value in MeCN of the redox wave of **169** against molar equivalents of (*S*)-**171** (blue diamonds) and (*R*)-**171** (pink squares). Reprinted with permission from ref 272. Copyright 2008 American Chemical Society.

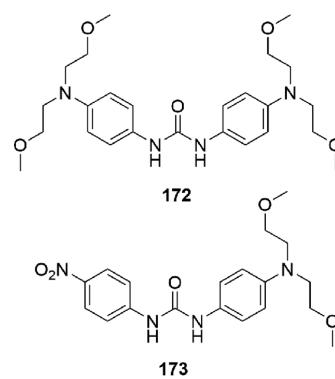


Figure 63. Structure of receptors **172** and **173**.

single one-electron oxidation at 180 mV relative to Fc/Fc^+ . For both receptors, the addition of substoichiometric quantities of CH_3COO^- , $\text{C}_6\text{H}_5\text{COO}^-$, and NO_2^- revealed a “two-wave” behavior. By determining the binding enhancement factor (BEF) the authors show that the most stable complex is **173**– CH_3COO^- .

Redox-active sensors have been reported for a whole range of other anions. Kim and collaborators reported an example of a redox-active sensor for dihydrogen phosphate in dichloro-

methane based on the neutral ferrocene-appended aryl triazole receptor **174** (Figure 64).²⁷⁴ Very recently, Lai and co-workers

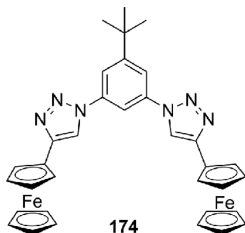


Figure 64. Structure of receptor **174** for the electrochemical recognition of H_2PO_4^- .

reported an interesting polythymine DNA-based electrochemical sensor for the detection of glutathione.²⁷⁵ Sensor signaling relies on glutathione's ability to chelate Hg(II), displacing it from the thymine–Hg(II)–thymine complex formed between the surface-immobilized DNA probes.

Along with molecular redox-active sensors, many anion-selective electrodes²⁷⁶ have been developed by immobilizing receptors inside a plastic membrane, often made of polyvinyl chloride (PVC) doped with a plasticizer such as 2-nitrophenyl octyl ether or bis(2-ethylbenzyl) sebacate.²⁷⁷ The potential of the selective electrode immersed in a solution of the target anion is measured versus the potential of a reference electrode. The potential difference can be related to the activity of the anion and hence to its concentration. A schematic representation of an anion-selective electrode is shown in Figure 65. In order to sense

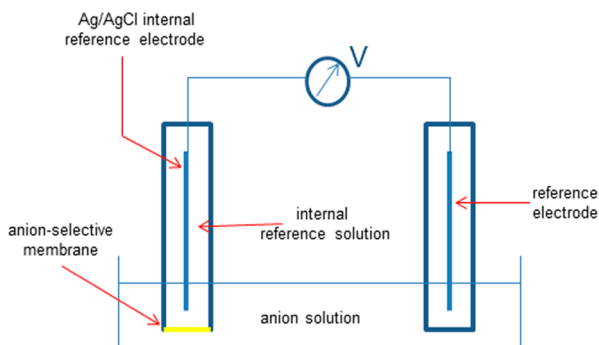


Figure 65. Schematic representation of an anion-selective electrode and reference electrode system.

anions with this type of device, the analyte should be extracted from the solution into the interior of the PVC membrane. In water it is more difficult to overcome the dominant extraction mechanism based on ion lipophilicity, which leads to a Hofmeister order of response for anions as $\text{ClO}_4^- > \text{SCN}^- > \text{NO}_3^- > \text{I}^- > \text{Br}^- > \text{Cl}^- > \text{F}^- > \text{HCO}_3^- > \text{SO}_4^{2-} > \text{HPO}_4^{2-}$.²⁷⁸ The selectivity of the receptors incorporated in the membrane should override the bias toward hydrophobic anionic species resulting in a more selective system capable of detecting specific hydrophilic anions. Only a few examples of ISEs will be discussed here; the reader is referred to more specialized reviews about electrochemical sensing for more details and additional examples.^{276,279}

Malinowski and co-workers reported that electrodes containing zirconium(IV)–salophens, such as **175** (Figure 66), exhibit very high fluoride selectivity over most lipophilic anions including perchlorate.^{280,281} The others also showed that the

electrodes function best when the membrane contains lipophilic anionic additives and in the pH range of 4.5–6.0. However, it was found that electrode function deteriorated over the course of a few days due to decomposition of **175**.

Zirconium(IV) tetraphenylporphyrins (tpp) were studied by Yuchi and co-workers, who found by UV-vis spectroscopy that the hydroxide-bridged dimerization equilibrium of these compounds in chlorobenzene depends on the concentration and nature of the contacting acid solution.²⁸² Furthermore, electrodes built from these complexes showed a strong preference for acetate (in the case of $[\text{Zr}^{\text{IV}}(\text{OH})\text{Cl}(\text{tpp})]$) or citrate (in the case of $[\text{Zr}^{\text{IV}}(\text{OH})_2(\text{tpp})]$) anions, although with significant super-Nernstian response slopes.

Qin and Bakker proposed covalently attaching In(III)–porphyrin derivatives such as **176** (Figure 66) to the polymer membrane of the electrode in order to minimize the hydroxide-bridged dimerization reactions of metalloporphyrins that normally cause super-Nernstian response slopes and short lifetime because of precipitation.²⁸³ The resulting membranes showed no evidence for dimer formation, had a longer lifetime, and displayed Nernstian response slopes to chloride, nitrite, and thiocyanate ions.

Ebdon and collaborators covalently attached a derivative of the phosphate-selective ionophore 3-decyl-1,5,8-triazacyclodecane-2,4-dione (**177**, Figure 66) to a cross-linked polystyrene-block-polybutadiene-block-polystyrene polymer for improved durability.²⁸⁴ Long-term stability was improved from 4 to 40 days, while the ion selectivity remained similar to that of a membrane containing freely dissolved ionophore.

Sanchez-Pedreño and co-workers explored tris(2-aminoethyl)amine derivative **178** (Figure 66) as an ionophore for the recognition of nitrate in ISEs.²⁸⁵ Receptor **178** was incorporated in plasticized PVC membranes, and the resulting electrodes exhibited a Nernstian response for nitrate, a wide working pH range (2–12), and a fast response time. It was also shown that the ISEs displayed good selectivity for nitrate over many common anions, particularly thiocyanate, perchlorate, and nitrite.

More recently, Diamond and Schazmann included urea-calix[4]arene **179** (Figure 66) into ISE membranes for nitrate sensing. An increase in sensitivity and selectivity for nitrate over chloride was observed compared to commercially available nitrate-selective electrodes.²⁸⁶

Very recently, Ortuño, Curiel, and collaborators synthesized a carbazole derivative **180** (Figure 66) to host dicarboxylate anions.²⁸⁷ The authors incorporated the compound as an ionophore into the membrane of an anion-selective electrode. The response of the electrode for oxalate, malonate, succinate, glutarate, and adipate showed very good detection limits, fast responses, and an unprecedented increase in selectivity for all dicarboxylates anions, with especially good results in the case of glutarate. The preferential binding of glutarate by carbazolo-carbazole **180** was also confirmed by ^1H NMR and fluorescence titrations.

2.4. Anion-Responsive Gels

Gels are soft materials that have attracted considerable attention in recent years due to their interesting peculiar properties. Gels are generally constituted by at least two components: a sample-spanning, fibrous solid network and a solvent or liquid component that is retained within the solid.²⁸⁸ In particular, supramolecular gels are dimensionally controlled assemblies of low-molecular-weight molecules held together by noncovalent

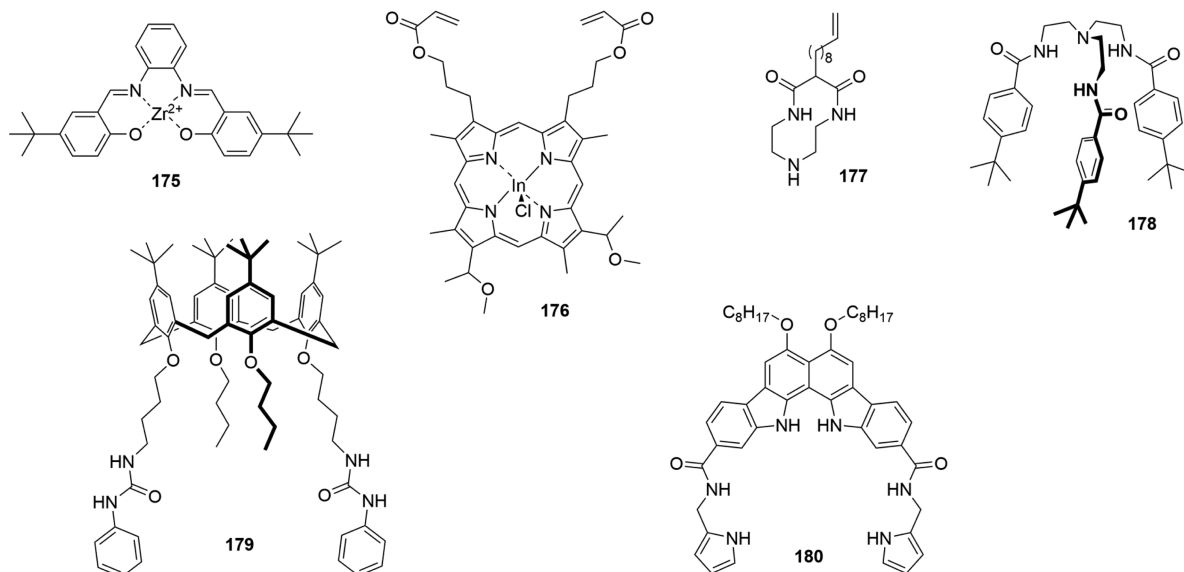


Figure 66. Structures of receptors **175–180** used in the development of anion-selective electrodes.

interactions, such as hydrogen bonds, metal coordination, van der Waals interaction, and π - π stacking. The initial step in the formation of a gel involves obtaining gelator molecules that can form fibril- or tape-like structures that compose gels. Such molecular assemblies are influenced by the external conditions, such as solvent, temperature, and concentration. Recently, the use of anions as external chemical stimuli for gel formation has been proposed. This section will focus on reports where a sol-gel transition can be employed as a means to sense the presence of a particular anion. A discussion of other aspects of anion-responsive gels will be given in section 5.2.

One of the first examples of anion-responsive gels has been reported by Cametti, Mandolini, Žinić, and co-workers.²⁸⁹ They reported that the anthraquinone-derived oxalamide **181** possesses excellent gelation properties toward aromatic solvents and alcohols. The anion binding properties of **181** toward a series of anionic guests (F^- , Cl^- , Br^- , I^- , AcO^- , $H_2PO_4^-$) in DMSO was investigated by means of UV-vis spectroscopy and revealed that only F^- is able to cause dramatic changes in the electronic absorption spectra with concomitant color changes visible to the naked eye. Upon the addition of fluoride in *p*-xylene a disruption of the gel is observed, because in this solvent the anion is poorly solvated and can compete with the NH gelator groups. In contrast, the better solvation of fluoride in EtOH makes it a less efficient competitor for the gelator NH groups, and a reddish-colored gel is obtained (Figure 67).

Clarke and Steed have shown that also urea-based gels can be influenced by the presence of anions.^{290a} A series of chiral gelators of type **182** have been synthesized. The compounds with an even number of methylene spacer units ($n = 2, 4, 6$, and 8) act as gelators in solvents such as acetonitrile and $CHCl_3$ (Figure 68). Upon addition of anions to a warmed MeCN solution of **182** 1:1 adducts are formed with a binding constant of $K_a = 18\,000\,M^{-1}$ for AcO^- determined by 1H NMR. The formation of host-anion complexes is in competition with dimerization (self-aggregation) of the urea in a fashion consistent with the beginning of gelation. Rheological measurements on the gel itself at room temperature (i.e., below T_{gel}) can give insight into the effect of the anion binding process upon gel strength, as measured by the storage modulus (G') and yield stress. These quantities were determined for $CHCl_3$ gels of **182** (Figure 68),

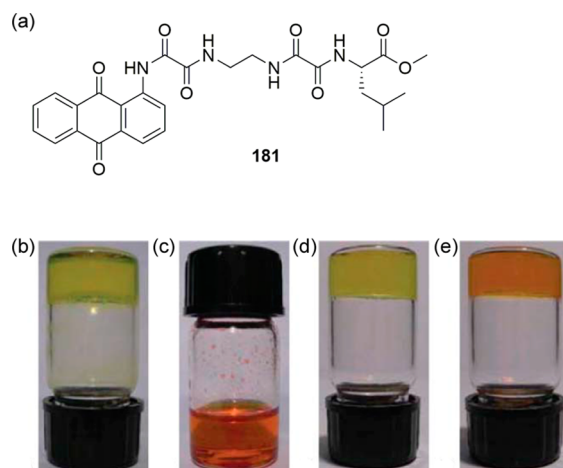


Figure 67. (a) Structure of compound **181**. (b) Gel of **181** in *p*-xylene. (c) *p*-Xylene solution from gel of **181** in the presence of F^- . (d) Gel of **181** in EtOH. (e) Gel of **181** in EtOH in the presence of F^- . Reprinted with permission from ref 289. Copyright 2007 Royal Society of Chemistry.

both for the free gelator and in the presence of 0.1 mol equiv of various anions. While weakly bound anions such as BF_4^- have almost no effect on the gel characteristics, anions with higher affinity reduce G' in a way that loosely correlates with anion-gel binding affinity. Thus, G' is reduced by ca. 1 order of magnitude in the presence of chloride anion and ca. 2 orders of magnitude by the more strongly bound acetate anion for the $n = 6$ compound.

de Mendoza and collaborators demonstrated that chiral bicyclic diguanidinium chloride **183** (Figure 69) forms gels in apolar aromatic solvents.^{290b} Interestingly, upon addition of different aqueous tetrabutylammonium salt solutions in toluene or *p*-xylene (*R*)-**183** gels and after heating up, mixing vigorously, and cooling down the biphasic system, different behaviors are observed. Chloride or bromide solutions lead to stable gels, whereas solutions containing AcO^- , BzO^- , NO_3^- , PF_6^- , and HSO_4^- ions cause the disruption of the aggregation. These observations suggest that the anion dependence on gel formation

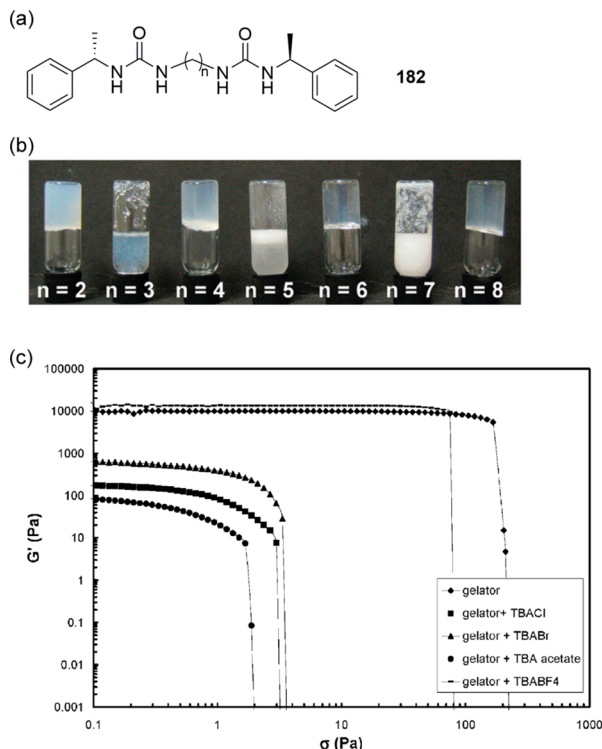


Figure 68. (a) Structure of gelator 182. (b) Picture of alternation of gel (even n) and sol (odd n) formation in CHCl_3 by 182. (c) Influence of different anions on the storage modulus (G') at 20°C as a function of oscillation stress (σ) of the 1% by weight gel of compound 182 with $n = 6$ in CHCl_3 . Reprinted with permission from ref 290. Copyright 2007 Royal Society of Chemistry.

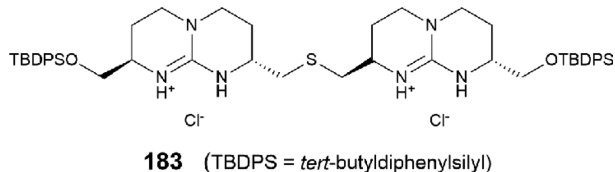


Figure 69. Structure of chiral gelator 183.

mainly responds to geometrical and spatial factors. Likely, spherical halides, such as chloride or bromide, allow a correct arrangement of aggregates, whereas the oxoanions with different geometries, such as acetates, sulfates, and nitrates, do not permit a suitable interaction between diguanidinium molecules, thus preventing gel formation.

Very recently, Lin, Wei, and co-workers described the ability of hydrazone gelator 184 to colorimetrically sense fluoride.²⁹¹ The peculiarity of this system, which can form stable gels in DMSO and DMF, is that the fluoride recognition process does not cause a gel–sol phase change. As shown in Figure 70, addition of solid TBAF to the gel causes a color change in the material, and this process is reversible upon addition of H^+ . Interestingly, scanning electron microscopy (SEM) demonstrates that although the macrophase of the gel is not affected by the presence of fluoride, its micromorphology is influenced by the presence of the anion: the entangled tape-like structure of the gel evolves into a layer structure upon addition of F^- (Figure 70). The authors attribute this phenomenon to the deprotonation of the N–H group caused by the anion. When the N–H group is deprotonated, hydrogen bonding between the gelator molecules does not occur and the gelator is assembled by van der Waals forces among the

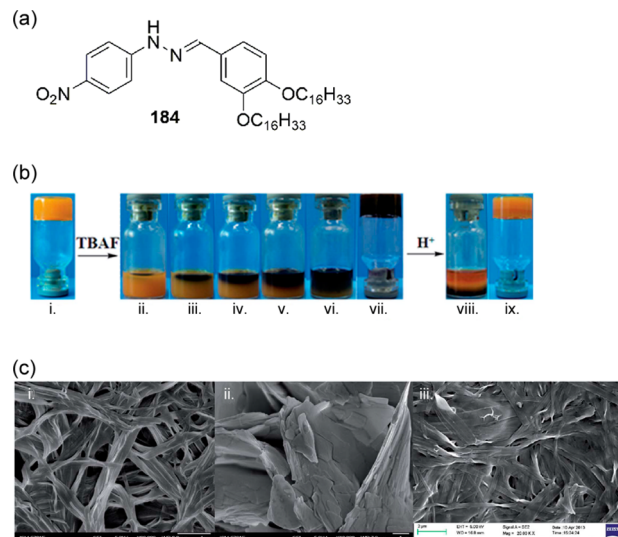


Figure 70. (a) Structure of gelator 184. (b) Color changes of the gel upon addition of fluoride: (i) free gel (0.8%, in DMSO); (ii) immediately after addition of solid TBAF (5 equiv); (iii) after 30 min; (iv) after 90 min; (v) after 150 min; (vi and vii) after 220 min; (viii) addition of 0.05 mL of HClO_4 (0.01 M) after 10 min; (ix) after 20 min. (c) SEM images of (i) xerogel of 184 (0.8%, in DMSO); (ii) after treatment with F^- in situ; (iii) xerogel treated with F^- in situ, then added HClO_4 (0.01 M). Reprinted with permission from ref 291. Copyright 2014 Royal Society of Chemistry.

long alkyl chains and π – π stacking interactions among the nitrophenyl groups. Upon addition of H^+ the micromorphology is restored (Figure 70).

Some examples of anion-responsive gels containing metals have also been reported. Aida and co-workers, for example, described the behavior of the trinuclear Au(I) pyrazolate complex 185.²⁹² In hexane this complex self-assembles via aurophilic interactions to form a red luminescent organogel ($\lambda_{\text{em}} = 640 \text{ nm}$). When a small amount of Ag(I) is added to the gel, the fluorescence turns to blue ($\lambda_{\text{em}} = 458 \text{ nm}$) without disrupting the structure of the gel. Interestingly, upon addition of chloride to the doped gel the red luminescence is restored because Ag(I) is removed by the anion. Upon heating, these organogels undergo gel-to-sol transition due to the destabilization of the metallophilic interactions. The red luminescence of the nondoped system becomes hardly visible, while the blue luminescence of the Ag(I) -doped system turns green ($\lambda_{\text{em}} = 501 \text{ nm}$). On cooling, these solutions undergo gelation and synchronously recover the original luminescence (Figure 71).

Lee and co-workers reported on the reversible sol–gel interconversion of Ag(I) coordination polymers of receptor 186 in aqueous media due to changes from folded helical chains to an unfolded zigzag conformation with counteranion exchange.²⁹³ As shown in Figure 72 the process is driven by depolymerization or conformational change. The Ag(I) complex of 186 in water undergoes spontaneous gelation at concentrations above 2.5% in weight. Upon addition of 1.2 equiv of TBAF to the gels, a fluid solution is obtained. This is due to the strong electrostatic interactions between Ag(I) and fluoride which causes the coordination polymer to depolymerize. Upon addition of 1.2 equiv of TBABF_4 the solution returns to the gel state. The gels also reversibly transform into a fluid solution with counteranion exchange of BF_4^- with a larger ion, $\text{C}_2\text{F}_5\text{CO}_2^-$.

An iodide-responsive hydrogel has been reported by Jiang and co-workers.²⁹⁴ This system is based on a Ag(I) GSH

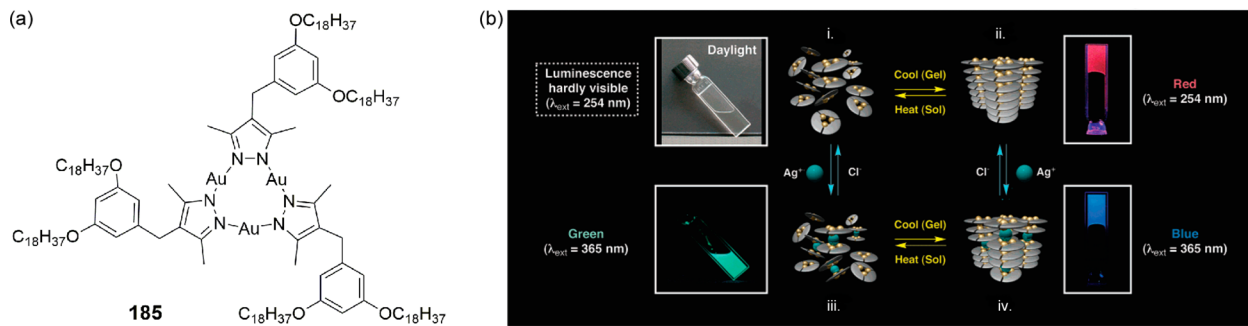


Figure 71. (a) Structure of the trinuclear Au(I) pyrazolate complex **185**. (b) Luminescence profiles of **185** in hexane. Pictures and schematic self-assembling structures: (i) sol, (ii) gel, (iii) sol containing AgOTf (0.01 equiv), and (iv) gel containing AgOTf (0.01 equiv). Reprinted with permission from ref 292. Copyright 2005 American Chemical Society.

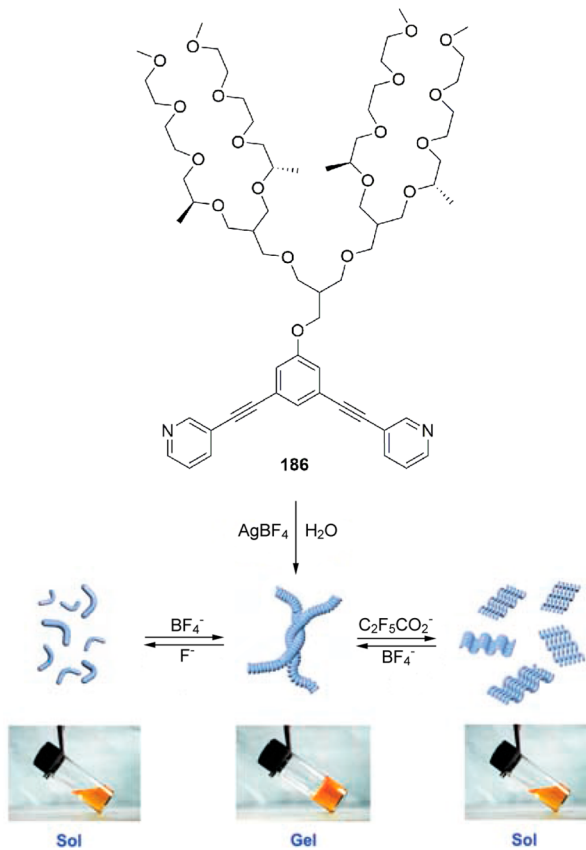
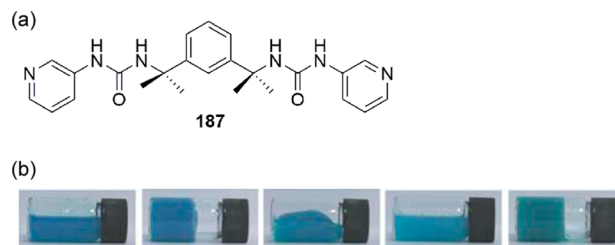


Figure 72. Structure of gelator **186**, and schematic representation of reversible polymerization and reversible conversion between folded and unfolded conformations of a coordination chain upon counteranion exchange. Reprinted with permission from ref 293. Copyright 2005 Wiley-VCH.

coordination polymer which undergoes gelation in water under acidic conditions. Upon addition of different anions (F^- , Cl^- , Br^- , I^- , and H_2PO_4^-) only iodide is able to trigger the hydrogel to perform a macroscopic gel–sol state transition with the formation of a slightly yellow fluid. Upon addition of 1 equiv of Ag(I) to the resulting sol solution a reversible sol–gel state transition can be performed.

Clarke and Steed described the behavior of the gelator **187** that contains both cation binding sites (the pyridyl groups) and anion binding sites (the urea groups).²⁹⁵ In MeOH in the presence of CuBr_2 a robust blue gel is formed upon shaking. The formation of the gel is unique in the presence of CuBr_2 and does

not occur for other anions such as Cl^- , AcO^- , NO_3^- , or BF_4^- . Acetate binding significantly influences the rheology of **187**/ CuBr_2 metallo-gel. As shown in Figure 73, upon addition of 1



equiv of tetrabutylammonium acetate (with respect to **187**) a dramatic disruption of the gel occurs after 30 min and a viscous liquid is obtained. Remarkably, the gel can be “healed” upon addition of an external stimuli, i.e., addition of 1 equiv of $\text{Cu}(\text{BF}_4)_2$.

2.5. Dual- and Triple-Channel Anion Sensors

When two or more different sensing reporters (a fluorophore and a redox-active unit, for example) are integrated in the same receptor, the system can give multiple outputs (responses) and we can describe them as multichannel sensors. The advantage of multichannel sensors lies in the fact that different anions can give a different set of outputs, allowing the selective discrimination of more than one type of anion at the same time and leading to increased selectivity and sensitivity.

Examples of dual-channel sensors that combine together fluorescence and redox sensing properties have been reported by Tarraga, Molina, and co-workers. Two examples of ferrocene benzobisimidazole-based systems **188** and **189** have been described by this research group in which the metallocene unit is directly linked to a π -extended imidazole ring such as 2,2'-biferrocenyl benzobisimidazole **188** and 2,2'-biferrocenylbisimidazole **189**.²⁹⁶ Compound **188** behaves as a highly selective redox, chromogenic, and fluorescent chemosensor molecule for AcO^- anions in $\text{DMSO}/\text{H}_2\text{O}$. The two receptors show only a reversible two-electron oxidation peak at $E_{1/2} = 0.57$ versus decamethylferrocene (DMFc), indicating that the two metal centers in these compounds are electronically decoupled. Upon

addition of AcO^- (in water) in a solution of **181** in DMSO a typical two-wave behavior, which is due to the anion complex, is clearly observed as shown in the evolution of the OSWV voltammetry reported in Figure 74. For receptor **189** under the

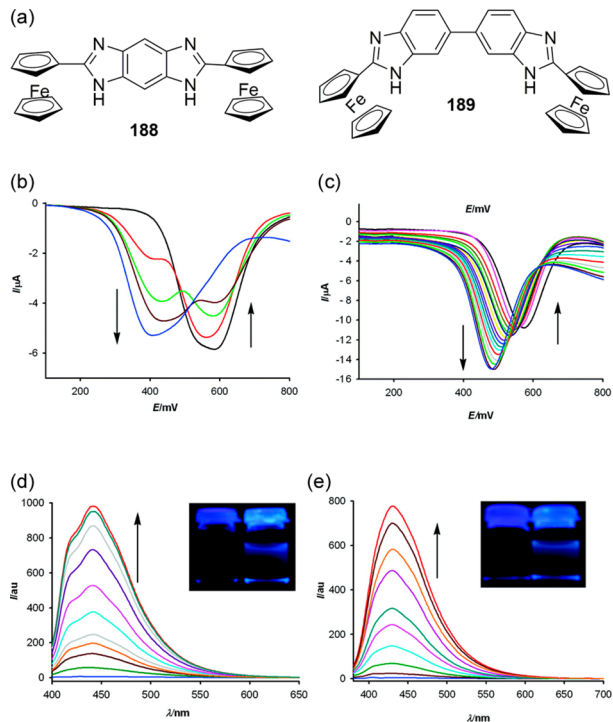


Figure 74. (a) Structures of receptors **188** and **189**. (b) Evolution of the OSWV of **188** with AcO^- . (c) Evolution of the OSWV of **189** with $\text{HP}_2\text{O}_7^{3-}$. (d) Changes in the emission properties of **188** with AcO^- . (e) Changes in the emission properties of **189** with H_2PO_4^- . Reprinted with permission from ref 296. Copyright 2010 American Chemical Society.

same electrochemical conditions the ferrocene/ferrocenium redox peak shows a “shifting behavior” and a new oxidation peak emerges at a potential cathodically shifted from that of the free receptor in the presence of the oxoanions $\text{HP}_2\text{O}_7^{3-}$ ($\Delta E_{1/2} = -90$ mV) and H_2PO_4^- ($\Delta E_{1/2} = -80$ mV). The anion binding ability of **188** and **189** has also been examined by UV-vis spectroscopy. In the case of receptor **188**, significant modifications in the absorption spectrum of the free receptor are observed only in the presence of AcO^- . Receptor **189**, instead, gives a different response upon addition of $\text{HP}_2\text{O}_7^{3-}$ and H_2PO_4^- : for the former a red shift of 10 nm for the band at 332 nm ascribed to ligand-centered $\pi-\pi^*$ electronic transitions ($L-\pi^*$) in the free receptor was observed, while for the latter the progressive appearance of a new band located at $\lambda = 384$ nm as well as a decrease of the band at 332 nm was observed. Finally, the selectivity toward anions has been assessed by means of fluorescence spectroscopy. Again, selectivity for AcO^- is observed for receptor **188** with an increase of the fluorescence band of the free receptor at 428 nm with a concomitant red shift of 13 nm (Figure 74). After addition of 1 equiv of aqueous H_2PO_4^- to a solution of receptor **189** in DMSO, the emission band is red shifted from 405 to 430 nm (Figure 74). Similar but smaller changes were observed in the presence of aqueous $\text{HP}_2\text{O}_7^{3-}$.

The same research group also described the binding properties of the ion-pair receptor **190**.²⁹⁷ As shown in Figure 75, this system exhibits a strong perturbation of the redox potential of the

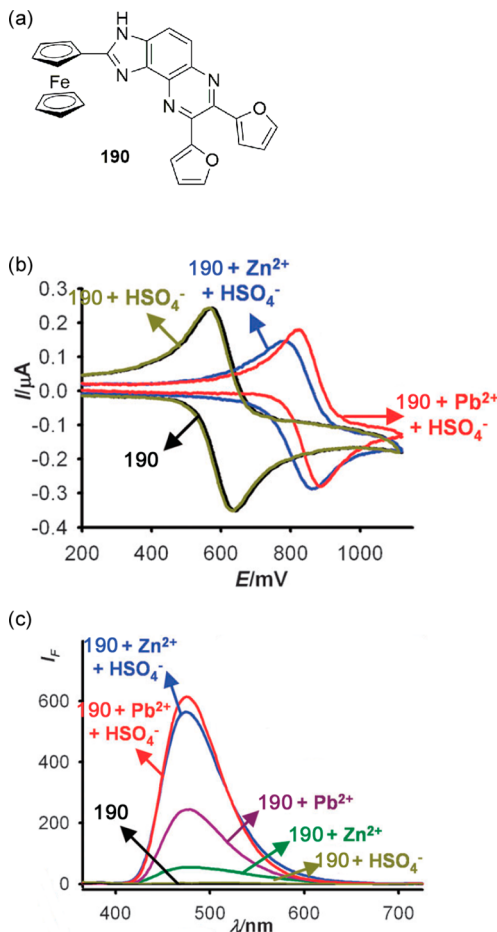


Figure 75. (a) Structure of receptor **190**. (b) Changes in the CV spectra in MeCN in the presence of 1 equiv of the indicated species. (c) Changes in the emission spectra in MeCN in the presence of 1 equiv of the indicated species. Reprinted with permission from ref 297. Copyright 2012 Royal Society of Chemistry.

ferrocene unit upon addition of HSO_4^- in MeCN only in the presence of Pb^{2+} , with a cathodic shift of the oxidation peak ($\Delta E_{1/2} = 245$ mV), and Zn^{2+} ($\Delta E_{1/2} = 220$ mV). The addition of only hydrogensulfate does not cause any changes in the redox potential of **190**. A remarkable enhancement of the fluorescence is also observed when to a solution of **190** and Pb^{2+} or Zn^{2+} 1 equiv of HSO_4^- is added.

Dual-channel sensors comprise also the combination of a sol-gel transition with color/fluorescence changes. Some examples have already been described in the previous section.^{289,291,292} Nonetheless, other examples of dual-channel sensors able to determine the presence of anions such as fluoride or acetate by a color change and a transition from gel to sol have been reported.^{298–300} In particular, Wei et al. described a dual-channel sensor that can recognize F^- , AcO^- , and H_2PO_4^- through proton-controlled reversible sol-gel transition and color changes.³⁰⁰ They reported the supergelator (a gelator able to gel at concentrations lower than 1% in weight) **191** bearing phenol O-H and acylhydrazone N-H groups with gelation ability in polar solvents such as DMF and DMSO. The organogel of **191** exhibits gel-sol transition according to the stimulus of anions. In particular, as shown in Figure 76, the addition of solid TBAF (5 equiv) to the DMF gel of **191** at 20 °C causes a gradual decomposition of the gelatinous state in about 15 min, yielding an wine-colored solution. Similarly, the addition of solid

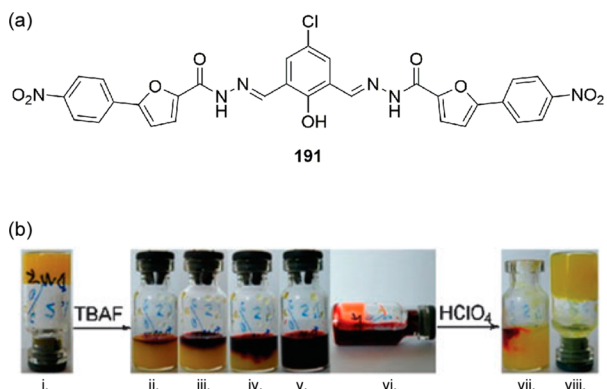


Figure 76. (a) Structure of the gelator **191**. (b) Pictures of the organogel formed from a solution of **191** in DMF (23.3 mM): (i) initial gel, (ii) immediately after addition of solid TBAF (5 equiv), (iii) after 2 min, (iv) after 8 min, (v and vi) after 15 min, (vii and viii) immediately after addition of 0.30 mL of HClO₄ (0.1 M) to the above obtained solution. Reprinted with permission from ref 300. Copyright 2010 Royal Society of Chemistry.

TBAAcO or TBAH₂PO₄ also leads to the gel–sol transition and color change, but the transition happens in a longer period of time. Under the same conditions, the addition of Cl⁻, Br⁻, I⁻, HSO₄⁻, and ClO₄⁻ (all used as solid TBA salts) did not lead to gel decomposition. Proton NMR titrations suggest that the deprotonation is the main cause of the disruption of the gel. For this reason, upon addition of an acid to a solution of **191** and TBAF, the solution regelates immediately.

It is worth highlighting here the work reported by Hamilton and Choi in 2001.³⁰¹ Macrocycle **192** is able to sense H₂PO₄⁻ over other anions (Cl⁻, p-TsO⁻, PhPO₃H⁻) in DMSO:1,4-dioxane (1:1, v/v) via a dual-channel fluorescence emission. Indeed, as shown in Figure 77 this system is able to give a double

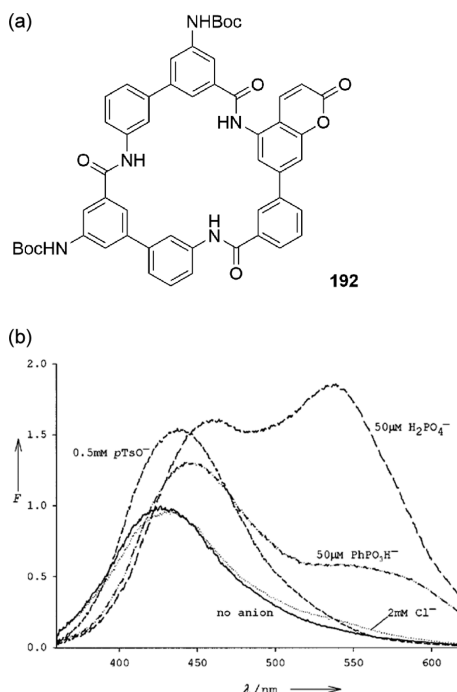


Figure 77. (a) Structure of receptor **192**. (b) Changes in the fluorescent emission of **192** upon addition of different anions. Reprinted with permission from ref 301. Copyright 2001 Wiley-VCH.

emission: anion binding close to the fluorophore can lead to the stabilization of the positive charge developed in the fluorophore excited state and to the opening of another fluorescence emission channel through intermolecular excited state proton transfer (ESPT). Emissions from the two channels show different anion dependencies, and as a result, more selective and sensitive sensing is achieved, although a single sensing technique (fluorescence in this case) is used. The binding of all tetrahedral anions studied causes an increase in the fluorescence intensity and a red shift of the peak maximum presumably due to the stabilization of the fluorophore excited state relative to the ground state on anion binding. However, only H₂PO₄⁻, the most basic among the anions considered, is able to open the second emission channel deriving from the proton transfer from the fluorophore excited state, and a second emission band at longer λ_{em} values is observed (Figure 77).

A very recent example of a sensor that can selectively detect Cys and GSH from different emission channels at two different excitation wavelengths has been reported by Guo and co-workers.³⁰² The chlorinated coumarin-hemicyanine dye **193** has three potential reaction sites which elicit three different chemical reactions toward Cys, Hcy, and GSH, as shown in Figure 78. Given the distinct chemical structures and absorption wavelengths (spanning from 360 to 450 nm for **193e**, **193f**, and **193h**) Cys, Hcy, and GSH can be simultaneously and selectively sensed by **193**. Effectively, different emission behaviors are observed upon addition of these thiols following time-dependent fluorescence spectra in the same conditions with N-acetylcysteine (NAC) as a control (Figure 78). In water buffered at pH 7.4, upon excitation at 360 nm (the maximum of emission of **193e**) a new emission peak appears at 420 nm and reaches equilibrium within 60 min in the presence of Cys, while Hcy, GSH, and NAC do not cause any change in the emission of **193**. Choosing the excitation wavelength of **193h** (450 nm), only the addition of GSH leads to the appearance of a new emission peak at 512 nm which reaches equilibrium within 60 min. Again, the response of the system is highly selective; when excitation at 500 nm (the maximum absorption wavelength for **193f**) is employed for this system, no fluorescence turn on is observed.

The ability of **193** to selectively sense Cys and GSH in biological systems has also been assessed. When COS-7 cells are incubated with **193** (10 μM), both blue and green emissions are observed, indicating that **193** is responsive to intracellular Cys and GSH. When COS-7 cells are pretreated with 0.5 mM Cys and then incubated with **193**, a marked increase in blue emission and a slight decrease in green emission are observed. When COS-7 cells were pretreated with 0.5 mM GSH and then incubated with **193**, a marked increase in green emission and a slight decrease in blue emission are observed.

2.6. Conclusions and Outlook on Anion Sensing

The examples discussed above demonstrate that anion sensing is a highly active area of supramolecular chemistry, and much effort has been put in the development of systems able to selectively sense anions in pure water. Most of the papers reported to date in the literature are devoted to molecular sensors, but recently, other types of sensors based on smart materials (gels and nanoparticles, for example) or on microarrays have been developed. We can expect the variety of methods used to sense anions to grow in the future along with the development of a wider range of anion detection methods in biological systems.

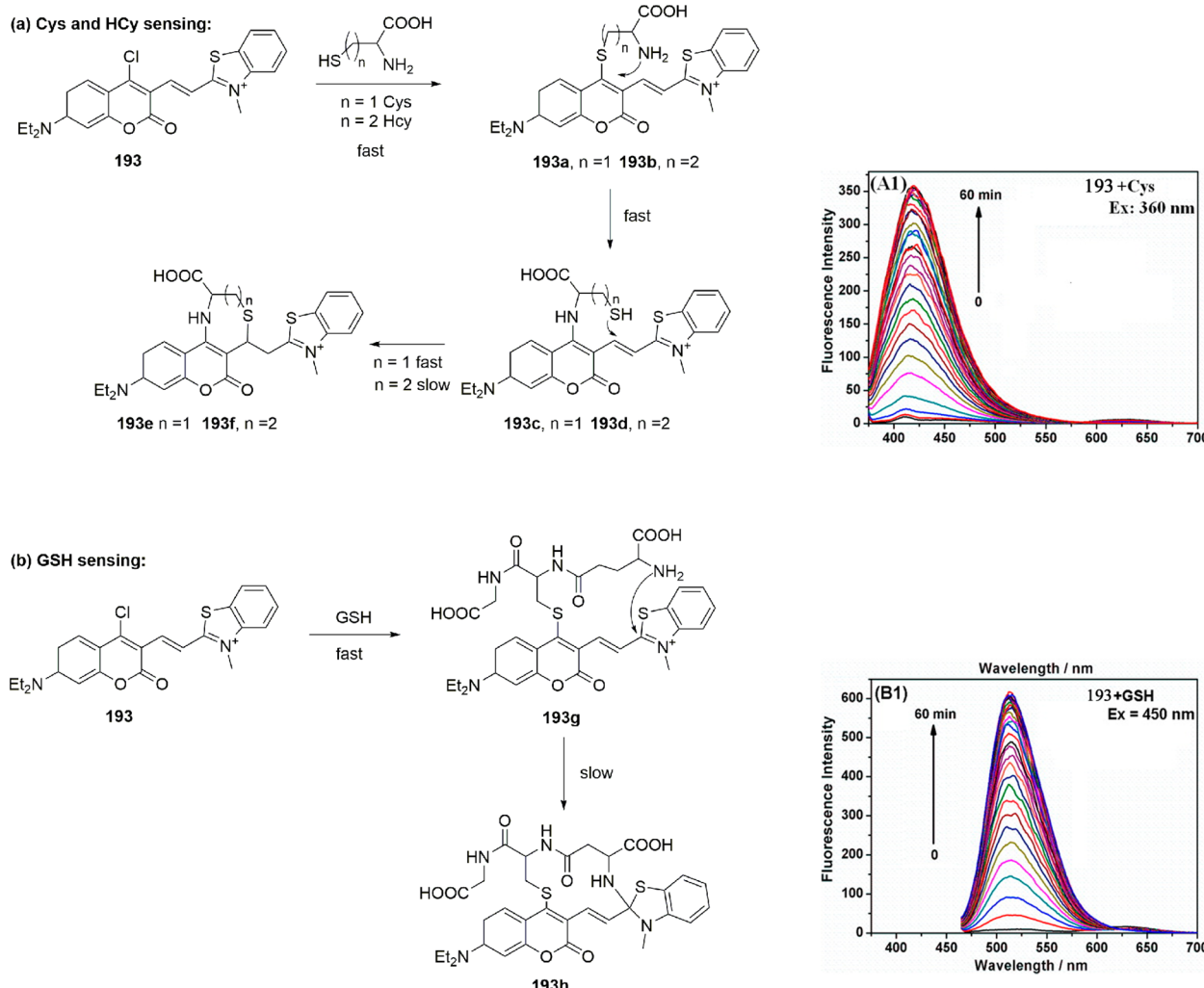


Figure 78. Proposed reaction mechanisms of compound **193** with Cys, Hcy, and GSH along with the time-dependent fluorescence response of **193** ($1\ \mu\text{M}$) in water buffered at pH 7.4 toward 10 equiv of Cys excited at 360 nm (A1) or 10 equiv of GSH excited at 450 nm (B1). Spectra reprinted with permission from ref 302. Copyright 2014 American Chemical Society.

3. EXTRACTION AND SEPARATION OF ANIONS

Anion extraction is another important application of supramolecular chemistry and mainly focuses on the removal of potentially harmful anions from the environment. This encompasses the removal of nitrates and phosphates to prevent algae bloom,³⁰³ the removal of radioactive anions such as TcO_4^- from waste waters,³⁰⁴ the removal of sulfate from radioactive waste to allow vitrification,³⁰⁵ and the removal of other toxic anions such as CN^- or AsO_4^{3-} , but anion extraction can also be employed in metallurgy through the extraction of metalate anions or ion pairs.³⁰⁶ These goals are usually achieved by liquid–liquid extraction techniques, but solid-phase extraction and selective crystallization have also gained popularity in recent years. There are a number of other techniques for removing or separating anions based on more analytical or chromatographical approaches (e.g., commercial anion-exchange resins), but this review will focus on the use of supramolecular concepts to achieve the extraction of anions.

Most extraction processes involve the removal of the anion from an aqueous solution and will therefore often depend on the hydrophobicity of both the receptor and the anion (similar to the design of ion-selective electrodes, see section 2.3). An important concept in extraction chemistry is therefore the Hofmeister

series, which orders anions according to their ability to “salt out” proteins and is widely considered to be related to the aqueous solvation (hydrophobicity) of the anions (Figure 79).^{307,308} This



Figure 79. Hofmeister series.

often results in an inherent Hofmeister bias during extraction processes, where more hydrophobic anions are extracted more easily into apolar solvents. In order to achieve selective extraction of one particular anion, it is therefore necessary to design anion receptors that can overcome this Hofmeister bias by strong binding.

It is also important to note that the extraction of an anion from one phase to another needs to be an overall electroneutral process, and hence, charge neutrality needs to be maintained. This can be achieved by using charged anion receptors where the original counteranion is exchanged for the anion to be extracted (Figure 80a), using ditopic receptors that can bind both an anion and a cation (either a metal cation or a proton) (Figure 80b), using a combination of an anion-extracting agent and a cation-

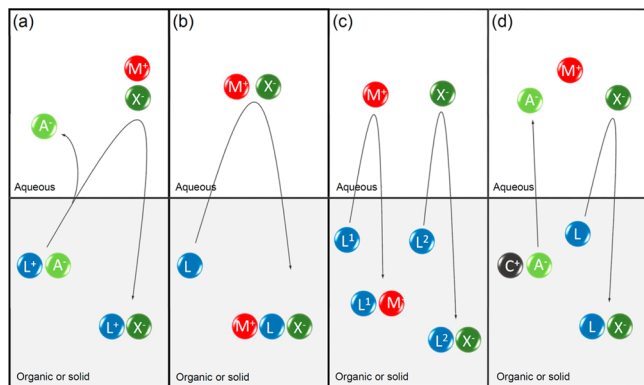


Figure 80. Various approaches to maintain charge neutrality in extraction experiments. (a) Employing a charged ligand L^+ . (b) Employing a ditopic ligand L that can bind both anions and cations. (c) Employing a mixture of ligands for cations, L^1 , and anions, L^2 . (d) Employing a lipophilic cation C^+ in combination with a neutral ligand L .

extracting agent (Figure 80c), or providing a separate lipophilic cation in the organic phase whose counteranion can be exchanged (Figure 80d). Additionally, in an industrial or environmental context, there needs to be a mechanism to recover the extracting agent and the extracted anion (stripping) so that the receptor can be reused multiple times. This aspect should be taken into account when designing and testing new potential anion receptors with anion extraction ability.

3.1. Liquid–Liquid Extraction

Liquid–liquid (or solvent) extraction is the most widely studied form of anion extraction and involves the transfer of a given anion from one liquid phase to another liquid phase (usually from an aqueous phase to an organic phase). This review focuses on the progress in this field in the past decade (2004–2014), and the reader is referred to other reviews and books for older examples.^{309–313} Moyer and co-workers also published a number of papers concerning in-depth investigations of the thermodynamics of anion extraction processes such as synergism and ion pairing.^{314,315}

3.1.1. Extraction of Halide Anions. Halide extraction can be useful for corrosion prevention but also as a means to coextract potentially harmful cations. Moyer, Sessler, Delmau, and co-workers investigated the solvent extraction ability of *meso*-octamethylcalix[4]pyrrole **194**.³¹⁶ Early studies had shown that this calixpyrrole can function as a ditopic receptor for CsCl and CsBr in both the solid state and solution, whereby the anion is bound by four hydrogen bonds to the pyrrole NHs and the cesium cation is bound in the electron-rich “cup” that is formed upon anion binding (see Figure 81).³¹⁷ This encouraged the authors to test if **194** can extract Cs^+ salts from an aqueous phase into nitrobenzene using a radiotracer (^{137}Cs) to determine the cesium concentrations in both the aqueous and the organic phases. It was observed that **194** is unable to extract $CsNO_3$ into nitrobenzene, in agreement with the low affinity of calix[4]-pyrrole for nitrate anions. On the other hand, **194** was found to extract both CsCl and CsBr into nitrobenzene, and the extraction efficiency for this process depended linearly on the initial Cs salt concentration and on the concentration of the receptor, suggesting the formation of a 1:1:1 cesium:halide:calixpyrrole ion-pair receptor complex. The dependence of the cesium extraction ability on the counteranion suggests that the extraction ability of **194** is due to its ability to function as a ditopic receptor, where only anions that can stabilize the cup

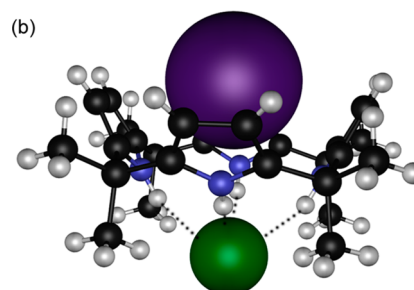
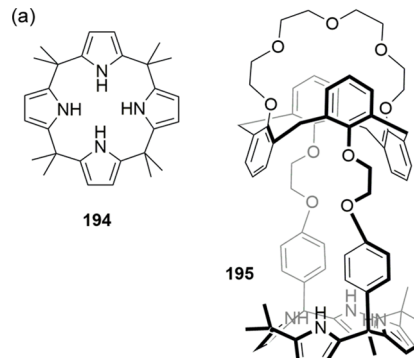


Figure 81. (a) Structure of calix[4]pyrroles **194** and **195**. (b) Crystal structure of the CsCl complex of **194**. Solvent molecules are omitted for clarity; the receptor is shown in ball-and-stick representation with the bound ions in space fill (0.6 times the van der Waals radius), and the atoms are color coded as follows: C (black), N (blue), H (white), Cl (green), Cs (purple). Hydrogen bonds are represented by dotted lines.

conformation of the calix[4]pyrrole and thereby allow the binding of cesium cations are able to induce extraction by **194**. Subsequent studies have found that the extraction selectivity of the calixpyrrole can be changed by appropriate structural modifications. Ditopic receptor **195**, for example, was shown to preferentially bind and extract KF over CsF from an aqueous solution into nitrobenzene.³¹⁸ Proton NMR studies and X-ray diffraction suggest that the K^+ ion is bound in the calix[4]arene-crown-5 unit, and the fluoride ion is bound by the pyrrole NH moieties.

In a later study, Akar, Bielawski, Sessler, and colleagues prepared a calix[4]pyrrole-appended methyl methacrylate copolymer **196** (Figure 82).³¹⁹ This polymer was found to be highly soluble in organic solvents, and the authors thus investigated the liquid–liquid anion extraction ability of **196** using a 1H NMR system with the anion present as a tetrabutylammonium (TBA) salt in a D_2O layer on top of a solution of **196** in CD_2Cl_2 and thermogravimetric analysis. It was found that **196** is able to extract TBA chloride and TBA fluoride into dichloromethane but not TBA phosphate. Furthermore, it was observed that the extraction ability was higher for chloride compared to fluoride. This finding does not agree with the anion affinity of calix[4]pyrrole in organic solvent ($F^- > Cl^- > H_2PO_4^-$) but is consistent with the Hofmeister series, and so the more hydrophobic chloride anion is extracted more easily. Interestingly, *meso*-octamethylcalix[4]pyrrole **194** and poly-(methyl methacrylate) alone were unable to extract TBA fluoride into dichloromethane, and the TBA chloride extraction ability was also significantly lower compared to copolymer **196**. Similar results were obtained by Aydogan and Akar for oligomeric calix[4]pyrroles.³²⁰ These findings suggest that polymer back-

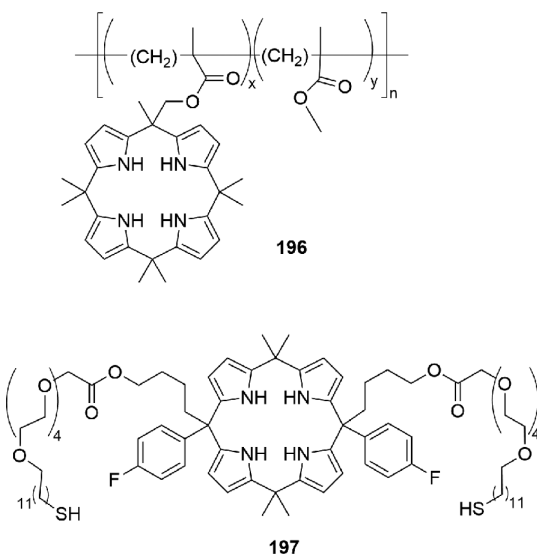


Figure 82. Structure of calix[4]pyrroles **196** and **197**.

bones can enhance the extraction ability of anion receptors through multivalency and introduce a means of easily fine tuning the solubility, stability, and other properties of the extracting agent. This was later shown by the same authors, who found that a poly(methyl methacrylate) copolymer appended with both calix[4]pyrrole and crown ether units is able to extract KCl and KF from aqueous media.³²¹ The advantage of multivalency was further established by Sessler, Lee, and colleagues by preparing gold nanoparticles decorated with double-armed calix[4]pyrrole 197.³²² It was shown that these nanoparticles were able to efficiently extract TBA fluoride from D₂O into CDCl₃, while the analogous monomeric calixpyrrole proved to be a poor anion extractor under similar conditions.

Flood and co-workers also employed the advantages of a polymeric backbone for the extraction of chloride salts.³²³ They synthesized PMMA copolymers such as 198 with triazole-containing appendages capable of binding anions through C–H···anion hydrogen bonding (Figure 83). ¹H NMR experiments

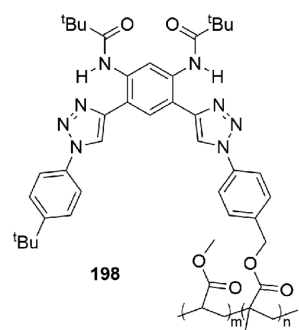


Figure 83. Structure of triazole-based receptor 198.

showed that the copolymers can extract tetrapropylammonium chloride from water to dichloromethane more effectively than a pure PMMA polymer. The ability of the copolymer to bind chloride was confirmed by ^1H NMR titrations in CD_2Cl_2 . The observed anion affinity and anion extraction ability is presumed to arise from hydrogen bonding to the triazole CH, which is strongly polarized due to the presence of the three nitrogen atoms in the ring and therefore serves as a good hydrogen-bond donor.

Davis and co-workers studied a range of cholic-acid-based receptors with appended hydrogen-bond-donating groups (coined cholapods). Initially the authors investigated the affinity of a series of 13 acyclic cholapods of general structure 199 (Figure 84) for 7 monovalent anions (Cl^- , Br^- , I^- , NO_3^- , AcO^- ,

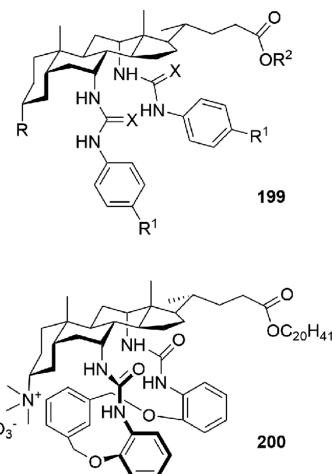


Figure 84. Structure of cholapods 199 and 200.

ClO_4^- , and EtSO_3^-) and used an extraction-based technique to determine the affinity constants.³²⁴ In brief, an aqueous solution of tetraethylammonium (TEA) salts was equilibrated against a chloroform solution of the cholapod and allowed to phase separate, and ^1H NMR integration against an internal 1,1,2,2-tetrachloroethane standard subsequently allowed the determination of extraction constants that can be converted into affinity constants. It was found that the cholapods are able to extract all investigated anions into chloroform, but the relative selectivities for chloride depend on both the geometry of the binding site and what the authors called the affinity-selectivity principle. It was observed that as the association constant toward Cl^- increased, the selectivity figures for Br^- , I^- , NO_3^- , ClO_4^- , and EtSO_3^- decreased (but increased for AcO^-), and thus, for receptors that bind anions mainly through hydrogen-bond formation, the stronger the binding to the anions, the higher the selectivity for anions that form stronger hydrogen bonds. In a later study, the same group attempted to increase the extraction selectivity by synthesizing cationic macrocyclic "cholaphanes" such as xylol-bridged **200** (Figure 84).³²⁵ Similar chloroform–water extraction experiments as described above revealed an anti-Hofmeister anion selectivity for **200** where the extractability changes as $\text{Br}^- > \text{I}^- \approx \text{Cl}^- > \text{NO}_3^- > \text{PF}_6^- > \text{AcO}^- \approx \text{EtSO}_3^-$. Thus, the most hydrophobic anion (PF_6^-) is extracted less efficiently than the spherical halide anions in an anti-Hofmeister selectivity. This preference for halides is presumably due to steric complementarity between the macrocycle and chloride anions, as suggested by computer modeling. This ability of the cholapods to extract chloride anions has prompted Davis and colleagues to also investigate the ability of the cholapods to transport chloride anions across phospholipid bilayers, which will be discussed in the following section (section 4.2).

Galbraith et al. investigated the anion extraction ability of *salen* derivatives containing additional protonatable sites and hydrogen-bond donors for anion binding (201–203, Figure 85).^{326a,b} The copper complexes of these receptors were shown to extract HCl and H₂SO₄ into chloroform solutions but with a higher selectivity for Cl⁻ extraction over SO₄²⁻ extraction. Bulk liquid

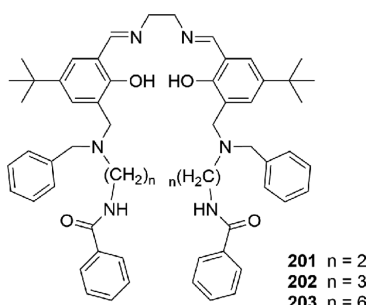


Figure 85. Structure of receptors **201–203**.

membrane transport studies, where the extraction of the anion from a source phase is combined with the stripping of the extracted anion in a receiving water phase, were also performed for a number of anions. The observed transport selectivity followed the Hofmeister series, and the halide anions (Cl^- , Br^-) and nitrate were transported most efficiently. Sulfate or phosphate transport was not observed in the presence of chloride, bromide, or nitrate. Although potentiometric titrations in 95:5 methanol:water suggested that the copper complexes can bind sulfate more strongly than chloride, the extraction selectivity of these compounds appears to be dominated by the hydrophobicity of the anions rather than the anion binding strength.

Gattuso et al. introduced halogen bonding as a useful noncovalent interaction for the extraction of iodide into a fluorous phase.³²⁷ Single crystals grown from an ethanol solution of CsI, cation receptor **204**, and 1,4-diiodoperfluorooctane (**205**) revealed the existence of a charge-separated supramolecular salt where the cesium cation is located in the crown-ether strap of calixarene **204** and is further screened by the picolyl and inverted phenol moieties, while the iodide anions are stabilized by hydrogen bonds to ethanol molecules and halogen bonds to **205** (Figure 86). Additional ^{19}F NMR experiments in chloroform/methanol showed that this halogen bond between iodide and **205** also persists in solution. The authors then checked if this system can be used to extract CsI into a water-immiscible fluorous phase. 1,4-Diiodoperfluorobutane (**206**) was chosen as the fluorous phase because it can simultaneously serve as a halogen-bond-donating replacement for **205**. ^1H NMR

and ion-exchange chromatography revealed that a solution of **204** in **206** is indeed able to extract CsI from a 2 mM aqueous solution with a distribution coefficient of 2.7. Both components (cesium extracting agent **204** and perfluorinated solvent **206**) were shown to be necessary for CsI extraction, as neither a solution of **204** in chloroform nor **206** alone was able to mediate CsI extraction. The system was found to be selective for CsI as neither CsNO_3 , NaI , nor KI was extracted into the fluorous phase.

Fluoride anions are an attractive target for anion extraction studies because high fluoride concentration can be detrimental for human health and due to the high hydrophilicity of this anion makes it a very challenging anion to extract from water. Ganguly, Das, and colleagues reported the fluoride sensing and extracting ability of phosphonium salt **207** (Figure 87).³²⁸ It was shown that

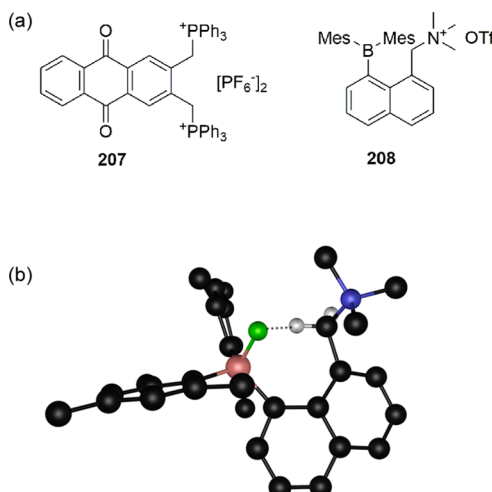


Figure 87. (a) Structures of **207** and **208**. (b) Crystal structure of the **208**-F complex shown in ball-and-stick representation, and the atoms are color coded as follows: C (black), N (blue), H (white), F (light green), B (pink). Noncoordinating hydrogen atoms are omitted for clarity, and hydrogen bonds are represented by dotted lines.

207 in CH_3CN functions as a selective colorimetric sensor for F^- over Cl^- , Br^- , I^- , HSO_4^- , NO_2^- , NO_3^- , N_3^- , AcO^- , ClO_4^- , IO_4^- , and H_2PO_4^- . ^1H and ^{31}P NMR studies as well as absorbance

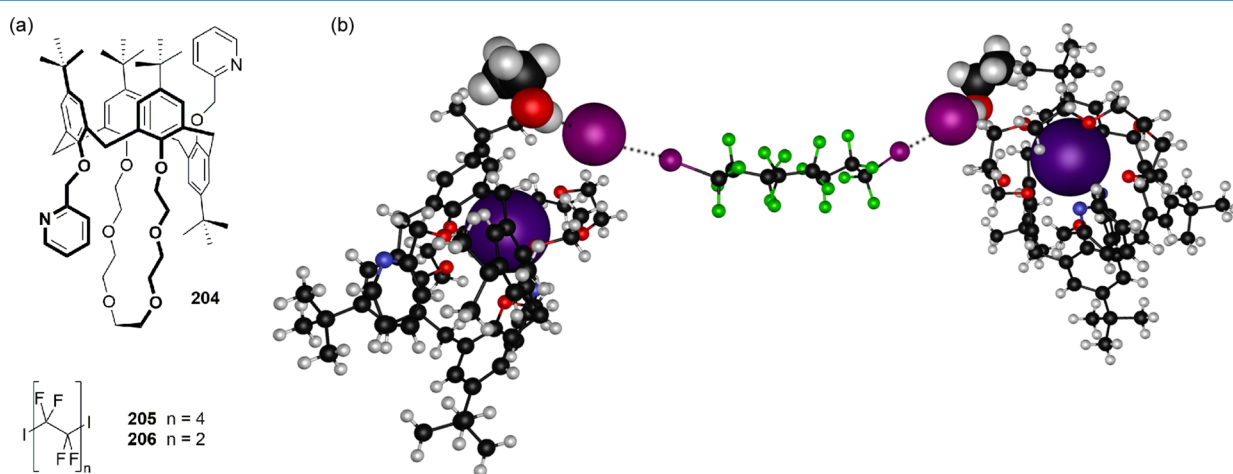


Figure 86. (a) Structures of **204–206**. (b) Crystal structure of the $\text{CsI}:204:205$ complex. Receptors are shown in ball-and-stick representation with the bound ions and solvent molecules in space fill (0.6 times the van der Waals radius), and the atoms are color coded as follows: C (black), N (blue), H (white), F (light green), Cs (dark purple), I (purple). Hydrogen and halogen bonds are represented by dotted lines.

measurements in acetonitrile suggest that this is due to the formation of a 2:1 fluoride:receptor complex via hydrogen bonding with the acidic methylene CH_2 protons and not due to deprotonation of the receptor by fluoride. Furthermore, **207** was able to quantitatively extract fluoride ions from an aqueous solution (NaF in water, seawater from the Arabian Sea, and water collected from the Sambhar lake in India) to a CH_2Cl_2 or CHCl_3 organic phase. The extraction of fluoride from seawater is remarkable, given the presence of many other competing anions in seawater.

Chiu and Gabbaï reported the fluoride extraction ability of cationic Lewis-acidic borane receptor **208** (Figure 87).³²⁹ The crystal structure of the fluoride adduct of **208** revealed the formation of a zwitterionic ammonium/fluoroborionate complex that contains an additional hydrogen bond between fluoride and a methylene proton of the ammonium group (Figure 87). The existence of this hydrogen bond in solution was confirmed by ^{19}F , ^{11}B , and ^1H NMR experiments on the fluoride adduct of **208** in acetone- d_6 . The fluoride extraction ability of **208** was shown by NMR experiments on a biphasic mixture of TBAF in D_2O and **208** dissolved in CDCl_3 , which revealed the formation of the fluoride adduct of **208** in the organic phase with an 82% conversion yield. Interestingly, borane receptors that do not contain the additional ammonium group were found to be unable to extract fluoride anions, and the authors ascribe this to the presence of additional hydrogen-bonding and electrostatic interactions that stabilize the B–F bond against hydrolysis in **208** but not in other borane receptors.

3.1.2. Extraction of Oxoanions. Sulfate extraction is of particular interest in the supramolecular chemistry of oxoanions due to its double negative charge and subsequent high hydration energy that renders this anion challenging to extract from aqueous media.^{330,331} Furthermore, the removal of sulfate from nitrate-rich radioactive waste is desired because sulfate is problematic when vitrifying nuclear waste for storage in geological repositories.³³² Nitrate is a much more lipophilic anion, and a potential receptor that can extract sulfate over nitrate will have to be able to overcome this Hofmeister bias. Moyer and Sessler published a number of macrocyclic ligands that might be useful in this respect. Originally, they investigated the properties of expanded porphyrin, cyclo[8]pyrrole **209** (Figure 88).³³³ Toluene extraction experiments from an aqueous Na_2SO_4 solution spiked with a $^{35}\text{SO}_4^{2-}$ tracer revealed that diprotonated **209** was a slow extracting agent by itself, but in combination with an additional synergistic phase-transfer catalyst such as Aliquat 336 (a lipophilic tetraalkyl ammonium salt) or trioctylamine the extraction ability greatly increased. Furthermore, the combination of **209** with trioctylamine was also able to extract sulfate anions from aqueous solutions that contain excess NaNO_3 . In subsequent manuscripts, Sessler and collaborators studied the extraction behavior of a series of other macrocycles, such as *meso*-octamethylcalix[4]pyrrole **194**, fluorinated calixpyrroles **210** and **211**, and tetraamides **212** and **213** (Figure 88).^{334,335} It was shown that the addition of these macrocycles to a chloroform solution of Aliquat 336 could significantly enhance the sulfate extraction ability of Aliquat 336 from an aqueous solution containing 10 mM sodium nitrate and 0.1 mM sodium sulfate. The best extracting agents were found to be **211** and **213**, which was attributed to stronger sulfate binding due to additional hydrogen-bond donors and lipophilicity effects. Interestingly, fluorinated calix[4]pyrrole **210** was found to be less effective at extracting sulfate than unsubstituted calix[4]pyrrole **194**, despite its higher anion binding ability. This was attributed

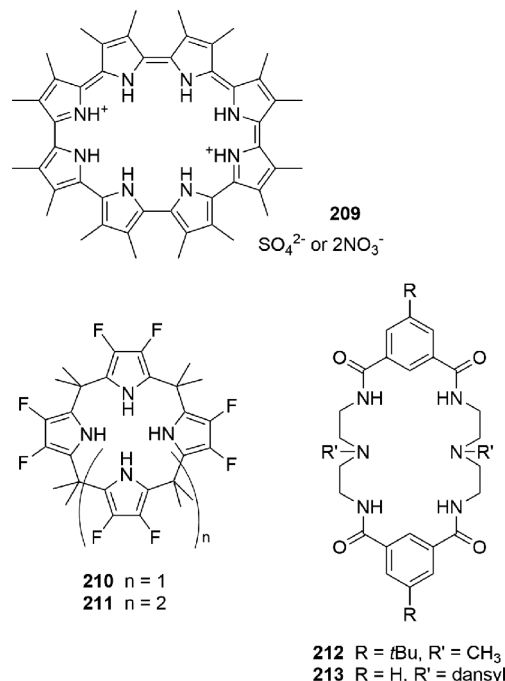


Figure 88. Structures of receptors 209–213.

to the potential ditopic nature of the calix[4]pyrrole (see Figure 81) where the sulfate complex of **194** might be stabilized by the binding of the Aliquat 336 cation into the cup of **194**. This hypothesis was later substantiated by a crystal structure of the tetramethylammonium (TMA) sulfate complex of **194**, where the TMA cation was located in the cup of the calixpyrrole, and the fact the sulfate extraction ability of **194** can be decreased in the presence of long-chain quaternary ammonium cations which, unlike methyl-containing ammonium salt Aliquat 336, cannot fit into the calixpyrrole cup.³³⁶ Recently, the same group found that the sulfate extraction ability of calix[4]pyrrole in the presence of Aliquat 336 can be significantly enhanced by strapping the receptor with bipyrrole units.³³⁷ This was attributed to the improved anion encapsulation by the strap and the increase in sulfate binding ability due to the additional hydrogen-bond donors. Furthermore, X-ray crystallography revealed that the strapped calix[4]pyrroles maintain their ability to coordinate tetramethylammonium cations (and possibly other methyl-containing alkyl–ammonium ions) in the cup of the calixpyrrole.

Wu, Li, and co-workers also developed an efficient extracting agent for sulfate anions.³³⁸ Theoretical calculations had shown that saturated sulfate coordination could be obtained with 12 hydrogen-bond donors in a tetrahedral arrangement,³³⁹ and receptor **214** was therefore designed as a single molecule capable of forming 12 hydrogen bonds. The X-ray crystal structure of the sulfate complex of **214** revealed that this compound is indeed able to adopt a tetrahedral cage-like conformation and bind sulfate anions inside the cage through 12 hydrogen bonds (Figure 89). Additional ^1H NMR titrations in $\text{DMSO}-d_6$ containing 0.5%, 10%, or 25% water revealed that this receptor is able to strongly bind sulfate anions in these highly competitive media ($K_a > 10^4 \text{ M}^{-1}$ in all solvent mixtures). This encouraged the authors to perform a series of liquid–liquid extraction experiments using ^1H NMR spectroscopy and gravimetric techniques and showed that **214** is able to effectively extract sulfate anions from a nitrate-rich aqueous solution (10 mM Na_2SO_4 and 100 mM NaNO_3) into a chloroform solution

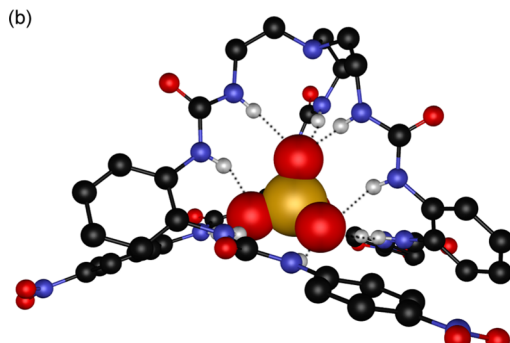
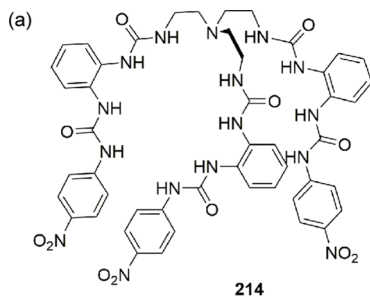


Figure 89. (a) Structure of 214. (b) Crystal structure of the 214–sulfate complex. Counter cations, solvent molecules, and noncoordinating hydrogen atoms are omitted for clarity. Hydrogen bonds are represented by dotted lines, and atoms are color coded as follows: C (black), N (blue), H (white), O (red), S (yellow).

containing 214 and TBACl as anion exchanger. Furthermore, the free receptor could be recovered by adding an aqueous BaCl₂ solution to the loaded chloroform solution, leading to the formation of a BaSO₄ precipitate in the aqueous phase.

Mezei and co-workers employed a self-assembly approach to sulfate extraction.³⁴⁰ It was found that the combination of CuSO₄, KOH, and pyrazole in the presence of a TBA⁺ source (TBAOH) led to the formation of neutral “nanojars” in organic solvents. Crystal structures of these nanojars revealed that they consist of a sulfate anion encapsulated within a stack of three [cis-Cu^{II}(μ-OH)(μ-pz)]_n rings ($n = 6 + 12 + 10$ or $8 + 14 + 9$) with the TBA⁺ counterion functioning as the “lid” of the jar (Figure 90). In this assembly, the polar hydrogen-bond donors and sulfate anions are located on the inside, while the hydrophobic pyrazolate and TBA units are located on the outside of the jar. This makes the jars highly soluble in organic solvents and a potential method for the extraction of sulfate anions. It was shown that the sulfate-containing nanojars can be extracted into an organic solvent by contacting an aqueous CuSO₄·SH₂O solution with a dichloromethane solution of pyrazole and triethylamine. Sulfate could subsequently be stripped by digesting the solid nanojars with 6 M HCl, followed by precipitation with BaCl₂. Selective crystallization of the sulfate nanojar could also be achieved in the presence of excess nitrate and perchlorate.

Plieger and co-workers employed a bis-salicylaldoximato–copper complex to achieve selective sulfate extraction³⁴¹ because previous studies had shown that receptor 215 can form a helical twisted 2:2 metallomacrocycle with Cu(II) that can encapsulate anions.³⁴² Single crystals grown from a methanol–water solution of 215, CuSO₄, and either NaCl, NaNO₃, or K₂HPO₄ resulted in mixed anion complexes where the sulfate anion is encapsulated by the metallomacrocycle and the other anions are coordinated

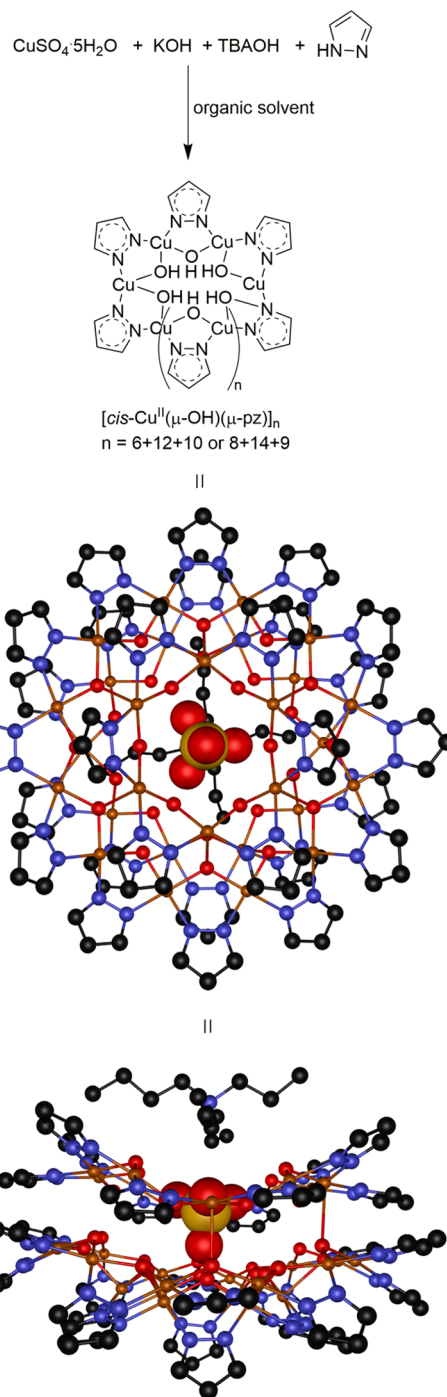


Figure 90. Synthetic pathway and two views on the X-ray crystal structure of the 6 + 12 + 10 nanojar developed by Mezei and co-workers, shown in ball-and-stick representation with the bound sulfate anion in space fill (0.6 times the van der Waals radius). Solvent molecules and hydrogen atoms are omitted for clarity, and atoms are color coded as follows: C (black), N (blue), O (red), S (yellow), Cu (orange).

on the outside of the complex (Figure 91). The preferential encapsulation of the sulfate anion over other anions encouraged the authors to investigate the sulfate extraction ability of the copper-only complex of 215. It was shown that copper-only [Cu₂(215)₂] was able to selectively extract sulfate into chloroform from an aqueous solution of sodium sulfate in the presence of excess sodium chloride, nitrate, or phosphate.

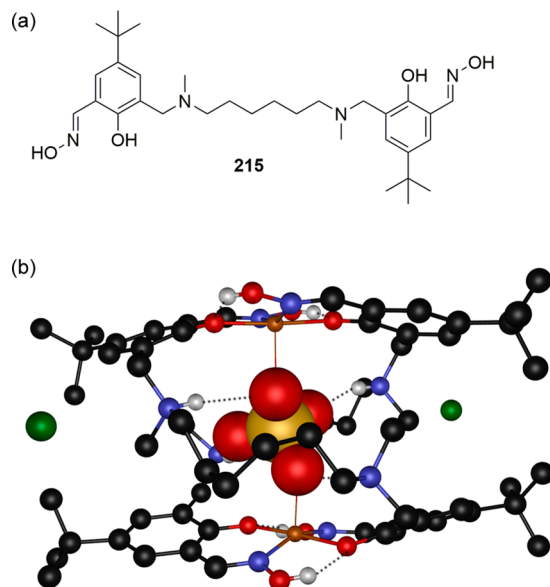


Figure 91. (a) Structure of 215. (b) Crystal structure of $[\text{SO}_4\text{CCu}_2(215+4\text{H})_2]\text{Cl}_2$ shown in ball-and-stick representation with the encapsulated sulfate anion shown in space fill (0.6 times the van der Waals radius). Solvent molecules and noncoordinating hydrogen atoms are omitted for clarity. Hydrogen bonds are represented by dotted lines, and atoms are color coded as follows: C (black), N (blue), H (white), O (red), S (yellow), Cl (green), Cu (orange).

Gale, Tasker, and colleagues employed a similar oxime (216) as the metal extracting agent in a dual-host approach for nickel sulfate extraction, where the sulfate extraction was achieved by bis-amides such as 217 (Figure 92).³⁴³ Although the bis-amides could improve the nickel extraction ability of oxime 216, the overall extraction ability was still quite low. Lindoy and co-workers also used a dual-host system for the extraction of metal(II) sulfates.³⁴⁴ Macrocycle 218 (Figure 92) was shown to mediate the extraction of metal chlorate salts from an aqueous solution at pH 7.2 to chloroform with the following selectivity:

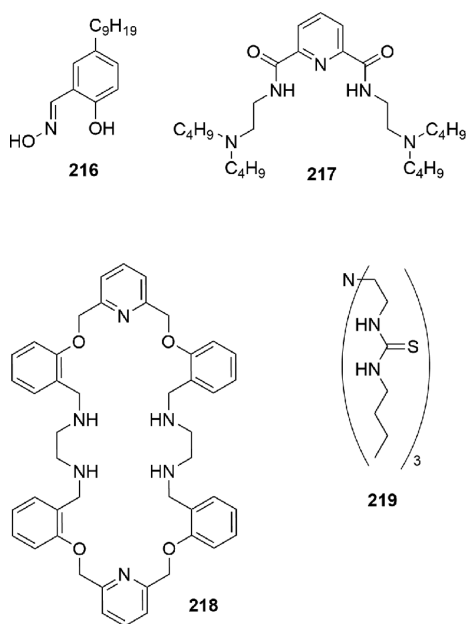


Figure 92. Structures of receptors 216–219.

$\text{Co}^{\text{II}} < \text{Ni}^{\text{II}} < \text{Zn}^{\text{II}} < \text{Cu}^{\text{II}} \approx \text{Cd}^{\text{II}}$. Furthermore, this macrocycle was shown to extract iodide and chromate anions at $\text{pH} \leq 5.5$. On the other hand, at higher pH (pH 7.7, where no anion extraction for 218 is observed), the combination of 218 and tripodal anion receptor 219 was found to be able to extract zinc(II) sulfate into chloroform.

Yilmaz and co-workers have been interested in the extraction of dichromate anions due to their high toxicity³⁴⁵ and presence in soils and waters.³⁴⁶ They investigated a number of calix[4]arene-based receptors (e.g., 220–226, Figure 93) that are capable of

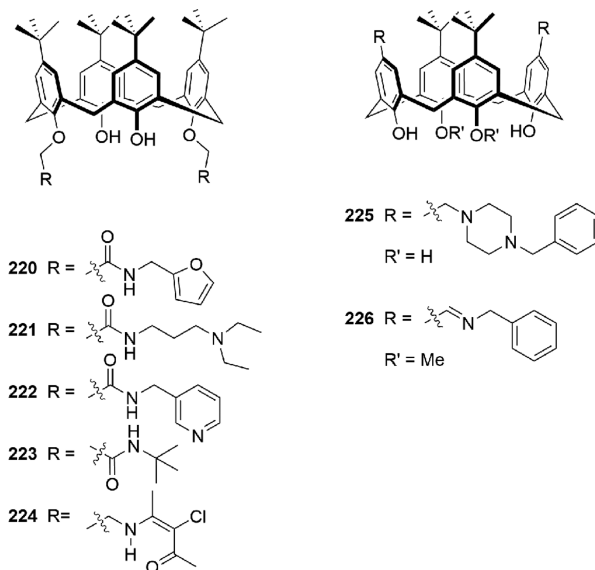


Figure 93. Structures of calixarenes 220–226.

extracting dichromate anions from an acidic aqueous $\text{Na}_2\text{Cr}_2\text{O}_7$ solution into dichloromethane.^{347–352} In general, it was observed that receptors bearing protonatable groups, such as tertiary amines (221, 225), pyridines (222), β -ketoimines (224), and Schiff bases (226), are able to extract dichromate anions into dichloromethane, while calixarenes that do not possess these functional groups are only poor extracting agents. This was ascribed to the fact that at low pH the acidic groups will become protonated and the dichromate anions (presumably as HCr_2O_7^- at low pH) can be extracted by an overall charge-neutral complex. More interestingly, calixarenes 225 and 226 were able to extract dichromate anions into dichloromethane from aqueous solutions that also contain F^- , Cl^- , Br^- , NO_3^- , NO_2^- , PO_4^{3-} , or SO_4^{2-} , showing that these calixarenes can be selective extracting agents for dichromate.

Pertechnetate (TcO_4^-) and perrhenate (ReO_4^-) extraction is another important target for supramolecular chemists as it provides a means of controlling the environmental exposure of radioactive ^{99}Tc and ^{188}Re . Both radioisotopes are used in medical diagnostics,^{353,354} but ^{99}Tc needs extra attention because it is also one of the isotopes responsible for the long-lived radioactivity of the nuclear waste produced in fission power plants.³⁰⁴ Perrhenate is a less important target in anion recognition and is often only used as a structurally similar isostere for the more regulated and hazardous pertechnetate anion. Early examples of pertechnetate and perrhenate recognition and extraction can be found in the 2009 review about this subject by Kataev and Sessler.³⁵⁵ Since then a number of new receptors for perrhenate and pertechnetate have emerged, but only a few were tested as potential extractants for these

anions.^{356–359} One of the few reports on pertechnetate extraction came from Sasaki and co-workers.^{360,361} They reported the ability of simple amine receptors 227 and 228 (Figure 94) to extract pertechnetate and perrhenate from

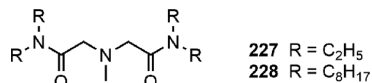


Figure 94. Structures of receptors 227 and 228.

aqueous HNO₃ solutions into dichloromethane (227) or *n*-dodecane (228). However, the crystal structure of the perrhenate complex of 227 revealed that perrhenate is bound primarily by electrostatic interactions with the protonated form of 227 as a simple ion-pair salt. The extraction selectivity is therefore not expected to be high, and it was found that increasing the HNO₃ concentration decreased the extraction ability of the receptors, presumably due to competition with NO₃[−] binding.

3.1.3. Extraction of Metalates. There are many other anions that can find applications through extraction. Anionic metalates, for example, can provide a target for the removal or recovery of metals in metallurgy.^{306,362} In this context, the more stable precious metal metalates such as [PtCl₆]^{2−} or [AuBr₄][−] are especially important due to their slow ligand exchange that requires outer-sphere coordination of the full anion during extraction. Tasker, Schröder, and co-workers investigated the ability of a series of tripodal ureas, amides, and sulfonamides such as 229–233 (Figure 95) to extract [PtCl₆]^{2−} from acidic solutions.^{363,364} The tripod scaffold was chosen because it complements the 3-fold symmetry of the metalate and because it possesses a protonatable bridgehead nitrogen atom that allows electroneutral extraction of the anion in acidic conditions. It was shown that most receptors were able to almost quantitatively extract [PtCl₆]^{2−} from an aqueous 0.6 M HCl solution into a chloroform phase, indicating that [PtCl₆]^{2−} is selectively extracted over chloride anions. Furthermore, industrially relevant back-extraction of platinum into an aqueous phase could be achieved by contacting the loaded chloroform phase with an aqueous NaOH solution, which results in the deprotonation of the anion receptor and subsequent release of the [PtCl₆]^{2−} anion. Yoshizawa plots suggested that the extracted complex displayed a 2:1 receptor:anion stoichiometry, which was confirmed by single-crystal X-ray diffraction experiments. A number of crystal structures of [PtCl₆]^{2−} complexes were obtained, and although none of them showed full encapsulation of the [PtCl₆]^{2−} anion within the tripodal scaffold, they all suggest that charge-neutral 2:1 complexes can be achieved between the receptors and this anion (see Figure 95b as an example).

Tasker, Schröder, and co-workers extended this work toward the extraction of other metalates such as tetrahedral zinc(II) and cobalt(II) chlorometalates. As a consequence of the more labile nature of these metalates, the authors designed ligands containing sterically hindered pyridine groups and amide functionalities (234–237, Figure 96).^{365,366} The protonatable pyridine group allows charge-neutral extraction, while the bulky *tert*-butyl substituents prevent the formation of inner-sphere metal complexes. It was shown that 235 and 236 are able to extract the metalates from an aqueous solution containing CoCl₂ or ZnCl₂ in 6 M HCl (to induce the formation of [ZnCl₄]^{2−} or [CoCl₄]^{2−} anions) into toluene. Furthermore, complete recovery of both zinc and cobalt could be achieved through contact of the toluene solution with deionized water, indicating that no inner-

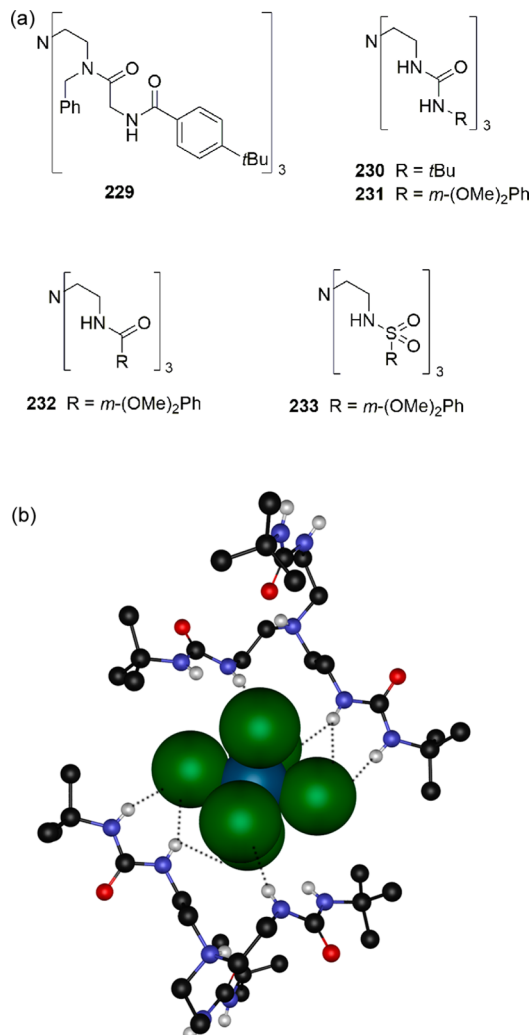


Figure 95. (a) Structures of 229–233. (b) Crystal structure of [(230H)₂PtCl₆]·2CH₃CN shown in ball-and-stick representation with the bound [PtCl₆]^{2−} anion in space fill (0.8 times the van der Waals radius). Solvent molecules are omitted, and only hydrogen atoms on heteroatoms are shown for clarity. Hydrogen bonds are represented by dotted lines, and atoms are color coded as follows: C (black), N (blue), H (white), O (red), Cl (green), Pt (metallic blue).

sphere complex was formed and that the extraction process was due to the extraction of the metalate anions. It is presumed that extraction occurs through the formation of a 2:1 complex between two protonated ligands of 235 or 236 and [ZnCl₄]^{2−} or [CoCl₄]^{2−} anions. Crystal structures of 235 with both [ZnCl₄]^{2−} or [CoCl₄]^{2−} revealed that the protonated pyridine NH does not hydrogen bond to the metalate but instead preorganizes the receptor through the formation of an intramolecular hydrogen bond with the amide oxygen atoms, while the amide NH functions and the pyridine CH groups are involved in hydrogen bonding to the metalate anion (Figure 96). ¹H NMR titrations, 2D NMR experiments, and DFT calculations suggest that similar anion complexes exist in solution and might be responsible for the extraction ability of 235 and 236.

The amidopyridyl ligands 234–237 are not suitable for industrial use due to their high cost, and Bailey, Tasker, and co-workers therefore investigated the metalate extraction ability of a series of simpler aliphatic amides 238–240 (Figure 97).³⁶⁷ Once again, these receptors possess a protonatable nitrogen atom to

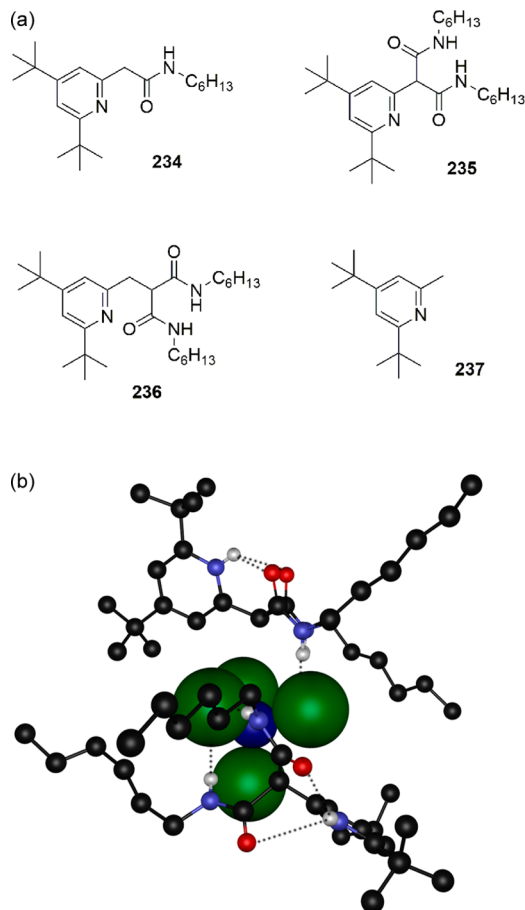


Figure 96. (a) Structures of 234–237. (b) Crystal structure of $[(235\text{H})_2\text{CoCl}_4]$ shown in ball-and-stick representation with the bound $[\text{CoCl}_4]^{2-}$ anion in space fill (0.8 times the van der Waals radius). Solvent molecules are omitted, and only hydrogen atoms on heteroatoms are shown for clarity. Hydrogen bonds are represented by dotted lines, and atoms are color coded as follows: C (black), N (blue), H (white), O (red), Cl (green), Co (bright blue).

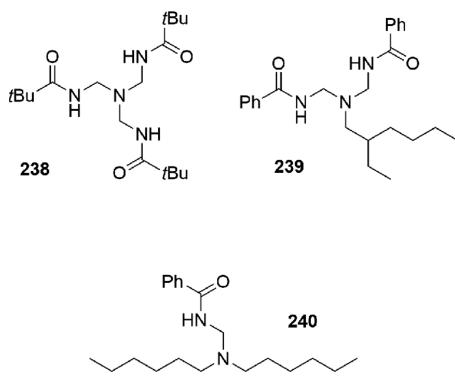


Figure 97. Structures of receptors 238–240.

allow the formation of charge-neutral 2:1 complexes with anions in acidic conditions. It was shown that these compounds are able to extract $[\text{ZnCl}_4]^{2-}$ into toluene from acidic chloride-rich ZnCl_2 solutions, suggesting that they can extract the metalate over the chloride anions. Surprisingly, the extraction ability decreased with increasing number of amides, and thus, the highest $[\text{ZnCl}_4]^{2-}$ extraction ability was seen for monoamide 240, while tris-amide 238 was virtually inactive. On the basis of extensive DFT calculations, the authors ascribe this effect to

intramolecular amide–amide hydrogen-bond formation that decreases the solubility of the tris-amides, lower proton affinity for bis- and tris-amides because protonation leads to the breaking of these amide–amide hydrogen bonds, and preferential binding of the tris-amide to chloride over $[\text{ZnCl}_4]^{2-}$ which reduces its extraction ability of the metalate from chloride-rich aqueous solutions due to competition with chloride extraction. Additionally, the DFT studies suggested that the gas-phase binding enthalpies for monoamide 240 increase as $[\text{FeCl}_4]^- < \text{Cl}^- \ll [\text{ZnCl}_4]^{2-}$, suggesting that this ligand can extract the zinc metalates selectively over chloride anions and iron metalates. This was also shown experimentally, as extraction of $[\text{ZnCl}_4]^{2-}$ into toluene from an acidic aqueous solution containing 2 M chloride was observed with 240 as extracting agent, while no extraction of $[\text{FeCl}_4]^-$ was observed under the same conditions. This selectivity could render receptor 240 a useful extraction agent in industrial processes.

Tasker and co-workers also developed a ditopic system for the extraction of zinc from ZnCl_2 solutions. Early work by the same group had shown that *salen*-type receptors such as 241 (Figure 98) can bind and extract metal(II)sulfates, where the metal is

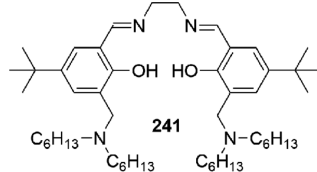


Figure 98. Structure of receptor 241.

bound by the N_2O_2 *salen* moiety and the sulfate anion is bound by the protonated tertiary ammonium groups.³⁶⁸ In a recent communication, it was shown that 241 can also extract zinc into chloroform from an aqueous 1 M ZnCl_2 solution.³⁶⁹ It was observed that the zinc loading of the chloroform solution of 241 was >100%, suggesting that 241 functions as a ditopic receptor. Presumably, zinc(II) is bound by the deprotonated *salen* moiety to form an overall neutral complex, whereas the positively charged tertiary ammonium groups coordinate a zinc(II) metalate such as $[\text{ZnCl}_4]^{2-}$ to provide an overall charge-neutral complex with two zinc atoms per receptor.

3.2. Liquid–Solid Extraction

In liquid–solid extraction, the anion to be extracted is transferred from a (aqueous) solution to a solid phase. This can be achieved by anion receptors in the solid state that can absorb the anions, by anion receptors grafted onto solid supports or membranes, or by adding anion receptors or building blocks to an aqueous solution to achieve precipitation of the anion–receptor complex or self-assembled structure (selective crystallization). The advantage of solid-phase extractions is that it is often easier to separate the liquid-donating phase from the receiving solid phase, making it a cost-effective technique. Extraction of anions in the solid state (salt) to a liquid organic solution is also possible,^{370,371} but this is less useful from an industrial point of view. In principle, commercial ion-exchange columns and membranes fall in this category, but they often utilize only nonspecific electrostatic interactions for anion separation. These techniques will therefore not be discussed here, and this section will be limited to supramolecular approaches toward solid-phase extraction.

3.2.1. Using Metal–Organic Frameworks (MOFs) or Other Anion Receptors in the Solid State. One of the most intuitive approaches to achieve liquid-to-solid extraction is by

employing anion receptors or assemblies in the solid state that can absorb or exchange anions. Metal–organic frameworks (MOFs) or coordination polymers are particularly useful in this respect as they are porous self-assembled materials built up from metal nodes and organic ligand. The metal nodes can provide the MOFs with a positive charge when neutral organic linkers are used, and thus, anions can be present in the porous channels of the MOF to ensure charge neutrality. When the MOFs are submerged into a solution, anion extraction can occur by exchange of these MOF-bound anions for the anions in solution through either a solid-state exchange mechanism or a dissolution–recrystallization process.^{372,373} Selectivity often arises through size exclusion, where anions that are too large to fit into the metal–organic framework cannot be extracted. Preference for the extraction of a certain anion can also be the result of the way in which the anions are bound inside the MOF. Anion binding is often the result of weak van der Waals and long-range electrostatic interactions between the anions and the metal nodes but can also be due to direct anion coordination to the metal nodes or via additional hydrogen bonds with the organic ligands in the framework. Depending on which interaction is dominant inside the MOF, the anion extraction selectivity can be altered. However, due to the hydrophobic interior of most MOFs and the fact that desolvation of the anion is required, the selectivity of anion exchange in MOFs is often also influenced by the Hofmeister series. Early examples of anion extraction by metal–organic frameworks can be found in the 2007 microreview by Custelcean and Moyer,³⁷⁴ and this section will focus on more recent examples.

Sun and co-workers reported a number of metal–organic frameworks and coordination polymers with anion-exchange properties based on flexible tridentate or tetradeятate ligands (e.g., 242–245, Figure 99) and Mn(II), Cd(II), Cu(II), Ni(II), or Zn(II) salts.^{375–381} The reaction of 245 with Cd(BF₄)₂, for example, yielded a 2D cationic double layer where each Cd(II) cation is coordinated by six imidazole nitrogen atoms from six different 245 ligands. The remaining BF₄[−] counterions are located in the voids between these 2D layers and are only loosely bound by C–H···F hydrogen bonds (Figure 99). When a powdered form of these crystals was suspended in an aqueous NaNO₃ or NaNO₂ solution for 24 h, it was shown by FT-IR and elemental analysis that the BF₄[−] counterions were quantitatively exchanged with NO₃[−] or NO₂[−] anions. Furthermore, the nitrate and nitrite anions could be recovered by suspending the newly formed solids in a NaClO₄ solution, which resulted in the complete exchange of the nitrate or nitrite anions by perchlorate anions. Hou and colleagues have shown that the trimethylbenzene analog of 245 can also be used to build MOFs with anion-exchange properties,³⁸² while Ziegler and co-workers obtained comparable results with another imidazole linker (246).³⁸³ They found that the combination of 246 with Pb(II) cations and 246 molecules form an extended 2D layered network with the nitrate anions positioned between the various 2D layers. It was found that the nitrate anions could be completely exchanged by iodide anions but not by the larger benzoate anions after suspending the solid into the appropriate salt solution.

Bu and co-workers were able to prepare an interpenetrating 3D metal–organic framework $\{[\text{Cu}(247)_2(\text{H}_2\text{O})_2](\text{ClO}_4)\}(\text{OH})(\text{H}_2\text{O})_{2.5}\}_n$ from the reaction between ligand 247 and Cu(ClO₄)₂·6H₂O.^{384,385} A series of other MOFs could be prepared by anion-exchange techniques where microcrystals of the original perchlorate-based MOF were suspended into an

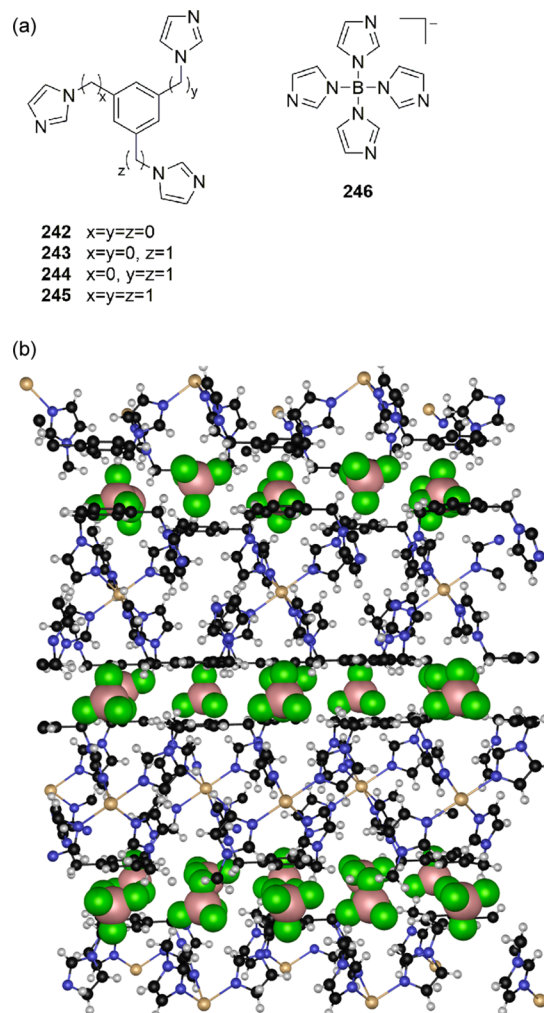
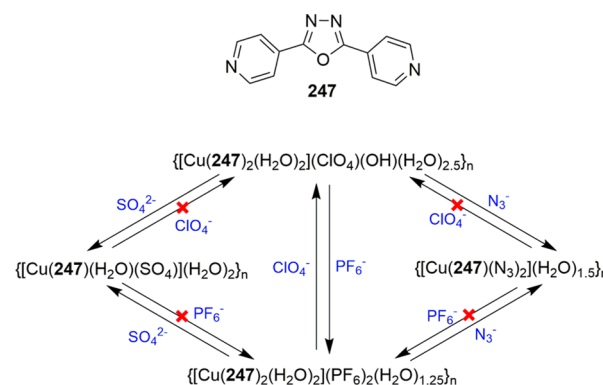


Figure 99. (a) Structures of 242–246. (b) Crystal structure of $[\text{Cd}(245)_2](\text{BF}_4)_2$ with the framework shown in ball-and-stick representation and the loosely coordinated BF_4^- anions shown in space fill (0.6 times the van der Waals radius). Atoms are color coded as follows: C (black), N (blue), H (white), Cd (pale yellow), F (light green), B (pink).

aqueous solution of NaPF₆, NaN₃, or Na₂SO₄, as shown by IR spectroscopy and single-crystal X-ray diffraction (Scheme 18). Due to the large structural changes that occurred during these reactions, the authors suggest that the anion exchange occurs

Scheme 18. Anion-Exchange Properties of Cu(II)–247-Based MOFs



through dissolution and subsequent recrystallization of the precursors rather than solid-state exchange. Du and co-workers reported a number of other MOFs with selective anion-exchange properties based on similar oxadiazole-containing ligands and Ag(I)³⁸⁶ or Cu(II)³⁸⁷ salts. For example, the assembly derived from Cu(ClO₄)₂·6H₂O and 2-(2-pyridyl)-5-(4-pyridyl)-1,3,4-oxadiazole was shown to be a highly selective anion exchanger where the original perchlorate anion could only be exchanged by benzoate anions and not by BF₄⁻, OAc⁻, NO₃⁻, Cl⁻, *o*-methylbenzoate, *m*-methylbenzoate, *p*-methylbenzoate, picolinate, nicotinate, or isonicotinate.

Oliver and co-workers reported a number of MOFs based on 4,4'-bipyridine, 1,2-ethanedisulfonate, and Cu(I), Ag(I), Zn(II), or Co(II) which are capable of selective anion exchange.^{388–391} These MOFs consist of a 1D coordination polymer based on the bipyridine and metal units, stacked together into a 2D layer by π - π interaction, with the disulfonate anions located between these 2D layers (Figure 100). In the case of the Ag(I)-based

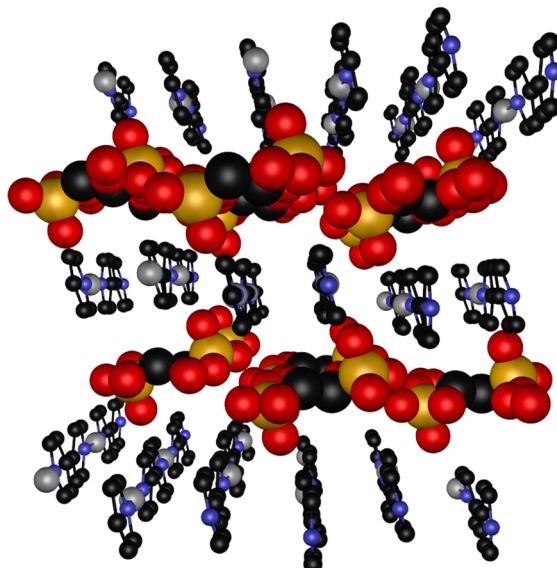


Figure 100. Crystal structure of $[\text{Ag}_2(4,4'\text{-bipy})_2(\text{O}_3\text{SCH}_2\text{CH}_2\text{SO}_3)_4\text{H}_2\text{O}]$ with the coordination polymer shown in ball-and-stick representation and the 1,2-ethanedisulfonate counteranions in space fill (0.6 times the van der Waals radius). Hydrogen atoms are omitted for clarity, and atoms are color coded as follows: C (black), N (blue), Ag (gray), S (yellow), O (red).

MOF the 1,2-ethanedisulfonate anions could be exchanged for other anions with selectivity MnO₄⁻ > ReO₄⁻ > ClO₄⁻ > CrO₄⁻ > NO₃⁻ > CO₃²⁻ by placing the solid form of the MOF into an aqueous solution of the appropriate salt. Furthermore, this MOF was able to quantitatively absorb MnO₄⁻ (or ReO₄⁻) from a solution containing a 100-fold excess of nitrate or carbonate. These results indicate that the Ag(I)-based MOF might be useful for the trapping of pertechnetate anions from nuclear waste solutions, as TcO₄⁻ often displays similar behavior to MnO₄⁻ and ReO₄⁻. Wang et al. reported a nanoporous cationic inorganic thorium borate framework capable of capturing pertechnetate but with a lower efficiency.³⁹²

Lippard and co-workers also reported a MOF capable of perrhenate trapping.³⁹³ They prepared a MOF based on the reaction of a tripodal ligand with three di(2-picoly)amine units (**248**, Figure 101) and CuCl₂ in the presence of NH₄PF₆. Single-crystal X-ray diffraction revealed that each dipicolyamine unit in

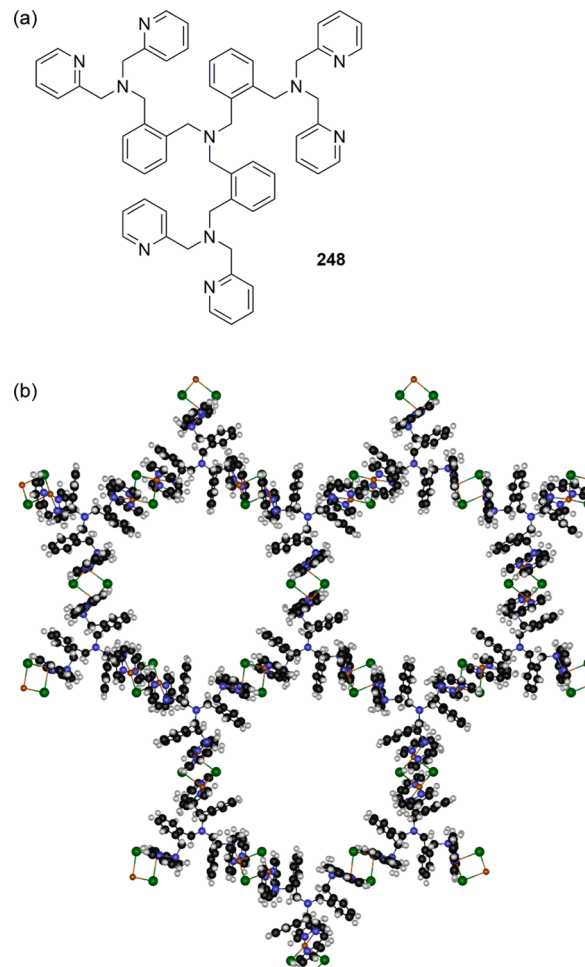


Figure 101. (a) Structure of **248**. (b) Crystal structure of $[(\text{CuCl})_3(248)](\text{PF}_6)_3 \cdot 5\text{H}_2\text{O}$ shown in ball-and-stick representation. Counter anions are omitted for clarity, and atoms are color coded as follows: C (black), N (blue), H (white), Cl (green), Cu (orange).

248 coordinates a single Cu(II) cation and is linked together in a 2D network via Cu(μ -Cl)₂Cu bridges (Figure 101). These cationic layers stack in an ABCABC manner with uncoordinated PF₆⁻ anions located between the layers. The liquid-to-solid extraction of perrhenate anions was achieved by immersing these crystals into a methanol solution of NaReO₄, which resulted in the complete displacement of the PF₆⁻ anions by ReO₄⁻ anions, as shown by FTIR, powder diffraction, and elemental analysis. Interestingly, the perrhenate anions could be recovered by back-exchange with a methanolic NaPF₆ solution, and this cycle could be repeated three times without loss of crystal morphology and exchange ability.

Fluoride anions can be challenging to extract from aqueous solutions due to their high hydration energy, and it has therefore been suggested that hydrated fluoride anions are a better target for fluoride removal. Gréard and Dastidar provided proof-of-principle that this can be achieved with metal-organic frameworks with large channels.³⁹⁴ The reaction of bis-amide **249** (Figure 102) with CuCl₂ in DMSO/MeCN resulted in the formation of a framework where the Cu²⁺ cations are coordinated in an octahedral fashion in which four **249** ligands are situated in the equatorial plane to form a 2D network and two chloride anions coordinate the axial positions and bridge the different 2D Cu-**249** layers. The framework does not display

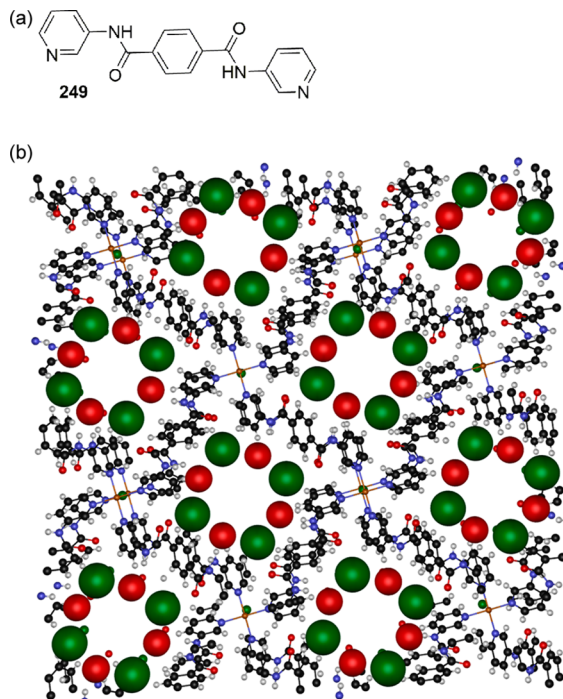


Figure 102. (a) Structure of ligand **249**. (b) Crystal structure of $[\text{Cu}(249)_2(\text{Cl})]\cdot\text{Cl}\cdot(\text{H}_2\text{O})_4$ shown in ball-and-stick representation with the chloride–water clusters shown in space fill (0.8 times the van der Waals radius). Atoms are color coded as follows: C (black), N (blue), H (white), O (red), Cl (green), Cu (orange).

interpenetration and possesses large octahedral channels that are occupied by chloride water clusters which are further stabilized by hydrogen bonding to the amide moieties of ligand **249** (Figure 102). When these crystals are submerged in an acetonitrile solution containing TBAF, the chloride–water clusters are exchanged for fluoride–water clusters, as suggested by single-crystal X-ray diffraction and solid-state ^{19}F NMR. Furthermore, time-resolved optical microscopy indicated that the crystals remain unchanged during the anion-exchange process and thus that the extraction occurs through solid-state exchange rather than dissolution–recrystallization. The ability of MOFs derived from similar pyridine-appended bis-amides and Cu(II) to exchange anions has also been shown by Sarkar and Biradha.³⁹⁵

Dong and co-workers reported a number of anion-separating MOFs based on various pyridine-containing ligands such as **250**,³⁹⁶ **251**,³⁹⁷ and **252**³⁹⁸ (Figure 103). The combination of **250** and Cu(NO₃)₂ leads to a 2D MOF with Cu(II) nodes linked via **250** ligands in a parallelogram-like fashion that create large nitrate-filled channels upon stacking. The nitrate anions in this MOF can be exchanged to Cl⁻, Br⁻, I⁻, SCN⁻, and N₃⁻ (but not F⁻) by immersing the neat crystals into an aqueous solution of the appropriate sodium salt. Interestingly, this anion exchange results in a naked-eye color change of the MOF crystals. X-ray powder diffraction and elemental analysis also revealed that this MOF can selectively absorb chloride from a NaCl/KBr mixture, thiocyanate from a KSCN/NaN₃ mixture, and iodide from a KBr/KI mixture. The MOF composed of ligand **251**, and AgPF₆, on the other hand, shows an interesting nanotube morphology. Coordination of Ag(I) into the Schiff base of ligand **251** results in a noncoplanar twist in the ligand, and upon further coordination of the pyridine moieties with Ag(I) a helical chain is formed (Figure 103). Four individual helical chains interpenetrate

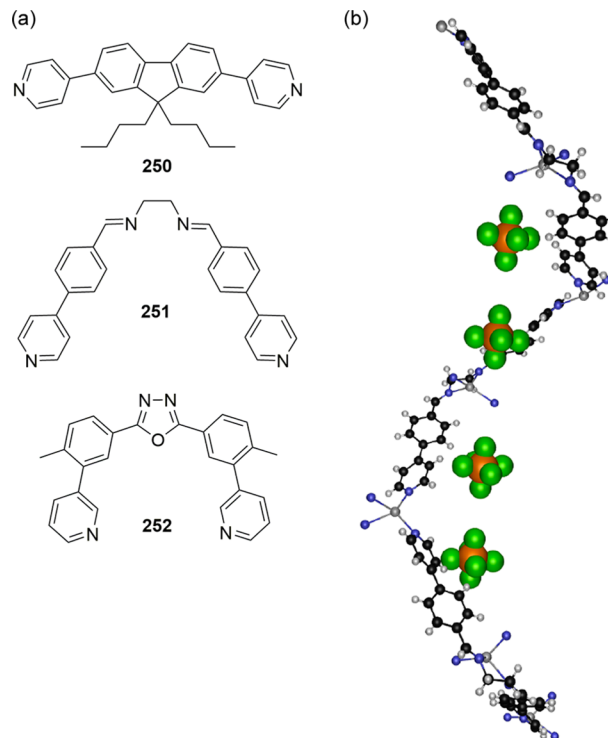


Figure 103. (a) Structures of ligands **250**–**252**. (b) Crystal structure of the nanotube formed of **251** and AgPF₆, shown in ball-and-stick representation with the PF₆⁻ anions in space fill. Only one helix that forms the nanotube is shown for clarity. Atoms are color coded as follows: C (black), N (blue), H (white), O (red), F (light green), P (orange), Ag (gray).

around a central axis to form an ellipsoidal nanotube filled with PF₆⁻ anions and solvent molecules. These PF₆⁻ anions could be exchanged for ClO₄⁻ or SbF₆⁻ anions but not for NO₃⁻ anions in 1:1 THF:MeOH. The same authors also reported a MOF based on **252** and Cd(NO₃)₂ capable of exchanging its nitrate counterions with chloride, bromide, iodide, azide, or isothiocyanate when the MOFs were dispersed in various MeOH solutions.

Lanthanides can be useful building blocks for metal–organic frameworks as their luminescent properties can provide a means for the simultaneous detection and extraction of anions.³⁹⁹ In this respect, Zhao and co-workers developed a heterometallic Dy/Zn-based MOF capable of sensing and extracting the toxic chromate anion. Single-crystal X-ray diffraction revealed that the MOF consists of a 3D network where the Zn²⁺ cations are coordinated by the nitrogen atoms of three **253** ligands and the Dy³⁺ cations form a bridged binuclear unit through coordination with the carboxylate units of **253** (Figure 104). Perchlorate counterions are located in the 1D channels present in the framework. UV-vis, inductive coupled plasma (ICP), X-ray photoelectron spectroscopy (XPS), and IR measurements indicated that these ClO₄⁻ anions could be exchanged in water by CrO₄²⁻ anions, even in the presence of other competing anions such as NO₃⁻, Cl⁻, Br⁻, and I⁻. Furthermore, the chromate anions could be partially recovered by submerging the loaded crystals in K₂CO₃ or Na₂SO₄ solutions. Additionally, these chromate exchange processes induced changes in the solid-state photoluminescence spectra, indicating that this MOF can also be used as a luminescent CrO₄²⁻ sensor. Su and co-workers also reported luminescent lanthanide-based MOFs that display anion-exchange ability.⁴⁰⁰

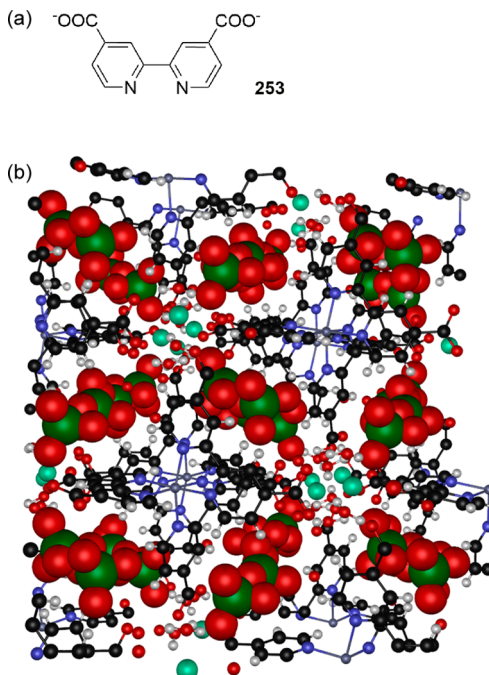


Figure 104. (a) Structure of ligand 253. (b) Crystal structure of 3D MOF $[Dy_2Zn(253)_3(H_2O)_4](ClO_4)_2 \cdot 10H_2O$ shown in ball-and-stick representation with the counteranions in the channels shown in space fill. Atoms are color coded as follows: C (black), N (blue), H (white), O (red), Cl (green), Dy (turquoise), Zn (gray).

Bu and co-workers studied the possibility of using cationic MOFs for the separation of larger, organic anions.⁴⁰¹ They prepared a series of indium-based MOFs prepared from $In(NO_3)_3$ and a number of mixed pyridine/carboxylate ligands (e.g., 254 and 255), where the In^{3+} cations form 9-connected indium trimers linked together by the ligands in a 3D network possessing various cages and channels filled with nitrate anions (Figure 105). The ability of the nitrate counterions to be exchanged by various azodyes was investigated. It was found that only negatively charged azodyes could be sequestered by the indium-MOF, while positively charged and neutral dyes could not. Furthermore, the dynamics of the exchange was found to depend on both the magnitude of the negative charge and the size of the dye, with higher charges and smaller dyes being exchanged faster. Furthermore, the dyes could be released by submerging the loaded MOF in a $NaNO_3$ solution in DMF. The fact that this MOF can separate relatively large organic anions (M_w 100–1000 Da) might make this type of MOF useful for the separation of peptides, nucleotides, or drug molecules.

In the past few years the number of MOFs with anion-exchange properties has grown, and most of them follow the same principles as described in Figure 105. Yang and Raptis built a MOF from 256 and $AgNO_3$ where the nitrate anions could be reversibly exchanged for perchlorate anions (Figure 106).⁴⁰² Zeller and co-workers reported a MOF made up from $Zn^{(II)}$, 4,4'-bipyridine, and *p*-aminobenzoate and showed that the original ClO_4^- anions could be reversibly exchanged with PF_6^- anions in water.⁴⁰³ Similarly, Phuengphai et al. reported a series of MOFs built from $Zn^{(II)}$ salts, 4,4'-bipyridine, and formate or propionate and showed that they possess reversible anion-exchange properties.⁴⁰⁴ Ligand 257 was shown by Bharadwaj and co-workers to form 2D networks with $Co^{(II)}$ cations that stack in an ABCABC fashion and contain BF_4^- anions in the voids, which

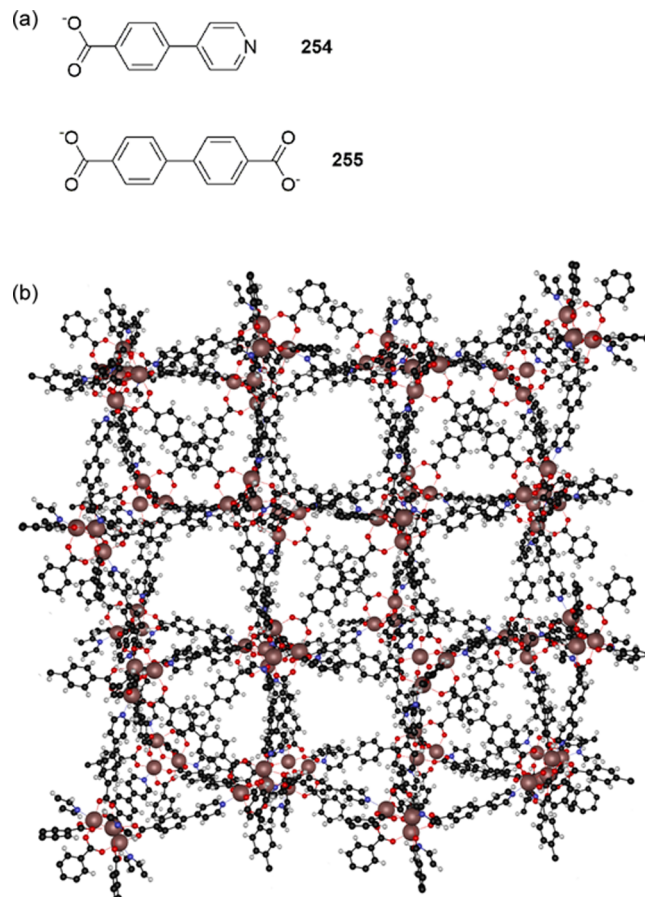


Figure 105. (a) Structures of ligands 254 and 255. (b) Crystal structure of one of the $In^{(III)}$ -MOF used for separating anionic azodyes $[In_3O(254)_3(255)_{1.5}](NO_3)_3$, shown in ball-and-stick representation with the $In^{(III)}$ ions shown in space fill for clarity. Atoms are color coded as follows: C (black), N (blue), H (white), O (red), In (gray-pink).

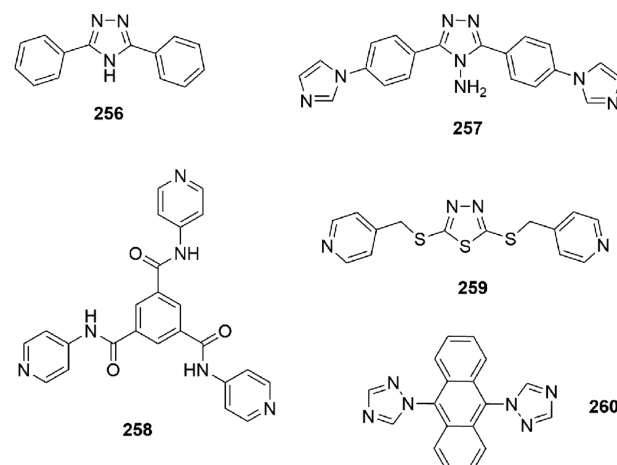


Figure 106. Structures of ligands 256–260.

can be exchanged for ClO_4^- , NO_3^- , and Cl^- but not for PF_6^- , BPh_4^- , or OBz^- in a size-selective manner.⁴⁰⁵ Analogously, Tzeng et al. found that a 3D MOF built from $Cd^{(II)}$ and trispyridyl-trisamide 258 displays size-selective exchange of its Cl^- counterions with ClO_4^- and PF_6^- but not with the larger BPh_4^- anion.⁴⁰⁶ Wei, Hong, and colleagues found that a coordination network made of $Ag^{(I)}$ and 259 displays anion-

exchange behavior that follows the Hofmeister series.⁴⁰⁷ Liu et al. have shown that a 3D MOF built from bis(1,2,4-triazole) ligand **260** and Cu(NO₃)₂ is capable of exchanging all of its nitrate anions for perchlorate anions when submerged into a 1:1 MeOH:water solution.⁴⁰⁸ Furthermore, both Cohen and co-workers⁴⁰⁹ and Liu and co-workers⁴¹⁰ reported various heterometallic MOFs that are able to exchange their counterions, while Michaelides and Skoulika⁴¹¹ reported a 1D coordination polymer based on lanthanide metals (Pr³⁺, Gd³⁺) and adipate that can exchange its counterions in an apparent crystal-to-crystal transformation.

It is not always necessary to use cationic MOFs to achieve anion adsorption. Yang, Wong, and co-workers prepared a neutral MOF from TbCl₃ and mucic acid (**261**) that forms a 2D coordination network in the solid state that generates 1D channels perpendicular to the 2D layers upon stacking (Figure 107).⁴¹² In the crystal structure the layers are connected by

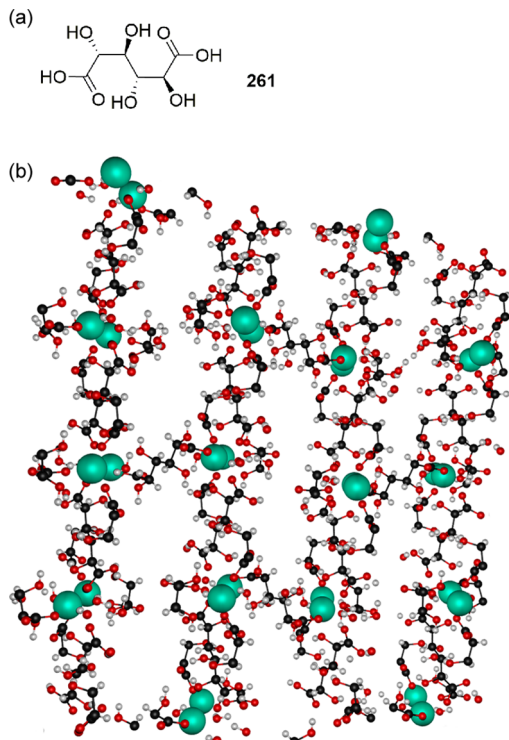


Figure 107. (a) Structure of mucic acid **261**. (b) Crystal structure of neutral MOF [Tb(**261**)_{1.5}(H₂O)₂]·SH₂O shown in ball-and-stick representation with the Tb(III) ions in space fill. Water molecules in the channels have been omitted for clarity, and atoms are color coded as follows: C (black), H (white), O (red), Tb (turquoise).

hydrogen bonding to water molecules, but the water can be removed by heating without collapse of the framework. It was found that this MOF was capable of extracting I⁻, Br⁻, Cl⁻, F⁻, CN⁻, and CO₃²⁻ anions (but not the larger SO₄²⁻ or PO₄³⁻ anions) from aqueous solutions, presumably due to hydrogen bonding of the anion with the hydroxyl groups of mucic acid. Due to the luminescent properties of the lanthanide metal ion (Tb³⁺), the anion uptake into the solid MOF could be monitored in the luminescence spectra. It was observed that the anion uptake was independent of the cation, with similar results obtained for NaCl, KCl, and Ca(Cl)₂, indicating that it is the hydrogen bonding to the anion that drives the extraction process.

Interestingly, the adsorbed salts could be recovered by placing the loaded crystals in pure water.

It is also possible to prepare purely inorganic 2D or 3D frameworks capable of anion exchange. Fogg and colleagues synthesized an ytterbium-containing framework (Yb₃O(OH)₆Cl·2H₂O) that consists of oxygen-centered Yb₄ tetrahedra bridged with hydroxyl groups to form a 3D network that contains 1D channels filled with uncoordinated, disordered chloride anions in the crystal structure (Figure 108).⁴¹³ Powder X-ray

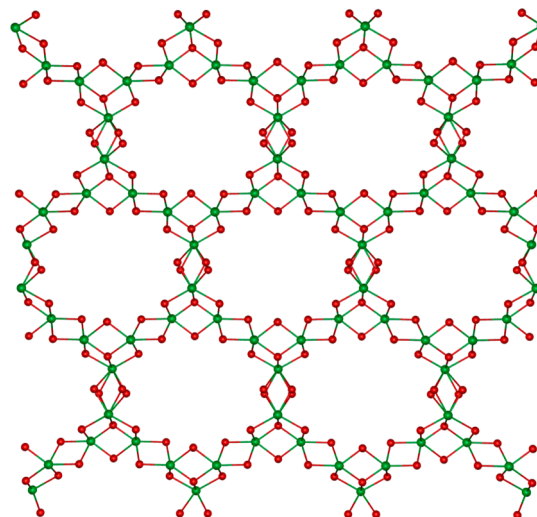


Figure 108. Crystal structure of cationic inorganic framework Yb₃O(OH)₆Cl·2H₂O shown in ball-and-stick representation. Atoms are color coded as follows: O (red), Yb (green).

diffraction, FTIR, and elemental analysis revealed that these chloride anions could be exchanged for a range of other anions (carbonate, oxalate, and succinate) when the solid framework is dispersed in the appropriate aqueous solution at room temperature. SEM images also showed that the crystals remain unchanged during this procedure, suggesting a solid-state anion exchange rather than a dissolution–crystallization mechanism. There are also other classes of inorganic anion exchangers, such as the layered double hydroxides (also known as hydrotalcites or anionic clays) which are 2D networks of hydroxides containing two different metal ions. They occur naturally but can also be synthesized and modified synthetically. However, their design is often not based on supramolecular principles, and they will therefore not be discussed here. A recent tutorial review by Scott Oliver provides more information on the use of these cationic inorganic materials for anion trapping.⁴¹⁴

It is theoretically possible to perform liquid–solid extraction with an insoluble discrete anion receptor in the solid state, but this is hard to achieve and is not very common. Danil de Namor and co-workers reported phenol-appended calix[4]pyrroles such as **262** and **263** (Figure 109) that can be reacted with

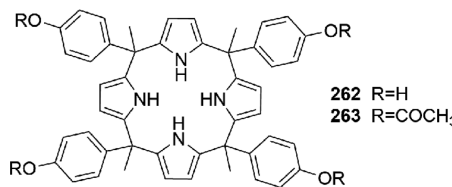


Figure 109. Structures of calixpyrroles **262** and **263**.

formaldehyde under basic conditions to form an oligomeric calix[4]pyrrole resin.^{415,416} It was shown that this oligomer is able to remove NaH_2PO_4 with a maximum capacity of 0.007 mmol of anion per gram of resin and NaF with a capacity of 5.64 mmol/g from aqueous solutions. The material could be recycled after fluoride extraction by washing with citric acid.

3.2.2. Using Modified Solid Supports and Membranes.

Modified solid supports are often used in industrial processes for separating anions, but many commercial anion-exchange columns consist of an organic polymer appended with cationic quaternary ammonium groups that bind anions through electrostatic interactions and are therefore often nonselective.⁴¹⁷ In principle, it should be possible to increase the selectivity of ion-exchange resins by appending a known anion receptor to a solid support. Although there have been a number of early examples of anion extraction by modified solid supports, including metalated porphyrins attached to polystyrene⁴¹⁸ or silica⁴¹⁹ and HPLC columns modified with calix[4]pyrrole,⁴²⁰ the progress in this field has been relatively limited in the past decade.

Calixarenes and calixpyrroles have remained the most popular receptors to be immobilized onto solid supports. Kaledkowski and Trochimczuk employed calixpyrrole **262** (Figure 109) and compared the anion sorption ability of resins obtained through immobilization onto a vinylbenzyl chloride/divinylbenzene copolymer, condensation of **262** with formaldehyde, and copolymerization of **262** with methacrylate and divinylbenzene.^{421,422} All resins were capable of extracting TBA halide salts from acetonitrile solutions with a selectivity of $\text{F}^- > \text{Cl}^- > \text{Br}^- > \text{I}^-$. The highest sorption ability was seen for the immobilized calixpyrrole, which was attributed to the fact that the anions can reach receptors immobilized onto the surface of a resin more easily than receptors that form an integer part of the resin. It was noted by the authors that the resins cannot be used to extract anions from aqueous solutions, but instead, water can be used to regenerate the resins by back-extraction of the anions. Another immobilized calixpyrrole was reported by Aydogan and Akar.⁴²³ They synthesized siloxane-functionalized calix[4]pyrrole **264** (Figure 110) which could be easily reacted with various silica-

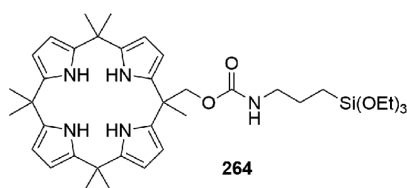


Figure 110. Structures of calixpyrrole **264**.

based solid supports to create a large range of different types of calixpyrrole resins, but the anion extraction ability of these resins was not reported.

Yilmaz and co-workers reported a number of solid supports immobilized with calix[4]arenes to achieve dichromate extraction (e.g., **265–267**, Figure 111). It was shown that both calixarenes loaded onto silica gel (**265**)⁴²⁴ and polysiloxane resin (**266**)⁴²⁵ are able to adsorb dichromate anions from acidic aqueous solutions (pH 1.5), while their analogous monomeric forms were found to be poor dichromate extractors in liquid–liquid extraction experiments. In both cases it was observed that Na^+ ions were also adsorbed by the calixarene-based resins to provide a counterion for the dichromate anions. More recent studies showed that piperazine-appended calix[8]arenes loaded

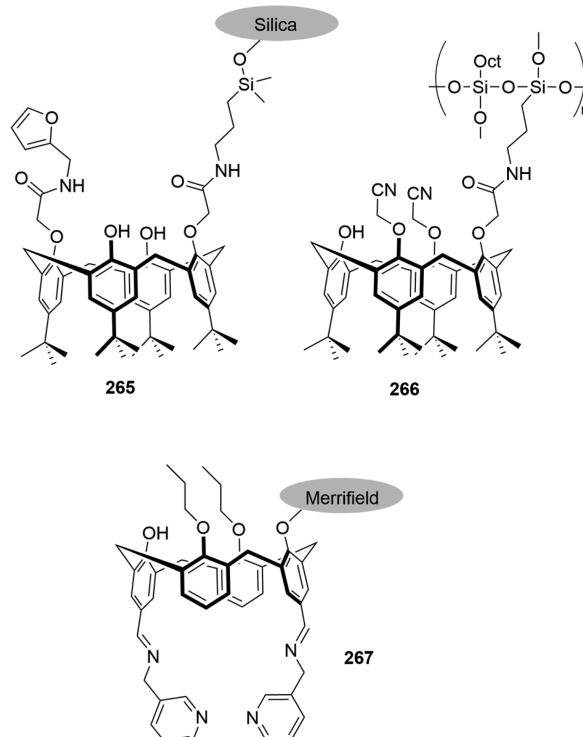


Figure 111. Structures of calixarene-based resins **265–267**.

onto Amberlite resins are also powerful dichromate extractors.⁴²⁶ On the other hand, calix[4]arenes loaded onto polymeric Merrifield resins (e.g., **267**) were shown to have a lower extraction ability toward dichromate anions than their monomeric counterparts.^{427,428} Although these results suggest that dichromate anions could be removed by immobilized calixarenes, other anions were not investigated by the authors, and it is not clear whether these resins can selectively adsorb dichromate over other anions. At neutral pH, the resins were able to extract transition metals such as Hg^{2+} as their picrate salt.

Attaching an anion receptor to a magnetic nanoparticle is another way of achieving liquid–solid extraction, as the anion can be easily removed from solution by an external magnetic field after complexation with the receptor. Yilmaz and co-workers prepared magnetite (Fe_3O_4) nanoparticles modified on the surface with 3-aminopropyltrimethoxysilane to allow the immobilization of calix[4]arene receptors (**268** and **269**, Figure 112).^{429,430} It was shown that **268** is able to efficiently remove dichromate anions from aqueous solutions at pH 2.5–4.5 with concomitant removal of sodium cations, while magnetic nanoparticle **269** was found to function as a solid-phase extracting agent for dichromate (66% removal at pH 1.5) and arsenate (86% removal at pH 3.5) when the tertiary amines are protonated. However, no selectivity experiments were conducted.

It is not always necessary to covalently bind the receptor to the solid support, as it is also possible to use noncovalent interactions. Lamb and colleagues adsorbed *cyclen*-based receptors **270** and **271** (Figure 113) onto a reversed-phase column for the separation and preconcentration of anions.⁴³¹ The long aliphatic tails attached to these receptors assure that they remain strongly adsorbed to the hydrophobic reversed-phase column when aqueous solutions are used as the eluent of the column. It was shown that with the correct eluent, the columns can be employed to separate a mixture of anions (F^- ,

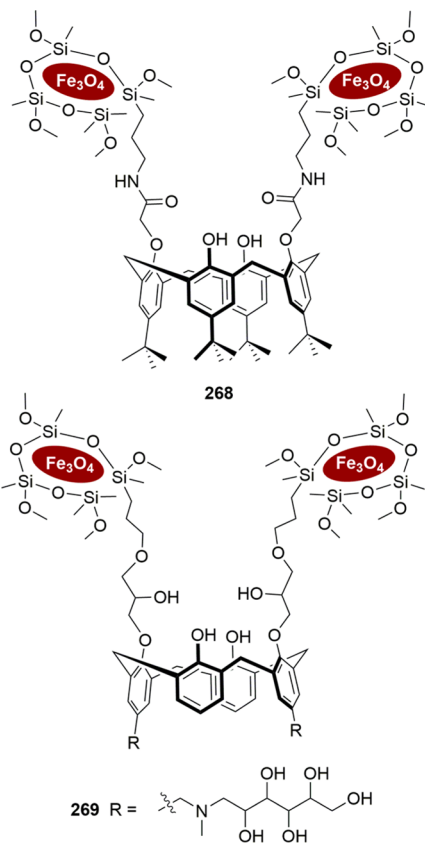


Figure 112. Structures of calixarene-based magnetic nanoparticles **268** and **269**.

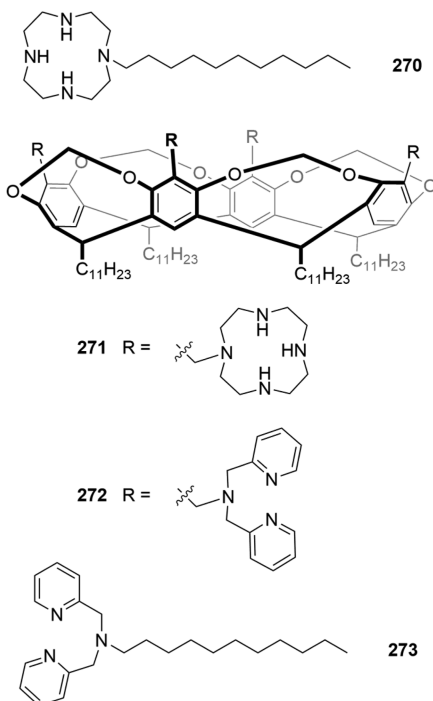


Figure 113. Structures of **270–273**.

Cl^- , NO_2^- , NO_3^- , SO_4^{2-} , PO_4^{3-} , and ReO_4^-). The column containing the resorcinarene-based receptor **271** possessed better separation ability than the simple *cyclen* receptor **270**. Furthermore, the authors showed that these columns can be used

to preconcentrate certain anions (ClO_4^- and ReO_4^-). When a mixture of anions was loaded onto the columns and a weak bicarbonate solution was used as eluent (under these conditions the *cyclen* amines are still partly protonated), most anions could be eluted except perchlorate and perrhenate which are retained on the column by electrostatic interactions. The latter two anions could subsequently be removed by using a NaOH solution as eluent to deprotonate all amine functionalities and release the anions.

Apart from receptors immobilized onto resin and silica columns, anion receptors could also be embedded into solid or liquid membranes to obtain anion-exchange membranes. The membranes can be seen as a liquid-to-solid extraction of the anion into the membrane, followed by a back-extraction of the anion into an aqueous solution at the other side of the membrane in a transport-like manner. While semipermeable membranes are popular in industry, most of them do not have specific anion receptors embedded in them, and there are only a few reports of supramolecular chemists trying to create anion-exchange membranes. Harrison, Lamb, and co-workers employed a strategy similar to the **271**-based column to develop a separation membrane.⁴³² They prepared a number of polymer inclusion membranes (PIMs) based on cellulose triacetate as the polymer support, Cu^{2+} , Zn^{2+} , or Fe^{3+} complexes of anion carriers **272** and **273** (Figure 113), and a range of plasticizers to help dissolve the carriers into the polymer. The transport of a range of halide anions (F^- , Cl^- , Br^- , I^-) and oxoanions (SO_4^{2-} , SeO_4^{2-} , NO_3^- , ReO_4^-) was investigated as a function of the carrier, metal, plasticizer, and source/receiving phases used. The permeability toward all anions was found to be higher for the metal complexes of **273** compared to **272**, which was attributed to the large size of **272**, resulting in slower diffusion rates. Similarly, the transport rates were dependent on the polarity and viscosity of the plasticizer, with increased anion permeability seen for more polar plasticizers (due to the stabilization of ions) and for less viscous plasticizers (due to faster diffusion of the carriers). In general, anion transport selectivities followed the Hofmeister series, but a number of other interesting selectivities were observed. A high perrhenate over nitrate selectivity, for example, was detected for the system with the Zn^{2+} complex of **273** as carrier, ethyl phthalyl ethyl glycolate (EPEG) as plasticizer, and a receiving phase containing KCl , indicating that these membranes can be used for the removal of the radioactive pertechnetate anion.

Duggan, Smith, and colleagues prepared a supported liquid membrane (SLM) containing ditopic receptor **274** (Figure 114)

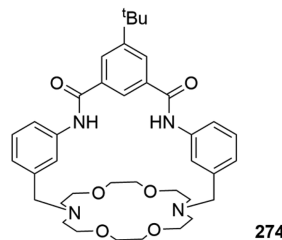


Figure 114. Structure of ditopic receptor **274**.

for the separation of halide salts.⁴³³ The SLM was prepared by dissolving receptor **274** into a minimal amount of 2-nitrophenyloctylether and immobilizing this solution in a thin sheet of porous polypropylene. It was found that the SLM allows the transport of cations and anions from a 1 M salt solution (donor phase) to a receiving phase consisting of distilled water with a

selectivity that follows the Hofmeister series $K^+ > Na^+ > Li^+$ for the cations and $I^- > Br^- > Cl^-$ for the anions. It was shown that this ditopic receptor creates faster fluxes through the SLM than a combination of an analogous anion receptor and cation receptor. Smith and co-workers also used this receptor across phospholipid bilayers (see section 4.2).

3.2.3. Using Selective Crystallization and Precipitation.

In recent years a new technique for extracting anions has emerged based on selective crystallization. This technique is related to liquid–solid extraction of anions by metal–organic frameworks or hosts in the solid state, but rather than adding a preformed crystal to the anion solution, the building blocks of the final complex are added to the solution and the anion-templated assembly crystallizes or precipitates out of solution. Ideally, the formed crystal/precipitate only contains one specific anion while the other anions remain in solution. There are a number of advantages associated with this type of anion separation. The self-assembly process allows more complex binding cavities that can be complementary to the size/shape of a particular anion, which is hard to achieve via traditional receptor synthesis. Furthermore, the rigidity present in the solid state can enhance the shape and size selectivity of the cavities, and the metal ion that is often involved in the self-assembly provides additional charge selectivity. Work in this field has been mainly conducted by Custelcean and co-workers, who published a number of reviews about the subject.^{434–437}

The first example of selective crystallization was based on the coordination behavior of bispyridyl monourea 275 (Figure 115).^{438,439} This ligand can form coordination polymers with

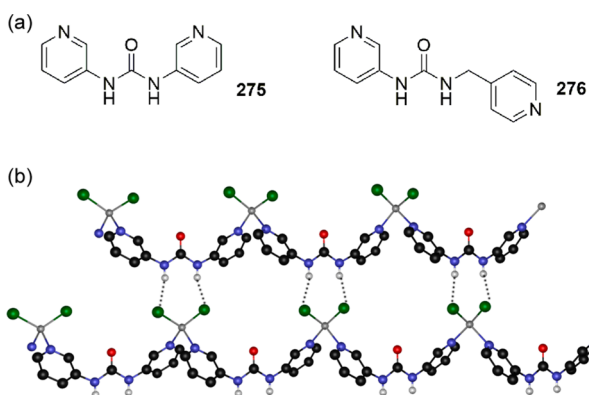


Figure 115. (a) Structure of ligands 275 and 276. (b) Crystal structure of the $ZnCl_2$ –275 coordination network shown in ball-and-stick representation. Noncoordinated hydrogen atoms are omitted for clarity. Hydrogen bonds are represented by dotted lines, and atoms are color coded as follows: C (black), N (blue), O (red), H (white), Cl (green), Zn (gray).

Zn^{2+} salts of chloride, bromide, iodide, and sulfate (but not nitrate and perchlorate). The $ZnCl_2$ complex consists of a 1D network where each Zn^{2+} coordinates with two pyridine N atoms of two different ligands and two chloride anions. The chloride anions are further stabilized by hydrogen bonding to the urea NHs to form a 2D layer (Figure 115). The $ZnBr_2$ and ZnI_2 complexes were found to be isostructural with the described $ZnCl_2$ coordination polymer. When ligand 275 was crystallized from a water:ethanol solution containing a mixture of $Zn(NO_3)_2$, $NaCl$, $NaBr$, NaI , $NaClO_4$, and Na_2SO_4 , the halide anions were selectively crystallized over the oxoanions, as shown by X-ray diffraction, FTIR, and elemental analysis. However, the

selectivity between the halides was not very high, and a mixed MOF with general composition $ZnCl_xBr_yI_z \cdot 275$ ($x + y + z = 2$) was obtained. Later studies with the same ligand found that 275 can also form coordination networks with HX acids.⁴⁴⁰ Upon monoprotonation by the acid the ligands are linked together via hydrogen bonding between the protonated pyridine of one ligand and the unprotonated pyridine of a neighboring ligand to form an infinite helical structure, with the counteranions hydrogen bonded to the urea functionalities. The helical pitch of this structure was found to vary between the different HX structures in order to adapt to the specific steric requirements of the anion. Pairwise competitive crystallization experiments revealed that the selectivity for acid crystallization agrees largely with the Hofmeister series ($I^- > ClO_4^- > NO_3^- > Br^- > Cl^-$). The lower selectivity observed for this system compared to the Zn^{2+} system was attributed to the soft and unspecific hydrogen bonds around the anion and the fact that the flexible helix structure can adapt to the size and shape of the anion. More recently, Dastidar and co-workers described a similar bispyridyl monourea ligand 276 (Figure 115) that was found to lead to the selective crystallization of a $CdSO_4$ network from an aqueous solution containing equal amounts of $CdSO_4$, $Cd(NO_3)_2$, $Cd(OAc)_2$, $Cd(ClO_4)_2$, $CdCl_2$, and $CdBr_2$.⁴⁴¹ However, the selectivity for sulfate was lost when excess amounts of the other anions were used.

After the pioneering work of Custelcean and co-workers, a number of research groups reported the selective crystallization of anions by monoureas and monoamides containing only one pyridine substituent. Banerjee and Dastidar, for example, found that fluorinated amide 277 is capable of separating ClO_4^- anions from an aqueous methanol/ethanol solution containing $CuSO_4$, $Cu(NO_3)_2$, $Cu(ClO_4)_2$, $Cu(BF_4)_2$, and $CuCl_2$ through the formation of a $[Cu(277)_4(ClO_4)] \cdot ClO_4 \cdot H_2O$ network where the perchlorate anion is stabilized by direct anion–metal coordination and anion–π interactions.⁴⁴² Similarly, Ghosh and co-workers showed that fluorinated monoureas 278 and 279 can selectively crystallize $CuSO_4$ from mixtures containing either equimolar amounts of $Cu(ClO_4)_2$, $CuSO_4$, $Cu(NO_3)_2$, and $CuCl_2$ or equimolar quantities of $CuSO_4$, $NiSO_4$, $CoSO_4$, and $ZnSO_4$, indicating selectivity toward both Cu^{2+} and SO_4^{2-} .^{443,444} The structure of the crystals formed from 279 and $CuSO_4$ in 4:1 DMF:water revealed that the Cu^{2+} cation is coordinated by two DMF molecules and four pyridine units, creating a bis-urea cleft in which the sulfate anion is bound through hydrogen bonding. Coordination of the sulfate anion to the ureas of another $Cu(279)_4$ unit creates a 1D coordination polymer where the sulfate is stabilized by approximately nine hydrogen bonds from four urea moieties (Figure 116). Another monopyridine urea 280 was shown by Wu, Yang, and co-workers to selectively crystallize the acid $HClO_4$ over HNO_3 from aqueous solutions (Hofmeister bias), in agreement with the results obtained for 275 by Custelcean.⁴⁴⁵

In an effort to increase the selectivity of the crystallization systems, Custelcean and co-workers investigated the liquid–solid extraction properties of metal complexes of bisurea 281 (Figure 117).⁴⁴⁶ When a 3:1 ethanol:DMF solution of 281 was mixed with an aqueous solution of $NiSO_4$, NaF , $NaCl$, $NaBr$, NaI , and $NaNO_3$, the sulfate anion was selectively crystallized with the Ni^{2+} network of the ligand. The crystal structure of this network consists of 2D layers made up from octahedral Ni^{2+} nodes coordinated by four equatorial pyridine units from four different ligands and two axial water molecules. These 2D layers stack on top of each other with a 0.5 offset, and the sulfate anions are

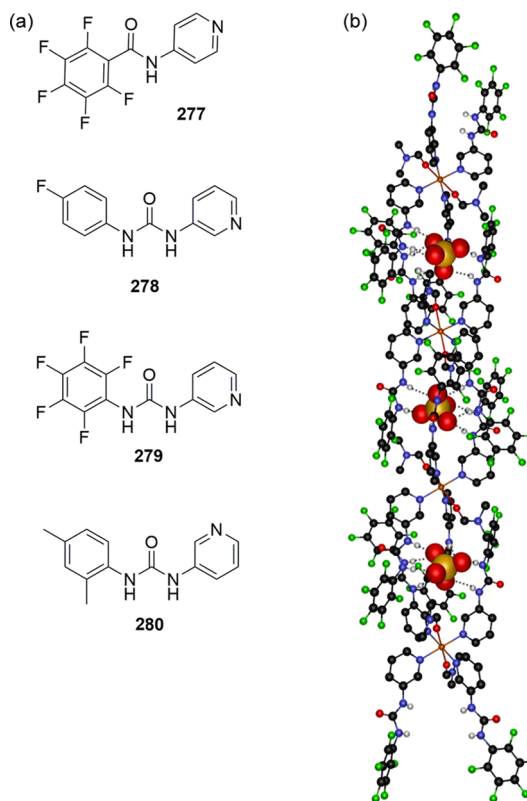


Figure 116. (a) Structures of ligands 277–280. (b) Crystal structure of the CuSO₄–279 coordination network shown in ball-and-stick representation with the bound sulfate anions in space fill (0.6 times the van der Waals radius). Noncoordinated hydrogen atoms are omitted for clarity. Hydrogen bonds are represented by dotted lines, and atoms are color coded as follows: C (black), N (blue), O (red), S (yellow), H (white), F (light green), Cu (orange).

located between the layers and hydrogen bonded to two water molecules and four urea groups from four different ligands in two adjacent layers (Figure 117). Furthermore, the same crystals could also be obtained from a solution containing a 20-fold excess of NaNO₃ (although in low yields), indicating that this selective crystallization approach could be used for the removal of sulfate from nitrate-rich radioactive waste. Similar results were obtained by Dastidar and co-workers, who reported on the selective crystallization of ZnSO₄ by 281,⁴⁴⁷ and by Wu and co-workers, who showed selective sulfate crystallization by similar bisurea 282 and Zn(II).⁴⁴⁸ Interestingly, Wu, Yang, and colleagues showed that related biscarbamate 283 can be employed for the selective crystallization of sulfuric acid from an ethanol:water solution containing 2 equiv of H₃PO₄, HClO₄, HCl, and HBr and 1 equiv of H₂SO₄.⁴⁴⁹ Cindrić and co-workers have shown that linear trisamine 284 can also selectively crystallize H₂SO₄ and HNO₃ from methanolic solutions containing competing anions, but no sulfate over nitrate selectivity was observed for this system.⁴⁵⁰

Dastidar and co-workers investigated the sulfate extraction properties of another series of bisureas and bisamides (285–287, Figure 118).^{451,452} All three ligands were capable of selectively crystallizing SO₄²⁻ from a mixture of ClO₄⁻, NO₃⁻, and CF₃COO⁻ (as Zn²⁺ salts in the case of 285 and 286 and as Cu²⁺ salts in the case of 287), as shown by FTIR, elemental analysis, and powder X-ray diffraction. The crystal structure of 285 in the presence of ZnSO₄ displays an interesting Borromean topology. The Zn(II) centers are coordinated by three ligands,

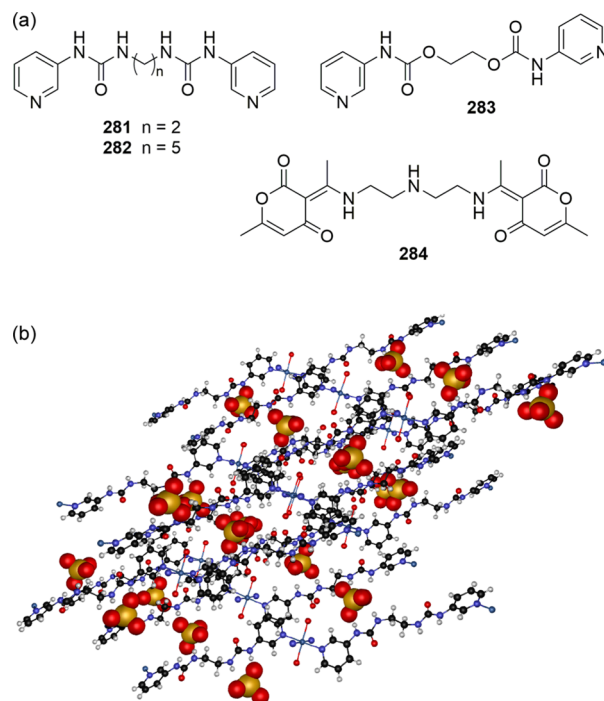


Figure 117. (a) Structure of ligands 281–284. (b) Crystal structure of the NiSO₄–281 coordination network shown in ball-and-stick representation with the bound sulfate anions in space fill (0.6 times the van der Waals radius). Atoms are color coded as follows: C (black), N (blue), O (red), S (yellow), H (white), Zn (gray).

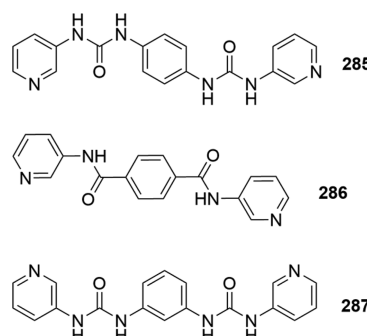


Figure 118. Structures of ligands 285–287.

one water, and one sulfate anion in a trigonal bipyramidal geometry, which results in a 2D honeycomb network. The 2D networks form a 3-fold interpenetrated structure displaying Borromean entanglement, where the sulfate anions are further hydrogen bonded by three urea groups from three different 2D layers in the Borromean network.

One of the best studied receptors for selective crystallization of anions is the tripodal trisurea 288 (Figure 119) that has been reported by the groups of both Custelcean and Wu. Initially, it was found that this ligand can crystallize into a 3D network in the presence of MgSO₄ (or similar M²⁺ salts).^{453–455} The crystal structure consists of 2:1 ligand:sulfate cages where the sulfate anion is coordinated by 12 hydrogen bonds from the six urea functionalities. Charge neutrality is maintained by Mg²⁺(H₂O)₆ clusters that also stabilize the cages and produce a 3D network via hydrogen bonding of the water molecules to the pyridine N atoms and carbonyl O atoms (Figure 119). Pairwise competitive crystallizations revealed that this system can crystallize dianions with a selectivity of SO₄²⁻ > SeO₄²⁻ >> CO₃²⁻ > SO₃²⁻, whereas

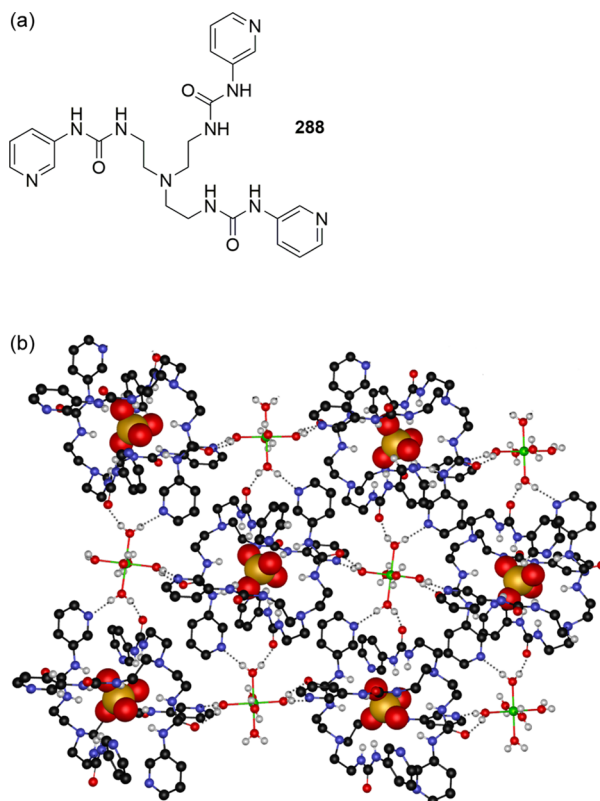


Figure 119. (a) Structure of ligand 288. (b) Crystal structure of the $\text{MgSO}_4\text{-}288$ coordination network shown in ball-and-stick representation with the bound sulfate anions in space fill (0.6 times the van der Waals radius). Noncoordinated hydrogen atoms are omitted for clarity. Hydrogen bonds are represented by dotted lines, and atoms are color coded as follows: C (black), N (blue), O (red), S (yellow), H (white), Mg (light green).

monoanions such as ClO_4^- , NO_3^- , HCO_3^- , HSO_4^- , H_2PO_4^- , F^- , Cl^- , Br^- , and I^- do not produce any crystals. The rejection of monoanions is presumably due to the charge mismatch with the $\text{Mg}^{2+}(\text{H}_2\text{O})_6$ clusters, while the selectivity for tetrahedral dianions (SO_4^{2-} , SeO_4^{2-}) over trigonal planar dianions (CO_3^{2-} , SO_3^{2-}) can be explained by the complementarity in shape between the cage and the tetrahedral guests. However, with the Mg^{2+} system the selectivity *between* tetrahedral anions was found not to be optimal. This was subsequently overcome by repeating the selective crystallization experiments with lithium salts. In this case very similar 2:1 cages were formed with sulfate, but the cages were found to be significantly smaller in the solid state, which resulted in an increased selectivity for the smaller sulfate anion

over the large selenate anion.⁴⁵⁶ Similar results were obtained with cages grown from Na^+ and K^+ salts, but the change in selectivity was less predictable.⁴⁵⁷ Recently, Custelcean and co-workers have shown that their system can potentially be applied to remove sulfate anions from nuclear wastes.^{458,459} The groups of Wu, Janiak, and Yang have also shown that ligand 288 can form 1:1 ligand:sulfate cages in the solid state when $[\text{Fe}(\text{bipy})_3]\text{SO}_4$ is used as the sulfate source, but this did not reduce the ability of this system to selectively crystallize SO_4^{2-} over NO_3^- , OAc^- , or ClO_4^- .⁴⁶⁰

Stoddart and co-workers used a similar selective crystallization/precipitation approach to achieve gold extraction by fast precipitation of α -cyclodextrin and KAuBr_4 in water.⁴⁶¹ Single crystals could be obtained for this assembly by slow-diffusion experiments, which revealed the existence of a 1D cable-like supramolecular polymer (Figure 120). In this structure, two α -cyclodextrin molecules form a head-to-head dimer by intermolecular hydrogen bonding between the secondary hydroxyl faces of the α -cyclodextrin molecules, and this dimer serves as a cage occupied by a $\text{K}^+(\text{H}_2\text{O})_6$ cation. These dimers are arranged into a 1D chain by square-planar $[\text{AuBr}_4]^-$ anions that are located between the primary hydroxyl faces of the α -cyclodextrin units of two adjacent dimers and are stabilized by $\text{C}-\text{H}\cdots\text{Br}-\text{Au}$ hydrogen bonding to the α -cyclodextrin units and $\text{O}-\text{H}\cdots\text{Br}-\text{Au}$ hydrogen bonding to the $\text{K}^+(\text{H}_2\text{O})_6$ cations. The existence of this structure was further corroborated by SEM, TEM, AFM, electron diffraction, and powder X-ray diffraction experiments. It is important to note that the fast precipitation of this complex only occurred for the combination KAuBr_4 and α -cyclodextrin, while combinations involving KAuCl_4 and β - or γ -cyclodextrin did not induce rapid precipitation. Furthermore, the precipitation also occurred in the presence of other metalates such as $[\text{PtBr}_4]^{2-}$, $[\text{PdBr}_4]^{2-}$, $[\text{PtCl}_4]^{2-}$, and $[\text{PdCl}_4]^{2-}$. This high selectivity inspired the authors to develop a lab-scale recovery process for gold. For this purpose, scrap gold-bearing alloys (containing Au, Zn, Cu, and Ag) were converted to HAuBr_4 using a HBr/HNO_3 etching mixture. KOH was subsequently used to convert the acid to the KAuBr_4 salt and to adjust the acidity to pH 4–6. Upon the addition of α -cyclodextrin, the precipitation of the $\text{KAuBr}_4:\alpha$ -cyclodextrin adduct occurred immediately and the precipitate could be filtered and subsequently treated with the reducing agent $\text{Na}_2\text{S}_2\text{O}_5$ to yield metallic gold. The success of this method suggests that it could serve as a potential environmentally friendly alternative to the traditional cyanide leaching method for gold recovery.

3.3. Conclusions and Outlook on Anion Extraction

The examples discussed in this section have shown that supramolecular chemistry can be a useful tool for extracting

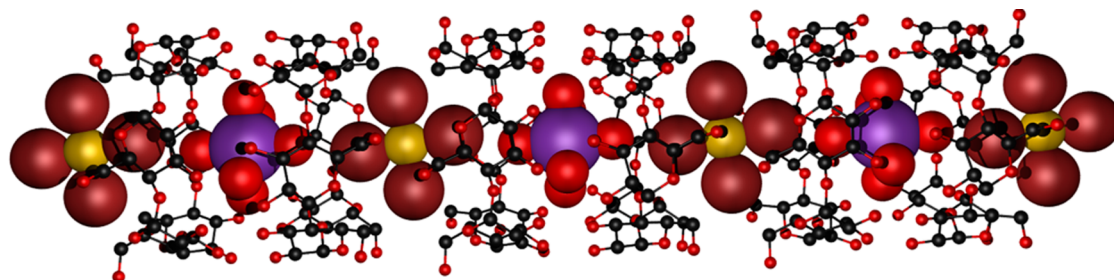


Figure 120. Structure of the $\text{KAuBr}_4:\alpha$ -cyclodextrin adduct reported by Stoddart and co-workers, shown in ball-and-stick representation with the bound $[\text{AuBr}_4]^-$ and $\text{K}^+(\text{H}_2\text{O})_6$ ions shown in space fill (0.8 times the van der Waals radius). Hydrogen atoms are omitted for clarity, and atoms are color coded as follows: C (black), O (red), Au (yellow), Br (brown), K (purple).

inorganic and organic anions and can also be employed in the recovery of metals by extraction of metalate anions. While the focus has been largely on liquid–liquid extraction methods, the past decade has also seen a rise in the number of papers concerning liquid-to-solid extraction methods for the separation of anions. The latter is mainly due to the growing popularity of metal–organic frameworks that can be used in neat solid-state anion-exchange processes, as well as in selective crystallization procedures. It is expected that the number of publication regarding anion extraction will continue to increase in the next years and that ever-increasing anion selectivities can be obtained for a wide range of anions.

4. TRANSMEMBRANE ANION TRANSPORT

Cells of all living organisms are surrounded by a phospholipid membrane that provides an apolar barrier for the free diffusion of large molecules and charged species such as anions. Instead, anions are transported in a controlled fashion by specialized proteins embedded within the cellular membranes in order to maintain the concentration of each anion within the cell and cellular compartments. However, defects in these proteins and the subsequent inability to transport anions have been linked to a number of diseases, such as cystic fibrosis,⁴⁶² Dent's disease,⁴⁶³ certain types of Bartter syndrome,^{464,465} Pendred syndrome,⁴⁶⁶ congenital chloride diarrhea,⁴⁶⁷ and other genetic diseases.⁴⁶⁸ This has motivated supramolecular chemists in recent years to develop synthetic molecules that can replace these malfunctioning proteins by creating anion receptors that can also transport anions across phospholipid membranes. While most synthetic transporters are still only tested in model liposomes, the ultimate goal is to create transporters that also function *in vitro* and *in vivo*. A number of excellent reviews regarding anion transport have been published during the past decade,^{469–475} and this section will thus be limited to an overview of the various methods that can be used to achieve transmembrane anion transport by synthetic molecules. Anion transporters are generally classified as functioning either as a “channel” or as a “mobile carrier” (Figure 121), although examples of anion transporters that function through different mechanisms also exist. Channels are membrane-spanning structures that provide a polar pathway (or pore) in the membrane through which anions can diffuse. They can be either a single molecule or a self-assembled supramolecular complex that spans the membrane. Mobile carriers, on the other hand, are structures that can bind an anion on one side of the membrane, diffuse through the membrane as an anion complex, and then release the anion on the other side of the membrane. The transport rates achieved by channels are generally faster than those achieved by mobile carriers, as the latter depend on a larger number of equilibria and require the diffusion of larger anion complexes. However, mobile carriers rely much more on anion binding and are therefore easier to design from a supramolecular perspective. It is important to note that for synthetic anion transporters the overall anion transport process needs to be electroneutral, and therefore, transmembrane anion transport will only occur either through symport/cotransport (both an anion and a cation are transported in the same direction) or through antiport/exchange (two anions are transported in opposite directions). In the following section, synthetic anion transporters will be classified according to their mechanism (channel, mobile carrier, or other).

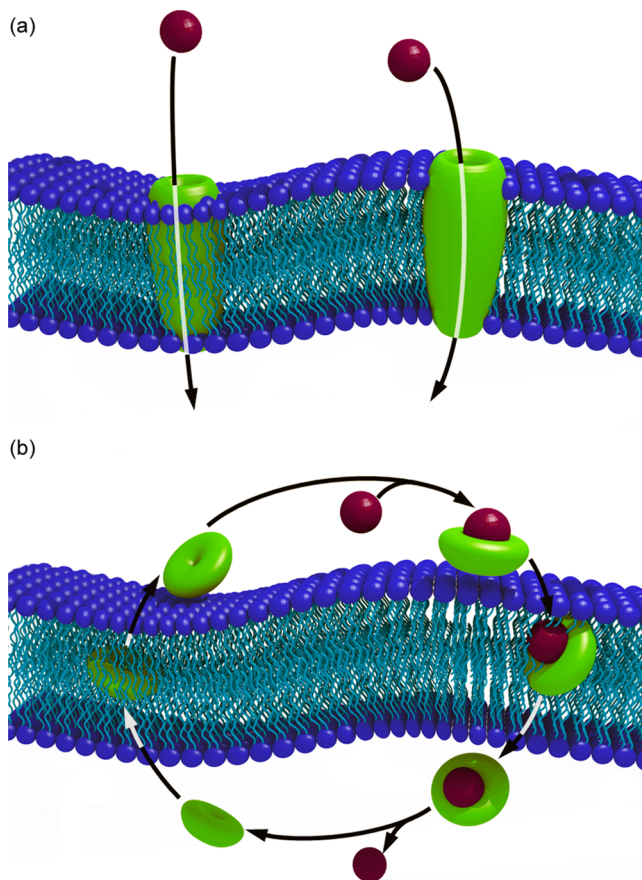


Figure 121. Schematic representation of anion transport by (a) an anion channel and (b) a mobile carrier.

4.1. Anion Transport via Synthetic Anion Channels

Over the years a number of strategies for designing synthetic anion channels have emerged. One strategy has been to create short peptides based on segments of naturally occurring anion transporting proteins (which are often channels), while other strategies included membrane-spanning “rigid rods” or “anion slides” and the design of tubular shaped molecules or assemblies. Synthetic ion channels do not always display a clear anion over cation selectivity and only channels that have shown to be selective for anions will be discussed here.

The first approach has been extensively used by Tomich and co-workers, who designed a large number of peptides based on the transmembrane segment of the brain glycine receptor. They were able to show that the naturally occurring transmembrane sequence 289 (Figure 122) can insert into membranes, form oligomeric channel-like structures and can facilitate anion transport in synthetic liposomes, planar lipid bilayers and living cells.^{476,477} By employing systematic modification of 289, followed by structure–activity relationship studies, Tomich and colleagues discovered that the addition of four lysines at the N-terminus,⁴⁷⁸ the removal of amino acids at the C-terminal⁴⁷⁹ and substitution of the C-terminal serine to tryptophan^{480,481} can improve the anion transport activity or the biophysical properties of the peptides. The same authors have also used a similar approach to develop synthetic peptides capable of anion transport based on a transmembrane segment of CFTR (Cystic Fibrosis Transmembrane conductance Regulator).⁴⁸²

Gokel and co-workers used a similar strategy and devised a series of synthetic peptides based on the CLC family of chloride

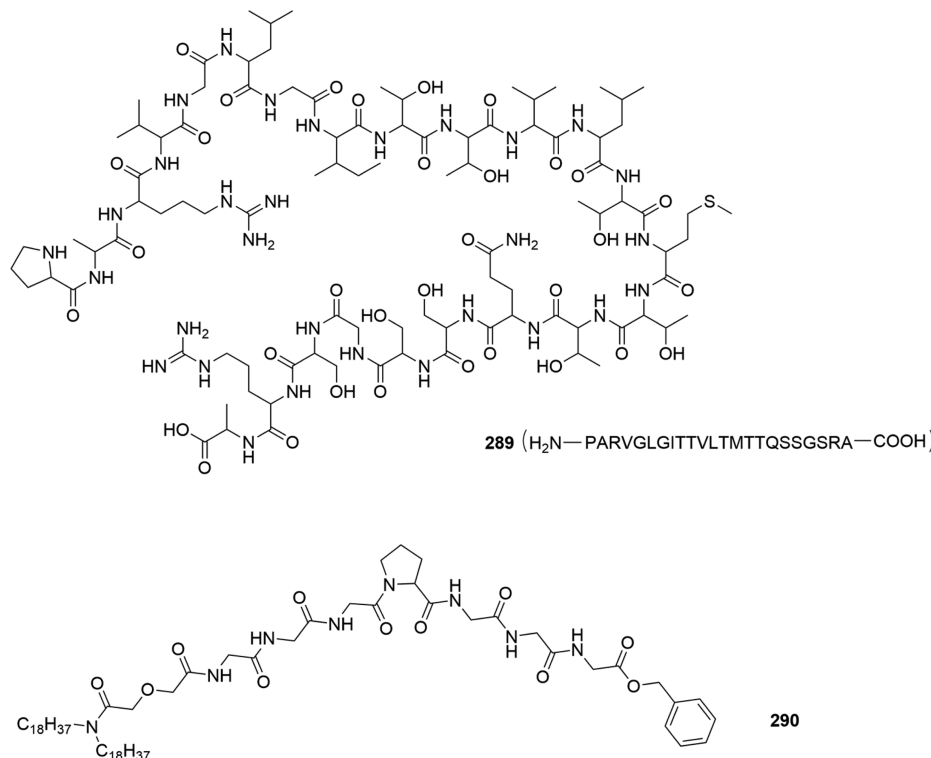


Figure 122. Structures of peptide-based anion channels **289** and **290**.

channels which contain a well-preserved amino acid sequence, namely GKxGP_xH. The authors' original design, **290** (Figure 122), therefore consisted of a proline residue flanked by a number of glycine residues with lipophilic anchor groups at both the N- and C-termini. ¹H NMR titrations showed that this peptide is able to bind chloride anions in CDCl₃,^{483,484} while voltage clamp techniques with planar lipid bilayers and ion selective electrode experiments with liposomes showed that the peptide is able to form an oligomeric channel capable of transporting chloride.⁴⁸⁵ Subsequent studies on modified analogues of **290** indicated that optimizing the N-and C-terminal anchor groups,⁴⁸⁶ covalently linking two peptides at the C- or N-terminus,⁴⁸⁷ decreasing the polarity of the midpolar region (i.e., the region between the N-terminus and the glycine residues)⁴⁸⁸ and extending the glycine sequence⁴⁸⁹ all resulted in improved chloride transport ability. On the other hand, mutating the central proline residue reduced the anion transport ability of the peptides, indicating that the "kink" in the conformation induced by the proline residue might be essential for chloride channel formation by this class of peptide.⁴⁹⁰ Furthermore, when one of the glycine residues is substituted by glutamate (containing a negatively charged carboxylate side chain), the chloride transport ability of the channel is diminished due to charge repulsion.⁴⁹¹ Similarly, replacement of glycine by tryptophan also reduced the transport activity of the peptides, presumably due to the higher ability of the tryptophan-containing peptides to form aggregates in aqueous solution.⁴⁹²

Matile and co-workers have been interested in designing rigid-rod molecules capable of transmembrane anion transport. Their original design (compounds **291–293**, Figure 123)^{493,494} was inspired by Amphotericin B, a natural product that is able to form ion channels and consists of a rigid lipophilic polyene backbone and a hydrophilic polyalcohol chain. Fluorescence studies with egg yolk phosphatidylcholine (EYPC) vesicles encapsulating a

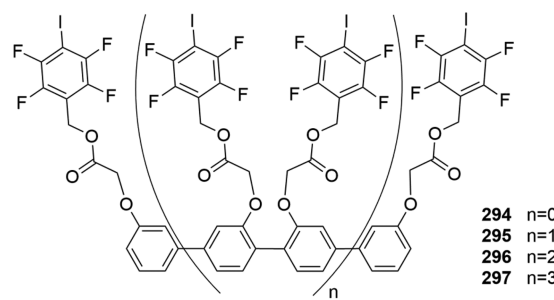
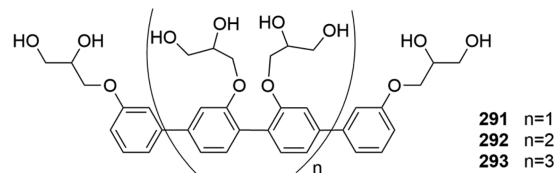


Figure 123. Structures of Matile's rigid rods **291–297**.

pH-sensitive dye indicated that **291–293** can function as channels capable of mediating both H⁺/M⁺ (M = Rb, Cs, K, Na) and OH⁻/Cl⁻ exchange. The highest activity was observed for **293**, which presumably acts as a unimolecular rigid rod that can span the full length of the EYPC lipid bilayer, while **291** and **292** are too short to function as ion channels. More recently, Matile and co-workers reported analogues of the original rigid rods where the hydroxyl groups were replaced with moieties capable of halogen bonding to anions (**294–297**, Figure 123).⁴⁹⁵ Similar studies with EYPC vesicles showed that these compounds are also able to function as ion channels, presumably via a Cl⁻/OH⁻ exchange mechanism where the anions can "hop" along the rigid rod from one halogen bonding site to the other in

a cascade-like manner. Once again, higher activities were observed for the longer rods **296** and **297** that are able to span the membrane. The same authors showed that related rigid rods can be employed to form higher order channels by self-assembling into a barrel-shaped channel. This was achieved by appending aromatic electron acceptors to the rigid rod, so that a 4-way barrel capable of OH⁻/Cl⁻ exchange is formed through π-π stacking when an aromatic electron donor is added (Figure 124).⁴⁹⁶

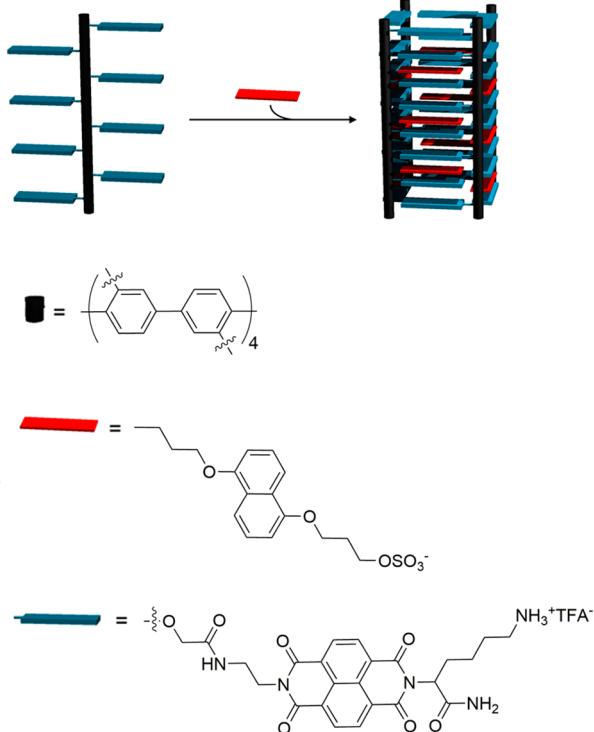


Figure 124. Barrel formation through π-π stacking between rigid-rod molecules and a dialkoxynaphthalene.

Matile and colleagues also performed a number of studies on rigid rods consisting of naphthalenediimides (NDI) linked together with benzene rings (e.g., **298**, Figure 125).^{497,498} The NDI units provide a π-acidic surface suitable for anion-π interactions, and the authors suggest that this class of compound can span EYPC lipid bilayers and allow anions to slide through the channel via anion-π interactions (hence, the name “π-slide”). Electrospray ionization Fourier transform ion cyclotron resonance tandem mass spectrometry (ESI-FTICR-MS-MS) on monomeric analogues of **298** provided evidence for the existence of anion-NDI complexes and the presence of anion-π interactions,⁴⁹⁹ while vesicle-based studies showed that the π-slides are also capable of transporting anions across lipid bilayers.⁵⁰⁰ Subsequent studies revealed that the activity and selectivity of the NDI-based rigid rods can be optimized by the addition of hydrophilic anchors at the termini of the slides.⁵⁰¹ In later studies, Matile and co-workers investigated similar perylenediimide (PDI) slides such as **299** (Figure 125) and showed that they are also capable of Cl⁻/OH⁻ exchange across EYPC membranes.⁵⁰² Furthermore, they found that these PDI slides are able to transport electrons and could have potential as artificial photosynthesis systems. Recently, Matile and co-workers employed analogues of their NDI and PDI systems to

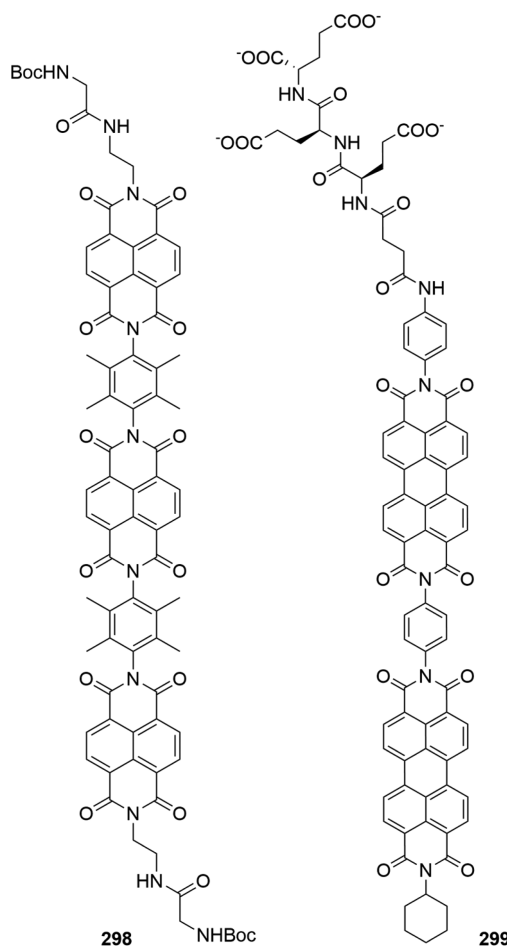


Figure 125. Structures of Matile's π-slides **298** and **299**.

create dynamic amphiphiles capable of sensing microdomains in giant unilamellar vesicles.⁵⁰³

Schmitzer and co-workers also investigated anion-π interactions for developing anion channels. They reported imidazole- and benzimidazole-containing transporters **300** and **301** (Figure 126) in the assumption that the positive charge close to the aromatic ring should allow strong anion-π interactions.^{504,505} Vesicle-based experiments with the chloride-selective dye lucigenin showed that these compounds are able to transport chloride. Channel formation was suggested by the observation of excimers in lipid bilayers. Furthermore, the authors showed that the addition of α-cyclodextrin or cucurbit[7]uril can inhibit the transport ability of **300** by the formation of an inclusion complex that enhances the partitioning of **300** into the aqueous phase. It was also observed that the counteranion of the imidazolium salt can be modulated to achieve enhanced chloride transport abilities.⁵⁰⁶ Recent studies by the Schmitzer group include the benzimidazole derivative **302**, which was shown to form anion-selective channels in liposomes,⁵⁰⁷ and imidazole-derivatized binols such as **303**, which were shown to facilitate anion transport across EYPC liposomes and possess antimicrobial activity against Gram-positive bacteria such as *Bacillus thuringiensis* and *Listeria seeligeri* (Figure 126).^{508,509}

Another approach to design ion channels is to develop inherently cylindrical molecules or self-assemblies that are able to span the membrane and hence provide a pore for anions to diffuse through. Cyclodextrins can be seen as ideal scaffolds for this as their diameter is large enough for anions to pass through.

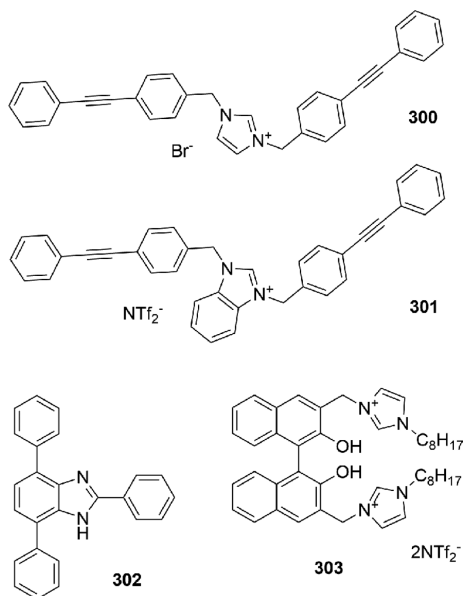


Figure 126. Structures of channels 300–303.

This was employed by Gin and co-workers, who developed two cyclodextrin-based ion channels **304** and **305** (Figure 127) that are able to selectively transport anions over cations.^{510,511} However, the halide transport ability of **304** was found to be dependent on the pH. In acidic conditions (pH 5.6) the amino

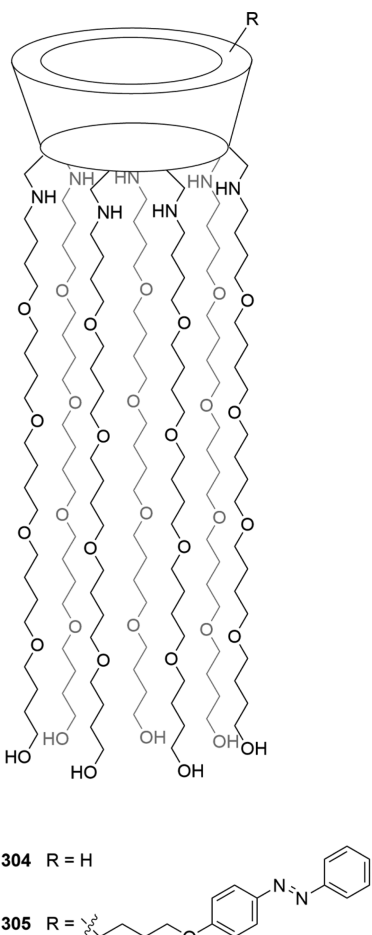


Figure 127. Structures of cyclodextrin-based channels 304 and 305.

groups are protonated and thus bind the halide anions more strongly through electrostatic interactions which results in a diminished anion transport ability of **304**. Furthermore, cyclodextrin **305**, which contains an additional azobenzene unit, was shown to be a photoswitchable ion channel. In the ground state (trans), the azobenzene units fits well into the cyclodextrin cavity and blocks the transport of anions (but not of cations). However, after photoswitch (cis), the diazobenzene units move out of the cavity and the anion transport ability is restored.

Montesarchia, Tecilla, and co-workers developed similar carbohydrate-containing channels, such as **306** (Figure 128),

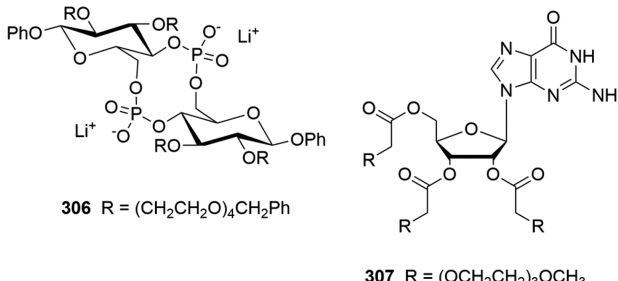


Figure 128. Structures of compounds 306 and 307.

that they coined CyPLOS (cyclic phosphate-linked oligosaccharide).^{512–514} Vesicle-based experiments using a pH-sensitive fluorophore indicated that **306** is able to quickly dissipate a pH gradient across the membrane. It was found that this ability to alter the pH was not influenced by the nature of the cation but instead was influenced by the nature of the anion (halogens, nitrate, and perchlorate were easily transported, but acetate, glutamate, and sulfate were not transported). Investigations on CyPLOS derivatives marked with the fluorescent dansyl dye indicated that the charged macrocycle lies on the surface of the membrane, while the ethylene glycol chains insert into the midpolar region of the bilayer.⁵¹⁵ The author suggests that transport therefore could occur through destabilization of the lipid bilayer, thereby causing changes in the permeability of the membrane. The same authors also reported a small series of sugar-modified guanosine derivatives (e.g., **307**, Figure 128).⁵¹⁶ Although K⁺-promoted G-quadruplex structures were observed in chloroform, no influence of potassium ions was seen during vesicle-based transport studies. On the other hand, the rate of transport observed during experiments with a pH-sensitive dye was strongly influenced by anions, indicating that these compounds are also able to transport anions. The authors suggest that a similar mechanism of membrane destabilization observed for the CyPLOS compounds also applies for the guanosine derivatives.

Metal–organic frameworks could in theory also be employed for self-assembly into pore-like structures that can span lipid bilayers and allow ions to pass through. However, most reported metal-based ion channels have low selectivity for anions. For example, Tecilla and co-workers employed a stable 4 + 4 metallacycle based on porphyrins appended with carboxylic acid groups as an ion channel.⁵¹⁷ The carboxylic acid groups allow the macrocycle to form dimeric structures that can span the membrane (Figure 129). Vesicle-based studies using HPTS indicated that the self-assembled structure is indeed able to form ion channels but with no selectivity toward alkali metals or inorganic anions.

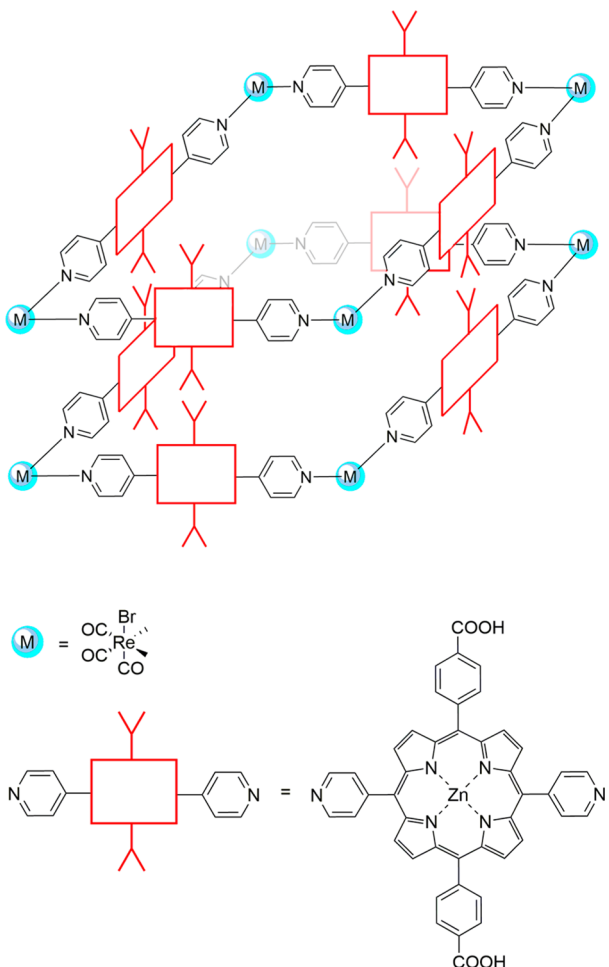


Figure 129. Schematic representation of a porphyrin metallacycle capable of ion transport by Tecilla and co-workers.

Calixarenes are another type of cylindrical molecule but with a smaller cavity than cyclodextrins and most metal–organic frameworks. Tecilla and colleagues developed a calix[4]arene in the 1,3-alt conformation appended with spermidine substituents as a potential anion channel (**308**, Figure 130).⁵¹⁸

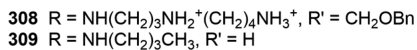
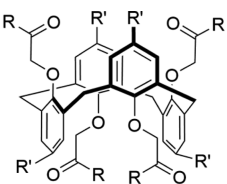


Figure 130. Structures of compounds **308** and **309**.

The spermidine arms are expected to be partially protonated in aqueous solution, and therefore, no cation transport activity was expected. Indeed, the authors were able to show using vesicle-based experiments with the pH-sensitive dye HPTS that **308** is able to transport halide anions but not cations or oxygenated anions (ClO₄⁻, glutamate, NO₃⁻, and SO₄²⁻). Similarly, Davis and co-workers designed calixarene-based transporter **309** (Figure 130).⁵¹⁹ Experiments conducted on liposomes encapsulating HPTS or lucigenin (halide-sensitive dye) indicated that

309 is able to transport chloride across EYPC membranes, presumably via a H⁺/Cl⁻ cotransport mechanism, while voltage-clamp experiments confirmed that **309** functions as an ion channel. However, the cavity of calix[4]arenes is believed to be too small for anions to pass through, and the authors therefore suggest that the ion channel activity is due to a self-assembled framework that was observed in a solid-state crystal structure of analogous calixarenes. Later studies showed that analogues of **309** in the *paco* and *cone* conformation are also able to transport chloride anions and that one of the arms of calixarene **309** can be left unsubstituted without loss of channel activity.^{520,521} Furthermore, Davis and co-workers also found that the macrocycle is not required for ion channel activity, as acyclic analogues of **309** were also able to function as anion channels.⁵²²

In recent years there have been a number of reports of intriguingly small molecules capable of forming anion channels, suggesting that it is not always necessary to develop large membrane-spanning structures to obtain anion channel activity. Yang and colleagues reported isophthalamide **310** containing two extra amide groups derived from α -aminoxy acids (Figure 131).⁵²³ They were able to show that **310** can transport chloride

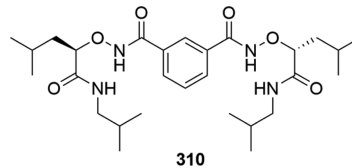


Figure 131. Structure of compound **310**.

anions across the lipid bilayers of both model liposomes and living cells (Madin-Darby canine kidney cells). Channel formation by **310** was suggested based on patch clamp experiments on giant unilamellar vesicles, but the mechanism of this channel formation has not yet been reported. Interestingly, Yang and co-workers also published a series of papers about the biological activity of **310**, including a report suggesting that the chloride transport activity of this compound is able to restore chloride conductance across cystic fibrosis epithelial cells.^{469,524–526}

Gokel and co-workers studied a series of similar isophthalamides and their pyridine analogues **311**–**318** (Figure 132).⁵²⁷

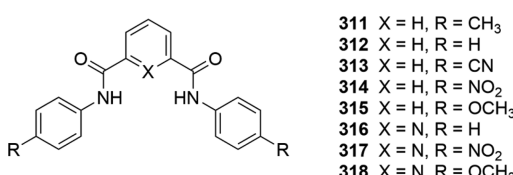


Figure 132. Structures of isophthalamides **311**–**318**.

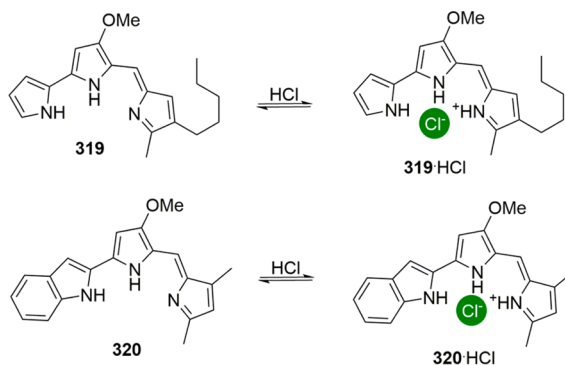
Vesicle-based assays with encapsulated lucigenin revealed that these compounds are able to transport chloride across DOPC (1,2-dioleoyl-sn-glycero-3-phosphocholine) bilayers. Furthermore, planar lipid bilayers techniques suggested that **314** might be able to form channels at high concentrations, which was also suggested by fluorescence studies. The authors speculate that the channel formation might be due to extensive stacking of the molecules in order to form an aggregate that can span the membrane. Subsequent studies on the same compounds revealed that they are not only able to transport chloride anions but also able to transport DNA into *E. coli* cells.⁵²⁸

4.2. Anion Transport via Synthetic Mobile Carriers

Mobile carriers are generally speaking smaller molecules than ion channels and function by binding to an anion, followed by diffusion of the anion-transporter complex through the bilayer. This means that many of the mobile carriers presented in this section will also function as potent anion receptors. There have been two main strategies in the development of mobile carriers for anions. One strategy has been to mimic the structure and behavior of natural products that function as anion carriers, while the other strategy has been to design carriers from scratch based on their behavior as anion receptors, followed by optimization of the anion transport activity by inducing small changes in the molecular properties (e.g., flexibility, anion binding ability, lipophilicity, etc.). In general, it has been observed that both the anion binding ability and the lipophilicity of the receptor need to be optimized. For both characteristics, too high values and too low values are detrimental for anion transport activity by the carrier.

The first strategy has been the result of the impressive anion transport ability of the natural compound “prodigiosin” (319).^{529,530} This tripyrrolic compound is isolated from certain strains of *Streptomyces* and *Serratia* and has been shown to possess anticancer,⁵³¹ antimalarial,⁵³² and immunosuppressive⁵³³ properties. Prodigiosin is able to bind chloride anions in a convergent array using three hydrogen bonds when protonated (Scheme 19). Early studies had therefore suggested that this

Scheme 19. Structures of Prodigiosin 319 and Obatoclax 320 and Their Respective HCl Salts



natural product is able to facilitate H^+/Cl^- symport across cell membranes and that this process might be responsible for the anticancer activity displayed by prodigiosin 319.^{534,535} More recent liposome-based studies, however, have revealed that 319 is also able to mediate $\text{Cl}^-/\text{NO}_3^-$ and $\text{Cl}^-/\text{HCO}_3^-$ antiport.^{536,537} Additionally, Quesada and co-workers investigated the anion transport ability of Obatoclax (320, Scheme 19), a synthetic analogue of prodigiosin that has also shown promising anticancer activity.^{538,539} A series of vesicle-based assays were employed to prove the ability of 320 to transport both chloride and bicarbonate anions across POPC (1-palmitoyl-2-oleoyl-sn-glycero-3-phosphocholine) membranes.⁵⁴⁰ It must be noted that the activity of prodigiosins 319 and 320 is exceptionally high and anion transport ability can be observed even at very low concentrations of the carrier, making them some of the best chloride carriers reported to date.

The high anion transport activity and potential therapeutic benefits of the natural prodigiosenes has inspired much research to develop analogues with similar activity. In 2005, Sessler and co-workers reported the chloride transport and anticancer

activity of a series of synthetic prodigiosenes and dipyrromethanes (e.g., 321 and 322, Figure 133).⁵⁴¹ It was found that

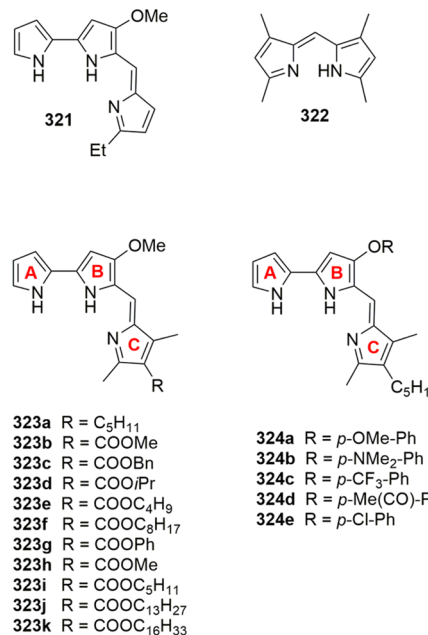


Figure 133. Structures of prodigiosenes 321–324.

these analogues are able to transport chloride across vesicle membranes and that they function mainly via an H^+/Cl^- cotransport mechanism. Furthermore, antiproliferative studies with A549 and PC3 cancer cell lines revealed that these prodigiosin mimics also possess anticancer activity. More recently, in 2013 and 2014, Davis, Thompson, and colleagues investigated the effect of B- and C-ring substitution on the pK_a , anion transport, and anticancer activity of synthetic prodigiosenes (323 and 324, Figure 133).^{542,543} It was found that the addition of an extra alkyl group on the B ring (323a) had little impact on the chloride transport activity of the prodigiosene, as observed during EYPC vesicle-based studies with the chloride-selective fluorophore lucigenin. On the other hand, the addition of electron-withdrawing groups on either the B ring (323b–n) or the C ring (324d–e) reduced the chloride transport activity of the prodigiosenes. This could be correlated with the apparent pK_a values of the prodigiosenes that were determined using UV-vis titrations in 1:1 CH_3CN :water at 25 °C, which revealed that the analogues with electron-withdrawing substituents have lower pK_a values. This implies that a higher percentage of these prodigiosenes will be present in their unprotonated form that is less able to bind and transport anions. Despite the good correlation between pK_a and transport activity, *in vitro* anticancer studies revealed no clear structure–activity relationship and all prodigiosin analogues were found to be similarly active in the anticancer assays.

Quesada and co-workers recently focused their research on the anion transport activity of a series of compounds that are structurally related to the prodigiosenes but synthetically easier to obtain, namely, the tambjamine alkaloids with general structure 325 (Figure 134).⁵⁴⁴ Their pK_a value is significantly higher than for the prodigiosenes ($\text{pK}_a \approx 10$ for the tambjamines versus $\text{pK}_a \approx 7.2$ for prodigiosin), and these compounds should therefore always be fully protonated at physiological pH. Indeed, initial studies showed that this class of compounds represents poor H^+/Cl^- cotransporters. On the other hand, experiments concerning

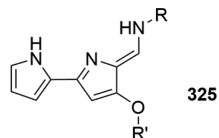


Figure 134. General structure of tambjamine 325; various substituents (R and R') have been investigated for anion transport.

the chloride transport activity of the tambjamines using chloride-selective electrode and ^{13}C NMR techniques on POPC vesicles revealed that these compounds are potent $\text{Cl}^-/\text{HCO}_3^-$ antiporters. Subsequent studies into their structure–activity relationships indicated that lipophilicity ($\log P$) plays an important role into the anion transport behavior of the tambjamines.⁵⁴⁵ It was found that tambjamines with too low $\log P$ values were poor transporters due to insufficient partitioning into the lipid bilayer, while compounds with too high $\log P$ values were also found to be poor transporters due to precipitation in the aqueous phase or the inability of the carriers to leave the membrane and pick up a new anion at the water–membrane interphase. The optimal $\log P$ value for anion transport by tambjamine derivatives was found to be $\log P \approx 4.2$. The same authors also investigated the anticancer activity of the tambjamines and discovered that the more potent anion transporters also possess anticancer activity by deacidifying acidic organelles in the cancer cells and thereby triggering apoptosis.⁵⁴⁶

The second approach toward the development of synthetic anion carriers, namely, the *de novo* design of small molecules that can transport anions, has become increasingly popular. The field has been dominated by synthetic ureas and thioureas, but in the past few years new hydrogen-bonding motives (squaramides, isophthalamides, pyrroles, hydroxyl groups, triazole, etc.) as well as nonclassical anion binding modes (halogen bonding, metal complexes) have emerged as potential building blocks for the design of new, more powerful anion carriers.

One of the earliest examples of synthetic mobile carriers for anions are the steroid-based ureas and thioureas developed by Davis and co-workers (coined “cholapods”, general structure 326, Figure 135).^{471,547,548} The steroid scaffold provides both preorganization of the anion binding site and high lipophilicity for sufficient partitioning into lipid bilayers. Early studies conducted with 7:3 POPC:cholesterol vesicles showed that the cholapods are able to mediate $\text{Cl}^-/\text{NO}_3^-$ antiport via a mobile carrier mechanism at concentrations as low as 1:250 000 transporter-to-lipid ratios.^{549,550} Later structure–activity studies revealed that for substituents in the 7 and 12 position, stronger anion complexation leads to increased anion transport ability, while for the substituents in the 3 position no correlation with anion affinity was found.⁵⁵¹ It was also observed that lipophilicity does not affect the chloride carrier activity of the cholapods,⁵⁵¹ that cationic cholapods are ineffective transporters,⁵⁵¹ that thioureas are generally better transporters than ureas,⁵⁵² and that macrocyclic analogues have enhanced chloride transport abilities due to stronger anion binding and improved screening of the anion from the lipophilic environment of the membrane.⁵⁵³ Recently, the Davis group discovered that the steroid scaffold is not necessary for anion transport, and equally powerful anion transporters that can function at concentrations of 1:500 000 (carrier-to-lipid) can be obtained when the cholic acid backbone is replaced with *trans*-decalin (e.g., 327)⁵⁵² or cyclohexane (e.g., 328)⁵⁵⁴ scaffolds (Figure 135). Furthermore, single-molecule anion transport analysis suggested that *trans*-decalin 327 is able

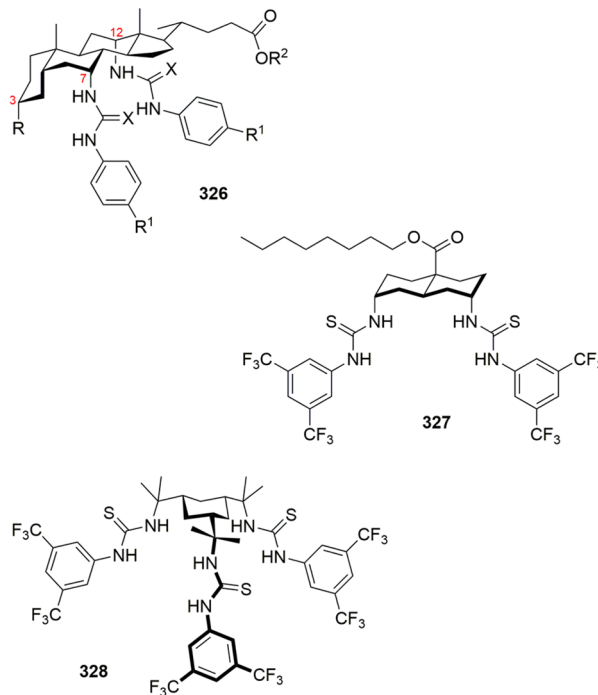


Figure 135. General structures of cholapods 326 for which various substituents (R and R') have been investigated for anion transport, as well as structures of analogues 327 and 328.

to transport chloride at an absolute rate of 850 chloride anions per seconds, which is similar to the activity of the natural chloride transporting protein CFTR when taking into account the low molecular weight of carrier 327.⁵⁵²

Gale and co-workers have been interested in preparing structurally simple receptors capable of transmembrane anion transport in an effort to make this type of anion carrier more “drug-like”. Initially, the authors studied a series of simple monoureas and monothioureas such as 329–332 (Figure 136).⁵⁵⁵ Chloride-selective electrode experiments conducted

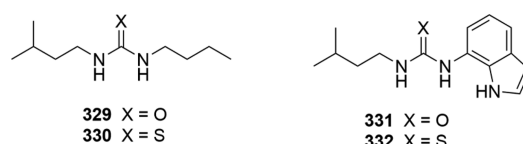


Figure 136. Structures of (thio)ureas 329–332.

on POPC vesicles revealed that these compounds are able to transport anions via $\text{Cl}^-/\text{NO}_3^-$ and $\text{Cl}^-/\text{HCO}_3^-$ antiport mechanisms at relatively low concentrations (1:25 000). It was observed that the thioureas outperformed the ureas, which was attributed to the higher acidity and lipophilicity of the thioureas. Interestingly, analogous monoamides and monothioamides were found not to be active as chloride carriers, indicating that thioureas provide an intrinsically good building block for the development of novel anion carriers. This was confirmed by a series of follow-up studies by the same authors, where ureas and thioureas attached to tris(2-aminoethyl)amine^{556,557} and cyclohexane⁵⁵⁸ all revealed the superiority of thioureas over ureas in anion transport assays.

Gale and colleagues subsequently tried to increase the potency of the carriers by introducing fluorination as a means of increasing both the lipophilicity and the anion binding strength

of the receptors. In this respect, fluorinated indole–ureas and indole–thioureas 333 and 334 (Figure 137) were prepared and

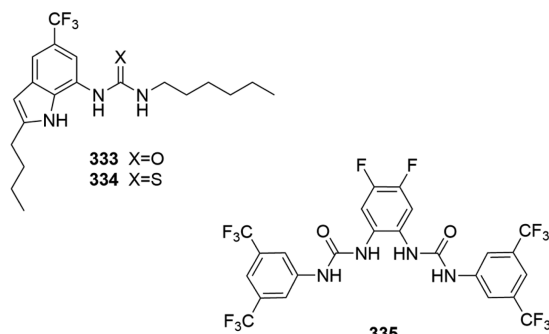


Figure 137. Structures of (thio)ureas 333–335.

their anion transport activities investigated.⁵⁵⁹ As expected, fluorination increased the chloride transport ability of the carriers during vesicle-based transport assays. Furthermore, the fluorinated indoles were also shown to induce apoptosis in vitro in cancer cell lines. This “fluorination effect” has been shown to be quite general, and the introduction of $-CF_3$ groups has now become common place in anion transport chemistry. For example, Gale and co-workers recently showed that highly fluorinated bis-urea 335 is able to challenge the Cl^-/HCO_3^- activity displayed by natural carrier prodigiosin 319.⁵⁶⁰

In order to gain more insight into the exact effect of substituents, such as $-CF_3$ groups, and the anion transport behavior of putative chloride carriers, Busschaert et al. synthesized a series of 22 monothioureas of general structure 336 containing various electron-donating and electron-withdrawing substituents (Figure 138).⁵⁶¹ Quantitative structure–

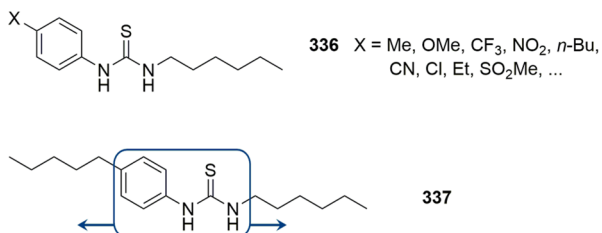


Figure 138. General structures of thioureas 336 and 337, which have been used to study the effect of substituents (336) and lipophilic balance (337) on anion transport ability.

activity relationship (QSR) techniques were employed to rationalize the anion transport properties of the thioureas. Although the anion binding ability of the thioureas correlated well with the electron-withdrawing or -donating effect of the substituents, statistical analysis revealed that the lipophilicity of the substituents has the largest effect on the anion transport ability of the thioureas, whereas the anion binding ability and the size of the receptor only cause minor changes in transport ability. However, a recent collaboration between Gale and Davis revealed that the effect of lipophilicity might be better explained in terms of “lipophilic balance”.⁵⁶² It was noted that in a series of monothioureas 337 with similar size, anion affinity, and overall lipophilicity (only the position of the thiourea functionality changes, Figure 138) the highest anion transport activity was displayed when the lipophilic substituents were symmetrically positioned around the binding site. This is presumably because

this arrangement allows better screening of the polar anion from the apolar lipid interior and helps the transfer of the complex into the membrane, while asymmetric lipophilic substitutions render the carriers more “surfactant like” and prevent the polar anion binding site to move into the core of the bilayer.

Although thioureas have been shown to be active anion transporters in model liposomes, there have been some concerns about the toxicity of thioureas,⁵⁶³ which might limit their use as potential treatments for anion transport-related pathologies. Gale and co-workers therefore studied the anion transport behavior of a number of thiourea isosteres (Figure 139), such as

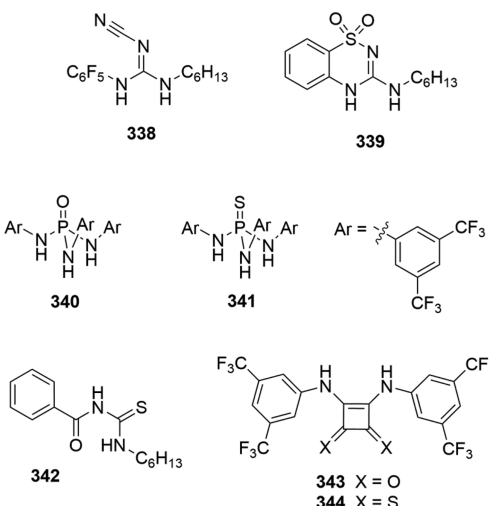


Figure 139. Structures of thiourea isosteres 338–344.

cyanoguanidines (e.g., 338),⁵⁶⁴ 3-amino-1,2,4-benzothiadiazine-1,1-dioxides (e.g., 339),⁵⁶⁴ phosphoric triamides (e.g., 340),⁵⁶⁵ thiophosphoric triamides (e.g., 341),⁵⁶⁵ acylthioureas (e.g., 342),⁵⁶⁶ and squaramides (e.g., 343).⁵⁶⁷ While all isosteres were found to facilitate chloride transport across POPC membranes, the cyanoguanidines, 3-amino-1,2,4-benzothiadiazine-1,1-dioxides, phosphoric triamides, and thiophosphoric triamides only displayed limited anion transport ability and could not rival the activity of the analogous thioureas. On the other hand, acylthioureas such as 342 and squaramides such as 343 were found to be significantly more active than their respective thiourea counterparts. For the acylthioureas this could be explained by the presence of an intramolecular hydrogen bond between the thiourea NH and the acyl oxygen atom. This intramolecular hydrogen bond shields the polar anion binding site from interactions with the environment and thereby increases the lipophilicity of the transporter. The high anion transport activity of the squaramides compared to the equivalent thioureas is presumably due to the fact that the lower lipophilicity of the squaramides can be overcome by their superior anion binding properties (association constants with TBA chloride in DMSO- d_6 /0.5% water were found to be 1 order of magnitude higher for the squaramides than for the thioureas). Since then, the anion transport ability of a cholic acid-derived squaramide has been reported by Deng et al.⁵⁶⁸ Recently, Gale, Jolliffe, and colleagues reported the properties of thiosquaramides such as 344.⁵⁶⁹ It was observed that at neutral pH a large fraction of the thiosquaramide is present as a negatively charged, deprotonated species due to the low pK_a values of the NH hydrogen atoms. This results in only minimal chloride transport mediated by the thiosquaramides in vesicles buffered to pH 7.2. However, anion

transport studies performed at lower pH ($\text{pH} < 6$) revealed that in these conditions the anion transport activity of the thiosquaramides is switched on because the carriers are present in their neutral fully protonated form.

Apart from (thio)ureas and their isosteres, isophthalamides and other convergent bis-amides have also been useful building blocks in the design of anion receptors. Davis, Gale, Quesada, and co-workers reported on the effect of preorganization on the anion transport ability of related isophthalamides **345** and **346** (Figure 140).⁵⁷⁰ The classic isophthalamide **345** prefers the

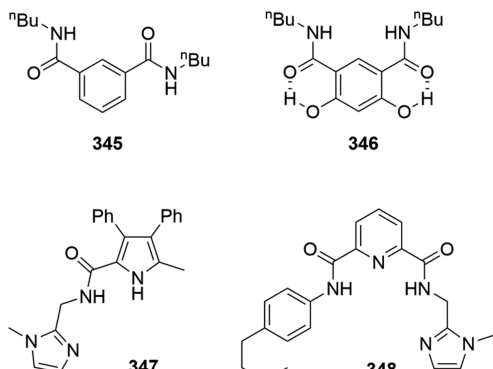


Figure 140. Structures of isophthalamides **345**–**348**.

nonconvergent syn-anti conformation and was found to be inactive in the anion transport assays. On the other hand, the hydroxyl groups in **346** can hydrogen bond to the amide oxygen atoms, thereby stabilizing the preorganized syn-syn conformation and enhancing the anion transport ability of the isophthalamide. Other bis-amide-based transporters are the ditopic isophthalamide–crown ether conjugate **274** capable of mediating both K^+/Cl^- and Na^+/Cl^- symport designed by Smith and colleagues (Figure 114, see section 3.2.2),⁵⁷¹ and bis-amides **347** and **348** that contain an imidazole group as a protonatable site to facilitate H^+/Cl^- symport activity (Figure 140).^{572,573}

Calix[4]pyrroles have also been proven versatile building blocks for anion carriers,⁵⁷⁴ which is unsurprising given their well-documented ability to extract anions from an aqueous phase into an organic phase (see section 3.1). Unsubstituted calix[4]pyrrole **194** (Figure 81) was found to only transport chloride anions across POPC vesicles in the presence of cesium cations and not in the presence of other group I cations, in agreement with the known ability of calixpyrroles to form ion pair complexes.⁵⁷⁵ However, later studies have shown that small modifications of the calix[4]pyrrole scaffold can switch this Cs^+/Cl^- symport process to an antiport process. Octafluorocalix[4]pyrrole **210** (Figure 88), for example, was shown by Gale, Sessler, and co-workers to function as a $\text{Cl}^-/\text{NO}_3^-$ and $\text{Cl}^-/\text{HCO}_3^-$ antiporter in POPC liposomes.⁵⁷⁶ The authors explained this observation by the increased anion affinity of the calixpyrrole due to the presence of the electron-withdrawing fluorine substituents. Similarly, calix[4]pyrroles strapped with additional hydrogen-bond donors, such as triazoles^{577,578} or isophthalamides,⁵⁷⁹ have also been shown to function as anion antiporters due to increased anion affinity.

Triazoles have become popular as a CH hydrogen-bond-donating motive since Flood's seminal report on triazolophanes,⁵⁸⁰ and it comes as no surprise that there have been some recent reports on the use of triazoles as transmembrane anion carriers. Shang et al. developed foldamer **349** containing amide

functionalities to provide a rigid receptor for anion binding via intramolecular hydrogen bonding (Figure 141), as confirmed by

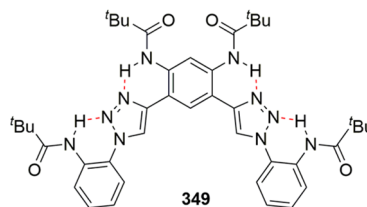


Figure 141. Structure of anion carrier **349**.

X-ray crystallography and 2D NOESY NMR in CDCl_3 .⁵⁸¹ Furthermore, ^1H NMR titrations with TBA chloride in CD_2Cl_2 revealed that receptor **349** is able to bind chloride anions in this solvent via CH hydrogen bonding to the triazoles, but the amide functionalities were found not to participate in the anion binding event. The chloride transport ability of **349** was investigated using the halide-sensitive dye lucigenin encapsulated in EYPC vesicles and confirmed the chloride transport ability of **349**. A mobile carrier mechanism was suggested by the absence of conductance signals in patch clamp experiments.

Hydroxyl groups are other alternative hydrogen-bond donors, but they are rarely used exclusively and usually come in combination with other anion binding groups. For example, Davis and co-workers investigated catechol-containing tris-amides **350**–**353** (Figure 142) and found that they were able

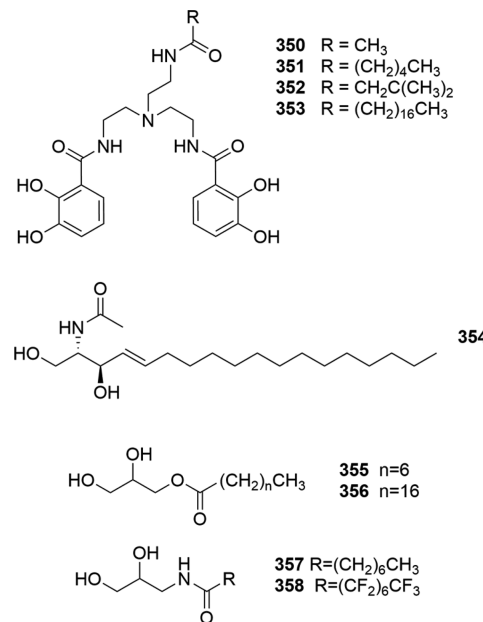


Figure 142. Structures of anion carriers **350**–**358**.

to transport anions across membranes.⁵⁸² It was also suggested that the OH functionalities of the catechol moiety are essential for transport, as analogous receptors without the OH groups were not able to facilitate anion transport. More recently, Davis and co-workers revealed that the naturally occurring sphingolipid ceramides such as **354** (Figure 142) are also able to bind anions and transport them across EYPC bilayers.⁵⁸³ It was previously shown that ceramides can aggregate into pores at high concentrations,⁵⁸⁴ but Davis and colleagues showed that they can also function as chloride carriers at low concentrations. Later,

the same group revealed that the structurally similar monoacylglycerols such as 355 and 356 (Figure 142) are capable of $\text{Cl}^-/\text{NO}_3^-$ antiport across EYPC membranes.⁵⁸⁵ Furthermore, the authors found that simple modifications such as the introduction of an extra NH hydrogen-bond donor (357) and fluorination (358) could greatly improve the transport ability of natural products 355 and 356.

Jeong and colleagues reported anion transporters that employ a similar chloride binding motive as the naturally occurring CLC chloride channels (i.e., two NH and two OH hydrogen-bond donors). Initially, the authors reported the properties of ureas 359–362 (Figure 143) and revealed that only the chlorinated

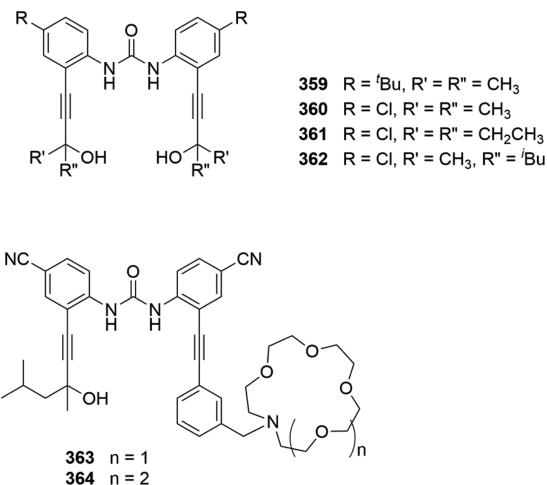


Figure 143. Structures of anion carriers 359–364.

analogues are potent transporters in lucigenin assays, with the best transport activity observed for the receptor with the more lipophilic isobutyl substituents (362).⁵⁸⁶ Various lucigenin assays with differing intra- and extravesicular salts revealed that these transporters function through a $\text{Cl}^-/\text{NO}_3^-$ antiport mechanism. In a subsequent manuscript, Jeong and co-workers reported analogous receptors 363 and 364 containing azacrown-ether appendages and showed that they were able to transport chloride across POPC membranes via either a Na^+/Cl^- (363) or a K^+/Cl^- (364) symport mechanism.⁵⁸⁷

Primary and secondary amines have also been employed in the design of transmembrane anion carriers. Davis and co-workers designed cholic-acid-based macrocycle 365 (Figure 144) containing primary amines that are expected to be protonated at neutral pH and therefore interact with anions through electrostatic interactions.⁵⁸⁸ It was shown that 365 can mediate chloride transport across EYPC membranes via an antiport mechanism. Furthermore, experiments with cholesterol-containing membranes suggested that 365 functions as a mobile carrier, rather than through self-assembly into membrane-spanning channels.

Guanidiniums are another type of charged NH-containing functional group that can be used for anion transport purposes. Tecilla and colleagues showed using a series of HPTS assays that polyguanidine calixarene 366 (Figure 144) can transport chloride anions across lipid bilayers.⁵⁸⁹ Calixarene 366 also transports chloride anions across bulk chloroform solutions (U tube), indicating that this compound functions as a mobile carrier. Interestingly, 366 displayed anti-Hofmeister behavior where chloride was preferentially transported over more lipophilic anions such as iodide and nitrate. Furthermore, the

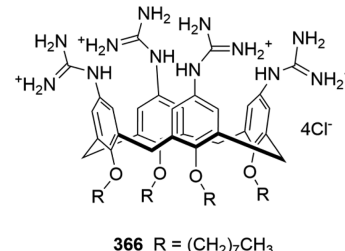
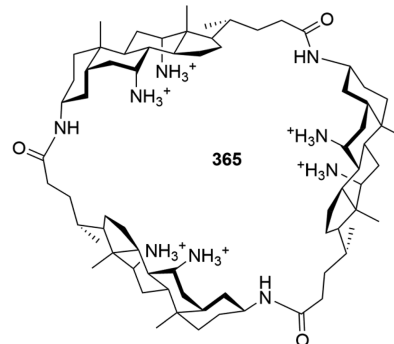


Figure 144. Structures of anion carriers 365 and 366.

chloride transport ability of 366 is significantly suppressed in the presence of iodide. However, this unusual behavior has not yet been fully explained by the authors.

Matile and co-workers reported a number of anion carriers that employ halogen bonding as the noncovalent interaction to coordinate anions. Originally, they investigated a series of calix[4]arenes substituted at the lower ring with halogenated phenyl substituents capable of halogen bonding.⁵⁹⁰ It was shown that these compounds can transport chloride anions only in the presence of tetramethylammonium cations, suggesting that they function through a biologically not relevant TMA^+/Cl^- symport mechanism. Furthermore, some of the compounds were found to be inactive due to too strong halogen bonding between the carrier and the anion. To overcome these problems, the same group subsequently reported a series of very simple halogenated compounds, including 367–374 (Figure 145), which were

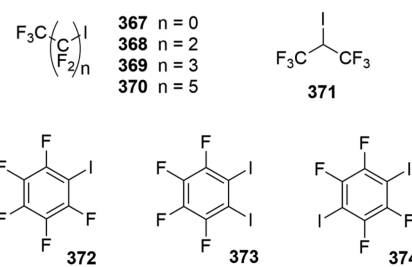


Figure 145. Structures of anion carriers 367–374.

shown to function as mobile carriers with anion antiport ability.⁵⁹¹ The surprisingly high anion transport ability of these small molecules is presumably partly due to the inherent hydrophobic nature of highly halogenated compounds, which implies that the often polar region of the anion binding site does not have to be compensated for by the addition of hydrophobic tails.

Iengo, Tecilla, and co-workers recently introduced metal complexes as potential transmembrane mobile carrier for anions.

They designed Pd(II) complex **375** (Figure 146) based on the fact that the diphosphine (dppp) ligand is inert toward ligand

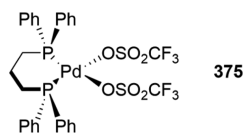


Figure 146. Structure of anion carrier **375**.

exchange and lipophilic enough to provide membrane solubility, while the triflate ligands are labile and should be easily exchanged with the anions to be transported.⁵⁹² Indeed, a series of HPTS and lucigenin assays in 95:5 EYPC:EYPG lipid vesicles revealed that **375** can transport chloride anions in an antiport fashion, while PdCl_2 or dppp alone cannot. U-tube experiments suggested that the metal complex is also able to transport chloride anions across bulk chloroform layers, indicating that this is the first report of a metal complex capable of transporting anions using a mobile carrier mechanism.

The examples mentioned thus far have focused on the transport of chloride anions. However, transmembrane transport of other anions can also be beneficial. Most chloride antiport systems function as chloride/nitrate or chloride/bicarbonate antiporters, and thus, Cl^- , NO_3^- , and HCO_3^- are the most commonly studied ions in anion transport, but it is also possible to transport other anions across lipid bilayers. It was already mentioned that isophthalimides can be used as DNA transporters. In principle, most nonviral chemical gene delivery systems can be seen as transmembrane DNA transporters,⁵⁹³ but a discussion of gene delivery systems is beyond the scope of this review. Sulfate is a common inorganic anion with a number of biological functions but is often seen as too hydrophilic to be transported across lipid bilayers by small molecules. Nonetheless, Gale, Jolliffe, and co-workers used ^{33}S NMR techniques to provide evidence for transmembrane sulfate transport by a series of tripod receptors and cages (e.g., **376** and **377**, Figure 147).⁵⁹⁴ The same group also employed the double anion binding site in *o*-phenylenediamine-based bis-ureas (e.g., **378** and **379**, Figure 147) to transport dicarboxylates such as maleate and fumarate across POPC bilayers, but the anions are presumably only transported in their monoionic form.⁵⁹⁵ Additionally, receptors **380** and **381**, containing additional hydrogen-bond acceptors, were designed in order to bind and transport L-lactate across lipid bilayers (see Figure 147).⁵⁹⁶ Assays using chloride-selective electrodes revealed that **380** and **381** are able to mediate chloride/lactate antiport and that this process is more favorable than chloride/pyruvate antiport, as the latter system does not benefit from an additional hydrogen bond between the receptor and the pyruvate anion. Very recently, Gale and co-workers achieved transmembrane amino acid transport by the combination of squaramide **343** (Figure 139) for binding to the carboxylate unit of the amino acid and a lipophilic aldehyde for dynamic binding to the amino functionality through reversible imine/enamine formation.⁵⁹⁷

4.3. Anion Transport via Other Mechanisms

In addition to the classic ion channels and mobile carriers, there are a number of synthetic transport systems that cannot be classified under one of these two mechanisms. For example, Davis and co-workers developed a series of modified phospholipids **382–384** (Figure 148) that function via a so-called “relay” mechanism.⁵⁹⁸ The structural similarity between

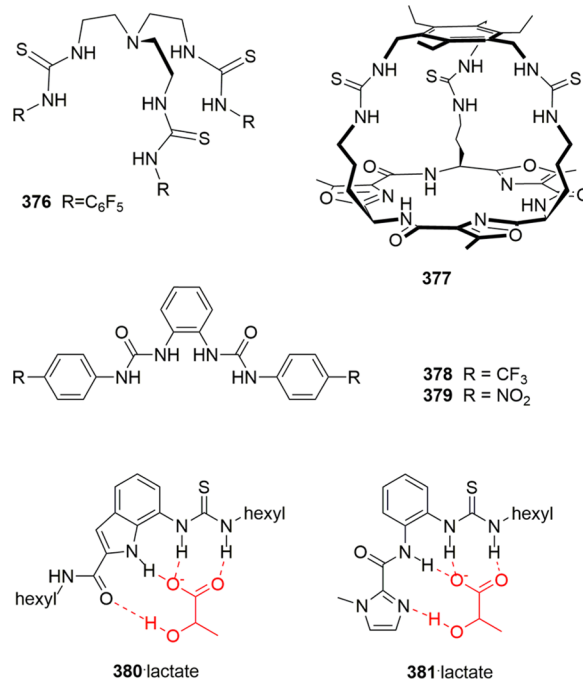


Figure 147. Structures of carriers **376–381** capable of transporting anions other than chloride.

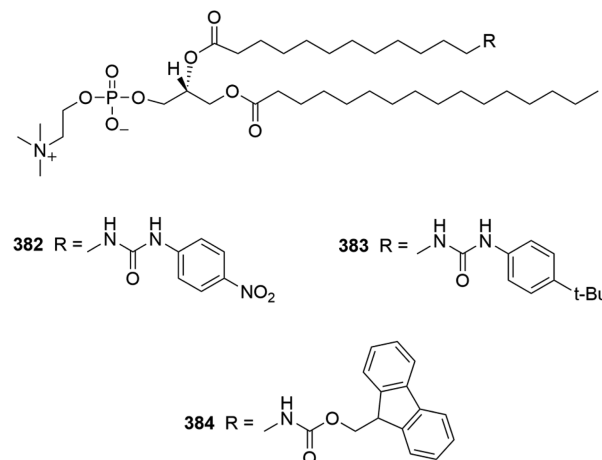


Figure 148. Structures of phospholipid–ureas **382–384** that function via a relay mechanism.

382–384 and the bulk of phospholipid bilayers suggests that these receptors will form an integral part of the membrane. However, the anion binding site attached to **382–384** allows the lipids in one leaflet of the bilayer to pick up an anion and subsequently hand it onto a modified lipid in the other leaflet, which can then release the anion on the other side of the bilayer. As this mechanism does not imply the formation of a transient pore nor the diffusion of the transporter within the membrane, this mechanism is neither a channel nor a mobile carrier mechanism.

Regen and co-workers worked on “molecular umbrellas” as a modified mobile carrier mechanism for transmembrane transport.⁵⁹⁹ The umbrellas consist of two or more facial amphiphiles (usually cholic acid derivatives) coupled to a hydrophilic core. When these umbrellas are submerged in a polar environment, they will adopt an “open” conformation that maximizes the contacts between the hydrophilic core and the amphiphile with

the environment. On the other hand, when the compounds are in an apolar environment such as a membrane, they will adopt a more “closed” conformation where the contacts between the apolar side of the amphiphile and the bilayer are maximized and the contacts between the hydrophilic core and the bilayer are minimized. In this closed conformation a polar or ionic guest can be entrapped within the umbrella and thus be shielded from the apolar environment. In this system, transmembrane transport occurs through the sequential opening and closing of the umbrella. Regen and colleagues employed this concept to transport a large variety of guests, including the anionic nucleotides AMP and ATP by guanidinium-containing umbrella 385 (Figure 149).^{600,601} Schmitzer and co-workers reported an analogous umbrella that is able to transport chloride anions across EYPC membranes.⁶⁰²

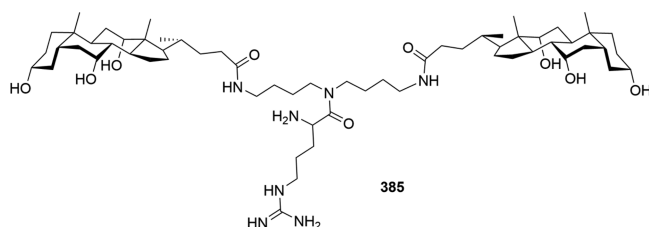


Figure 149. Structure of molecular umbrella 385.

Matile and his group postulated another type of transmembrane ion transport, coined the “Jacobs ladder”, based on the activity of a number of mixed cyclic oligoureas and oligoamides such as 386 and 387 (Figure 150).⁶⁰³ Experiments using EYPC vesicles encapsulating the pH-sensitive dye HPTS suggested that this class of receptor can facilitate HCl transport. X-ray crystallography showed that 386 forms tubular stacks in the solid state through dipole–dipole interactions and hydrogen

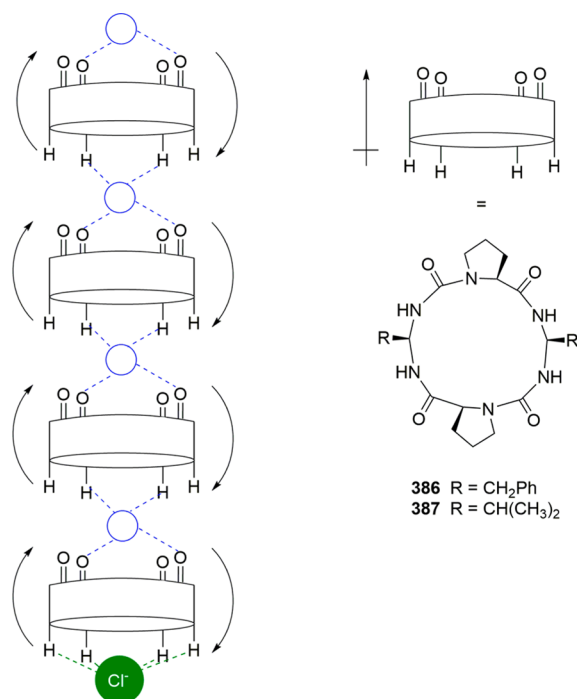


Figure 150. Schematic representation of the Jacobs ladder mechanism for anion transport by 386 and 387.

bonding with bridging water molecules.⁶⁰⁴ However, anions are generally too large to pass through these macrocycles, and the authors therefore suggested a different mechanism but note that it is purely speculative and no evidence for this mechanism is given. The proposed mechanism consists of a membrane-spanning stack of macrocycles, similar to that observed in the solid state. An anion can then be bound on one side of the membrane via NH hydrogen-bonding and anion–dipole interactions. Rotation of this complex then allows the following macrocycle to bind this anion, and multiple repetitions of this event will eventually lead to the release of the anion on the other side of the membrane (Figure 150).

Another type of anion transport that cannot be classified as either channel or mobile carrier is so-called “flippase” activity. This is not exactly the transport of an anion *through* a membrane but consists instead of the binding of a phospholipid headgroup in one leaflet of the bilayer, followed by the translocation of this lipid molecule to the other leaflet of the bilayer. In biological systems, this process is carried out by specialized proteins in order to maintain the asymmetric lipid distribution between the inner and the outer leaflets of the cell membrane, which is important for normal cellular function and signaling.⁶⁰⁵ Synthetic flippases have been mainly developed by Smith and colleagues (Figure 151). Initially, they found that tris-sulfonamide 388 is

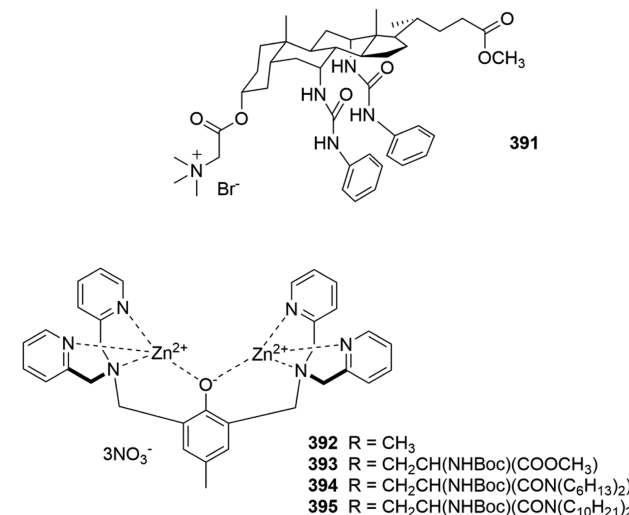
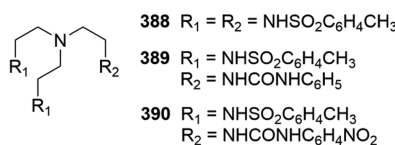


Figure 151. Structures of synthetic flippases 388–395.

able to translocate PC (phosphatidylcholine) lipids in both model vesicles and erythrocytes,^{606,607} while later studies revealed that urea-containing analogues 389 and 390,^{608–610} as well as cationic cholapod 391,^{611,612} are capable of PS (phosphatidylserine) flippase activity in both liposomes and erythrocytes. In another study, Smith and co-workers investigate the transport properties of Zn²⁺-containing receptors 392–395.⁶¹³ Zn²⁺ complexes often have a high affinity for phosphates and were therefore considered good candidates for phospholipid flippase activity. Flippase studies with fluorescently labeled lipids revealed that 392–395 can translocate negatively charged lipids

such as POPG but not zwitterionic lipids such as POPC. It was also shown that the Zn^{2+} complexes can transport carboxy-fluorescein and chloride anions across POPC membranes. Furthermore, 392 was found to be an effective antibiotic against *Staphylococcus aureus*, which could potentially be due to its ion transport and flippase ability.

Not only is the division between ion channel and mobile carrier not always clear, the division between symport and antiport can also be circumvented. The transporters discussed so far function either through a symport or an antiport mechanism where one transporter conducts both steps of the overall electroneutral transmembrane transport process. However, in biological systems there are many natural ion channels present that can influence the overall transport process. Gale and co-workers therefore devised a “dual-host” approach to anion transport to mimic this situation. They combined a known potassium carrier (valinomycin, 396, Figure 152) with a known

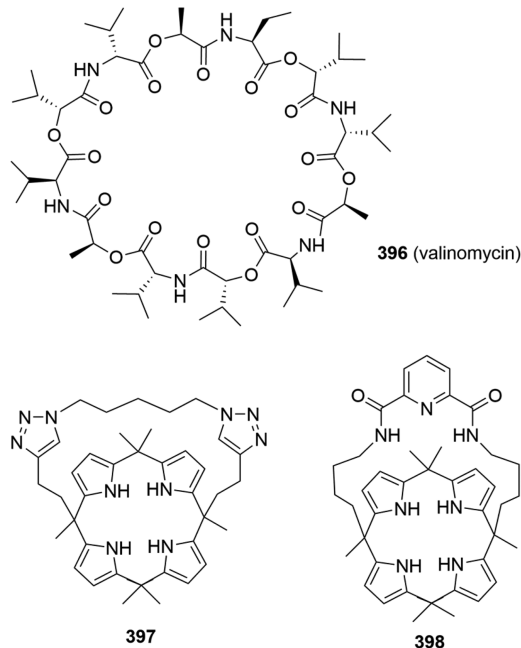


Figure 152. Structures of compounds 396–398 used in dual-host-type ion transport.

chloride transporter (e.g., calixpyrrole 397, Figure 152) and found that the overall transport process was a K^+/Cl^- symport system that functioned significantly faster than any of the components alone.⁶¹⁴ Similarly, the combination of a known chloride transporter with a known bicarbonate transporter led to significantly increased ion transport with an overall Cl^-/HCO_3^- antiport mechanism.⁶¹⁵ In collaboration with Sessler and Shin, Gale and co-workers then employed this strategy to design anion transporters with anticancer activity.⁵⁷⁹ In model POPC vesicles, diamide-strapped calixpyrrole 398 (Figure 152) was shown to be a poor chloride transporter by itself, but the transport ability was significantly enhanced in the presence of known Na^+ transporter monensin. Additionally, 398 was found to possess anticancer activity *in vitro*, which was attributed to the ability of 398 to alter both the Cl^- and the Na^+ concentrations within the cancer cells. However, when the natural Na^+ channels were blocked with amiloride, the ability of 398 to alter the intracellular chloride concentrations was reduced. These results suggest that the anticancer activity of this calixpyrrole is due to the transport of

Cl^- mediated by 398 that is compensated by concomitant transport of Na^+ through natural sodium channels in an overall dual-host symport process.

4.4. Conclusions and Outlook on Transmembrane Anion Transport

The examples given in this section show that anion transport has developed into a major subfield of supramolecular chemistry, and it now involves a large range of molecules, from simple (thio)ureas and squaramides to halogen bond donors, metal complexes, and large membrane-spanning structures. Furthermore, structure–activity studies have highlighted the importance of optimal lipophilicity and optimal anion binding (not too strong and not too weak) in the design of novel anion transporters. The challenge now is to move into biological systems with early work showing much promise.

5. ANION-DRIVEN SUPRAMOLECULAR ARCHITECTONICS

The self-assembly of fragments such as sugars, amino acids, and fatty acids occurs throughout nature and plays an essential role in the construction of biological macrostructures.^{616,617} Moreover, these building blocks self-sort into one of the most efficient and complex systems known in nature to build the functional basic unit of life: a cell. A profound understanding of self-assembly and self-sorting phenomena is therefore essential for the comprehension of such complex supramolecular systems and can be used for innovation toward novel functional materials.^{618,619} Complementary to metal-driven assembly, the use of anionic templates opens up a whole new aspect of influencing the assembly processes. The interaction with anions has been shown to provide novel characteristics, such as electron transfer, to supramolecular architectures.⁶²⁰ Here we review how anions can influence large topologies and drive the self-assembly of macroscopic structures. In the past few years a number of reviews have emerged regarding this topic, and this section will therefore be kept relatively brief.^{621,622} Furthermore, some reports on anion-mediated assemblies have already been discussed in the previous sections where they were used for anion sensing (sections 2.2 and 2.4) or anion extraction by selective crystallization (section 3.2.3), and the reader is referred to these sections for additional examples.

5.1. Anion-Templated Topologies

A very early example of the anion-templated synthesis of an organometallic system was found by Hawthorne and co-workers upon combining 1,2-dilithiocarbonane with mercury(II) chloride.⁶²³ In the presence of chloride the reaction afforded tetranuclear [12]mercuracarborand-4 in 80% yield, as confirmed by X-ray diffraction (Figure 153). The absence of a proper anion template, when mercury acetate is used as a mercury source, resulted in trinuclear [9]mercuracarborand-3 as the exclusive product, while a more linear template such as thiocyanate gave cyclic pentameric species.⁶²⁴

Inspired by the double helix of DNA, which is assembled via the interaction of two complementary chains of nucleotides through hydrogen bonding, Lehn and colleagues introduced the use of a chloride-templating effect to control the structure of circular helicates.⁶²⁵ The combination of a tris-bipyridine ligand with iron(II) chloride afforded circular double-helicate 399 with a central chloride ion stabilized via $CH\cdots Cl^-$ interactions (Figure 154a). Each Fe(II) ion has a distorted octahedral coordination sphere occupied by three bipyridine groups. The metal ions lie almost in one plane and form the corners of a pentagon. When

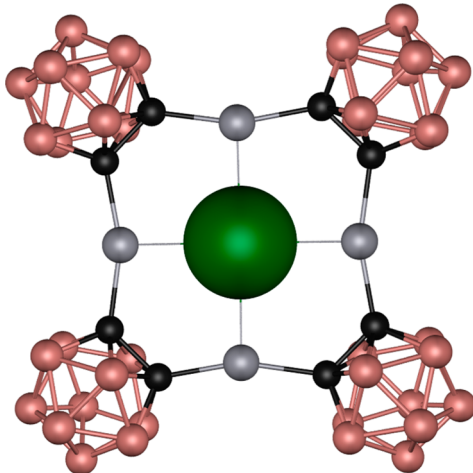


Figure 153. X-ray crystal structure of the chloride-templated tetranuclear [12]mercuracarborand-4, shown in ball-and-stick representation with the bound chloride anion in space fill. Atoms are color coded as follows: C (black), B (pink), Hg (gray), Cl (green).

other anions such as sulfate were used it was found that a hexameric circular helicate formed.⁶²⁶

Recently, Leigh and co-workers adapted Lehn's strategy to synthesize a pentafoil knot templated by chloride.⁶²⁷ In Leigh's system the ligands contain terminal aldehydes that can react dynamically with diamines to form bridges, resulting in completely covalent knotted structure **400** (Figure 154b). Treatment of this chloride complex with a large excess of silver hexafluorophosphate caused the exchange of chloride for hexafluorophosphate and generated an empty cavity pentafoil knot. The addition of different anions, such as bromide and iodide, to this emptied system did not introduce significant spectral changes, with the exception of the administration of TBACl which allowed a smooth regeneration of the chloride complex, demonstrating that this pentafoil knot is a selective cavitan for chloride anions.

Biological systems are dynamic and protean, and the use of anions as templates can introduce this characteristic in metal organic systems, as shown by Nitschke and co-workers.⁶²⁸ Mixing *p*-toluidine, 6,6'-diformyl-3,3'-bipyridine, and cobalt(II) triflimide hydrate ($\text{Co}[\text{N}(\text{SO}_2\text{CF}_3)_2]_2 \cdot \text{H}_2\text{O}$) gave a dynamic library of coordination complexes of ligand **401**. On the other hand, the use of cobalt(II) triflate hexahydrate ($\text{Co}(\text{SO}_2\text{CF}_3)_2 \cdot 6\text{H}_2\text{O}$) instead of the triflimide salt produced a tetrahedral Co_4L_6 cage ($\text{L} = \text{401}$, Figure 155b). Furthermore, the addition of lithium perchlorate to either the dynamic library or the tetrahedral cage resulted in the transformation into a $\text{Co}_{10}\text{L}_{15}$ pentagonal prism with both enantiomers present in the crystal structure ($\text{L} = \text{401}$, Figure 155c). The interweaving of the ligands created six distinct anion binding pockets, five of which lie along the 2-fold symmetry axis between the upper and the lower rings. A central channel surrounded by 10 inward-pointing pyridyl hydrogen atoms forms up the sixth binding site, occupied by a chloride anion, presumably introduced as an impurity.

Metal coordination of organic ligands into cages templated by various anionic guests, such as the examples given above, makes up the largest group of anion-templated topologies. Recently, Custelcean and Dunbar summarized the influence of anions on the topology of these anion binding coordination cages and described in detail the dynamics and specific interactions that drive anion encapsulation.^{629,630} Here, we will only update their

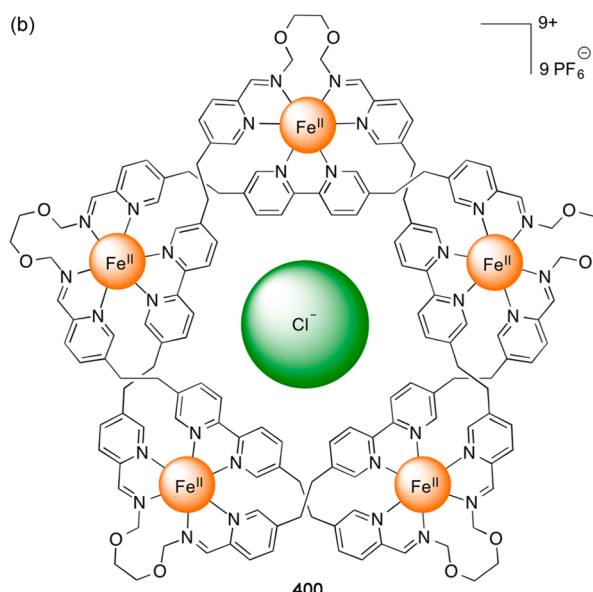
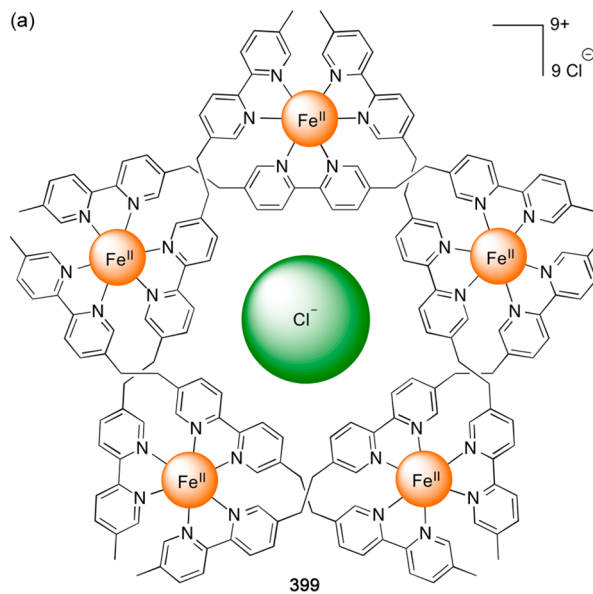


Figure 154. (a) Chloride-templated circular double helicate **399** by Lehn and co-workers. (b) Chloride-templated pentafoil knot **400** by Leigh and co-workers.

comprehensive reviews with the latest contribution to this field, focusing on metal-free anion-templated architectures. Additionally, extra attention will be drawn to those cases where evidence of anion-templated assembly in solution has been given rather than to those where assembly was solely observed in the solid state by X-ray diffraction.

Edge-directed M_4L_6 tetrahedra represent the most common class of anion-encapsulating coordination cages. In 2014 a novel addition to this class of compounds was made by Hooley and co-workers.⁶³¹ Combination of 2,7-diaminofluorinol, 2-formylpyridine (to create ligand **402**), and iron(II) perchlorate afforded the $[(\text{ClO}_4)\text{CFe}_4(\text{402})_6]^{+}$ complex (Figure 156). A combination of metal–ligand interactions and self-complementary hydrogen bonding allowed stereocontrol in the self-assembly of the prochiral ligands into a tetrahedral-like arrangement. In

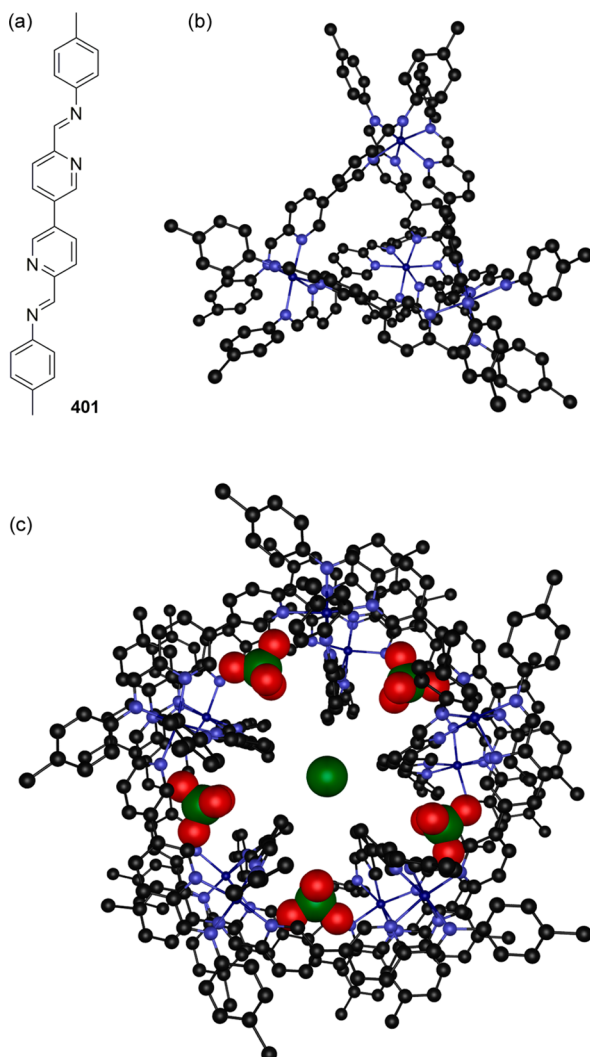


Figure 155. (a) Structure of ligand **401**. (b) Crystal structure of tetrahedral Co_4L_6 cage ($\text{L} = \text{401}$) shown in ball-and-stick representation. (c) Crystal structure of pentagonal prism $\text{Co}_{10}\text{L}_{15}$ cage ($\text{L} = \text{401}$) shown in ball-and-stick representation with the coordinated perchlorate and chloride anions in space fill (0.6 times the van der Waals radius). Solvent molecules, noncoordinating counterions, and hydrogen atoms are omitted for clarity. Atoms are color coded as follows: C (black), N (blue), O (red), Cl (green), Co (vivid blue).

addition, four out of six alcohol groups of the fluorene moiety formed hydrogen bonds with a single bound perchlorate ion in the interior cavity, which exerts a templating effect that forms the basis of the structure. While the majority of the energy of formation of the cage comes from the favorable metal–ligand interactions, the discrimination between different isomers arises from the directing hydrogen bonding. This resulted in a shift of the equilibrium toward a single main diastereomer, observed both in the crystalline state by X-ray diffraction and in solution by NMR analysis. Other anions with similar dimensions and hydrogen-bond acceptor characteristics such as NO_3^- , SO_4^{2-} , and BF_4^- also proved to be good templates, while CF_3SO_3^- , $\text{S}_2\text{O}_4^{2-}$, $\text{Ph}_3\text{SiF}_2^-$, PF_6^- , and halide ions, which all have significantly different geometries and dimensions compared to ClO_4^- , did not promote cage formation.

Until 2013 well-defined cage complexes lacking metal atoms had not been explored. Wu and co-workers were the first to use a tris(bisurea) triphenylamine ligand (**403**) that can form a

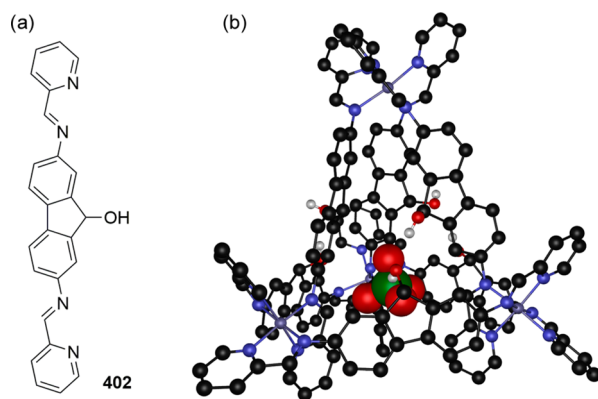


Figure 156. (a) Structure of ligand **402**. (b) Crystal structure of perchlorate templated cage $[(\text{ClO}_4)\text{CFe}_4(\text{402})_6]^{7+}$ shown in ball-and-stick representation with the coordinated perchlorate anion in space fill (0.6 times the van der Waals radius). Solvent molecules, non-coordinating counterions, and hydrogen atoms are omitted for clarity. Atoms are color coded as follows: C (black), N (blue), O (red), Cl (green), Fe (gray).

tetrahedral $[(\text{PO}_4)_4\text{L}_4]$ -type cage and a “pinwheel” helical $[(\text{SO}_4)_3\text{L}_2]$ complex with PO_4^{3-} and SO_4^{2-} ions, respectively (Figure 157).⁶³² The tetrahedral cage could be readily disassembled and reassembled via the addition of weak acids and bases, indicating good control over the assembly process. Each phosphate ion was bound to six urea groups from three different ligands through 12 strong N–H···O hydrogen bonds. The cage also displayed good thermal and solvent stability, thereby initiating interest in metal-free anionic cages. Similarly, in the pinwheel complex each sulfate ion is bound by four urea groups through eight N–H···O hydrogen bonds with additional C–H···O hydrogen bonds further stabilizing the system.

Even though metal-free cages were only prepared recently, noncage-like anion-driven assemblies have been reported earlier. In 1996 Sessler et al. reported anion-predicated self-assembly of polypyrrolic macrocycles.⁶³³ Sapphyrin and calixpyrrole monocarboxylates such as **404**, deprotonated by tetrabutylammonium fluoride (TBAF), were shown to self-assemble into dimers via anion chelation. The calixpyrrole adopted the cone conformation, allowing every carboxylate ion to form four hydrogen bonds (Figure 158). The dimers were observed in the gas phase, in solution, and in the solid-state.

During a collaboration between the Sessler and Gale groups calix[4]pyrrole dimers were assembled via bis-imidazolium and bis-pyridinium linkers (e.g., **405**).⁶³⁴ Hydrogen bonding of calix[4]pyrrole **194** to the bromide counterion caused the macrocycles to adopt a cone-like conformation, which in turn provided an electron-rich binding pocket encapsulating a single imidazolium or pyridinium ion, affording the envisioned dimers (Scheme 20a). Later, Sessler applied that same strategy to form a self-assembled polymer using imidazolium-functionalized calix[4]pyrrole **406** (Scheme 20b).⁶³⁵ In this case, the binding pocket enclosed the tethered imidazolium ion of a neighboring molecule forming the supramolecular polymer chain.

de Mendoza and co-workers observed a double-strand helical self-assembly of bicyclic guanidinium dimers (**407**) and tetramers (**408**) around sulfate ions (Figure 159).⁶³⁶ The short CH_2SCH_2 linker between the guanidinium moieties prevents the strand to wrap around a single anion and drive two strands to work together wrapping up the sulfate anion in the double-helical structure of the predictable handedness imposed by the chiral

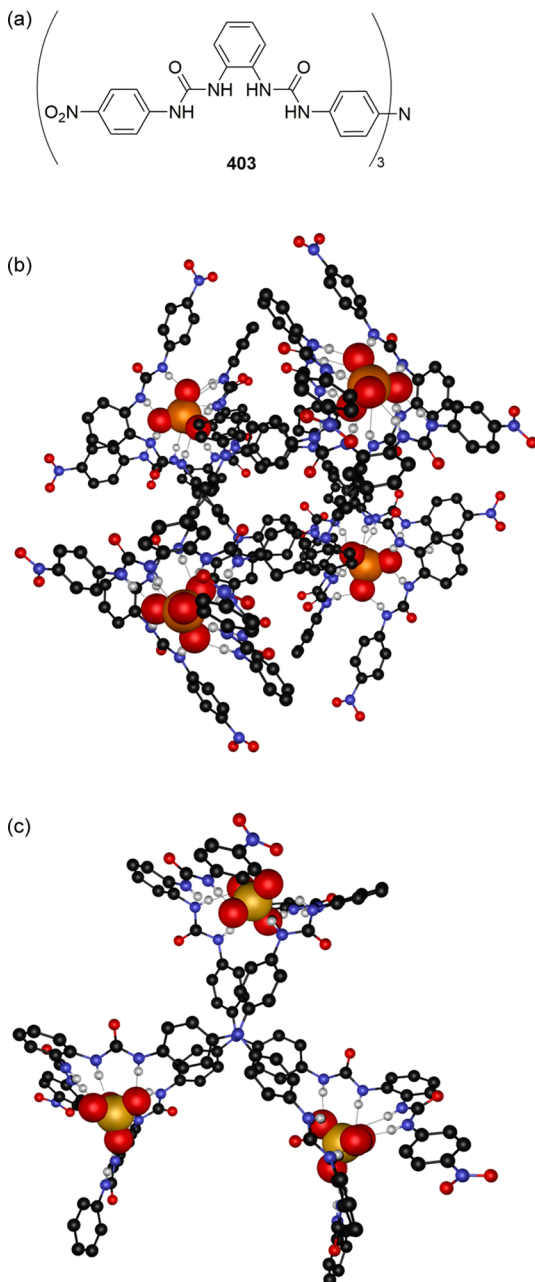


Figure 157. (a) Structure of ligand **403**. (b) Crystal structure of tetrahedral $[(\text{PO}_4)_4(\mathbf{403})_4]$ -type cage shown in ball-and-stick representation with the coordinated phosphate anions in space fill (0.6 times the van der Waals radius). (c) Crystal structure of pinwheel helical $[(\text{SO}_4)_3(\mathbf{403})_2]$ complex shown in ball-and-stick representation with the coordinated sulfate anions in space fill (0.6 times the van der Waals radius). Solvent molecules, noncoordinating counterions, and hydrogen atoms are omitted for clarity. Atoms are color coded as follows: C (black), H (white), N (blue), O (red), Cl (green), P (orange), S (yellow).

nature of the receptor. The helical conformation of the oligomers was elucidated by NMR and CD spectroscopy.

Schmidtchen and his team developed compound **409** (Figure 160) in order to use the bicyclic guanidinium moiety to form highly ordered chiral porphyrin assemblies in aqueous solutions without the help of polyionic helical templates.⁶³⁷ The $\pi-\pi$ stacking of the central porphyrin units was combined with the Coulombic and hydrogen-bonding attraction forces governed by

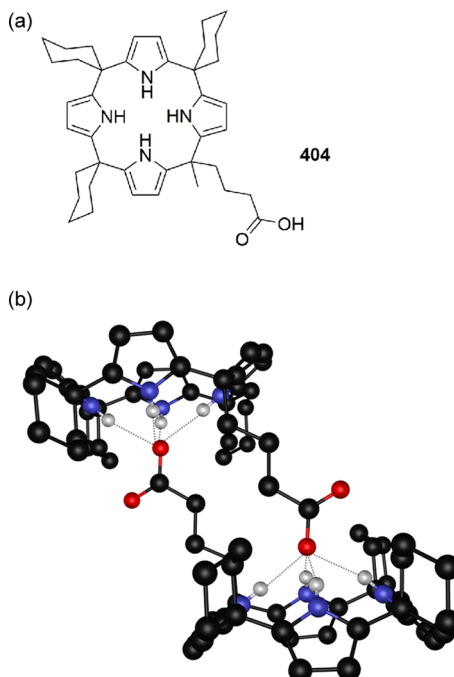


Figure 158. (a) Structure of calix[4]pyrrole carboxylic acid **404**. (b) Crystal structure of $[\mathbf{404}-\text{H}]_2$ dimer shown in ball-and-stick representation. Solvent molecules, noncoordinating counterions, and hydrogen atoms are omitted for clarity. Hydrogen bonds are shown as dotted lines, and atoms are color coded as follows: C (black), H (white), N (blue).

the peripheral guanidinium moieties and the counteranions. These interactions impose geometrical restrictions with respect to the intermolecular distance and orientation of the chiral guanidinium species. The exact spacing and chemical nature of the counteranions control the actual chirality of the system, whereby the anions serve as linkers that diminish the repulsion forces between the porphyrin moieties.

Gao et al. reported the formation of micelle nanoparticles consisting of poly(ethylene oxide)-block-PR copolymers (Scheme 21).⁶³⁸ The PR polymer, providing ionizable tertiary amines, allowed for chaotropic anion (CA^-) induced micellization. The PR block polymer with the most hydrophobic side chains resulted in the most sensitive induction of micellization in the presence of ClO_4^- ions. In anion-free conditions or in the presence of kosmotropic anions only monomers were found. These findings indicate an anti-Hofmeister trend in which the presence of chaotropic anions (lipophilic anions, e.g., ClO_4^-) but not kosmotropic anions (hydrophilic anions, e.g., SO_4^{2-}) result in micellization.

Sánchez and co-workers visualized (by scanning electron microscopy) an interesting effect that anions can have on the crystalline morphology of a surface deposit.⁶³⁹ When free of anions, bis(triazole)benzamide receptor **410** aggregates into needles where the microcrystals grow anisotropically in a direction perpendicular to the active plane of a small cluster of molecules by means of $\pi-\pi$ stacking. Assembly in the presence of gallic acid, however, gives rise to flower-like structures on a graphite surface by complexation of the receptor with gallic acid in a 1:2 receptor:acid ratio forming flat ribbons (Figure 161). The interdigitation of the aliphatic chains and the $\pi-\pi$ stacking between the aromatic moieties form lamellae consisting of the flat ribbons.

Scheme 20. Schematic Representation of (a) Calixpyrrole Dimerization Induced by Bis-imidazolium 405 and (b) Imidazolium-Based Calix[4]pyrrole 406 Supramolecular Polymer Formation

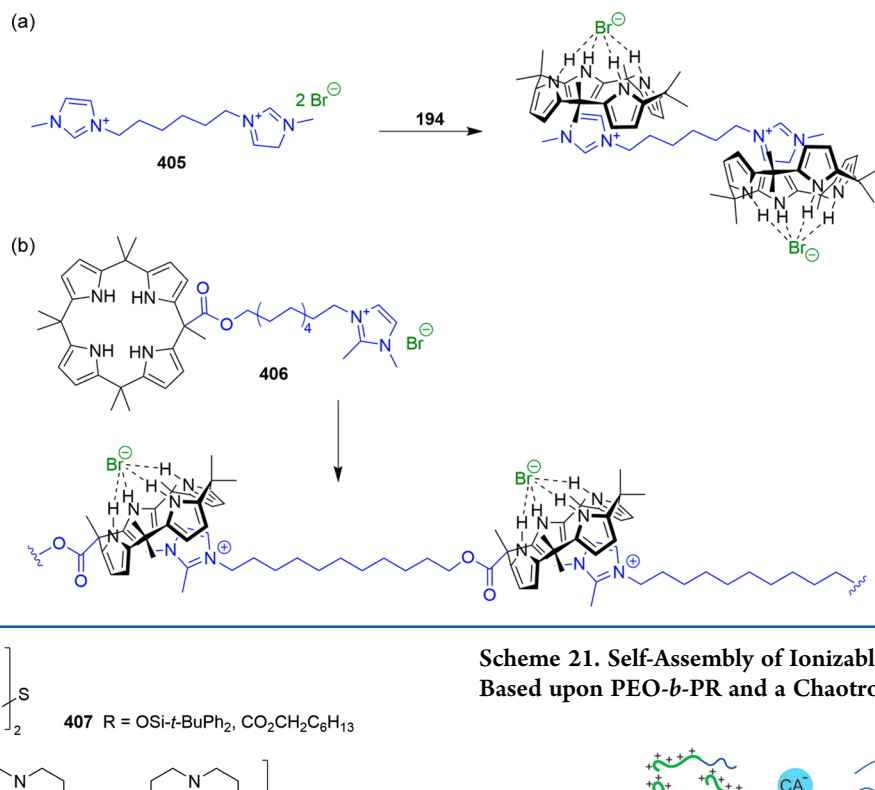


Figure 159. Structure of bicyclic guanidinium oligomers 407 and 408.

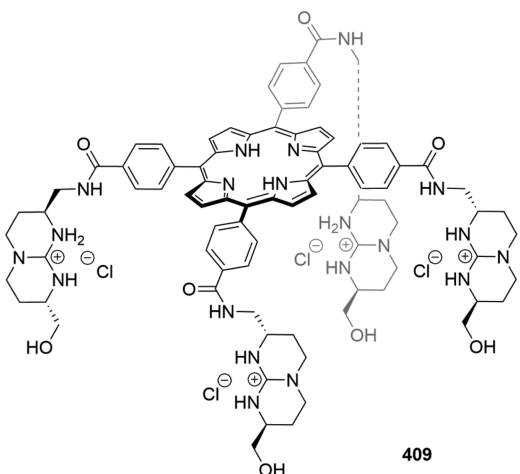
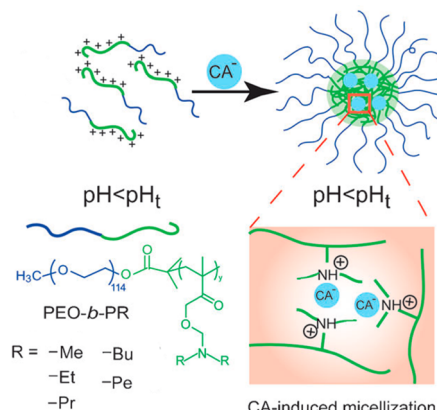


Figure 160. Structure of bicyclic guanidinium porphyrin 409.

Bottom-up self-assembly of materials requires a profound knowledge of how to encode contacts between the molecular building blocks to program their packing. Flood and co-workers found that pentagonal macrocycles with cyanostilbene CH donors ("cyanostar", 411 and 412) stack into dimers with various anions both in solution and in the solid state (Figure 162).⁶⁴⁰ These systems were further investigated to gain a deeper understanding of the solution-phase intermolecular coupling, which could then be exploited for three-dimensional growth on surfaces.⁶⁴¹ Interestingly, when a drop of host solution mixed

Scheme 21. Self-Assembly of Ionizable Polymeric Micelles Based upon PEO-*b*-PR and a Chaotropic Anion (CA^-)^a



^aReprinted with permission from ref 638. Copyright 2014 Wiley-VCH.

with TBAPF_6 was deposited on highly ordered pyrolytic graphite, the scanning tunnelling microscopy (STM) image revealed anisotropic lateral crystalline domains (Figure 162). The darker spots in the STM image correspond to individual cyanostar rings sitting directly on the graphite surface, while the brighter spots resemble dimers holding a single PF_6^- ion between two cyanostars molecules, similar to what was observed in solution. This first report of anion-driven dimerization on a surface holds great promise for the rational design of surface-active supramolecular assemblies. The principles of dimerization found for the cyanostar macrocycle were further applied to interlock two cyanostars simultaneously on a single dialkyl-substituted phosphate thread, forming an anion-templated [3]rotaxane (413) with 18 short hydrogen bonds ($<3\text{ \AA}$) among the two cyanostars with the threaded phosphate moiety (Scheme 22).⁶⁴⁰

The use of anions to interlock different molecules is a well-studied aspect in supramolecular chemistry. In 2013 Beer and co-workers published a review on the anion-templated assembly of

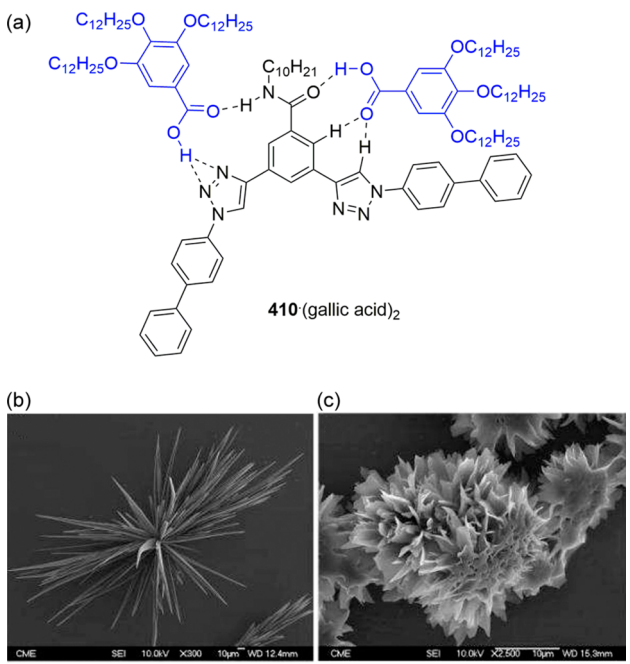


Figure 161. (a) Structure of the in-silico-predicted **410**-(gallic acid)₂ complex. (b) SEM image of the aggregates formed by self-assembly of **410**. (c) SEM image of the aggregates formed by self-assembly of **410** in the presence of a gallic acid derivative. Reprinted with permission from ref 639. Copyright 2012 Royal Society of Chemistry.

mechanically interlocked structures.²⁴⁸ Additionally, in 2014 Beer et al. summarized the progress in the synthesis and exploitation of catenanes and the application of rotaxanes and catenanes for sensing of charged guests.^{249,642} In this section we will therefore give a detailed picture of anion-templated interlocking pseudorotaxanes, rotaxanes, and catenanes by providing an up-to-date overview of seminal work not included in these reviews.

Beer and co-workers have been pioneers in investigating the ability of anions to template pseudorotaxane formation. Using the ability of both triazole C–H and amide N–H functionalities to form hydrogen bonds with halide ions and oxoanions, bis(triazole)pyridinium (e.g., **414**) and bis(amide)pyridinium (e.g., **415**) molecules can be held into the cavity of an isophthalamide-based macrocycle (e.g., **416**) to form pseudorotaxanes (Figure 163).⁶⁴³ Both solution and solid-state analysis revealed that both halide ions and oxoanions template interpenetration without a notable selectivity. Following this anion-templating strategy applying both C–H and N–H hydrogen bonding, a number of similar pseudorotaxanes, rotaxanes, and catenanes were obtained by combining various isophthalamide- and bistriazolium-based macrocycles with different triazolium-based threads.⁶⁴⁴

The concept of halogen bonding is a rather novel contribution to the field of supramolecular chemistry,^{645,646} and consequently, there are only a few examples of anion template architectures that employ this type of interaction. Beer's group exploited the halogen–halogen bond between a 2-iodo-imidazolium thread and a chloride ion, held within the cavity by hydrogen bonding, to guide the thread into an isophthalamide-based macrocycle and form pseudorotaxane **417** (Figure 164).⁶⁴⁷ Even though the authors anticipated that a larger cavity might be required to embed the larger iodo-substituted thread, the macrocycle with the smallest cavity was shown to have the strongest association. A feasible explanation for this is the greater contribution of the

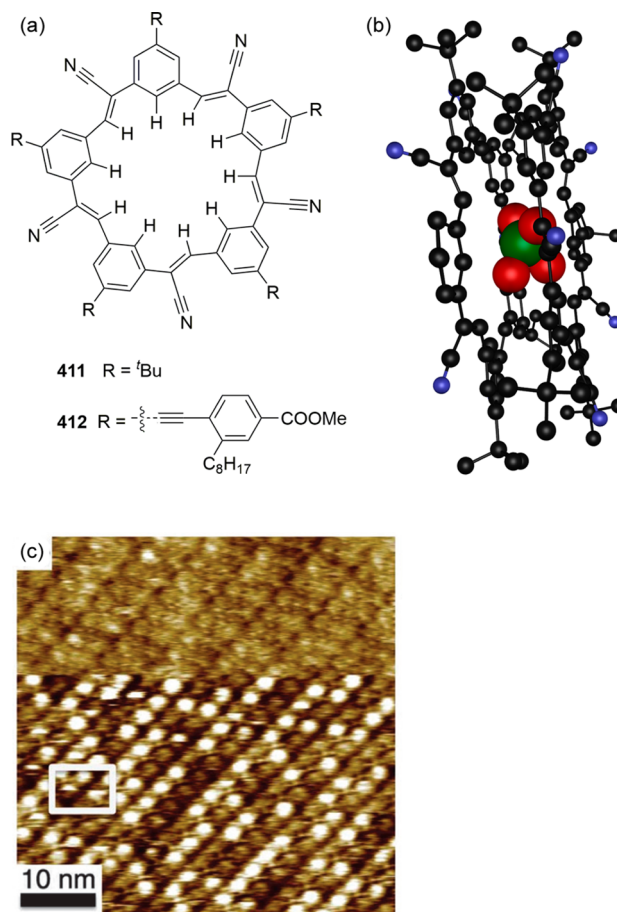


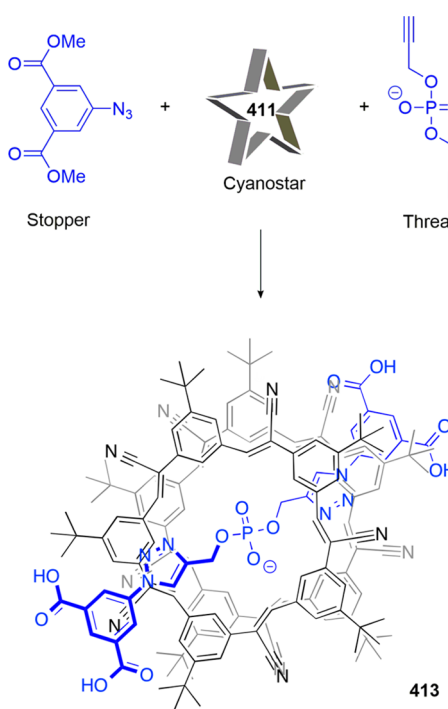
Figure 162. (a) Structures of cyanostar **411** and **412**. (b) Crystal structure of the $[(411)_2 \cdot \text{ClO}_4]^-$ dimer shown in ball-and-stick representation with the bound perchlorate anion in space fill (0.6 times the van der Waals radius). Solvent molecules, noncoordinating counterions, and hydrogen atoms and other disorder are omitted for clarity. Atoms are color coded as follows: C (black), H (white), N (blue), O (red), Cl (green). (c) STM image showing the bright features assigned to dimers of the PF_6^- complex of **412**. Reprinted with permission from ref 641. Copyright 2014 Royal Society of Chemistry.

polar interactions between the polyether and the positive imidazolium moiety.

Beer and colleagues also reported the first nitrate-templated assembly of [2]rotaxanes.⁶⁴⁸ An asymmetric bidentate isophthalamide-3,5-bis(amide)pyridinium thread was designed, which after complexation with a nitrate ion was capped via the Huisgen reaction, leaving an isophthalamide-based macrocycle interlocked system **418** (Figure 165). In the absence of nitrate no evidence of rotaxane formation was observed. The trigonal nitrate anion was found to bind strongly within the rotaxane host's complementary cavity with a notable weaker binding for other oxoanions such as bicarbonate and dihydrogen phosphate.

A valid alternative for capping the thread after interpenetration of the central component into the macrocycle is synthesizing the macrocycle around the completed thread. Beer and co-workers applied the metathesis reaction using a Grubbs catalyst as a very successful way to close macrocyclic rings around a thread forming different [2]rotaxanes (e.g., rotaxane **421**, Scheme 23).^{649–651} The macrocycle precursor was positioned on the various threading components via a combination of hydrogen-bonding and electrostatic interactions with a chloride ion as template.

Scheme 22. Formation of Phosphate-Templated Cyanostar [3]Rotaxane 413



The same metathesis strategy also allows the preparation of [2]catenanes, as shown by Beer and his group.^{652,653} By employing both hydrogen- and halogen-bonding interactions and using different anions as template (e.g., bromide and nitrate), a second macrocycle precursor could be interlocked around an existing macrocycle. Subsequent ring-closure metathesis afforded [2]catenanes such as 422 (Figure 166).

5.2. Anion-Controlled Gelation

Compared to the topologies that combine a limited number of molecules, supramolecular gels consist of an almost infinite number of assembled molecules that form a continuous network withholding a second component, such as a gas in the case of aerogels or a liquid in the case of hydrogels and organogels. Gels have a permanent structure on the analytical time scale, which is solid like in its rheological behavior, lacking flow. A large number of gelators are polymers, and these systems have been studied extensively and will not be discussed here. Supramolecular gels, on the other hand, often consist of low molecular weight gelators (LMWGs) which interact through the formation of noncovalent interactions resulting in the construction of fibrous aggregates.^{288,654,655} The addition of anions often results in dissolution of the supramolecular gel, as the anions perturb the noncovalent interactions between the LMWGs resulting in a gel–sol transition. This property has been applied as mode of detection (discussed previously in section 2.4) as well as a means to alter the properties of supramolecular gels.

The chemically diverse nature of the LMWGs provides access to a wide range of solvent systems, making these systems a versatile tool in pharmaceutical polymorph screening, as described by Steed and co-workers, who conducted a detailed study of crystallization processes involving a series of pharmaceutical substances.⁶⁵⁶ They employed the established gel-forming abilities of bis-ureas such as 423–426 (Figure 167) to create gels with a wide range of solvents and at various temperatures and critical gelator concentrations. Crystallization

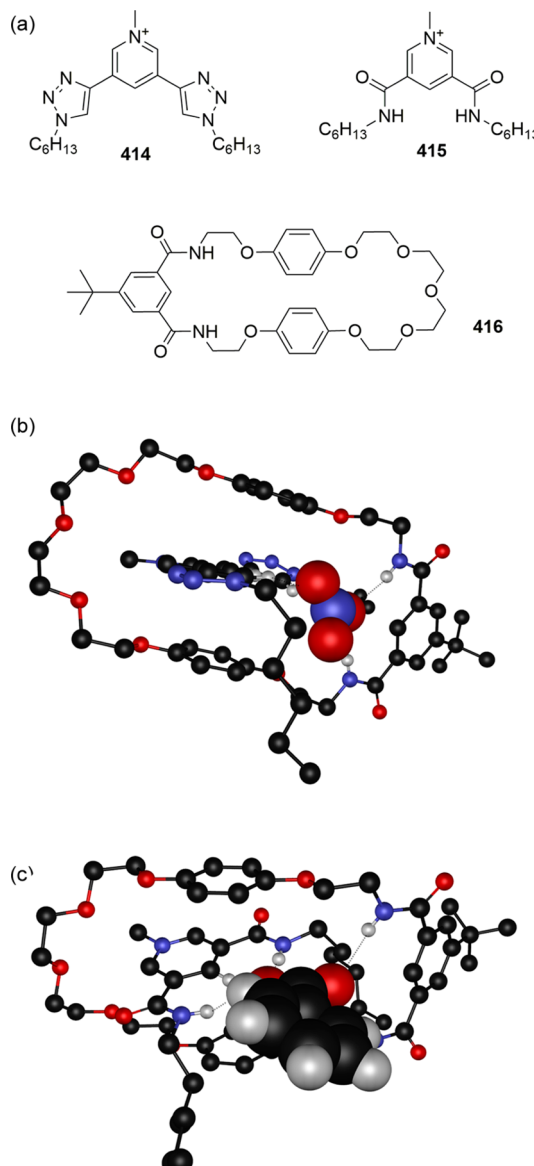


Figure 163. (a) Structures of compounds 414–416. (b) Crystal structure of the nitrate-templated pseudorotaxane from 414 and 416 shown in ball-and-stick representation with the bound nitrate anion in space fill (0.6 times the van der Waals radius). (c) Crystal structure of the benzoate-templated pseudorotaxane from 415 and 416 shown in ball-and-stick representation with the bound benzoate anion in space fill (0.6 times the van der Waals radius). Solvent molecules and noncoordinating hydrogen atoms are omitted for clarity. Hydrogen bonds are shown by dotted lines, and atoms are color coded as follows: C (black), H (white), N (blue), O (red).

experiments were then undertaken with a range of drug and nondrug compounds in both gel- and solution-based media. The crystals tended to grow larger and with more regular faces in the supramolecular gels than in the gelator-free reference solutions. Moreover, the conversion of metastable polymorphs was inhibited. In many cases the crystals could conveniently be obtained by acetate-triggered gel dissolution (Figure 167). Crystals of substances that themselves bind to the anions, however, were shown to dissolve along with the gel.

Several reports have recently been made showcasing the development of fibrillar growth and moderation of supramolecular gels formation by salting out using different

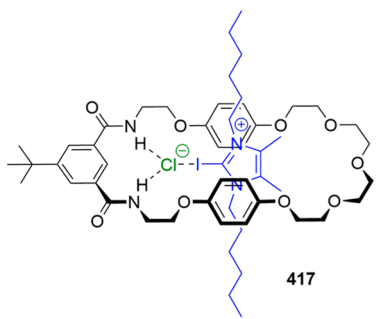


Figure 164. Structure of halogen-bonding-templated pseudorotaxane 417.

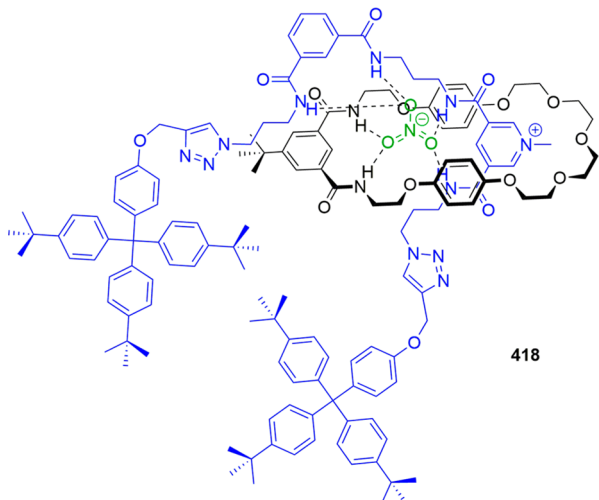


Figure 165. Structure of nitrate-templated [2]rotaxane 418.

salts.^{657–659} Strongly hydrated anions are referred to as salting-out or kosmotropic ions, and less hydrated anions are salting-in or chaotropic ions, following the Hofmeister series (Figure 79). In general, the tendency to form gels displays a Hofmeister bias, with the kosmotropic ions resulting in a liquid phase, whereas the chaotropic ions tend to induce gelation.⁶⁶⁰ Superimposed on this trend is crystallization, which is presumably driven by factors such as solubility and lattice energy. In between these extremes there is a specific region where the most stable gels are formed.

The effective anion-induced gel formation of LMWGs, without the presence of a metal counterion, was reported recently when Tripathi and Pandey stumbled onto hydrogen sulfate stimulated gelation.⁶⁶¹ While studying the host:guest interactions of the hexafluorophosphate salt of bile-acid-based macrocycle 427 with various anions in $\text{CHCl}_3\text{--DMSO}$ (5:1) a gel was formed when TBA HSO_4^- was added (Figure 168). Among the anions tested (F^- , Cl^- , Br^- , AcO^- , H_2PO_4^- , and HSO_4^-), only HSO_4^- ions effectively induce gel formation. Interestingly, replacement of the central benzene ring in the macrocycle for a pyridine ring (428) prevents gel formation, most probably due to an improved imbedding of the HSO_4^- ion inside the cavity.

Charged species and electron-rich anionic and electron-deficient cationic building blocks can be used to form assemblies on the basis of electrostatic attractive and repulsive interactions between opposite and identical charges. Other parameters, such as van der Waals interactions, enable the alteration of the packing of these charged species within the assemblies. Next to salting out, these charge-by-charge assemblies applying different anions

Scheme 23. Chloride-Templated Synthesis of [2]Rotaxane 421 via a Metathesis Reaction

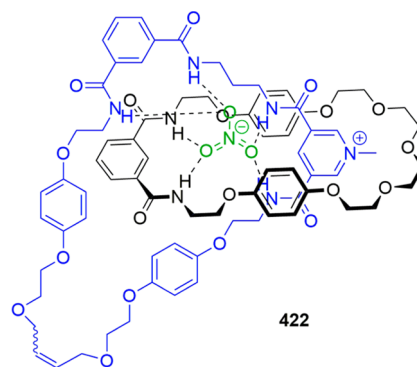
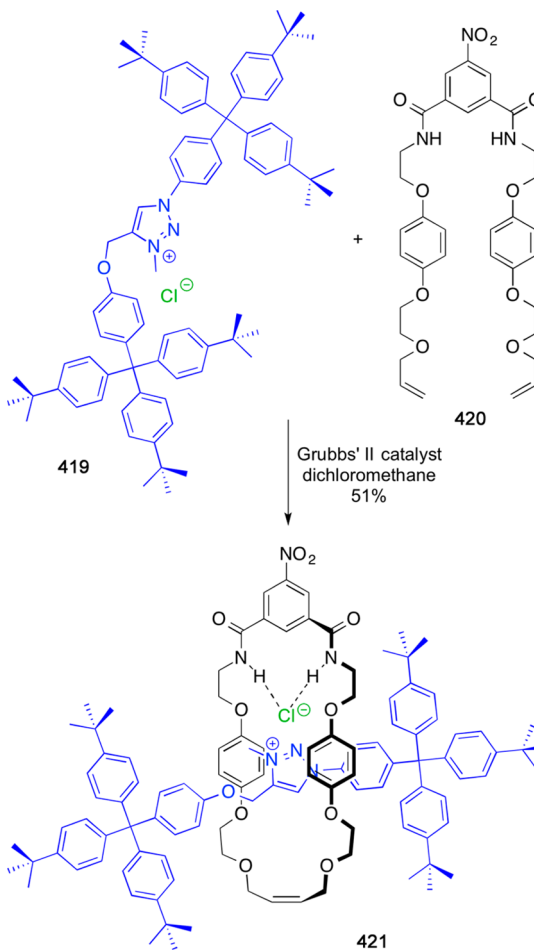


Figure 166. Structure of nitrate-templated [2]catenane 422.

is the most common technique to introduce anion-dependent gelation. In 1998, Huc and co-workers used LMWGs based on gemini surfactants to form a set of transparent gels. Dimers of cetyltrimethylammonium ions 429 displayed a remarkable high dependence on the nature of the negatively charged counterion (Figure 169).⁶⁶² Dissolving 429-L-tartrate or 429-D-tartrate in organic solvents resulted in the formation of stable gels, even at concentrations as low as 10 mM. When the two isomers were mixed together, however, no gelation was observed. Notably, residual amounts of water were required to allow gels to form, and the gels were disrupted by small amounts of alcohol, indicating the crucial role of hydrogen bonding for gel cohesion.

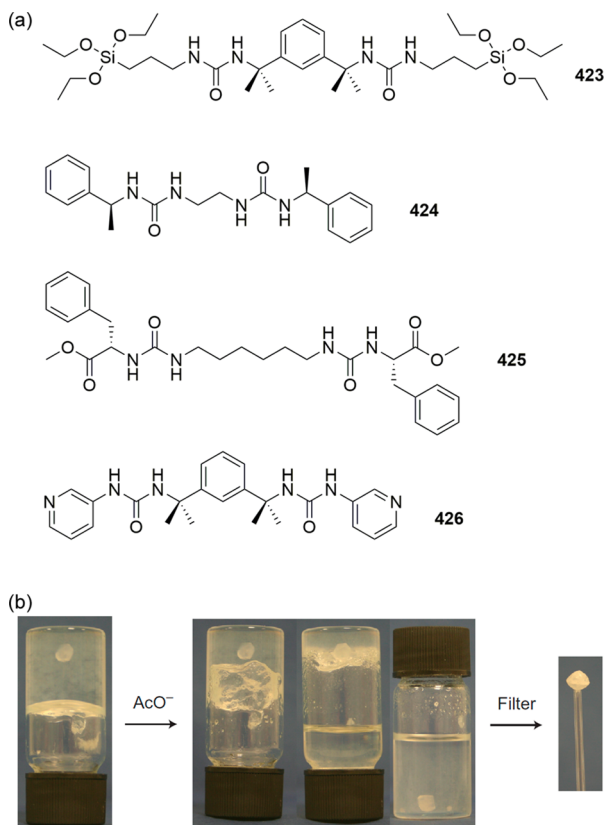


Figure 167. (a) Structures of bis-urea gelators 423–426. (b) Recovery of a single crystal of carbamazepine by acetate-triggered gel dissolution of a 1:9 CHCl₃:toluene gel of gelator 425. Reprinted with permission from ref 656. Copyright 2010 Macmillan Publishers Limited.

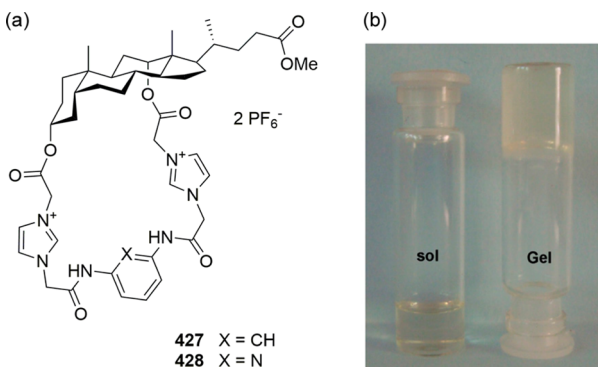


Figure 168. (a) Structures of compounds 427 and 428. (b) Photographs of a solution of 427 in 5:1 CDCl₃:DMSO-*d*₆ in the absence (left) and presence (right) of 1.4 equiv of TBA HSO₄. Reprinted with permission from ref 661. Copyright 2011 Elsevier Ltd.

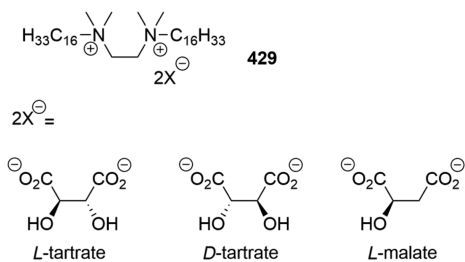


Figure 169. Structures of various salts of cetyltrimethylammonium dimer 429.

The latter was further supported by 429-L-malate failing to form gels. The tartrate gelators (*L*, *D*, and *D*+*L*-tartrate) displayed the ambiguous property to gelate in water (even at concentrations as low as 1 mM).

Maeda and co-workers elaborated on the charge-by-charge gelation technique by combining negatively and positively charged planar species.^{663–665} Dipyrrolyldiketone boron complexes such as 430 afford negatively charged planar building blocks by binding chloride ions, while planar 4,8,12-trialkyl-4,8,12-triazatragulenium (TATA) cations such as 431 can be applied as positive moieties (Figure 170). The alternating stacks

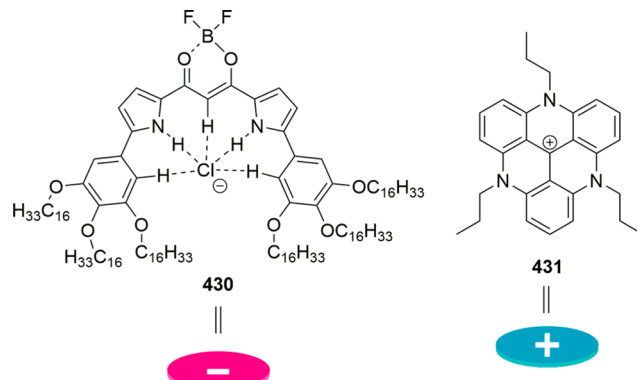


Figure 170. Structures of the negatively charged dipyrrolyldiketone 430 chloride complex and positively charged 431 building blocks.

of these moieties form fibrillars through $\pi-\pi$ stacking and electrostatic interactions, along with van der Waals forces, allowing for gelation in octane with a solution–gel transition temperature ($T_{\text{sol-gel}}$) of 27 °C (10 mg/mL). The introduction of longer alkyl chains on the anion receptor helps to stabilize the hexagonal columnar phase based on a trimeric assembly via intertwining of the alkyl chains of proximal columns. Longer alkyl chains on the TATA units, on the contrary, provided less-ordered morphologies. The propyl-substituted cation 431 resulted in the most stable gels, while anion receptor 430 even exhibited gelation in octane on its own with a gel–sol transition upon addition of TBACl. Variation of the boron substituents, such as replacing the fluorides by phenyl groups or catechol, had only a minor influence on $T_{\text{sol-gel}}$ (22.5 and 27.5 °C, respectively).⁶⁶⁶ The catechol–boron complexes formed mesophases similar to the BF₂ complexes but with broader temperature ranges, whereas diphenylboron complexes showed crystal–crystal transitions upon heating. Moreover, variation of the anion used allowed for tuning of the assemblies formed.⁶⁶⁷

Alkylation and fluorination of the pyrrole β position in 430 prevents the anion receptors to gelate spontaneously in octane (10 mg/mL).⁶⁶⁸ In sharp contrast with the β -unsubstituted gelator, however, the β -fluorinated receptor forms a gel upon the addition of TBACl. In the presence of 431, the fluorinated and alkylated analogues of 430 align into charge-segregated assemblies rather than charge-by-charge assemblies, presumably due to the distorted aryl rings owing to the β substituents (Figure 171).⁶⁶⁹ Study of these columnar mesophases revealed a high charge-carrier mobility in the assemblies, with a larger contribution from the charge-segregated arrangements than from the charge-by-charge assembly. The materials constructed out of the anisotropically ordered arrangements of π -conjugated charged species exhibited well-balanced ambipolar charge-carrier transport behavior with a relative high mobility, making them

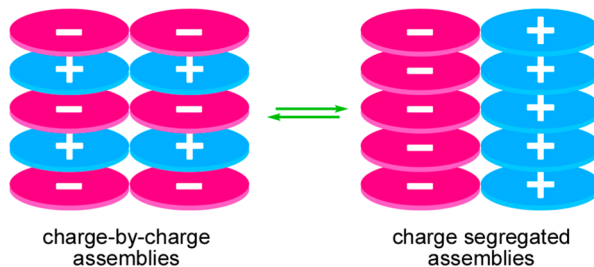


Figure 171. Illustration of charge-by-charge and charge-segregated assemblies.

potentially applicable as stable liquid crystalline electric-transporting materials.

Maeda's group also varied the positively charged building blocks in order to investigate their effect on the supramolecular assembling properties.^{670–672} Bis(imidazolium) dicationic anion receptors such as 432 and 433 (Figure 172) form planar

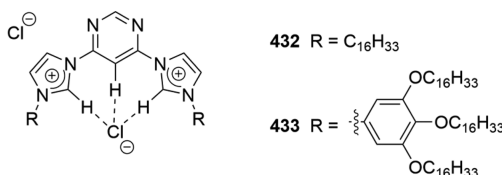


Figure 172. Structures positively charged 432 and 433.

monocationic receptor–chloride complexes that are accompanied by free chloride ions. Subsequently, the electronically neutral dipyrrolylketone boron complex (e.g., 430) forms negatively charged receptor–chloride complexes with the free chloride ions. The combination of the positively and negatively charged planar species stimulated the formation of supramolecular octane gels through self-organization into lamellar structures with a $T_{\text{sol-gel}}$ of 6 °C. Upon thermal annealing more ordered hexagonal columnar mesophases were obtained in line with a charge-by-charge assembly.

5.3. Conclusions and Outlook on Anion-Driven Assemblies

Anions have been shown to be able to alter and form supramolecular assemblies. They take up various functions within the assembling process and often play essential roles toward the final outcome. Anions can template or disrupt well-organized topologies and stimulate or perturb gelation. It is clear that anions are no longer just counterions for the undoubtedly important metal centers but are now considered full-fledged centers on their own capable of making a difference.

6. ANION-DRIVEN ORGANOCATALYSIS

An often overlooked application of supramolecular anion receptors is their use as organocatalysts. In order to improve the sustainability and lessen the environmental impact of chemical processes, the study of organocatalytic alternatives to reactions that typically employ metal-based systems is essential. In nature, chemical transformations are catalyzed by enzymes that have evolved to perform these transformations with the utmost accuracy and efficiency. Research has been pursued on the use of enzymes to catalyze industrial-scale reactions, but many drawbacks have been encountered. For example, the majority of enzymes require an aqueous environment. The mimicry of enzymatic modes of action by small synthetic organic molecules has become a field on its own, coined “biomimetic

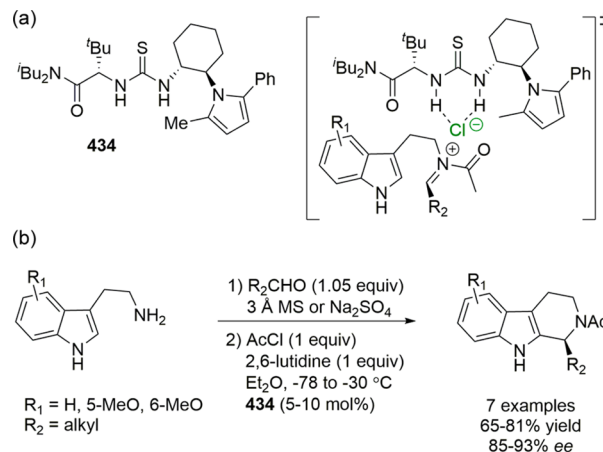
chemistry”, aimed at the development of artificial enzymes.^{673,674} Molecular recognition is of central importance in bio- and organocatalysis, relying on noncovalent interactions such as hydrogen bonding, anion–π interactions, and ionic and hydrophobic effects. Even though anions play a crucial role in living organisms and the majority of enzyme substrates and cofactors are anionic,⁶⁷⁵ their contribution to the field of organocatalysis has been recognized only recently.^{676,677} For example, the role of urea- and thiourea-based compounds in organocatalysis has been reviewed by Connolly.^{678,679} In this section, we seek to highlight the success of organocatalysis based on interactions with anionic moieties.

6.1. Organocatalysis Based on Interactions with Halide Anions

Halide anions are spherical species, which readily undergo interactions with hydrogen-bond donors.^{680–682} These interactions have been applied to catalyze halide-producing reactions and obtain enantioselective outcomes. The development of chloride binding catalysis has initiated a rather novel approach to organocatalysis, which opens up many new opportunities for molecular design and synthesis.

The first report of organocatalysis via halide binding was by Taylor and Jacobsen, who performed an intramolecular enantioselective Pictet–Spengler cyclization mediated by thioureas such as 434 (Scheme 24).⁶⁸³ This new methodology

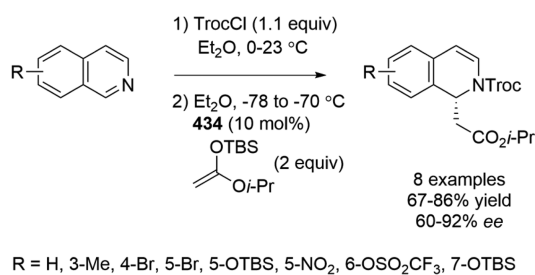
Scheme 24. (a) Structure of Catalyst 434 and of the Acyl Iminium Transition State Stabilized by 434. (b) Enantioselective Pictet–Spengler Cyclization Reaction Catalyzed by 434



provides facile access to enantiopure tetrahydro-β-carbolines, avoiding the use of harsh conditions. The hydrogen-bond-donating thiourea group of the catalyst interacts with the chloride counterion and results in the activation of the acyl iminium ion (Scheme 24). The presence of the chiral thiourea derivative bearing a bulky 2-methyl-5-phenylpyrrole substituent (434) afforded the highest enantiomeric excess (ee) values.

The same strategy was also successfully applied in the acyl–Mannich reaction of isoquinolines with tributylsilyl-protected ester enolates to obtain dihydroquinolines (Scheme 25).⁶⁸⁴ The formation of a chiral N-acyl iminium chloride–thiourea complex through hydrogen bonding allows good enantioselectivity. Furthermore, it was found that the enantioinduction strongly depends on the nature of the nucleophile, the acylating agent,

Scheme 25. Enantioselective Acyl–Mannich Reaction Catalyzed by 434

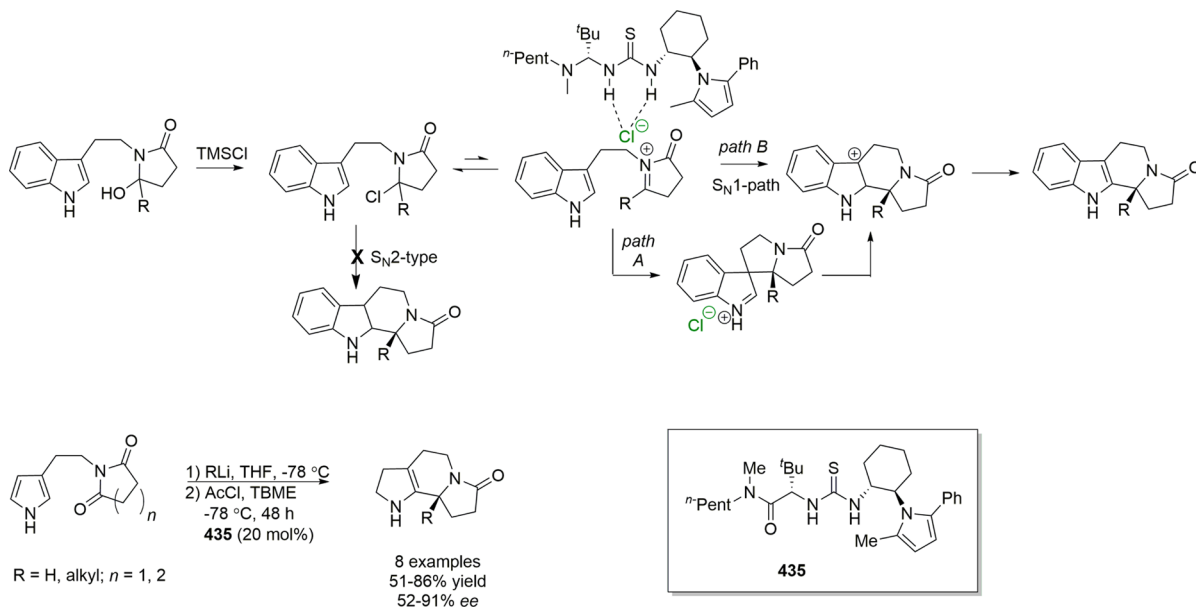


and the solvent but much less on the isoquinoline substitution pattern.

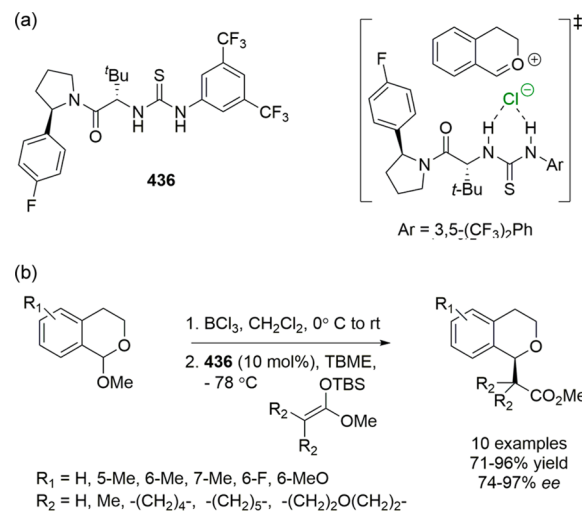
Jacobsen continued to investigate halide binding catalysis by analogues of 434 (e.g., 435) via the activation of the acyl iminium ion in an asymmetric Pictet–Spengler cyclization of β -indolyl ethyl hydroxylactams, assisted by in-situ dehydration with trimethylsilyl chloride as dehydrating agent.⁶⁸⁵ Experimental observations allowed for a clear insight into the reaction mechanism. The authors propose that the catalysis and enantioinduction result from initial abstraction of the chloride counterion in an S_N1-type rate-determining step, followed by an asymmetric cyclization (following path A or B) mediated by the chiral anion-bound thiourea derivative (Scheme 26a). Interestingly, when the same thiourea catalyst and similar reaction conditions were applied to β -pyrrolo ethyl hydroxylactams, access to pyrroloindolizidinones and pyrroloquinolizidinones could be obtained (Scheme 26b).⁶⁸⁶ The cyclization was found to proceed in both a good enantio- and regioselective manner.

The halide anion binding catalysis concept is not limited to nitrogen-stabilized carbocations, but also oxonium ions can act as electrophilic species. The earlier findings encouraged Jacobsen and co-workers to apply an identical strategy for the activation of cationic oxocarbenium ions by coordinating to the negatively charged counteranion during the enantioselective addition of nucleophiles to the oxocarbenium cations (Scheme 27).⁶⁸⁷

Scheme 26. (a) Mechanism of the Enantioselective Pictet–Spengler Cyclization Reaction Catalyzed by 435; (b) Enantioselective Pictet–Spengler-Type Reaction Catalyzed by 435



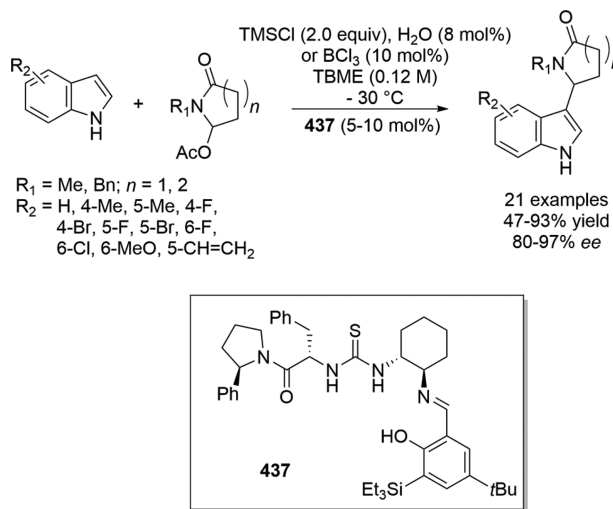
Scheme 27. (a) Structures of Catalyst 436 and of the Oxocarbenium Transition State Stabilized by 436; (b) Enantioselective Addition to Oxocarbenium Ions Catalyzed by 436



Systematic evaluation of the catalyst revealed that both a bis(trifluoromethyl)aniline and an appropriately constrained amide component were required to provide high yields and good enantioselectivities for the reaction of a 1-chloroisochroman with a silyl ketene acetal in a one-pot two-stage procedure, with thiourea 436 found to be the optimal catalyst for this reaction.

In subsequent manuscripts, Jacobsen et al. widened the scope of thiourea-catalyzed reactions with the enantioselective addition of indoles to hydroxylactam-derived cyclic N-acyl iminium ions mediated by 437 and analogues (Scheme 28).⁶⁸⁸ The synergistic improvement of the reaction outcome by trimethylsilyl chloride and catalytic H₂O suggests that the in-situ evolving of HCl leads to the formation of a chlorolactam, which proceeds to be the actual substrate in the alkylation. The proposed catalytic cycle is based on the S_N1-type anion binding mechanism reported earlier

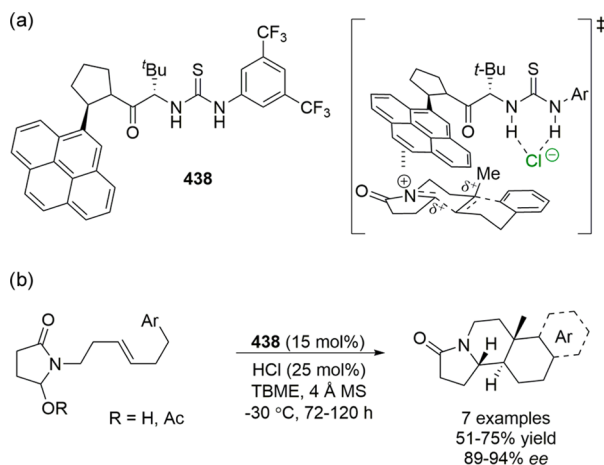
Scheme 28. Enantioselective Addition of Indoles to Cyclic N-Acyl Iminium Ions Catalyzed by 437



for the acyl-Pictet-Spengler and oxocarbenium ion alkylation reactions (Schemes 26 and 27). Coordination of the catalyst to the chloride counterion results in activation of the cationic species.

Later, the same group developed the enhanced bifunctional catalyst **438**, which was shown to be capable of electrostatically stabilizing both poles of the reactive ion pair in a spatially resolved manner (Scheme 29).⁶⁸⁹ This novel catalyst consists of

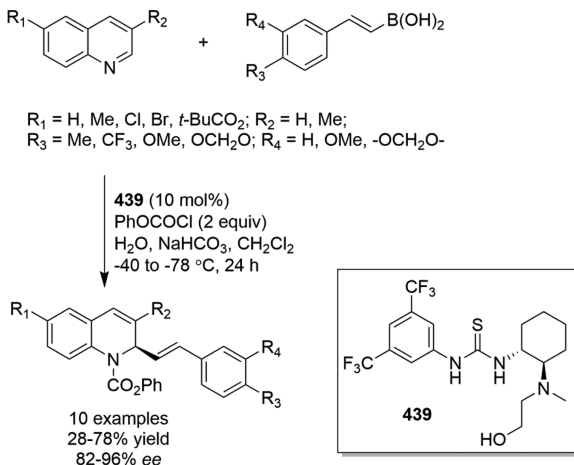
Scheme 29. (a) Structures of Catalyst 438 and of the Transition State Stabilized by 438; (b) Enantioselective Bicyclization Reaction Catalyzed by 438



a thiourea moiety that interacts with the chloride ion generated by in-situ dehydration by HCl of the hydroxylactam starting material and a pyrenyl function that allows cation–π interactions to stabilize the dominant cationic transition state resulting in bicyclization reactions with ee values up to 94%.

Takemoto and colleagues also recognized the value of a secondary interaction within a single catalyst and performed the first catalytic enantioselective variant of the Petasis transformation of quinolones using catalyst **439**.⁶⁹⁰ A proton-donating thiourea moiety, activating the acyl iminium ion, was combined with a 1,2-amino alcohol functionality to stimulate the nucleophile, giving ee values up to 96% (Scheme 30). At that time an intriguing, albeit speculative, mechanistic hypothesis was

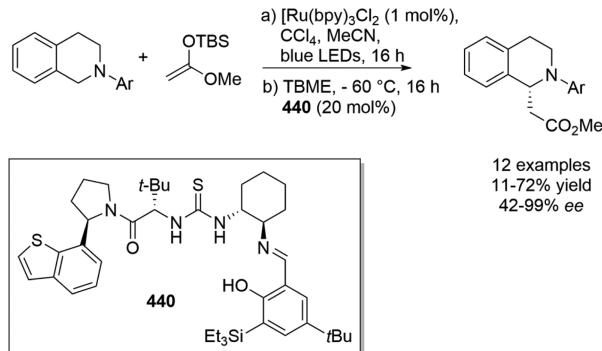
Scheme 30. Enantioselective Petasis Reaction Catalyzed by 439



proposed where only neutral activation was considered. Currently, however, an alternative mechanism has been described where the anion binding activation of the *N*-acylated quinolinium ion is taken into account.⁶⁷⁷

Recently, the Stephenson group, in collaboration with Jacobsen and co-workers, combined the enantioselective halide binding organocatalysis by thiourea **440** with a ruthenium-stimulated photoredox activation, resulting in a dual-catalytic enantioselective synthesis (Scheme 31).⁶⁹¹ With CCl4 as the

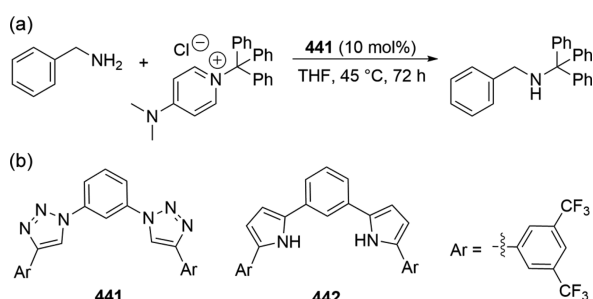
Scheme 31. Combination of Photoredox Activation with Chloride Binding Catalysis by 440



stoichiometric oxidant and halide donor, the oxidative Mannich reaction of *N*-aryltetrahydroisoquinolines with silyl ketene acetals provided β-amino esters in good yields and ee's between 42% and 99%.

Several research groups have taken on the challenge of exploring other hydrogen-bonding motifs for use in catalysis. The use of polarized C–H bonds to bind anions has attracted significant interest in the past decade.⁶⁹² The triazole ring in particular has received special attention due to its highly polarized character and facile synthesis.⁵⁸⁰ Mancheño and co-workers therefore explored the use of 1,2,3-triazole-based anion receptors as neutral chloride-accepting catalysts.⁶⁹³ The aryltriazole oligomer with the highest chloride affinity (**441**) proved to be the best catalyst in the amine alkylation reaction (Scheme 32). In a selectivity assay toward chloride the triazole-based catalyst outcompeted a thiourea analog. Inspired by this system, Van Rossum et al. prepared arylpyrrole oligomers of similar structure (e.g., **442**, Scheme 32).^{694,695} The greatly

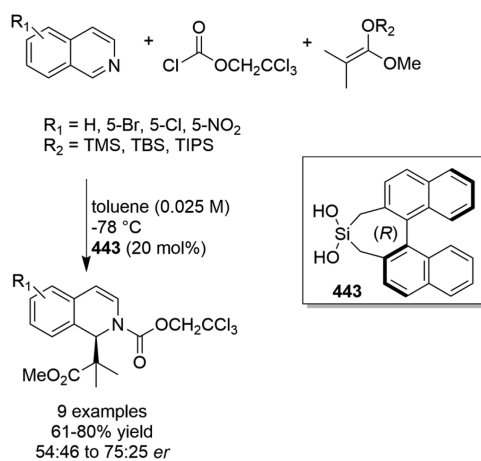
Scheme 32. (a) Amine Alkylation Reaction Catalyzed by 441; (b) Structures of Organocatalyst 441 and Pyrrole Analog 442



improved anion binding properties of these pyrrole derivatives over the triazole compounds makes them promising compounds for use in the development of future non(thio)urea-based catalysts.

Mattson and co-workers employed silanediols as alternative hydrogen-bond donor catalysts.⁶⁹⁶ Enantiopure (*R*)-2,2'-dimethyl-1,1'-naphthalene silanediol 443 was found to catalyze the addition of silyl ketene acetals to *N*-acylisoquinolines in good yields and with promising levels of stereocontrol (Scheme 33). Further exploration of silane derivatives may provide another alternative for the commonly explored (thio)urea organocatalysts.

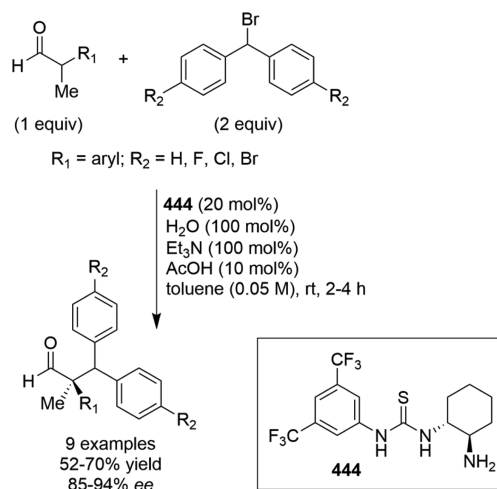
Scheme 33. Silandiol 443 Catalyzed Alkylation Reaction



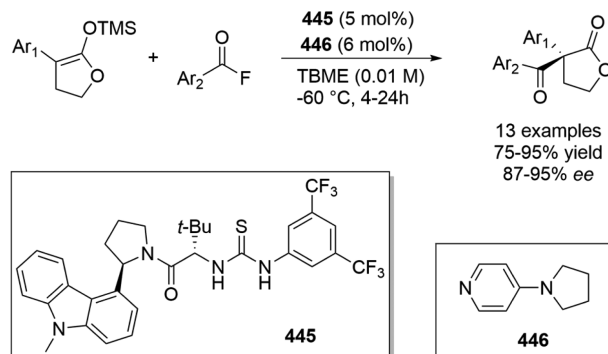
While the main focus of halide binding catalysis still lies in the binding of chloride, the first reports of the effective use of other halides in organocatalysis have also emerged in recent years. Jacobsen and co-workers found that primary aminothiourea derivatives such as 444 were unique in inducing good reactivity and enantioselectivity during the asymmetric α -alkylation of 2-arylpropionaldehydes with diarylbromomethanes (Scheme 34).⁶⁹⁷ Mechanistic studies revealed strong evidence that the reaction proceeds via a catalyst-stabilized carbocation via binding of the bromide ion in an $S_{N}1$ -like substitution mechanism.

Jacobsen and colleagues employed a duo of a thiourea-based catalyst (445) and a 4-pyrrolidinopyridine catalyst (446) for the promotion of the enantioselective alkylation of silyl ketene acetals with acyl fluorides to form α,α -disubstituted butyrolactone products (Scheme 35).⁶⁹⁸ The right-hand *tert*-leucine-thiourea-3,5-bis(trifluoromethyl)anilide fragment of catalyst 445 was shown to be essential for a selective reaction outcome, while the identity of the aryl group on the left-hand 2-arylpiperidino

Scheme 34. Alkylation through Bromide Binding Catalysis by 444



Scheme 35. Acylation through Fluoride Binding Catalysis by a Combination of 445 and 446



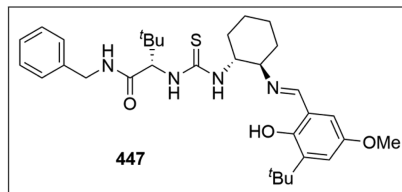
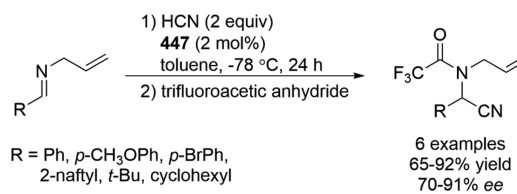
fragment had only a minor influence on the outcome. Interestingly, benzoyl chloride was completely unreactive in the model reaction, whereas excellent yields and ee values were obtained with benzoyl fluoride. A plausible reason might be the greater affinity of fluoride over chloride ions for the silyl group,⁶⁹⁹ and therefore, this also seems to be the rate-determining step in the catalytic cycle as suggested by the authors.

Huber and co-workers pioneered halogen-bonding approaches to organocatalysts. For example, this group used 5-iodo-1,2,3-triazolium-based multidentate halogen-bond donor compounds and diazo-linked halogen-functionalized pyridinium compounds as activators in halide-abstraction reactions.⁷⁰⁰⁻⁷⁰² Similar systems have been applied to activation of carbonyl compounds.⁷⁰³

6.2. Organocatalysis Based on Interactions with Cyanide Anions

As with halide binding organocatalysis, the potential of cyanide binding catalysis had not been recognized until after its synthetic use. Jacobsen and co-workers reported the first examples of cyanide binding catalysis while investigating a combinatorial library of tridentate Schiff-base ligands (e.g., 447) to optimize the enantioselective outcome of an asymmetric Strecker reaction (Scheme 36).⁷⁰⁴ It was observed that the ligands could catalyze the reaction even without the presence of a metal center, motivating the group to explore the organocatalytic activity of this class of compounds. The first mechanistic explorations

Scheme 36. Enantioselective Strecker Reaction Catalyzed by 447



pointed toward the activation of the electrophile by hydrogen bonding with the thiourea moiety;^{705,706} however, this hypothesis was re-evaluated later once the concept of anion binding catalysis was established (vide infra).

Shortly after the initial report of cyanide binding catalysis, Corey and Grogan reported the enantioselective synthesis of α -amino nitriles from *N*-benzhydryl imines and HCN with chiral C_2 -symmetric guanidine catalyst 448 giving excellent yields and good ee values (Scheme 37).⁷⁰⁷ In addition, a compelling

Scheme 37. (a) Structures of Catalyst 448 and of the Transition State Stabilized by 448; (b) Enantioselective Hydrocyanation of a *N*-Benzhydryl Imine Catalyzed by 448

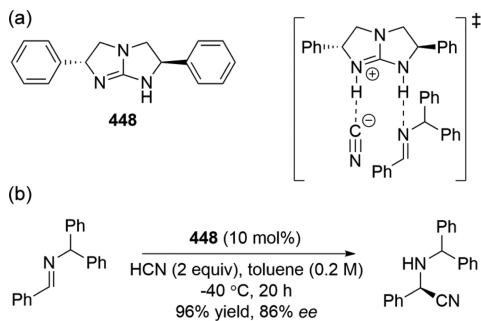
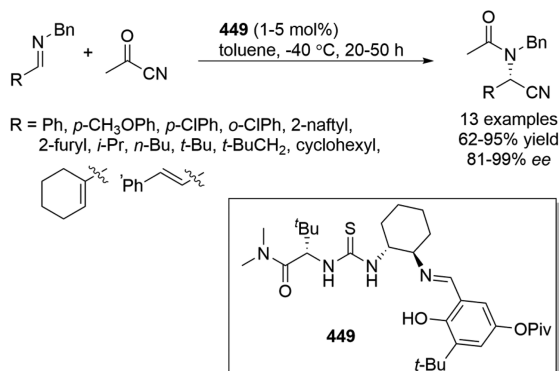


illustration of the potential mechanism was provided, indicating that the bifunctional character of the catalyst allowed both the formation of a guanidinium cyanide complex, between the catalyst and HCN through the basic nitrogen, and stereoinduction onto the aldimine via hydrogen-bond formation with the substrate (Scheme 37).

In 2007 List et al. communicated the screening of hydrogen-bond-donating catalysts (e.g., 449) in the asymmetric catalysis of acylcyanation of imines to derive the corresponding α -amino-nitriles in excellent yields and enantioselectivities.⁷⁰⁸ Notably, acetyl cyanide was used as the cyanation reagent in the asymmetric Strecker reaction, which had not been reported before. It was only when this work was further elaborated by the same authors that two mechanisms were proposed of which one suggested the binding of the cyanide anion to create a chiral nucleophile in analogy with the chloride binding mechanism (Scheme 38).⁷⁰⁹

In 2009 Jacobsen and co-workers published a detailed experimental and computational mechanistic study on their original thiourea-catalyzed Strecker reaction (vide supra, Scheme

Scheme 38. Enantioselective Strecker Reaction Using Acetyl Cyanide Catalyzed by 449



36).⁷¹⁰ The authors concluded that activation of the imine function by the thiourea moiety, as was initially suggested, does not coincide with the productive catalytic cycle. Hence, while stabilization of the cyanide anion by the thiourea is important for the catalytic process, differences in enantioselectivity could not be traced to the degree of anion stabilization. Instead, the degree of stabilization of the iminium ion was principally responsible for control of the enantioselectivity in the asymmetric imine hydrocyanation. Furthermore, they also demonstrated that these thiourea-catalyzed Strecker syntheses are scalable and that even inexpensive sources of cyanide such as KCN can be applied to obtain unnatural α -amino acids in excellent yields and enantioselectivities.⁷¹¹

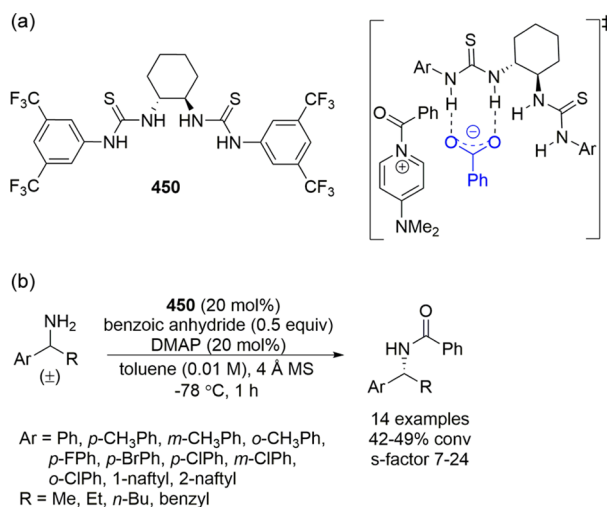
6.3. Organocatalysis Based on Interactions with Carboxylate Anions

The carboxylate ion with its particular Y shape is one of the most common anions found in nature. Carboxylate binding catalysts have now found their own place within the field of organocatalysis, albeit slightly later than chloride and cyanide binding catalysts. In 2009, Seidel and co-workers anticipated that the introduction of 4-(*N,N*-dimethylamino)pyridine (DMAP) together with a chiral hydrogen-bond-donating catalyst (450) could transform a simple anhydride into a chiral electrophilic acyl reagent (Scheme 39).⁷¹² Due to the stabilization of the carboxylic counterion by the thiourea moiety, the new chiral acylation agent is more active than the initial anhydride, allowing for in-situ generation of the complex. This insightful strategy was successfully applied to the kinetic resolution of amines forming benzylamines.

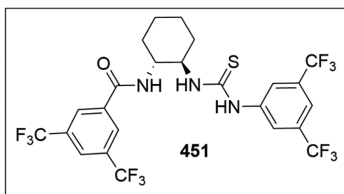
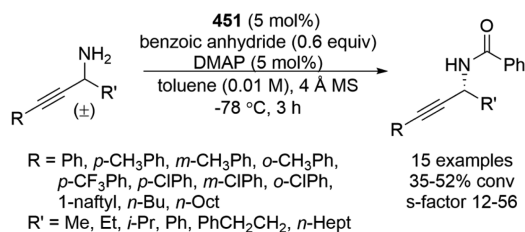
After the initial proof-of-principle study on the kinetic resolution of benzylic amines, Seidel and colleagues extended this approach to other classes of amines and improved the hydrogen-bonding cocatalyst.⁷¹³ Replacement of one thiourea unit by an electron-deficient aryl amide (451) led to a substantial improvement in selectivity, resulting in an increase in the *s* factor from 11 to 38 for the kinetic resolution of propargylic amines by acylation (Scheme 40).⁷¹⁴ Even when the amount of both nucleophile and the new anion receptor was reduced from 20 to 2 mol% no substantial loss in conversion was observed.

The scope of reactions for which the dual-catalyst concept was effective was expanded via the desymmetrization of *meso*-1,2-diaryl-1,2-diaminoethanes by enantioselective monobenzoylation (Scheme 41).⁷¹⁵ Notably, until that time, no organocatalytic enantioselective monoacetylation of *cis*-1,2-diamines had been reported. With DMAP and the amide–thiourea receptor 451 as catalyst duo, substrates with electron-withdrawing groups in the

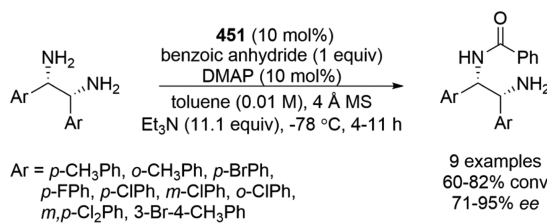
Scheme 39. (a) Structures of Catalyst 450 and of the Transition State Stabilized by 450; (b) Kinetic Resolution of Benzylic Amines by 450 and DMAP



Scheme 40. Kinetic Resolution of Propargylic Amines by 451 and DMAP



Scheme 41. Enantioselective Monobenzoylation Reaction Catalyzed by 451 and DMAP



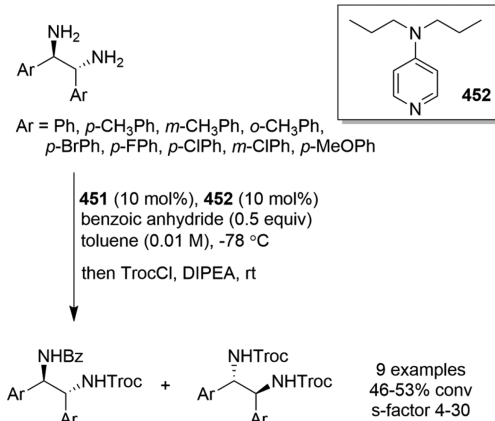
para positions provided the corresponding products in good yields and with enantioselectivities up to 95%. Other substrates gave rise to slightly reduced ee values, and all other thiourea-based catalysts tested resulted in lower yields and/or enantioselectivities.

In 2011 Seidel et al. continued to improve the catalytic system but shifted their attention from the hydrogen-bond donor to the nucleophilic cocatalyst and investigated the effect of new catalyst duo compositions on the kinetic resolution of racemic allylic amines.⁷¹⁶ Combination of the previously applied amide-thiourea receptor 451 with the more nucleophilic 4-(1-

pyrrolidinyl)pyridine afforded the desired products with *s* factors up to 20.

More recently, Seidel and co-workers found a remarkable dependence of the reaction's selectivity on the achiral nucleophilic cocatalyst while evaluating a broad scope of nucleophilic derivatives.⁷¹⁷ From the wide spectrum of achiral nucleophiles investigated 4-di-*N*-propylaminopyridine 452, in combination with the chiral amide-thiourea anion receptor 451, proved to give superior results with *s* factors up to 67. Using this improved set of cocatalysts, a number of 1,2-diaryl-1,2-diaminoethanes were resolved efficiently by monobenzoylation and subsequent addition of 2,2,2-trichlorethoxycarbonyl chloride showing *s* factors up to 30 (Scheme 42).⁷¹⁸

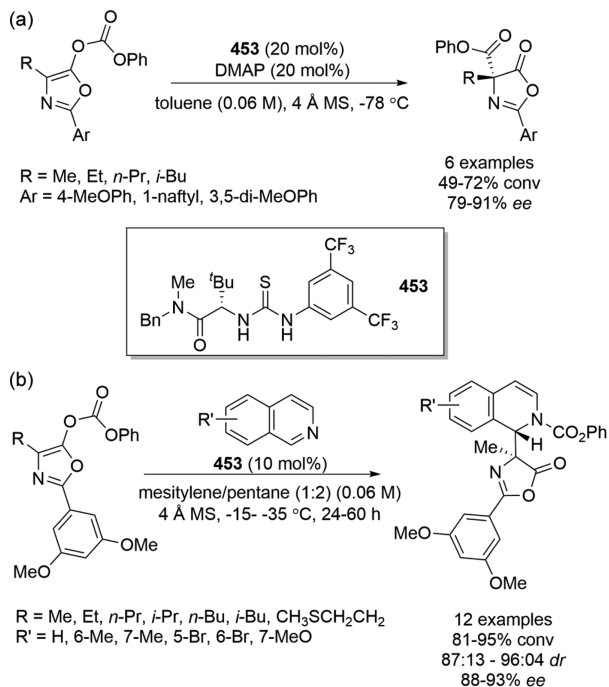
Scheme 42. Kinetic Resolution of 1,2-Diaryl-1,2-diaminoethanes by 451 and 452



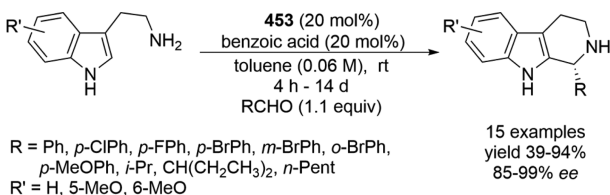
A similar cooperative action of two small-molecule catalysts was used by the same group to facilitate a Steglich reaction, which is a rearrangement of an *O*-acylated azlactone to the corresponding *C*-acylated oxazolone, providing α,α -disubstituted amino acid derivatives in a highly enantioselective fashion (Scheme 43a).⁷¹⁹ Interestingly, the former hydrogen-bonding cocatalysts 450 and 451, which gave good results for the acetyl-transfer reactions of benzylic, propargylic, and allylic amines, achieved only poor enantioselectivities. Fortunately, inspired by the pioneering work of Jacobsen (vide supra), DMAP was combined with a *tert*-leucine-based thiourea receptor 453 to form a catalytic system offering ee values up to 91%. The nature of the aryl group on the azlactone proved to have a pronounced effect on the product selectivity, with a 3,5-dimethoxyphenyl substituent providing the best results. In addition, an alternative reaction pathway was found when DMAP was replaced with a more “imine-like” nucleophile such as *N*-isoquinazoline. In this case, the acetylisoquinolinium ion was attached by the enolate in the 1 position of the isoquinoline ring to afford α,β -diamino acid derivatives (Scheme 43b).

The Jacobsen group also embarked on the field of carboxylate binding catalysis in 2009 when they investigated the protio-Pictet–Spengler reaction (Scheme 44).⁷²⁰ A protio-iminium formation induced by a weak Brønsted acid in combination with *tert*-leucine-based thiourea catalyst 453 preceded the Pictet–Spengler cyclization. The final tetrahydro- β -carbolines were obtained directly from tryptamine and aldehyde precursors in high yield and ee levels as high as 99%. Benzoic acid proved to be superior over acetic acid, affording higher reaction rates and enantiometric excess.

Scheme 43. (a) Enantioselective Steglich Reaction Catalyzed by 453 and DMAP; (b) Azlactone Addition to Isoquinolines Catalyzed by 453



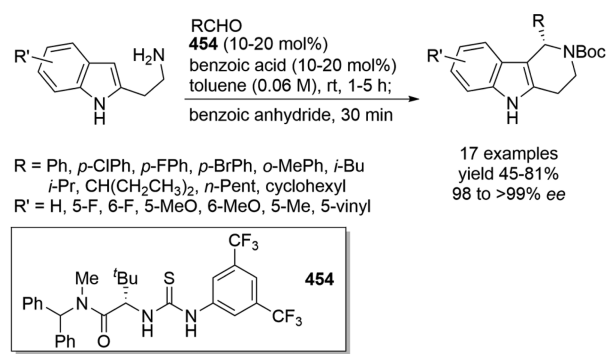
Scheme 44. Enantioselective Pictet–Spengler Reaction Catalyzed by 453 and Benzoic Acid



A very similar chiral thiourea/benzoic acid dual-catalyst system (**454**/benzoic acid) was used to facilitate a one-pot condensation of isotryptamines and aldehydes (Scheme 45).⁷²¹ This iso-Pictet–Spengler reaction offers a facile route to optically pure *N*-Boc tetrahydro- γ -carbolines after treatment of the crude products with Boc_2O followed by simple trituration or crystallization.

Through the binding of the carboxylate counterion, Jacobsen et al. also succeeded in synthesizing indolo- and benzoquinolinolines.

Scheme 45. Enantioselective Iso-Pictet–Spengler Reaction Catalyzed by 454 and Benzoic Acid



zidine derivatives in a highly enantio- and diastereoselective fashion (Scheme 46).⁷²² Bifunctional primary aminothiourea catalyst **455** was applied to coordinate the formal aza-Diels–Alder reaction between enones and cyclic imines. In the proposed cooperative mechanism the catalyst achieves activation of the enone through the formation of the corresponding covalently bound dienamine, while the imine is simultaneously activated as a thiourea-bound iminium ion. As before, a crucial role was played by the weak Brønsted acid additive ascribed to the acceleration of the condensation and/or hydrolysis steps integral to the enamine catalysis cycle.

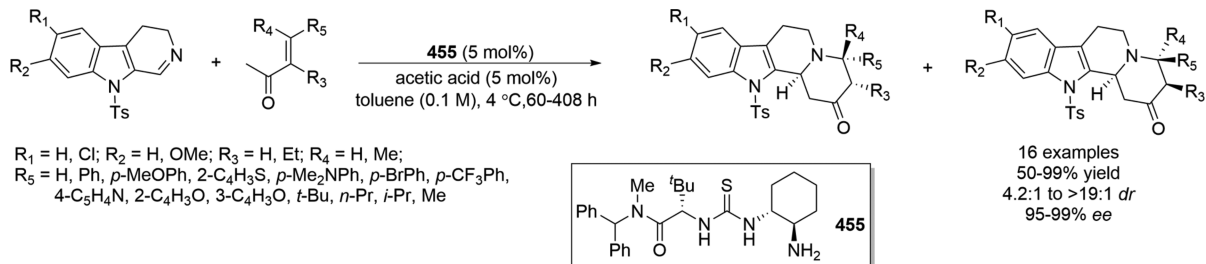
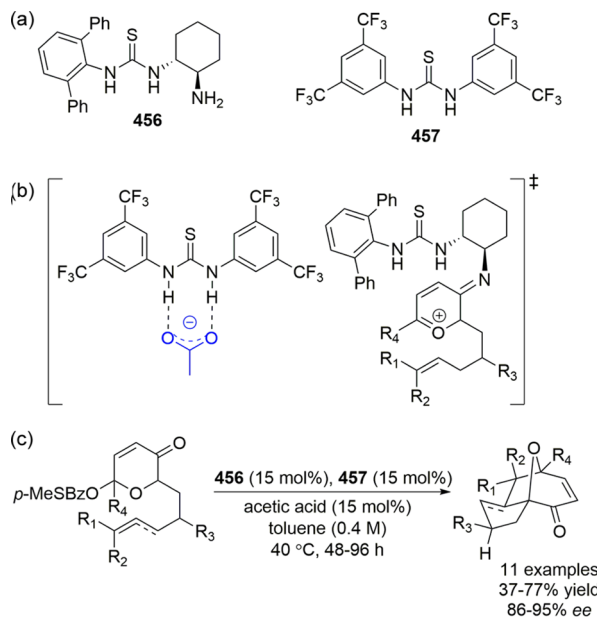
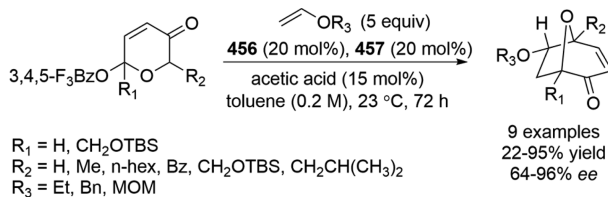
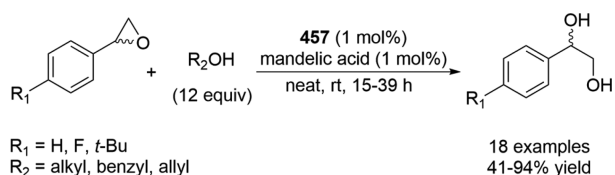
In 2011 Jacobsen and co-workers reported a novel anion binding cooperative catalysis.⁷²³ This method combined a chiral aminothiourea and an achiral thiourea receptor to catalyze oxidopyrylium-based intramolecular [5 + 2]-cycloadditions of racemic acetopyranones (Scheme 47). The chiral catalyst decorated with a bulky 2,6-diphenylanilide and a primary amine component (**456**) was identified to be the most enantioselective in combination with a symmetric thiourea cocatalyst bearing two 3,5-bis(trifluoromethyl)phenyl groups (**457**). The observation that the primary amine is necessary for catalysis as well as the fact that acetic acid increases the rate of the reaction are consistent with an operative enamine catalysis mechanism with generation of a catalyst–pyrylium adduct. Interestingly, reversal in the sense of enantioinduction was observed using a primary amine catalyst decorated with a carbazole rather than a 2,6-diphenylanilide moiety.

A few years later, Jacobsen and co-workers revisited the multicatalyst concept for the synthesis of 8-oxabicyclo[3.2.1]-octanes by intermolecular [5 + 2]-pyrylium cycloaddition using the same catalyst system (Scheme 48).⁷²⁴ The observed enantioselectivity appeared to be dependent on the substitution pattern of the 5 π component, suggesting a critical role of the 6 substituent in controlling the transition structure geometry in the catalytic reaction.

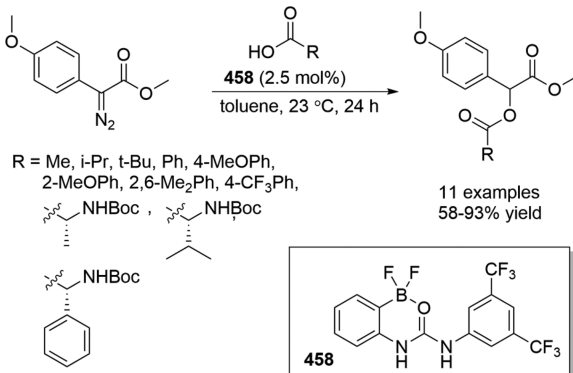
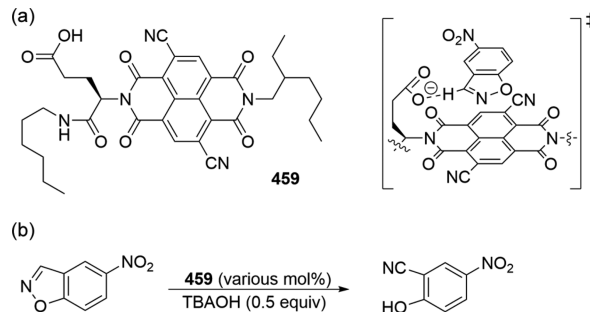
Schreiner and co-workers reported the catalytic epoxide ring opening applying mandelic acid and fluorinated thiourea **457** as catalyst partners.⁷²⁵ The authors speculated that mandelic acid protonates the epoxide, affording mandelate ion, which is stabilized by the thiourea cocatalyst, shifting the reaction toward alcoholysis of the styrene oxide into a β -alkoxy alcohol in good to excellent yields (Scheme 49). Simple aliphatic and sterically demanding as well as unsaturated alcohols were employed successfully, confirming the versatility of this method.

While conventional urea and thiourea catalysts were unable to promote carboxylic acid and mercaptan insertion on α -aryldiazoacetates, Mattson et al. found that difluoroboronate urea compounds work as acidity amplifiers and enable the formation of α -acyloxyesters and α -mercaptoesters (Scheme 50).⁷²⁶ It was found that the internal boron activation and appropriate electron-withdrawing substitution pattern activate the catalyst with the 3,5-bis(trifluoromethyl) derivative (**458**), resulting in good to excellent yields for this catalyst. The authors' working hypothesis of the catalytic cycle involves an initial proton transfer, and the cycle concludes with the diazonium species reacting with the urea-stabilized anion to generate the insertion product. The weak interaction of the product with the difluoroboronate urea can subsequently free the urea to re-enter the catalytic cycle.

In 2013 Matile and co-workers published the first organocatalysis that employs anion– π interactions.⁷²⁷ Applying a π -acidic naphthalenediimide with a covalently attached carboxylate base (e.g., **459**), the Kemp elimination of benzisoxazole was

Scheme 46. Stereoselective Formal Aza-Diels–Alder Reaction Catalyzed by 455 and Acetic Acid**Scheme 47.** (a) Structures of Catalysts 456 and 457, (b) Proposed Roles of the Thiourea Catalysts, and (c) Intramolecular [5 + 2] Cycloaddition Reaction Catalyzed by 456 and 457**Scheme 48.** Intramolecular [5 + 2] Pyrylium Cycloaddition Reaction Catalyzed by 456 and 457**Scheme 49.** Alcoholysis of Styrene Oxides Catalyzed by 457 and Mandelic Acid

notably accelerated (Scheme 51). It was anticipated that π stacking between the substrate and the π -acidic surface of the catalyst stabilizes the transition state, allowing the injection of a negative charge over 5 atoms (from the carboxylate oxygen to the benzisoxazole oxygen). A substantial acceleration of the reaction

Scheme 50. Carboxylate Insertion Catalyzed by 458**Scheme 51.** (a) Structure of Catalyst 459 and Proposed Role of the Catalyst; (b) Anion– π Interaction Catalyzing Kemp Elimination

upon addition of the catalyst demonstrated the concept of anion– π catalysis, which is unprecedented in nature and has the potential to open up a new area in anion binding catalysis.

The Matile group furthered their work in this area by investigating in more detail the dependence of the catalytic activity on the π acidity of the catalyst's surface and the nature of the linker.⁷²⁸ The experimental results were reinforced with computational simulations to evaluate the interaction between anion– π surface and substrate. While the length of the linker between the naphthalenediimide and the carboxylate base strongly influences the activity, its preorganization only moderately affects the activity. This suggests that ideal positioning of the carboxylate base on the π -acidic surface is achieved by intramolecular anion– π interactions rather than an optimized structure of the linker. Decorating the body of naphthalenediimide with electron-withdrawing substituents resulted in an increase in π acidity, which in turn was shown to increase the recognition and stabilization of the anionic transition state and thus improve the performance of the catalyst. The introduction of sulfoxide moieties afforded the most active

anion- π catalyst so far (**460**, Figure 173). The poor performance of a similar pyrylenediimide catalyst indicated that the

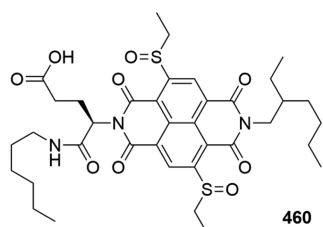


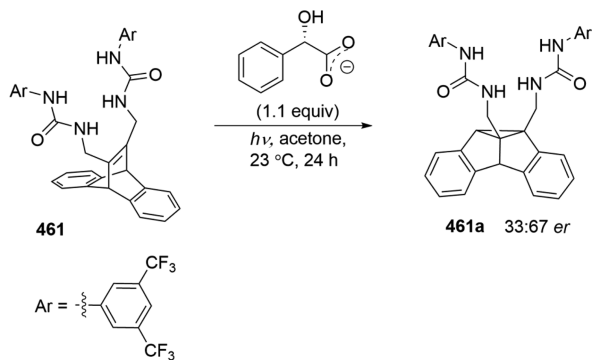
Figure 173. Structure of anion- π catalyst **460**.

contributions of π - π interactions between catalyst and substrate to anion- π catalysis are nearly irrelevant compared to the anion- π interactions.

Shortly after Matile's initial reports, Lu and Wheeler addressed the exact role of the different interactions in Matile's anion- π catalysis and quantified their net impact via *in silico* analyses.⁷²⁹ The data indicated that there is no electrostatic stabilization during the course of the reaction as the noncovalent interactions preferentially stabilize the catalyst–substrate complex over the transition state. The gain in anion- π interaction between catalyst and substrate is overshadowed by the loss of anion- π interaction between the carboxylate ion and the π -acidic surface. From the newly gained insights, the authors predicted a set of new catalysts, which were believed to achieve significant lowering of the activation energy through anion- π interactions.

A different approach toward the use of carboxylates is found in the work of Ihmels and co-workers.⁷³⁰ The hydrogen-bonding receptors are subjected to an asymmetric photoreaction themselves. Bisureido- and bisthioureido-substituted dibenzobarrelene derivatives (e.g., **461**) undergo a di- π -methane rearrangement to the corresponding dibenzosemibullvalene derivatives in the presence of chiral carboxylate ions with rather low selectivities so far (Scheme 52); however, these observations demonstrate that anion-controlled stereoselective di- π -methane rearrangements may be accomplished in principle.

Scheme 52. Photostimulated Dibenzobarrelene Di- π -methane Rearrangement of **461**



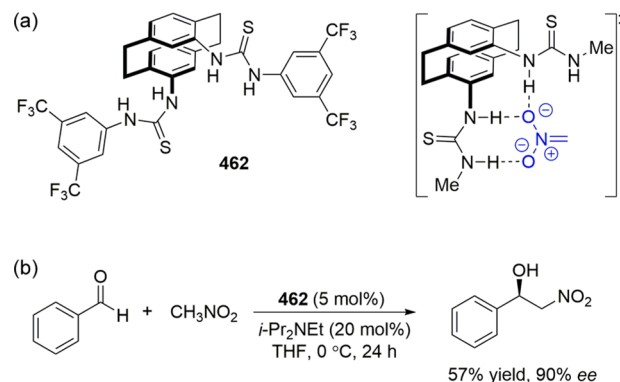
6.4. Organocatalysis Based on Interactions with Nitronate Anions

The interaction of hydrogen-bond-donating receptors with nitronate ions is studied rarely, and only a few examples are reported in the literature, which includes examples of anion transport and anion-selective sensors. This lack of nitronate receptors is surprising given that there is a clear electronic

similarity between the well-studied carboxylate and nitronate ions. In the field of anion binding organocatalysis, however, the nitronate ion has been applied abundantly to satisfy synthetic needs. Since the first notion of nitronate binding catalysis reported in 1992 by Davis and co-workers, a number of contributions have been made on the subject by different research groups.⁷³¹ Cobb et al. recently (2013) summarized the application of nitronate binding catalysis in detail, and we will therefore limit this subsection to an overview of the advances since 2013.⁷³² The reader is referred to the review by Cobb and co-workers for older examples.

The design of new organocatalysts often relies on the detailed understanding of the underlying factors controlling the stereochemistry. Thus, Breugst and Houk undertook a computational analysis of the bisthiourea-[2.2]paracyclophe (**462**) catalyzed Henry reaction between benzaldehyde and nitromethane anion employing density functional theory (DFT).⁷³³ The original experimental work by Mukai and colleagues showed that the reaction product could be obtained in good yield and with high enantioselectivity (Scheme 53).⁷³⁴ On the basis of the *in silico*

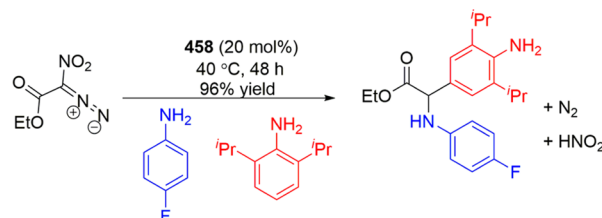
Scheme 53. (a) Structure of Catalyst **462** and the Energetically Most Likely Interaction between Catalyst and Substrate Calculated by Breugst and Houk; (b) Enantioselective Henry Reaction Catalyzed by **462**



generated data, the authors concluded that the reaction occurs between a thiourea–nitronate complex and an uncoordinated aldehyde, and the formation of the experimentally observed major stereoisomer is preferred kinetically by 3.8 kcal·mol⁻¹ as a result of a better hydrogen arrangement.

Mattson and co-workers harnessed difluoroboronate urea catalyst **458** (Scheme 50) to elicit and control the loss of nitrite followed by addition of anilines and indoles forming aryl glycines in good yields (Scheme 54).⁷³⁵ The difluoroboronate group was strategically incorporated into the catalyst's design to increase the overall acidity of the urea moiety by coordinating to the urea

Scheme 54. N–H Insertion/Multicomponent Coupling Catalyzed by Difluoroboronate Urea **458**

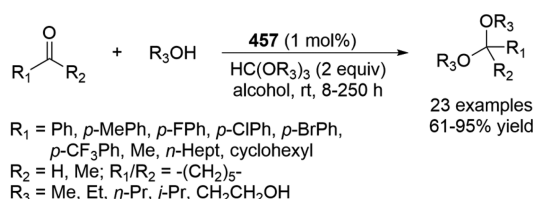


carbonyl and thus improving the hydrogen-bonding capacity and catalytic activity. The experimental and computational data suggested that the reaction proceeds according to a concerted N–H insertion mechanism rather than a urea-stabilized nitrocarbene.

6.5. Organocatalysis Based on Interactions with Other Oxoanions

The stabilization of noncarboxylate oxoanionic intermediates (or transition state moieties) and subsequent catalysis was first revealed in 2006 by Kotke and Schreiner for the acid-free, organocatalytic acetalization of aldehydes and ketones by fluorinated thiourea 457 (Scheme 55).⁷³⁶ The addition of

Scheme 55. Organocatalytic Acetalization of Aldehydes and Ketones Catalyzed by Thiourea 457



catalyst loadings as low as 0.01 mol% afforded excellent yields up to 95%. The thiourea catalyst was assigned several roles in the mechanistic proposal, among which was the stabilization of the hydroxide ion; unfortunately little experimental evidence was provided.

After the concept of anion binding catalysis became well accepted, Jacobsen and co-workers introduced a cooperative catalysis system for an enantioselective Pavarov reaction, a [4 + 2] cycloaddition of *N*-aryl imines and electron-rich olefins.⁷³⁷ The combination of bifunctional sulfinamido urea 463 with *o*-nitrobenzenesulfonic acid in a 2:1 ratio provided the best structure-reactivity/enantioselectivity outcome (Scheme 56). As a model for the mechanistic analysis the authors referred to triflic acid (or other sulfonic acids). After the initial protonation by the sulfonic acid, the protio-iminium triflate is solubilized in the presence of the urea cocatalyst through the formation of a 1:1 complex. The character of the complex causes a substantial decrease in reactivity, which suppresses the relatively fast nonstereoselective Brønsted-acid-catalyzed reaction and allows

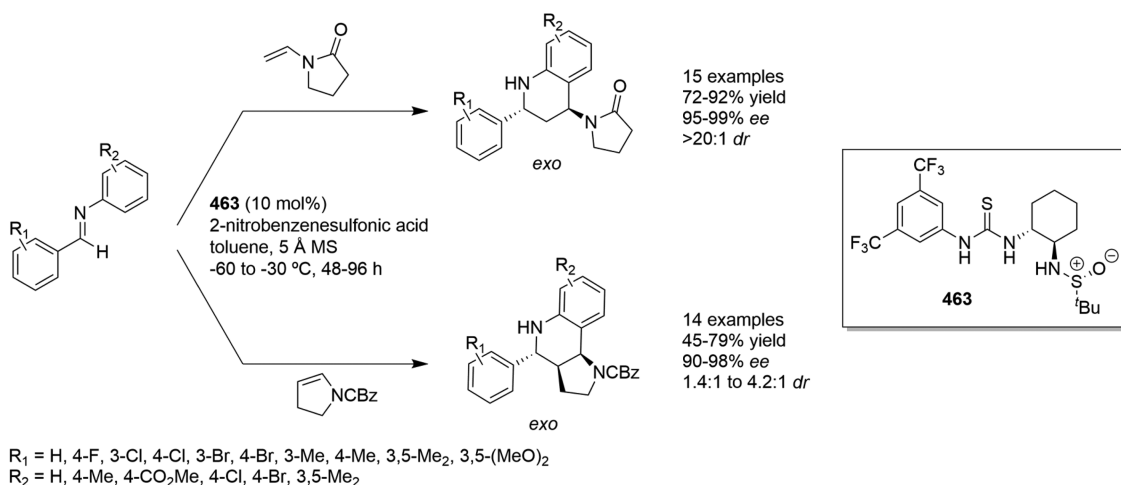
a higher stereoinduction control. The experimental data (binding constants, kinetic analysis), in combination with DFT calculations, suggests that the high ee values were obtained exactly as a result of the strong interaction between the protio-iminium triflate and the sulfinamido urea cocatalyst.

Lin and Jacobsen also found a strong contribution of anion binding in an organocatalyzed Friedel–Crafts-type indole alkylation reaction.⁷³⁸ The phenanthrylpiperidino amido thiourea 464 and *p*-nitrobenzenesulfonic acid catalyst duo enhances the enantioselective nucleophilic ring opening of episulfonium ions by indoles, giving excellent yields (16–99%) and ee values up to 95% (Scheme 57). While variation of the indole's substituents was well tolerated, a sharp drop in yield and enantioselectivity for the *N*-methylindole substrate suggests that the indole N–H motif may be involved in a key interaction during the ee determining transition state. Interestingly, variations on the carbon backbone of the electrophilic episulfonium ion precursor revealed that aryl groups with para functionalities, regardless of their electronic properties, resulted in substantially lower yields and enantioselectivity. Computational studies indicated that in the transition state leading to the major enantiomeric product one of the *para*-C–H bonds is engaged in an attractive, electrostatic interaction with the thiourea-bound sulfonate, causing a disorganized structure. A plausible catalytic cycle was elucidated from both experimental and computational data, showing the importance of the thiourea–sulfonate interaction in combination with the catalyst amide–indole N–H interaction and a cation–π interaction between the phenanthrene of the catalyst and the benzylic protons of the episulfonium ion (Scheme 57).

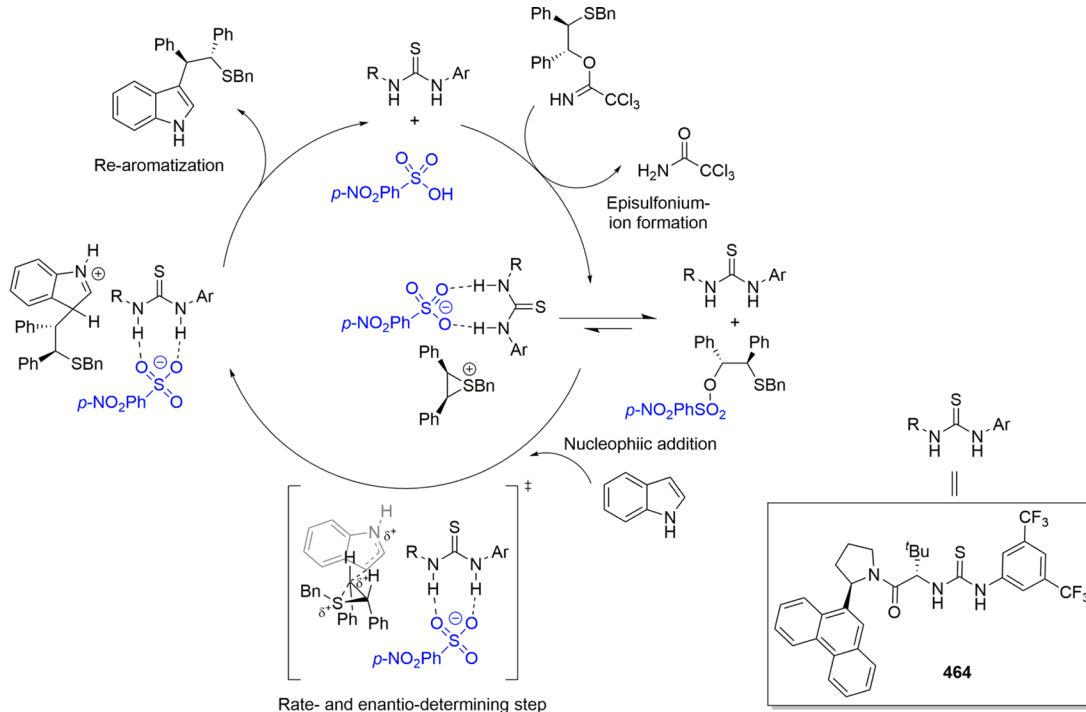
Recently, Palomo and co-workers contributed to the field of oxyanion binding catalysis by introducing ureidopeptide-based catalysts prepared from valine or *tert*-leucine derivatives (e.g., 465) for a Michael reaction between thiazoles and nitro-olefins and a Mannich-type reaction between *N*-Boc imines and (arylsulfonyl)acetonitriles providing β-amino nitriles.⁷³⁹ The latter was explored for a broad scope of substrates and provided good to excellent yields and high enantioselectivities with only a minimal influence of the electronic nature of the substrate's substitution pattern (Scheme 58).

Next to the numerous urea and thiourea catalysts that have been reported, Lennon and co-workers took on the quest to evaluate a series of bisamides (e.g., 466) for Baylis–Hillman

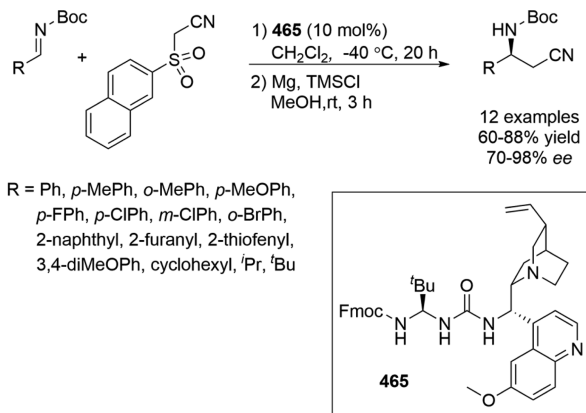
Scheme 56. Diastereoselective and Enantioselective Povarov Reaction Catalyzed by Thiourea 463



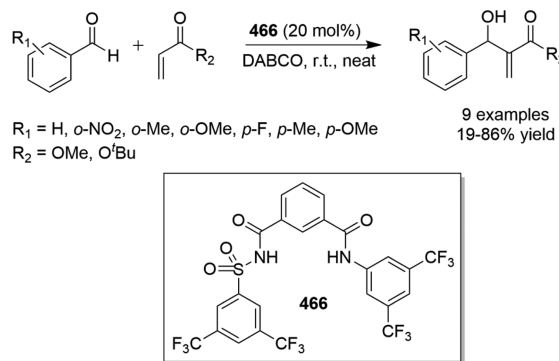
Scheme 57. Proposed Catalytic Cycle for Friedel–Crafts-Type Indole Alkylation Reaction Catalyzed by Thiourea 464



Scheme 58. Enantioselective Mannich Reaction Catalyzed by Urea 465



Scheme 59. Baylis–Hillman Reaction Catalyzed by Bisamide 466

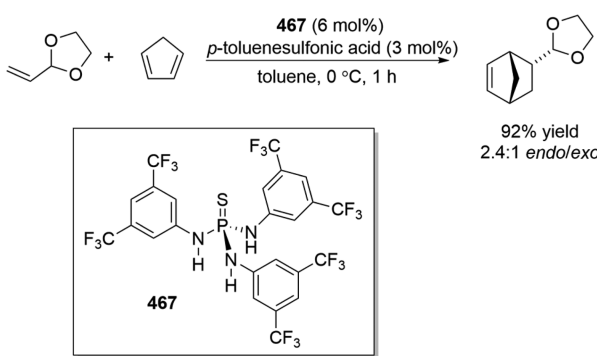


reactions (Scheme 59).⁷⁴⁰ After testing the anion binding properties, the authors proposed that the increased reaction rates and yields could be assigned to the interaction of the anion receptors with the negatively charged intermediates in the reaction medium.

Nagorny et al. reported the first use of a three hydrogen-bond donor for anion binding catalysis.⁷⁴¹ The combination of *p*-toluenesulfonic acid with a thiophosphoramido cocatalyst such as 467 gave higher yields compared to the thiourea or squaramide derivatives for ionic [2 + 4] cycloaddition reactions under mild reaction conditions (Scheme 60). The authors ascribed this to the fact that the thiophosphoramido appears to have the perfect structure to bind all three of the oxygen atoms of the sulfonate counterions.

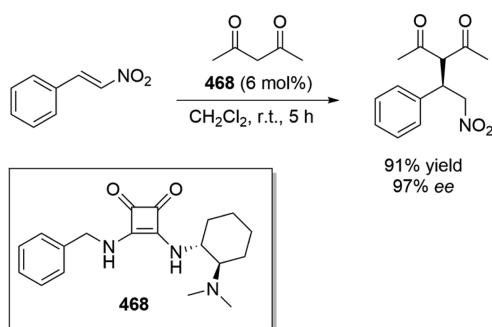
In the Soos group the focus was directed to bifunctional squaramide–amine catalyst 468, which was shown to induce excellent yields (up to 96%) and ee values (up to 97%) for the Michael addition of acetylacetone to *trans*- β -nitrostyrene

Scheme 60. Diels–Alder Reaction Catalyzed by Thiophosphoramido 467



(Scheme 61).⁷⁴² A thorough DFT analysis was performed to figure out the mechanism in place. The data pointed toward the binding of the deprotonated nucleophile by the squaramide,

Scheme 61. Michael Addition Catalyzed by Squaramide–Amine 468

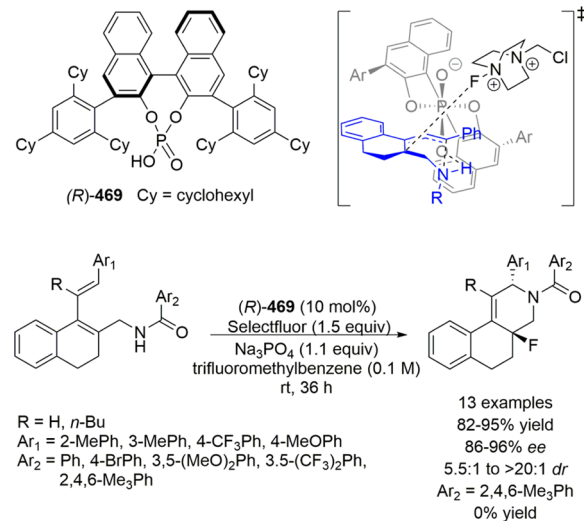


while the protonated amine activates and positions the electrophile.

Several research groups approached the aspect of oxoanion-driven organocatalysis from a different angle. Their work focused on the use of chiral anions as phase-transfer catalysts, instead of the interaction of the catalyst with an anionic intermediate or transition state. As several reviews have been published on the matter recently, only an update on the latest advances on the subject of “the use of chiral anions in organocatalysis” will be given here.^{743,744}

Toste and co-workers reported extensively on the use of chiral-anion phase-transfer catalysts in various reactions. They reported the first catalytic asymmetric 1,4-aminofluorination of conjugated dienes using Selectfluor (Scheme 62).⁷⁴⁵ The mild

Scheme 62. (a) Structure of Chiral anion (*R*)-469 and the Proposed Transition State; (b) Asymmetric 1,4-Aminofluorination of Conjugated Dienes Using Chiral Anion (*R*)-469

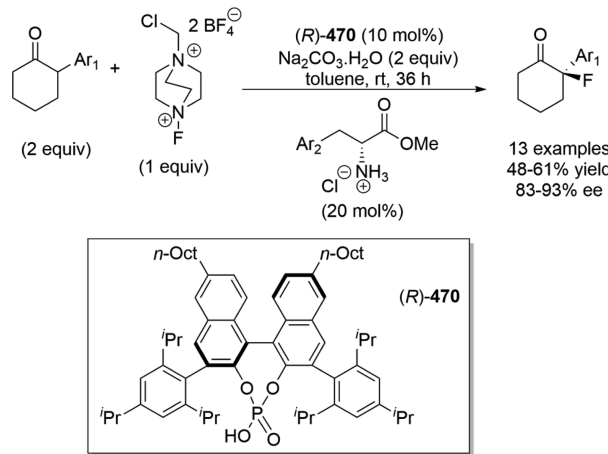


conditions and chiral phosphate catalyst (*R*)-469 allowed the fluorination of substrates that are typically incompatible with homogeneous Selectfluor conditions. The resulting benz[f]-isoquinoline derivatives were formed with high levels of enantiomeric excess and excellent yields of up to 95%.

The same group found that a multicatalyst system using a similar 1,1'-bi-2-naphthol (BINOL)-based phosphonate cocatalyst enhanced the asymmetric fluorination of branched cyclohexanones.⁷⁴⁶ The combination of a chiral anion phase-transfer catalyst, activating Selectfluor, with an enamine activation of the

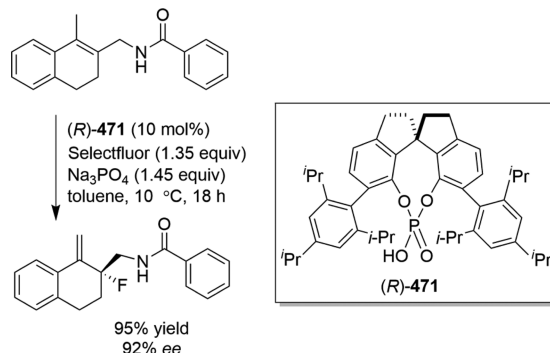
ketone by an amino acid cocatalyst gave two separate chiral catalytic cycles operating together to afford the fluorinated compounds in moderate yields but with good ee values (Scheme 63). The more lipophilic chiral phosphoric acid (*R*)-470 was found to give the most optimal results with ee levels up to 93%.

Scheme 63. Asymmetric Fluorination of Branched Cyclohexanones Using Chiral Anion (*R*)-470



Toste and colleagues applied the same strategy as above for the enantioselective electrophilic fluorination of alkenes to generate β -amino- and β -phenolic allylic fluorides (Scheme 64).⁷⁴⁷ An

Scheme 64. Enantioselective Electrophilic Fluorination of Alkenes Using Chiral Anion (*R*)-471



altered chiral phosphate transfer reagent (*R*)-471 was applied, replacing the commonly used BINOL by a diindenophenol derivative, to afford modest to good yields but with good to excellent ee values. Furthermore, Toste and co-workers demonstrated a one-pot tandem dihalogenation–cyclization reaction using the same catalytic system twice but with an analogous electrophilic brominating reagent in the second step. The resulting indeno-1,3-oxazine was formed in good yields with high diastereoselectivity and enantioselectivity with creation of adjacent stereocenters and two carbon–halogen bonds.

6.6. Conclusions and Outlook on Anion-Driven Organocatalysis

By making the link between enzymatic catalysis and anion recognition, the importance of anion coordination in organocatalysis has been realized in the past few years. The exploration of anions as substrates will undoubtedly expand the scope of existing “artificial enzymes”. Currently, anion-driven catalysis has

covered some of the most common anions; however, much of this area is left to explore. Undoubtedly, this approach will become a powerful tool in organic synthesis.

The vast amount of work on anion recognition performed by various groups has paved the way to readily understand the underlying principles of anion binding organocatalysis. Hydrogen bonding is the main driving force of anion binding organocatalysis; however, the first reports of halogen bonding and anion- π coordinating catalysis have found their way into the field. We may expect many novel classes of anion binding catalysts to be developed and to find them applied in various new reactions in future years to ensure a steady progress toward a more sustainable future and a cleaner environment.

7. CONCLUSIONS

Over the last 10 years anion complexation has transitioned from being a predominantly academic pursuit to one in which there are demonstrable applications. This review has highlighted the application of this area of supramolecular chemistry in the production of anion sensors, the extraction of anions from mixtures of species, the transport of anions across lipid bilayers with potential future application in the treatment of disease, the use of anions to template the formation of molecular ensembles, and the role anion complexation can play in organocatalysis. These exciting subdisciplines have blossomed over the past decade, and we can expect to see their growth and the emergence of new areas over the coming years. Areas that have seen particular growth in recent years include the development of halogen-bonding-based anion receptors, sensors, and organocatalysts. The fact that halogen bonding operates more effectively in water than analogous hydrogen-bonding receptors again opens up this chemistry to real-world application. Other developments recently include new classes of receptor employing CH hydrogen-bond donor groups that show contrasting anion selectivity^{692,748,749} to receptors containing NH hydrogen-bond donor groups. Also there are recent examples of self-sorting and self-assembly of anion clusters.^{750,751} It will be fascinating to see the applications which develop from these new discoveries.

AUTHOR INFORMATION

Corresponding Author

*Phone: +44 23 8059 3332. Fax: +44 23 8059 6805. E-mail: philip.gale@soton.ac.uk

Present Address

[§]Nathalie Busschaert present address: Chemistry Research Laboratory, Department of Chemistry, University of Oxford, Mansfield Road, Oxford OX1 3TA, United Kingdom.

Author Contributions

The manuscript was written through contributions of all authors. All authors have given approval to the final version of the manuscript.

Notes

The authors declare no competing financial interest.

Biographies



Nathalie Busschaert completed her B.Sc. degree in Chemistry at the Catholic University of Leuven (Belgium) and continued studying for her M.Sc. degree in Chemistry at the same university. She then moved to the University of Southampton (U.K.) in 2010 to undertake Ph.D. studies under the supervision of Professor Philip A. Gale, with research stays at A*STAR, Singapore, and the University of Ljubljana, Slovenia. She is currently working as a postdoctoral researcher in the group of Professor Andrew Hamilton at the University of Oxford. Her research interests are anion coordination chemistry, transmembrane anion transport, and medicinal applications of supramolecular systems.



Claudia Caltagirone graduated in Chemistry in 2001 and received her Ph.D. degree in Chemistry in 2006 at the University of Cagliari under the supervision of Prof. Vito Lippolis. She spent 2 years as a visitor at the University of Southampton (U.K.), where she worked on anion recognition in the group of Professor Philip Gale. She is currently Assistant Professor in Inorganic Chemistry at the University of Cagliari. Her research interests mainly focus on optical sensors for anions and cations recognition and fluorescent nanoparticles for imaging and therapeutic purposes.



Wim Van Rossom graduated in Chemistry in 2006 and received his Ph.D. degree in Chemistry in 2010 at the Catholic University of Leuven under the supervision of Prof. Wim Dehaen and Prof. Wouter Maes. He spent 2 years as a JSPS Postdoctoral Fellow at the National Institute for Materials Science in Japan supported by Prof. Katsuhiko Ariga and Dr. Jonathan P. Hill. He was selected for a Marie Curie CIG in 2013 to continue his research at the University of Southampton as Research Fellow under the guidance of Prof. Philip A. Gale. His research interests mainly focus on synthetic approaches toward macrocyclic structures and the study and application of transmembrane anion transport.



Philip A. Gale was born in Liverpool and grew up in Woolton attending Gateacre Community Comprehensive School. He then moved to the University of Oxford, where he received his B.A. (Hons) degree in 1992 and M.A. and D.Phil. degrees in 1995. In 1995, he moved to the University of Texas at Austin, where he spent 2 years as a Fulbright Scholar before returning to Oxford in 1997 as a Royal Society University Research Fellow. In 1999 he moved as a Lecturer to the University of Southampton and was promoted through the ranks to a Personal Chair in Supramolecular Chemistry in 2007. Since 2010 he has been the Head of Chemistry at Southampton. In 2014 he was awarded a Doctor of Science degree by the University of Oxford and was listed by Thomson Reuters as a highly cited researcher in chemistry. His research interests focus on the supramolecular chemistry of anionic species and, in particular, the molecular recognition, sensing, and lipid bilayer transport of anions. He has won a number of research prizes including the RSC 2014 Supramolecular Chemistry Award, a Royal Society Wolfson Research Merit Award, and the RSC Corday Morgan medal and prize. He currently serves as the chair of the *Chemical Society Reviews* Editorial Board and is a member of the Advisory Board of *Chemical Science*. He is also the coeditor of the journal *Supramolecular Chemistry*. In 2012 he was elected chair of the RSC Macroyclic and Supramolecular Chemistry Group.

ACKNOWLEDGMENTS

P.A.G. thanks the EPSRC for a postdoctoral fellowship (N.B.) (EP/J009687/1) and the European Union for a Marie Curie Career Integration grant (W.V.R.). P.A.G. also thanks the Royal Society and the Wolfson Foundation for a Royal Society Wolfson Research Merit Award. C.C. would like to thank Regione Autonoma della Sardegna (CRP-59699) for funding.

ABBREVIATIONS

TBA	tetrabutylammonium
LDA	lithium diisopropylamide
BM	Brooker's merocyanine
EHEC	ethyl(hydroxyethyl)-cellulose
PA	<i>Pseudomonas aeruginosa</i>
GFP	green fluorescent protein
HNL	hydroxynitrile lyase
PET	photoinduced electron transfer
ICT	intramolecular charge transfer
DLS	dynamic light scattering
CLSM	confocal laser scanning microscopy
CTP	cytidine triphosphate
GTP	guanosine triphosphate
TPP	thymidine triphosphate
UTP	uridine triphosphate
FRET	fluorescence resonance energy transfer
PPi	pyrophosphate
NP	β -naphthyl phosphate
CT	charge transfer
CD	circular dichroism
CPL	circular polarized luminescence
PKU	phenylketonuria
BINOL	1,1'-bi-2-naphthol
ROS	reactive oxygen species
GSH	glutathione
Cys	cysteine
HCy	homocysteine
IDA	indicator displacement assay
RC	red cresol
BG	bromocresol green
AR	alizarine red S
AIDA	allosteric indicator displacement assay
HPTS	8-hydroxypyrene-1,3,6-trisulfonic acid
IIDA	intramolecular indicator displacement assay
QDA	quencher displacement assay
PCA	principal component analysis
LDA	linear discriminant analysis
ANN	artificial neural networks
HCA	hierarchical cluster analysis
MAP	mitogen-activated protein
IMP	isopropylmethyl phosphonate
MP	methyl phosphonate
PDA	polydiacetylene
NOE	nuclear Overhauser effect
NIR	near infrared
PiBP	phosphate binding protein
CFP	cyan fluorescent protein
YFP	yellow fluorescent protein
Pi	phosphate
ISEs	ion-selective electrodes
OSWV	Osteryoung squarewave voltammetry
p-TMPD	tetramethyl-p-phenylenediamine
BEF	binding enhancement factor

SEM	scanning electron microscopy
DMFc	decamethylferrocene
ESPT	excited state proton transfer
NAC	N-acetylcysteine
EYPC	egg yolk phosphatidylcholine
NDI	naphthalenediimide
PDI	perylene diimide
DOPC	1,2-dioleoyl-sn-glycero-3-phosphocholine
POPC	1-palmitoyl-2-oleoyl-sn-glycero-phosphatidylcholine
POPG	1-palmitoyl-2-oleoyl-sn-glycero-3-phosphatidylglycerol
PC	phosphatidylcholine
PS	phosphatidylserine
STM	scanning tunneling microscopy
LMWG	low molecular weight gelator
ee	enantiomeric excess
DMAP	4-(<i>N,N</i> -dimethylamino)pyridine
DFT	density functional theory

REFERENCES

- (1) Shriver, D. F.; Biallas, M. J. Observation of the Chelate Effect with a Bidentate Lewis Acid, $\text{F}_2\text{BCH}_2\text{CH}_2\text{BF}_2$. *J. Am. Chem. Soc.* **1967**, *89*, 1078–1081.
- (2) Park, C. H.; Simmons, H. E. Macrobicyclic Amines. iii. Encapsulation of Halide Ions by *in,in-1,(k + 2)*-Diazabicyclo[*k.l.m.*]-Alkane Ammonium Ions. *J. Am. Chem. Soc.* **1968**, *90*, 2431–2432.
- (3) Graf, E.; Lehn, J.-M. Anion Cryptates: Highly Stable and Selective Macrotricyclic Anion Inclusion Complexes. *J. Am. Chem. Soc.* **1976**, *98*, 6403–6405.
- (4) Gale, P. A.; Busschaert, N.; Haynes, C. J. E.; Karagiannidis, L. E.; Kirby, I. L. Anion Receptor Chemistry: Highlights from 2011 and 2012. *Chem. Soc. Rev.* **2014**, *43*, 205–241.
- (5) Wenzel, M.; Hiscock, J. R.; Gale, P. A. Anion Receptor Chemistry: Highlights from 2010. *Chem. Soc. Rev.* **2012**, *41*, 480–520.
- (6) Evans, N. H.; Beer, P. D. Advances in Anion Supramolecular Chemistry: From Recognition to Chemical Applications. *Angew. Chem., Int. Ed.* **2014**, *53*, 11716–11754.
- (7) Gale, P. A.; Caltagirone, C. Anion Sensing by Small Molecules and Molecular Ensembles. *Chem. Soc. Rev.* **2015**, DOI: 10.1039/C4CS00179F.
- (8) Duke, R. M.; Veale, E. B.; Pfeffer, F. M.; Kruger, P. E.; Gunnlaugsson, T. Colorimetric and Fluorescent Anion Sensors: An Overview of Recent Developments in the Use of 1,8-Naphthalimide-Based Chemosensors. *Chem. Soc. Rev.* **2010**, *39*, 3936–3953.
- (9) Martínez-Máñez, R.; Sancenón, F. Chemodosimeters and 3D Inorganic Functionalised Hosts for the Fluoro-Chromogenic Sensing of Anions. *Coord. Chem. Rev.* **2006**, *250*, 3081–3093.
- (10) Gunnlaugsson, T.; Glynn, M.; Tocci, G. M.; Kruger, P. E.; Pfeffer, F. M. Anion Recognition and Sensing in Organic and Aqueous Media Using Luminescent and Colorimetric Sensors. *Coord. Chem. Rev.* **2006**, *250*, 3094–3117.
- (11) dos Santos, C. M. G.; Harte, A. J.; Quinn, S. J.; Gunnlaugsson, T. Recent Developments in the Field of Supramolecular Lanthanide Luminescent Sensors and Self-Assemblies. *Coord. Chem. Rev.* **2008**, *252*, 2512–2527.
- (12) Moragues, M. E.; Martínez-Máñez, R.; Sancenón, F. Chromogenic and Fluorogenic Chemosensors and Reagents for Anions. A Comprehensive Review of the Year 2009. *Chem. Soc. Rev.* **2011**, *40*, 2593–2643.
- (13) Li, A.-F.; Wang, J.-H.; Wang, F.; Jiang, Y.-B. Anion Complexation and Sensing Using Modified Urea and Thiourea-Based Receptors. *Chem. Soc. Rev.* **2010**, *39*, 3729–3745.
- (14) Santos-Figueroa, L. E.; Moragues, M. E.; Climent, E.; Agostini, A.; Martínez-Máñez, R.; Sancenón, F. Chromogenic and Fluorogenic Chemosensors and Reagents for Anions. A Comprehensive Review of the Years 2010–2011. *Chem. Soc. Rev.* **2013**, *42*, 3489–3613.
- (15) Kaminsky, L. S.; Mahoney, M. C.; Leach, J.; Melius, J.; Miller, M. J. Fluoride: Benefits and Risks of Exposure. *Crit. Rev. Oral Biol. Med.* **1990**, *1*, 261–281.
- (16) Polhuijs, M.; Langenberg, J. P.; Benschop, H. P. New Method for Retrospective Detection of Exposure to Organophosphorus Anticholinesterases: Application to Alleged Sarin Victims of Japanese Terrorists. *Toxicol. Appl. Pharmacol.* **1997**, *146*, 156–161.
- (17) Jakubowski, E. M.; McGuire, J. M.; Evans, R. A.; Edwards, J. L.; Hulet, S. W.; Benton, B. J.; Forster, J. S.; Burnett, D. C.; Muse, W. T.; Matson, K.; Crouse, C. L.; Mioduszewski, R. J.; Thomson, S. A. Quantitation of Fluoride Ion Released Sarin in Red Blood Cell Samples by Gas Chromatography-Chemical Ionization Mass Spectrometry Using Isotope Dilution and Large-Volume Injection. *J. Anal. Toxicol.* **2004**, *28*, 357–363.
- (18) Cametti, M.; Rissanen, K. Recognition and Sensing of Fluoride Anion. *Chem. Commun.* **2009**, 2809–2829.
- (19) Zhou, Y.; Zhang, J. F.; Yoon, J. Fluorescence and Colorimetric Chemosensors for Fluoride-Ion Detection. *Chem. Rev.* **2014**, *114*, 5511–5571.
- (20) Marcus, Y. Thermodynamics of Solvation of Ions. Part 5.-Gibbs Free Energy of Hydration at 298.15 K. *J. Chem. Soc., Faraday Trans.* **1991**, *87*, 2995–2999.
- (21) Camiolo, S.; Gale, P. A.; Hursthouse, M. B.; Light, M. E.; Shi, A. J. Solution and Solid-State Studies of 3,4-Dichloro-2,5-Diamidopyrroles: Formation of an Unusual Anionic Narcissistic Dimer. *Chem. Commun.* **2002**, 758–759.
- (22) Camiolo, S.; Gale, P. A.; Hursthouse, M. B.; Light, M. E. Nitrophenyl Derivatives of Pyrrole 2,5-Diamides: Structural Behaviour, Anion Binding and Colour Change Signalled Deprotonation. *Org. Biomol. Chem.* **2003**, *1*, 741–744.
- (23) Gunnlaugsson, T.; Kruger, P. E.; Jensen, P.; Pfeffer, F. M.; Hussey, G. M. Simple Naphthalimide Based Anion Sensors: Deprotonation Induced Colour Changes and CO_2 Fixation. *Tetrahedron Lett.* **2003**, *44*, 8909–8913.
- (24) Gunnlaugsson, T.; Kruger, P. E.; Lee, T. C.; Parkesh, R.; Pfeffer, F. M.; Hussey, G. M. Dual Responsive Chemosensors for Anions: The Combination of Fluorescent PET (Photoinduced Electron Transfer) and Colorimetric Chemosensors in a Single Molecule. *Tetrahedron Lett.* **2003**, *44*, 6575–6578.
- (25) Boiocchi, M.; Del Boca, L.; Gómez, D. E.; Fabbrizzi, L.; Licchelli, M.; Monzani, E. Nature of Urea–Fluoride Interaction: Incipient and Definitive Proton Transfer. *J. Am. Chem. Soc.* **2004**, *126*, 16507–16514.
- (26) Boiocchi, M.; Del Boca, L.; Esteban-Gómez, D.; Fabbrizzi, L.; Licchelli, M.; Monzani, E. Anion-Induced Urea Deprotonation. *Chem.—Eur. J.* **2005**, *11*, 3097–3104.
- (27) Esteban-Gómez, D.; Fabbrizzi, L.; Licchelli, M. Why, on Interaction of Urea-Based Receptors with Fluoride, Beautiful Colors Develop. *J. Org. Chem.* **2005**, *70*, 5717–5720.
- (28) Amendola, V.; Boiocchi, M.; Fabbrizzi, L.; Palchetti, A. What Anions Do inside a Receptor's Cavity: A Trifurcate Anion Receptor Providing Both Electrostatic and Hydrogen-Bonding Interactions. *Chem.—Eur. J.* **2005**, *11*, 5648–5660.
- (29) Amendola, V.; Esteban-Gómez, D.; Fabbrizzi, L.; Licchelli, M. What Anions Do to N–H-Containing Receptors. *Acc. Chem. Res.* **2006**, *39*, 343–353.
- (30) Rostami, A.; Colin, A.; Li, X. Y.; Chudzinski, M. G.; Lough, A. J.; Taylor, M. S. *N,N'*-Diarylsquaramides: General, High-Yielding Synthesis and Applications in Colorimetric Anion Sensing. *J. Org. Chem.* **2010**, *75*, 3983–3992.
- (31) Pfeffer, F. M.; Gunnlaugsson, T.; Jensen, P.; Kruger, P. E. Anion Recognition Using Preorganized Thiourea Functionalized [3]-Polynorbornane Receptors. *Org. Lett.* **2005**, *7*, 5357–5360.
- (32) Jiang, J.; Xiao, X.; Zhao, P.; Tian, H. Colorimetric Naked-Eye Recognizable Anion Sensors Synthesized Via Raft Polymerization. *J. Polym. Sci. A: Polym. Chem.* **2010**, *48*, 1551–1556.
- (33) Bose, P.; Ghosh, P. Visible and Near-Infrared Sensing of Fluoride by Indole Conjugated Urea/Thiourea Ligands. *Chem. Commun.* **2010**, *46*, 2962–2964.

- (34) Bose, P.; Ahamed, B. N.; Ghosh, P. Functionalized Guanidinium Chloride Based Colourimetric Sensors for Fluoride and Acetate: Single Crystal X-Ray Structural Evidence of -NH Deprotonation and Complexation. *Org. Biomol. Chem.* **2011**, *9*, 1972–1979.
- (35) Vázquez, M.; Fabbrizzi, L.; Taglietti, A.; Pedrido, R. M.; González-Noya, A. M.; Bermejo, M. R. A Colorimetric Approach to Anion Sensing: A Selective Chemosensor of Fluoride Ions, in Which Color Is Generated by Anion-Enhanced π Delocalization. *Angew. Chem., Int. Ed.* **2004**, *43*, 1962–1965.
- (36) Han, F.; Bao, Y.; Yang, Z.; Fyles, T. M.; Zhao, J.; Peng, X.; Fan, J.; Wu, Y.; Sun, S. Simple Bisthiocarbonohydrazone as Sensitive, Selective, Colorimetric, and Switch-on Fluorescent Chemosensors for Fluoride Anions. *Chem.—Eur. J.* **2007**, *13*, 2880–2892.
- (37) Raposo, M. M. M.; García-Acosta, B.; Ábalos, T.; Calero, P.; Martínez-Máñez, R.; Ros-Lis, J. V.; Soto, J. Synthesis and Study of the Use of Heterocyclic Thiosemicarbazones as Signaling Scaffolding for the Recognition of Anions. *J. Org. Chem.* **2010**, *75*, 2922–2933.
- (38) Lu, W.; Zhang, M.; Liu, K.; Fan, B.; Xia, Z.; Jiang, L. A Fluoride-Selective Colorimetric and Fluorescent Chemosensor and Its Use for the Design of Molecular-Scale Logic Devices. *Sens. Actuators, B* **2011**, *160*, 1005–1010.
- (39) Lu, W.; Chen, D.; Jiang, H.; Jiang, L.; Shen, Z. Polymer-Based Fluoride-Selective Chemosensor: Synthesis, Sensing Property, and Its Use for the Design of Molecular-Scale Logic Devices. *J. Polym. Sci. A: Polym. Chem.* **2012**, *50*, 590–598.
- (40) Zhuang, X.; Liu, W.; Wu, J.; Zhang, H.; Wang, P. A Novel Fluoride Ion Colorimetric Chemosensor Based on Coumarin. *Spectrochim. Acta, Part A: Mol. Biomol. Spectrosc.* **2011**, *79*, 1352–1355.
- (41) Bhosale, S. V.; Bhosale, S. V.; Kalyankar, M. B.; Langford, S. J. A Core-Substituted Naphthalene Diimide Fluoride Sensor. *Org. Lett.* **2009**, *11*, 5418–5421.
- (42) Lv, Y.; Guo, Y.; Xu, J.; Shao, S. Simple Indole-Based Colorimetric Sensors with Electron-Withdrawing Chromophores: Tuning Selectivity in Anion Sensing. *J. Fluorine Chem.* **2011**, *132*, 973–977.
- (43) Peng, X.; Wu, Y.; Fan, J.; Tian, M.; Han, K. Colorimetric and Ratiometric Fluorescence Sensing of Fluoride: Tuning Selectivity in Proton Transfer. *J. Org. Chem.* **2005**, *70*, 10524–10531.
- (44) Batista, R. M. F.; Oliveira, E.; Costa, S. P. G.; Lodeiro, C.; Raposo, M. M. M. Synthesis and Ion Sensing Properties of New Colorimetric and Fluorimetric Chemosensors Based on Bithienyl-Imidazo-Anthraquinone Chromophores. *Org. Lett.* **2007**, *9*, 3201–3204.
- (45) Elmes, R. B. P.; Gunnlaugsson, T. Luminescence Anion Sensing Via Modulation of MLCT Emission from a Naphthalimide–Ru(II)–Polypyridyl Complex. *Tetrahedron Lett.* **2010**, *51*, 4082–4087.
- (46) Kumar, B.; Kaloo, M. A.; Raja Sekhar, A.; Sankar, J. A Selective Fluoride Sensor and a Digital Processor with “Write-Read-Erase-Read” Behaviour. *Dalton Trans.* **2014**, *43*, 16164–16168.
- (47) Bhardwaj, V. K.; Hundal, M. S.; Hundal, G. A Tripodal Receptor Bearing Catechol Groups for the Chromogenic Sensing of F⁻ Ions Via Frozen Proton Transfer. *Tetrahedron* **2009**, *65*, 8556–8562.
- (48) Sui, B.; Kim, B.; Zhang, Y.; Frazer, A.; Belfield, K. D. Highly Selective Fluorescence Turn-on Sensor for Fluoride Detection. *ACS Appl. Mater. Interfaces* **2013**, *5*, 2920–2923.
- (49) Gunnlaugsson, T.; Kruger, P. E.; Jensen, P.; Tierney, J.; Ali, H. D. P.; Hussey, G. M. Colorimetric “Naked Eye” Sensing of Anions in Aqueous Solution. *J. Org. Chem.* **2005**, *70*, 10875–10878.
- (50) Fillaut, J.-L.; Andriès, J.; Perruchon, J.; Desvergne, J.-P.; Toupet, L.; Fadel, L.; Zouchoune, B.; Saillard, J.-Y. Alkynyl Ruthenium Colorimetric Sensors: Optimizing the Selectivity toward Fluoride Anion. *Inorg. Chem.* **2007**, *46*, 5922–5932.
- (51) Perez-Ruiz, R.; Diaz, Y.; Goldfuss, B.; Hertel, D.; Meerholz, K.; Griesbeck, A. G. Fluoride Recognition by a Chiral Urea Receptor Linked to a Phthalimide Chromophore. *Org. Biomol. Chem.* **2009**, *7*, 3499–3504.
- (52) Jo, Y.; Chidalla, N.; Cho, D.-G. Bis-Ureidoquinoline as a Selective Fluoride Anion Sensor through Hydrogen-Bond Interactions. *J. Org. Chem.* **2014**, *79*, 9418–9422.
- (53) Guha, S.; Saha, S. Fluoride Ion Sensing by an Anion- π Interaction. *J. Am. Chem. Soc.* **2010**, *132*, 17674–17677.
- (54) Galbraith, E.; James, T. D. Boron Based Anion Receptors as Sensors. *Chem. Soc. Rev.* **2010**, *39*, 3831–3842.
- (55) Nishiyabu, R.; Kubo, Y.; James, T. D.; Fossey, J. S. Boronic Acid Building Blocks: Tools for Sensing and Separation. *Chem. Commun.* **2011**, *47*, 1106–1123.
- (56) Hudnall, T. W.; Chiu, C.-W.; Gabbaï, F. P. Fluoride Ion Recognition by Chelating and Cationic Boranes. *Acc. Chem. Res.* **2009**, *42*, 388–397.
- (57) Katz, H. E. Hydride Sponge: Complexation of 1,8-Naphthalenediylbis(Dimethylborane) with Hydride, Fluoride, and Hydroxide. *J. Org. Chem.* **1985**, *50*, 5027–5032.
- (58) Williams, V. C.; Piers, W. E.; Clegg, W.; Elsegood, M. R. J.; Collins, S.; Marder, T. B. New Bifunctional Perfluoroaryl Boranes. Synthesis and Reactivity of the *ortho*-Phenylene-Bridged Diboranes 1,2-[B(C₆F₅)₂]₂C₆X₄ (X = H, F). *J. Am. Chem. Soc.* **1999**, *121*, 3244–3245.
- (59) Yamaguchi, S.; Akiyama, S.; Tamao, K. Colorimetric Fluoride Ion Sensing by Boron-Containing π -Electron Systems. *J. Am. Chem. Soc.* **2001**, *123*, 11372–11375.
- (60) Yamaguchi, S.; Shirasaka, T.; Akiyama, S.; Tamao, K. Dibenzoborole-Containing π -Electron Systems: Remarkable Fluorescence Change Based on the “on/off” Control of the P π –P π * Conjugation. *J. Am. Chem. Soc.* **2002**, *124*, 8816–8817.
- (61) Kubo, Y.; Yamamoto, M.; Ikeda, M.; Takeuchi, M.; Shinkai, S.; Yamaguchi, S.; Tamao, K. A Colorimetric and Ratiometric Fluorescent Chemosensor with Three Emission Changes: Fluoride Ion Sensing by a Triarylboration–Porphyrin Conjugate. *Angew. Chem., Int. Ed.* **2003**, *42*, 2036–2040.
- (62) Reetz, M. T.; Niemeyer, C. M.; Harms, K. Crown Ethers with a Lewis Acidic Center: A New Class of Heterotopic Host Molecules. *Angew. Chem., Int. Ed.* **1991**, *30*, 1472–1474.
- (63) Cooper, C. R.; Spencer, N.; James, T. D. Selective Fluorescence Detection of Fluoride Using Boronic Acids. *Chem. Commun.* **1998**, 1365–1366.
- (64) Liu, Z.-Q.; Shi, M.; Li, F.-Y.; Fang, Q.; Chen, Z.-H.; Yi, T.; Huang, C.-H. Highly Selective Two-Photon Chemosensors for Fluoride Derived from Organic Boranes. *Org. Lett.* **2005**, *7*, 5481–5484.
- (65) Arimori, S.; Davidson, M. G.; Fyles, T. M.; Hibbert, T. G.; James, T. D.; Kociok-Kohn, G. I. Synthesis and Structural Characterisation of the First Bis(Bora)Calixarene: A Selective, Bidentate, Fluorescent Fluoride Sensor. *Chem. Commun.* **2004**, 1640–1641.
- (66) Galbraith, E.; Fyles, T. M.; Marken, F.; Davidson, M. G.; James, T. D. Fluorescent Boron Bis(Phenolate) with Association Response to Chloride and Dissociation Response to Fluoride. *Inorg. Chem.* **2008**, *47*, 6236–6244.
- (67) Xu, Z.; Kim, S. K.; Han, S. J.; Lee, C.; Kociok-Kohn, G.; James, T. D.; Yoon, J. Ratiometric Fluorescence Sensing of Fluoride Ions by an Asymmetric Bidentate Receptor Containing a Boronic Acid and Imidazolium Group. *Eur. J. Org. Chem.* **2009**, *2009*, 3058–3065.
- (68) Jun, E. J.; Xu, Z.; Lee, M.; Yoon, J. A Ratiometric Fluorescent Probe for Fluoride Ions with a Tridentate Receptor of Boronic Acid and Imidazolium. *Tetrahedron Lett.* **2013**, *54*, 2755–2758.
- (69) Sole, S.; Gabbaï, F. P. A Bidentate Borane as Colorimetric Fluoride Ion Sensor. *Chem. Commun.* **2004**, 1284–1285.
- (70) Melaimi, M.; Gabbaï, F. P. A Heteronuclear Bidentate Lewis Acid as a Phosphorescent Fluoride Sensor. *J. Am. Chem. Soc.* **2005**, *127*, 9680–9681.
- (71) Hudnall, T. W.; Kim, Y.-M.; Bebbington, M. W. P.; Bourissou, D.; Gabbaï, F. P. Fluoride Ion Chelation by a Bidentate Phosphonium/Borane Lewis Acid. *J. Am. Chem. Soc.* **2008**, *130*, 10890–10891.
- (72) Kim, Y.; Gabbaï, F. P. Cationic Boranes for the Complexation of Fluoride Ions in Water Below the 4 ppm Maximum Contaminant Level. *J. Am. Chem. Soc.* **2009**, *131*, 3363–3369.
- (73) Lee, M. H.; Agou, T.; Kobayashi, J.; Kawashima, T.; Gabbaï, F. P. Fluoride Ion Complexation by a Cationic Borane in Aqueous Solution. *Chem. Commun.* **2007**, 1133–1135.
- (74) Hudnall, T. W.; Gabbaï, F. P. Ammonium Boranes for the Selective Complexation of Cyanide or Fluoride Ions in Water. *J. Am. Chem. Soc.* **2007**, *129*, 11978–11986.

- (75) Badugu, R.; Lakowicz, J. R.; Geddes, C. D. A Wavelength-Ratiometric Fluoride-Sensitive Probe Based on the Quinolinium Nucleus and Boronic Acid Moiety. *Sens. Actuators, B* **2005**, *104*, 103–110.
- (76) Wade, C. R.; Ke, I.-S.; Gabbaï, F. P. Sensing of Aqueous Fluoride Anions by Cationic Stibine–Palladium Complexes. *Angew. Chem., Int. Ed.* **2012**, *51*, 478–481.
- (77) Tripier, R.; Platas-Iglesias, C.; Boos, A.; Morfin, J.-F.; Charbonnière, L. Towards Fluoride Sensing with Positively Charged Lanthanide Complexes. *Eur. J. Inorg. Chem.* **2010**, *2010*, 2735–2745.
- (78) Lima, L. M. P.; Lecointre, A.; Morfin, J.-F.; de Blas, A.; Visvikis, D.; Charbonnière, L. J.; Platas-Iglesias, C.; Tripier, R. Positively Charged Lanthanide Complexes with Cyclen-Based Ligands: Synthesis, Solid-State and Solution Structure, and Fluoride Interaction. *Inorg. Chem.* **2011**, *50*, 12508–12521.
- (79) Liu, T.; Nonat, A.; Beyler, M.; Regueiro-Figueroa, M.; Nchimi Nono, K.; Jeannin, O.; Camerel, F.; Debaene, F.; Cianfrani-Sanglier, S.; Tripier, R.; Platas-Iglesias, C.; Charbonnière, L. J. Supramolecular Luminescent Lanthanide Dimers for Fluoride Sequestering and Sensing. *Angew. Chem., Int. Ed.* **2014**, *53*, 7259–7263.
- (80) Rochat, S.; Severin, K. A Simple Fluorescence Assay for the Detection of Fluoride in Water at Neutral pH. *Chem. Commun.* **2011**, *47*, 4391–4393.
- (81) Yamaguchi, S.; Akiyama, S.; Tamao, K. Photophysical Properties Changes Caused by Hypercoordination of Organosilicon Compounds: From Trianthrylfluorosilane to Trianthryldifluorosilicate. *J. Am. Chem. Soc.* **2000**, *122*, 6793–6794.
- (82) Saxena, A.; Fujiki, M.; Rai, R.; Kim, S.-Y.; Kwak, G. Highly Sensitive and Selective Fluoride Ion Chemosensing, Fluoroalkylated Polysilane. *Macromol. Rapid Commun.* **2004**, *25*, 1771–1775.
- (83) Descalzo, A. B.; Jimenez, D.; Haskouri, J. E.; Beltran, D.; Amoros, P.; Marcos, M. D.; Martínez-Mañez, R.; Soto, J. A New Method for Fluoride Determination by Using Fluorophores and Dyes Anchored onto MCM-41. *Chem. Commun.* **2002**, *562*–563.
- (84) Kim, T.-H.; Swager, T. M. A Fluorescent Self-Amplifying Wavelength-Responsive Sensory Polymer for Fluoride Ions. *Angew. Chem., Int. Ed.* **2003**, *42*, 4803–4806.
- (85) Li, B.; Zhang, C.; Liu, C.; Chen, J.; Wang, X.; Liu, Z.; Yi, F. Chemodosimeter for Fluoride Ions Based on F-Triggered Si–O Cleavage Followed by the Deprotonation/Autoxidation of Secondary Nitrile C–H Group. *RSC Adv.* **2014**, *4*, 46016–46019.
- (86) Cao, J.; Zhao, C.; Zhu, W. A near-Infrared Fluorescence Chemodosimeter for Fluoride Via Specific Si–O Cleavage. *Tetrahedron Lett.* **2012**, *53*, 2107–2110.
- (87) Li, X.; Hu, B.; Li, J.; Lu, P.; Wang, Y. Fluoride Anion Detection Based on the Excited State Intramolecular Proton Transfer (ESIPT) of 2-(O-Hydroxyphenyl)Imidazole Induced by the Si–O Cleavage of Its Silyl Ether. *Sens. Actuators, B* **2014**, *203*, 635–640.
- (88) Buckland, D.; Bhosale, S. V.; Langford, S. J. A Chemodosimeter Based on a Core-Substituted Naphthalene Diimide for Fluoride Ion Detection. *Tetrahedron Lett.* **2011**, *52*, 1990–1992.
- (89) Cao, X.; Lin, W.; Yu, Q.; Wang, J. Ratiometric Sensing of Fluoride Anions Based on a Bodipy-Coumarin Platform. *Org. Lett.* **2011**, *13*, 6098–6101.
- (90) Kim, S. Y.; Hong, J.-I. Chromogenic and Fluorescent Chemodosimeter for Detection of Fluoride in Aqueous Solution. *Org. Lett.* **2007**, *9*, 3109–3112.
- (91) Kim, S. Y.; Park, J.; Koh, M.; Park, S. B.; Hong, J.-I. Fluorescent Probe for Detection of Fluoride in Water and Bioimaging in A549 Human Lung Carcinoma Cells. *Chem. Commun.* **2009**, 4735–4737.
- (92) Hu, R.; Feng, J.; Hu, D.; Wang, S.; Li, S.; Li, Y.; Yang, G. A Rapid Aqueous Fluoride Ion Sensor with Dual Output Modes. *Angew. Chem., Int. Ed.* **2010**, *49*, 4915–4918.
- (93) Baker, M. S.; Phillips, S. T. A Small Molecule Sensor for Fluoride Based on an Autoinductive, Colorimetric Signal Amplification Reaction. *Org. Biomol. Chem.* **2012**, *10*, 3595–3599.
- (94) Perry-Feigenbaum, R.; Sella, E.; Shabat, D. Autoinductive Exponential Signal Amplification: A Diagnostic Probe for Direct Detection of Fluoride. *Chem.—Eur. J.* **2011**, *17*, 12123–12128.
- (95) Li, G.; Gong, W.-T.; Ye, J.-W.; Lin, Y.; Ning, G.-L. Unprecedented Intramolecular Cyclization of Pyridinium to Pyrido[1,2-a]Benzimidazole: A Novel Chemodosimeter for Fluoride Ions. *Tetrahedron Lett.* **2011**, *52*, 1313–1316.
- (96) Padie, C.; Zeitler, K. A Novel Reaction-Based, Chromogenic and “Turn-on” Fluorescent Chemodosimeter for Fluoride Detection. *New J. Chem.* **2011**, *35*, 994–997.
- (97) Zelder, F. H.; Männel-Croisé, C. Recent Advances in the Colorimetric Detection of Cyanide. *Chimia* **2009**, *63*, 58–62.
- (98) Ma, J.; Dasgupta, P. K. Recent Developments in Cyanide Detection: A Review. *Anal. Chim. Acta* **2010**, *673*, 117–125.
- (99) Xu, Z.; Chen, X.; Kim, H. N.; Yoon, J. Sensors for the Optical Detection of Cyanide Ion. *Chem. Soc. Rev.* **2010**, *39*, 127–137.
- (100) Wang, F.; Wang, L.; Chen, X.; Yoon, J. Recent Progress in the Development of Fluorometric and Colorimetric Chemosensors for Detection of Cyanide Ions. *Chem. Soc. Rev.* **2014**, *43*, 4312–4324.
- (101) Kumari, N.; Jha, S.; Bhattacharya, S. Colorimetric Probes Based on Anthraimidazolediones for Selective Sensing of Fluoride and Cyanide Ion Via Intramolecular Charge Transfer. *J. Org. Chem.* **2011**, *76*, 8215–8222.
- (102) Housecroft, C. E.; Sharpe, A. G. *Inorganic Chemistry*, 3rd ed.; Pearson Education Ltd.: Harlow, 2008.
- (103) Gulyey, R.; Ozturk, S.; Sahin, E.; Akkaya, E. U. Expanded Bodipy Dyes: Anion Sensing Using a Bodipy Analog with an Additional Difluoroboron Bridge. *Org. Lett.* **2012**, *14*, 1528–1531.
- (104) Jia, J.; Xue, P.; Zhang, Y.; Xu, Q.; Zhang, G.; Huang, T.; Zhang, H.; Lu, R. Fluorescent Sensor Based on Dimesitylborylthiophene Derivative for Probing Fluoride and Cyanide. *Tetrahedron* **2014**, 5499–5504.
- (105) Gimeno, N.; Li, X.; Durrant, J. R.; Vilar, R. Cyanide Sensing with Organic Dyes: Studies in Solution and on Nanostructured Al₂O₃ Surfaces. *Chem.—Eur. J.* **2008**, *14*, 3006–3012.
- (106) Nandi, L. G.; Nicoleti, C. R.; Bellettini, I. C.; Machado, V. G. Optical Chemosensor for the Detection of Cyanide in Water Based on Ethyl(Hydroxyethyl)Cellulose Functionalized with Brooker’s Merocyanine. *Anal. Chem.* **2014**, *86*, 4653–4656.
- (107) Hudnall, T. W.; Gabbaï, F. P. Ammonium Boranes for the Selective Complexation of Cyanide or Fluoride Ions in Water. *J. Am. Chem. Soc.* **2007**, *129*, 11978–11986.
- (108) Kim, Y.; Zhao, H.; Gabbaï, F. P. Sulfonium Boranes for the Selective Capture of Cyanide Ions in Water. *Angew. Chem., Int. Ed.* **2009**, *48*, 4957–4960.
- (109) Song, K. C.; Lee, K. M.; Nghia, N. V.; Sung, W. Y.; Do, Y.; Lee, M. H. Synthesis and Anion Binding Properties of Multi-Phosphonium Triarylboranes: Selective Sensing of Cyanide Ions in Buffered Water at pH 7. *Organometallics* **2013**, *32*, 817–823.
- (110) Brooms Grove, A. E. J.; Addy, D. A.; Bresner, C.; Fallis, I. A.; Thompson, A. L.; Aldridge, S. AND/NOT Sensing of Fluoride and Cyanide Ions by Ferrocene-Derivatised Lewis Acids. *Chem.—Eur. J.* **2008**, *14*, 7525–7529.
- (111) Chung, S. Y.; Nam, S. W.; Lim, J.; Park, S.; Yoon, J. A Highly Selective Cyanide Sensing in Water Via Fluorescence Change and Its Application to *in vivo* Imaging. *Chem. Commun.* **2009**, 2866–2868.
- (112) Chen, X.; Nam, S. W.; Kim, G. H.; Song, N.; Jeong, Y.; Shin, I.; Kim, S. K.; Kim, J.; Park, S.; Yoon, J. A near-Infrared Fluorescent Sensor for Detection of Cyanide in Aqueous Solution and Its Application for Bioimaging. *Chem. Commun.* **2010**, *46*, 8953–8955.
- (113) Reddy, G. U.; Das, P.; Saha, S.; Baidya, M.; Ghosh, S. K.; Das, A. A CN-Specific Turn-on Phosphorescent Probe with Probable Application for Enzymatic Assay and as an Imaging Reagent. *Chem. Commun.* **2013**, *49*, 255–257.
- (114) Tetilla, M. A.; Aragoni, M. C.; Arca, M.; Caltagirone, C.; Bazzicalupi, C.; Bencini, A.; Garau, A.; Isaia, F.; Laguna, A.; Lippolis, V.; Meli, V. Colorimetric Response to Anions by a “Robust” Copper(II) Complex of a [9]aneN₃ Pendant Arm Derivative: CN[−] and I[−] Selective Sensing. *Chem. Commun.* **2011**, *47*, 3805–3807.
- (115) Gee, H.-C.; Lee, C.-H.; Jeong, Y.-H.; Jang, W.-D. Highly Sensitive and Selective Cyanide Detection via Cu²⁺ Complex Ligand Exchange. *Chem. Commun.* **2011**, *47*, 11963–11965.

- (116) Liu, H.; Shao, X. B.; Jia, M. X.; Jiang, X. K.; Li, Z. T.; Chen, G. J. Selective Recognition of Sodium Cyanide and Potassium Cyanide by Diaza-Crown Ether-Capped Zn-Porphyrin Receptors in Polar Solvents. *Tetrahedron* **2005**, *61*, 8095–8100.
- (117) Worlinsky, J. L.; Halepas, S.; Brückner, C. Pegylated meso-Arylporpholactone Metal Complexes as Optical Cyanide Sensors in Water. *Org. Biomol. Chem.* **2014**, *12*, 3991–4001.
- (118) Swamy, P. C. A.; Mukherjee, S.; Thilagar, P. Dual Binding Site Assisted Chromogenic and Fluorogenic Recognition and Discrimination of Fluoride and Cyanide by a Peripherally Borylated Metalloporphyrin: Overcoming Anion Interference in Organoboron Based Sensors. *Anal. Chem.* **2014**, *86*, 3616–3624.
- (119) Chen, C. L.; Chen, Y. H.; Chen, C. Y.; Sun, S. S. Dipyrrrole Carboxamide Derived Selective Ratiometric Probes for Cyanide Ion. *Org. Lett.* **2006**, *8*, 5053–5056.
- (120) Ekmekci, Z.; Yilmaz, M. D.; Akkaya, E. U. A Monostyryl-Boradiazaindacene (Bodipy) Derivative as Colorimetric and Fluorescent Probe for Cyanide Ions. *Org. Lett.* **2008**, *10*, 461–464.
- (121) Lee, K. S.; Kim, H. J.; Kim, G. H.; Shin, I.; Hong, J. I. Fluorescent Chemodosimeter for Selective Detection of Cyanide in Water. *Org. Lett.* **2008**, *10*, 49–51.
- (122) Park, S.; Kim, H. J. Highly Activated Michael Acceptor by an Intramolecular Hydrogen Bond as a Fluorescence Turn-on Probe for Cyanide. *Chem. Commun.* **2010**, *46*, 9197–9199.
- (123) Gotor, R.; Costero, A. M.; Gil, S.; Parra, M.; Martínez-Máñez, R.; Sancenón, F.; Gaviña, P. Selective and Sensitive Chromogenic Detection of Cyanide and HCN in Solution and in Gas Phase. *Chem. Commun.* **2013**, *49*, 5669–5671.
- (124) Dong, M.; Peng, Y.; Dong, Y. M.; Tang, N.; Wang, Y. W. A Selective, Colorimetric, and Fluorescent Chemodosimeter for Relay Recognition of Fluoride and Cyanide Anions Based on 1,1'-Binaphthyl Scaffold. *Org. Lett.* **2012**, *14*, 130–133.
- (125) Lee, C. H.; Yoon, H. J.; Shim, J. S.; Jang, W. D. A Boradiazaindacene-Based Turn-on Fluorescent Probe for Cyanide Detection in Aqueous Media. *Chem.—Eur. J.* **2012**, *18*, 4513–4516.
- (126) Chen, B.; Ding, Y.; Li, X.; Zhu, W.; Hill, J. P.; Ariga, K.; Xie, Y. Steric Hindrance-Enforced Distortion as a General Strategy for the Design of Fluorescence “Turn-on” Cyanide Probes. *Chem. Commun.* **2013**, *49*, 10136–10138.
- (127) Yang, Y. K.; Tae, J. Acridinium Salt Based Fluorescent and Colorimetric Chemosensor for the Detection of Cyanide in Water. *Org. Lett.* **2006**, *8*, 5721–5723.
- (128) Robbins, T. F.; Qian, H.; Su, X.; Hughes, R. P.; Aprahamian, I. Cyanide Detection Using a Triazolopyridinium Salt. *Org. Lett.* **2013**, *15*, 2386–2389.
- (129) Kim, H. J.; Ko, K. C.; Lee, J. H.; Lee, J. Y.; Kim, J. S. KCN Sensor: Unique Chromogenic and ‘Turn-on’ Fluorescent Chemodosimeter: Rapid Response and High Selectivity. *Chem. Commun.* **2011**, *47*, 2886–2888.
- (130) Huang, X.; Gu, X.; Zhang, G.; Zhang, D. A Highly Selective Fluorescence Turn-on Detection of Cyanide Based on the Aggregation of Tetraphenylethylene Molecules Induced by Chemical Reaction. *Chem. Commun.* **2012**, *48*, 12195–12197.
- (131) Tomasulo, M.; Sortino, S.; White, A. J. P.; Raymo, F. M. Chromogenic Oxazines for Cyanide Detection. *J. Org. Chem.* **2006**, *71*, 744–753.
- (132) Ren, J.; Zhu, W.; Tian, H. A Highly Sensitive and Selective Chemosensor for Cyanide. *Talanta* **2008**, *75*, 760–764.
- (133) Zhang, X.; Li, C.; Cheng, X.; Wang, X.; Zhang, B. A near-Infrared Croconium Dye-Based Colorimetric Chemodosimeter for Biological Thiols and Cyanide Anion. *Sens. Actuators, B: Chem.* **2008**, *129*, 152–157.
- (134) Afkhami, A.; Sarlak, N. A Novel Cyanide Sensing Phase Based on Immobilization of Methyl Violet on a Triacetylcellulose Membrane. *Sens. Actuators, B: Chem.* **2007**, *122*, 437–441.
- (135) Kaur, P.; Sareen, D.; Kaur, S.; Singh, K. An Efficacious “Naked-Eye” Selective Sensing of Cyanide from Aqueous Solutions Using a Triarylmethane Leuconitrile. *Inorg. Chem. Commun.* **2009**, *12*, 272–275.
- (136) Qian, G.; Li, X.; Wang, Z. Y. Visible and Near-Infrared Chemosensor for Colorimetric and Ratiometric Detection of Cyanide. *J. Mater. Chem.* **2009**, *19*, 522–530.
- (137) Adams, R. L. P.; Knowler, J. T.; Leader, D. P. *The Biochemistry of the Nucleic Acids*, 10th ed.; Chapman and Hall: New York, 1986.
- (138) Saenger, W. *Principles of Nucleic Acid Structure*; Springer-Verlag: New York, 1984.
- (139) *Phosphorus in the Global Environment: Transfers, Cycles, and Management*; Wiley: New York, 1995.
- (140) Mason, C. F. *Biology of Freshwater Pollution*; Longman: New York, 1991.
- (141) Hargrove, A. E.; Nieto, S.; Zhang, T.; Sessler, J. L.; Anslyn, E. V. Artificial Receptors for the Recognition of Phosphorylated Molecules. *Chem. Rev.* **2011**, *111*, 6603–6782.
- (142) Hirsch, A. K. H.; Fischer, F. R.; Diederich, F. Phosphate Recognition in Structural Biology. *Angew. Chem., Int. Ed.* **2007**, *46*, 338–352.
- (143) Marcus, Y.; Rashin, A. A Simple Empirical Model Describing the Thermodynamics of Hydration of Ions of Widely Varying Charges, Sizes, and Shapes. *Biophys. Chem.* **1994**, *51*, 111–127.
- (144) Czarnik, A. W. Chemical Communication in Water Using Fluorescent Chemosensors. *Acc. Chem. Res.* **1994**, *27*, 302–308.
- (145) Bazzicalupi, C.; Bencini, A.; Lippolis, V. Tailoring Cyclic Polyamines for Inorganic/Organic Phosphate Binding. *Chem. Soc. Rev.* **2010**, *39*, 3709–3728.
- (146) Bazzicalupi, C.; Biagini, S.; Bencini, A.; Faggi, E.; Giorgi, C.; Matera, I.; Valtancoli, B. ATP Recognition and Sensing with a Phenanthroline-Containing Polyammonium Receptor. *Chem. Commun.* **2006**, 4087–4089.
- (147) Malojčić, G.; Piantanida, I.; Marinić, M.; Žinić, M.; Marjanović, M.; Kralj, M.; Pavelić, K.; Schneider, H. J. A Novel Bis-Phenanthridine Triamine with pH Controlled Binding to Nucleotides and Nucleic Acids. *Org. Biomol. Chem.* **2005**, *3*, 4373–4381.
- (148) Descalzo, A. B.; Marcos, M. D.; Martínez-Máñez, R.; Soto, J.; Beltran, D.; Amoros, P. Anthrylmethylamine Functionalised Mesoporous Silica-Based Materials as Hybrid Fluorescent Chemosensors for ATP. *J. Mater. Chem.* **2005**, *15*, 2721–2731.
- (149) Aucejo, R.; Diaz, P.; García-España, E.; Alarcon, J.; Delgado-Pinar, E.; Torres, F.; Soriano, C.; Guillem, M. C. Naphthalene-Containing Polyamines Supported in Nanosized Boehmite Particles. *New J. Chem.* **2007**, *31*, 44–51.
- (150) Kim, S. K.; Singh, N. J.; Kwon, J.; Hwang, I. C.; Park, S. J.; Kim, K. S.; Yoon, J. Fluorescent Imidazolium Receptors for the Recognition of Pyrophosphate. *Tetrahedron* **2006**, *62*, 6065–6072.
- (151) Yoon, J.; Kim, S. K.; Singh, N. J.; Lee, J. W.; Yang, Y. J.; Chellappan, K.; Kim, K. S. Highly Effective Fluorescent Sensor for H_2PO_4^- . *J. Org. Chem.* **2004**, *69*, 581–583.
- (152) Singh, N. J.; Jun, E. J.; Chellappan, K.; Thangadurai, D.; Chandran, R. P.; Hwang, I. C.; Yoon, J.; Kim, K. S. Quinoxaline-Imidazolium Receptors for Unique Sensing of Pyrophosphate and Acetate by Charge Transfer. *Org. Lett.* **2007**, *9*, 485–488.
- (153) Xu, Z.; Singh, N. J.; Lim, J.; Pan, J.; Ha, N. K.; Park, S.; Kim, K. S.; Yoon, J. Unique Sandwich Stacking of Pyrene-Adenine-Pyrene for Selective and Ratiometric Fluorescent Sensing of ATP at Physiological pH. *J. Am. Chem. Soc.* **2009**, *131*, 15528–15533.
- (154) Ahmed, N.; Shirinfar, B.; Geronimo, I.; Kim, K. S. Fluorescent Imidazolium-Based Cyclophane for Detection of Guanosine-5'-Triphosphate and I^- in Aqueous Solution of Physiological pH. *Org. Lett.* **2011**, *13*, 5476–5479.
- (155) Jung, J. Y.; Jun, E. J.; Kwon, Y.-U.; Yoon, J. Recognition of myo-Inositol 1,4,5-Trisphosphate Using a Fluorescent Imidazolium Receptor. *Chem. Commun.* **2012**, *48*, 7928–7930.
- (156) Duke, R. M.; O’Brien, J. E.; McCabe, T.; Gunnlaugsson, T. Colorimetric Sensing of Anions in Aqueous Solution Using a Charge Neutral, Cleft-Like, Amidothiourea Receptor: Tilting the Balance between Hydrogen Bonding and Deprotonation in Anion Recognition. *Org. Biomol. Chem.* **2008**, *6*, 4089–4092.
- (157) Duke, R. M.; McCabe, T.; Schmitt, W.; Gunnlaugsson, T. Recognition and Sensing of Biologically Relevant Anions in Alcohol and

- Mixed Alcohol-Aqueous Solutions Using Charge Neutral Cleft-Like Glycol-Derived Pyridyl-Amidothiourea Receptors. *J. Org. Chem.* **2012**, *77*, 3115–3126.
- (158) García-Garrido, S. E.; Caltagirone, C.; Light, M. E.; Gale, P. A. Acridinone-Based Anion Receptors and Sensors. *Chem. Commun.* **2007**, 1450–1452.
- (159) Sanchez, G.; Espinosa, A.; Curiel, D.; Tarraga, A.; Molina, P. Bis(Carbazolyl)Ureas as Selective Receptors for the Recognition of Hydrogenpyrophosphate in Aqueous Media. *J. Org. Chem.* **2013**, *78*, 9725–9737.
- (160) Caltagirone, C.; Bazzicalupi, C.; Isaia, F.; Light, M. E.; Lippolis, V.; Montis, R.; Murgia, S.; Olivari, M.; Picci, G. A New Family of Bis-Ureidic Receptors for Pyrophosphate Optical Sensing. *Org. Biomol. Chem.* **2013**, *11*, 2445–2451.
- (161) Plitt, P.; Gross, D. E.; Lynch, V. M.; Sessler, J. L. Dipyrrolyl-Functionalized Bipyridine-Based Anion Receptors for Emission-Based Selective Detection of Dihydrogen Phosphate. *Chem.—Eur. J.* **2007**, *13*, 1374–1381.
- (162) Bencini, A.; Bartoli, F.; Caltagirone, C.; Lippolis, V. Zinc(II)-Based Fluorescent Dyes: Luminescence Modulation by Phosphate Anion Binding. *Dyes Pigm.* **2014**, *110*, 169–192.
- (163) Ngo, H. T.; Liu, X.; Jolliffe, K. A. Anion Recognition and Sensing with Zn(II)-Dipicolylamine Complexes. *Chem. Soc. Rev.* **2012**, *41*, 4928–4965.
- (164) Sakamoto, T.; Ojida, A.; Hamachi, I. Molecular Recognition, Fluorescence Sensing, and Biological Assay of Phosphate Anion Derivatives Using Artificial Zn(II)-DPA Complexes. *Chem. Commun.* **2009**, 141–152.
- (165) Madden, D. P.; da Mota, M. M.; Nelson, S. M. Five-Coordination in Molecular Complexes of Zinc, Cadmium, and Mercury(II) with Potentially Ter- or Tetra-Dendate Ligands with Nitrogen Donor Atoms. *J. Chem. Soc. A: Inorg., Phys., Theor.* **1970**, 790–794.
- (166) Anai, T.; Nakata, E.; Koshi, Y.; Ojida, A.; Hamachi, I. Design of a Hybrid Biosensor for Enhanced Phosphopeptide Recognition Based on a Phosphoprotein Binding Domain Coupled with a Fluorescent Chemosensor. *J. Am. Chem. Soc.* **2007**, *129*, 6233–6239.
- (167) Ojida, A.; Mito-Oka, Y.; Sada, K.; Hamachi, I. Molecular Recognition and Fluorescence Sensing of Monophosphorylated Peptides in Aqueous Solution by Bis(Zinc(II)-Dipicolylamine)-Based Artificial Receptors. *J. Am. Chem. Soc.* **2004**, *126*, 2454–2463.
- (168) Ojida, A.; Nonaka, H.; Miyahara, Y.; Tamaru, S. I.; Sada, K.; Hamachi, I. Bis(DPA-Zn^{II}) Appended Xanthone: Excitation Ratio-Metric Chemosensor for Phosphate Anions. *Angew. Chem., Int. Ed.* **2006**, *45*, 5518–5521.
- (169) Ojida, A.; Takashima, I.; Kohira, T.; Nonaka, H.; Hamachi, I. Turn-on Fluorescence Sensing of Nucleoside Polyphosphates Using a Xanthenone-Based Zn(II) Complex Chemosensor. *J. Am. Chem. Soc.* **2008**, *130*, 12095–12101.
- (170) Kurishita, Y.; Kohira, T.; Ojida, A.; Hamachi, I. Rational Design of Fret-Based Ratiometric Chemosensors for *in vitro* and in Cell Fluorescence Analyses of Nucleoside Polyphosphates. *J. Am. Chem. Soc.* **2010**, *132*, 13290–13299.
- (171) Bazzicalupi, C.; Bencini, A.; Puccioni, S.; Valtancoli, B.; Gratteri, P.; Garau, A.; Lippolis, V. Selective Binding and Fluorescence Sensing of Diphosphate in H₂O via Zn²⁺-Induced Allosteric Regulation of the Receptor Structure. *Chem. Commun.* **2012**, *48*, 139–141.
- (172) Zeng, Z.; Torriero, A. A. J.; Bond, A. M.; Spiccia, L. Fluorescent and Electrochemical Sensing of Polyphosphate Nucleotides by Ferrocene Functionalised with Two Zn^{II}(TACN)(pyrene) Complexes. *Chem.—Eur. J.* **2010**, *16*, 9154–9163.
- (173) Kumar Pathak, R.; Kumar Hinge, V.; Rai, A.; Panda, D.; Pulla Rao, C. Imino-Phenolic-Pyridyl Conjugates of Calix[4]arene (L1 and L2) as Primary Fluorescence Switch-on Sensors for Zn²⁺ in Solution and in HeLa Cells and the Recognition of Pyrophosphate and ATP by [ZnL2]. *Inorg. Chem.* **2012**, *51*, 4994–5005.
- (174) Zhang, M.; Ma, W. J.; He, C. T.; Jiang, L.; Lu, T. B. Highly Selective Recognition and Fluorescence Imaging of Adenosine Polyphosphates in Aqueous Solution. *Inorg. Chem.* **2013**, *52*, 4873–4879.
- (175) Khatua, S.; Choi, S. H.; Lee, J.; Kim, K.; Do, Y.; Churchill, D. G. Aqueous Fluorometric and Colorimetric Sensing of Phosphate Ions by a Fluorescent Dinuclear Zinc Complex. *Inorg. Chem.* **2009**, *48*, 2993–2999.
- (176) Luxami, V.; Paul, K.; Jeong, I. H. Pyrophosphate Selective Fluorescent Probe and Molecular Flip-Flop. *Dalton Trans.* **2013**, *42*, 3783–3786.
- (177) Kim, M. J.; Swamy, K. M. K.; Lee, K. M.; Jagdale, A. R.; Kim, Y.; Kim, S. J.; Yoo, K. H.; Yoon, J. Pyrophosphate Selective Fluorescent Chemosensors Based on Coumarin-DPA-Cu(II) Complexes. *Chem. Commun.* **2009**, 7215–7217.
- (178) Swamy, K. M. K.; Kwon, S. K.; Lee, H. N.; Shantha Kumar, S. M.; Kim, J. S.; Yoon, J. Fluorescent Sensing of Pyrophosphate and ATP in 100% Aqueous Solution Using a Fluorescein Derivative and Mn²⁺. *Tetrahedron Lett.* **2007**, *48*, 8683–8686.
- (179) Zhou, L. L.; Sun, H.; Li, H. P.; Wang, H.; Zhang, X. H.; Wu, S. K.; Lee, S. T. A Novel Colorimetric and Fluorescent Anion Chemosensor Based on the Flavone Quasi-Crown Ether-Metal Complex. *Org. Lett.* **2004**, *6*, 1071–1074.
- (180) Li, S. H.; Yuan, W. T.; Zhu, C. Q.; Xu, J. G. Species-Differentiable Sensing of Phosphate-Containing Anions in Neutral Aqueous Solution Based on Coordinatively Unsaturated Lanthanide Complex Probes. *Anal. Biochem.* **2004**, *331*, 235–242.
- (181) Nadella, S.; Sahoo, J.; Subramanian, P. S.; Sahu, A.; Mishra, S.; Albrecht, M. Sensing of Phosphates by Using Luminescent Eu^{III} and Tb^{III} Complexes: Application to the Microalgal Cell Chlorella Vulgaris. *Chem.—Eur. J.* **2014**, *20*, 6047–6053.
- (182) Pope, S. J. A.; Burton-Pye, B. P.; Berridge, R.; Khan, T.; Skabara, P. J.; Faulkner, S. Self-Assembly of Luminescent Ternary Complexes between Seven-Coordinate Lanthanide(III) Complexes and Chromophore Bearing Carboxylates and Phosphonates. *Dalton Trans.* **2006**, 2907–2912.
- (183) Filby, M. H.; Dickson, S. J.; Zaccheroni, N.; Prodi, L.; Bonacchi, S.; Montalti, M.; Paterson, M. J.; Humphries, T. D.; Chiorboli, C.; Steed, J. W. Induced Fit Interanion Discrimination by Binding-Induced Excimer Formation. *J. Am. Chem. Soc.* **2008**, *130*, 4105–4113.
- (184) Engle, J. M.; Carroll, C. N.; Johnson, D. W.; Haley, M. M. Synthesis and Optoelectronic Properties of 2,6-Bis(2-Anilinoethyl)Pyridine Scaffolds. *Chem. Sci.* **2012**, *3*, 1105–1110.
- (185) Chifotides, H. T.; Schottel, B. L.; Dunbar, K. R. The π-Accepting Arene Hat(CN)₆ as a Halide Receptor through Charge Transfer: Multisite Anion Interactions and Self-Assembly in Solution and the Solid State. *Angew. Chem., Int. Ed.* **2010**, *49*, 7202–7207.
- (186) Maeda, H.; Bando, Y.; Shimomura, K.; Yamada, I.; Naito, M.; Nobusawa, K.; Tsumatori, H.; Kawai, T. Chemical-Stimuli-Controllable Circularly Polarized Luminescence from Anion-Responsive π-Conjugated Molecules. *J. Am. Chem. Soc.* **2011**, *133*, 9266–9269.
- (187) Ghosh, K.; Sen, T. Adenine-Based Urea Receptors in Fluorescent Recognition of Iodide. *Tetrahedron Lett.* **2008**, *49*, 7204–7208.
- (188) Singh, N.; Jung, H. J.; Jang, D. O. Cu(II) Complex of a Flexible Tripodal Receptor as a Highly Selective Fluorescent Probe for Iodide. *Tetrahedron Lett.* **2009**, *50*, 71–74.
- (189) Zhao, Y.; Yao, L.; Zhang, M.; Ma, Y. A Simple Sensitive Colorimetric/Fluorometric Probe for Iodide. *Talanta* **2012**, *97*, 343–348.
- (190) Patil, S. R.; Nandre, J. P.; Jadhav, D.; Bothra, S.; Sahoo, S. K.; Devi, M.; Pradeep, C. P.; Mahulikar, P. P.; Patil, U. D. Imatinib Intermediate as a Two in One Dual Channel Sensor for the Recognition of Cu²⁺ and I[−] Ions in Aqueous Media and Its Practical Applications. *Dalton Trans.* **2014**, *43*, 13299–13306.
- (191) Chen, W.; Elfeky, S. A.; Nonne, Y.; Male, L.; Ahmed, K.; Amiable, C.; Axe, P.; Yamada, S.; James, T. D.; Bull, S. D.; Fossey, J. S. A Pyridinium Cation-π Interaction Sensor for the Fluorescent Detection of Alkyl Halides. *Chem. Commun.* **2011**, *47*, 253–255.

- (192) Okamoto, M.; Teranishi, H. Effect of Pressure on the External Heavy Atom Quenching of Pyrene Fluorescence in Fluid Solution. *J. Phys. Chem.* **1984**, *88*, 5644–5646.
- (193) Curiel, D.; Cowley, A.; Beer, P. D. Indolocarbazoles: A New Family of Anion Sensors. *Chem. Commun.* **2005**, 236–238.
- (194) Hiscock, J. R.; Caltagirone, C.; Light, M. E.; Hursthouse, M. B.; Gale, P. A. Fluorescent Carbazolylurea Anion Receptors. *Org. Biomol. Chem.* **2009**, *7*, 1781–1783.
- (195) Miao, R.; Zheng, Q. Y.; Chen, C. F.; Huang, Z. T. A Novel Calix[4]arene Fluorescent Receptor for Selective Recognition of Acetate Anion. *Tetrahedron Lett.* **2005**, *46*, 2155–2158.
- (196) Costero, A. M.; Colera, M.; Gavina, P.; Gil, S. Fluorescent Sensing of Maleate Versus Fumarate by a Neutral Cyclohexane Based Thiourea Receptor. *Chem. Commun.* **2006**, 761–763.
- (197) Stepinski, J.; Pawlowska, D.; Angielski, S. Effect of Lithium on Renal Gluconeogenesis. *Acta Biochim. Polym.* **1984**, *31*, 229–240.
- (198) Liu, S. Y.; Law, K. Y.; He, Y. B.; Chan, W. H. Fluorescent Enantioselective Receptor for S-Mandelate Anion Based on Cholic Acid. *Tetrahedron Lett.* **2006**, *47*, 7857–7860.
- (199) Liu, S. Y.; He, Y. B.; Chan, W. H.; Lee, A. W. M. Cholic Acid-Based High Sensitivity Fluorescent Sensor for α,ω -Dicarboxylate: An Intramolecular Excimer Emission Quenched by Complexation. *Tetrahedron* **2006**, *62*, 11687–11696.
- (200) Xu, K. X.; He, Y. B.; Qin, H. J.; Qing, G. Y.; Liu, S. Y. Enantioselective Recognition by Optically Active Chiral Fluorescence Sensors Bearing Amino Acid Units. *Tetrahedron: Asymmetry* **2005**, *16*, 3042–3048.
- (201) Bencini, A.; Coluccini, C.; Garau, A.; Giorgi, C.; Lippolis, V.; Messori, L.; Pasini, D.; Puccioni, S. A Binol-Based Chiral Polyammonium Receptor for Highly Enantioselective Recognition and Fluorescence Sensing of (S,S)-Tartaric Acid in Aqueous Solution. *Chem. Commun.* **2012**, *48*, 10428–10430.
- (202) Descalzo, A. B.; Rurack, K.; Weisshoff, H.; Martínez-Máñez, R.; Marcos, M. D.; Amorós, P.; Hoffmann, K.; Soto, J. Rational Design of a Chromo- and Fluorogenic Hybrid Chemosensor Material for the Detection of Long-Chain Carboxylates. *J. Am. Chem. Soc.* **2005**, *127*, 184–200.
- (203) Mishra, A.; Vajpayee, V.; Kim, H.; Lee, M. H.; Jung, H.; Wang, M.; Stang, P. J.; Chi, K. W. Self-Assembled Metalla-Bowls for Selective Sensing of Multi-Carboxylate Anions. *Dalton Trans.* **2012**, *41*, 1195–1201.
- (204) Ballistreri, F. P.; Pappalardo, A.; Tomaselli, G. A.; Toscano, R. M.; Trusso Sfrazzetto, G. Heteroditopic Chiral Uranyl-Salen Receptor for Molecular Recognition of Amino Acid Ammonium Salts. *Eur. J. Org. Chem.* **2010**, 3806–3810.
- (205) Niu, L. Y.; Guan, Y. S.; Chen, Y. Z.; Wu, L. Z.; Tung, C. H.; Yang, Q. Z. A Turn-on Fluorescent Sensor for the Discrimination of Cystein from Homocysteine and Glutathione. *Chem. Commun.* **2013**, *49*, 1294–1296.
- (206) Qin, H.; He, Y.; Qing, G.; Hu, C.; Yang, X. Novel Chiral Fluorescent Macroyclic Receptors: Synthesis and Recognition for Amino Acid Anions. *Tetrahedron: Asymmetry* **2006**, *17*, 2143–2148.
- (207) Qing, G. Y.; He, Y. B.; Zhao, Y.; Hu, C. G.; Liu, S. Y.; Yang, X. Calix[4]arene-Based Chromogenic Chemosensor for the α -Phenylglycine Anion: Synthesis and Chiral Recognition. *Eur. J. Org. Chem.* **2006**, 1574–1580.
- (208) Lin, Z.; Wu, M.; Schäferling, M.; Wolfbeis, O. S. Fluorescent Imaging of Citrate and Other Intermediates in the Citric Acid Cycle. *Angew. Chem., Int. Ed.* **2004**, *43*, 1735–1738.
- (209) Pal, R.; Parker, D.; Costello, L. C. A Europium Luminescence Assay of Lactate and Citrate in Biological Fluids. *Org. Biomol. Chem.* **2009**, *7*, 1525–1528.
- (210) Singh, A. S.; Sun, S. S. Recognition, Encapsulation, and Selective Fluorescence Sensing of Nitrate Anion by Neutral C₃-Symmetric Tripodal Podands Bearing Amide Functionality. *J. Org. Chem.* **2012**, *77*, 1880–1890.
- (211) Sasakura, K.; Hanaoka, K.; Shibuya, N.; Mikami, Y.; Kimura, Y.; Komatsu, T.; Ueno, T.; Terai, T.; Kimura, H.; Nagano, T. Development of a Highly Selective Fluorescence Probe for Hydrogen Sulfide. *J. Am. Chem. Soc.* **2011**, *133*, 18003–18005.
- (212) Wang, M. Q.; Li, K.; Hou, J. T.; Wu, M. Y.; Huang, Z.; Yu, X. Q. Binol-Based Fluorescent Sensor for Recognition of Cu(II) and Sulfide Anion in Water. *J. Org. Chem.* **2012**, *77*, 8350–8354.
- (213) Liu, C.; Pan, J.; Li, S.; Zhao, Y.; Wu, L. Y.; Berkman, C. E.; Whorton, A. R.; Xian, M. Capture and Visualization of Hydrogen Sulfide by a Fluorescent Probe. *Angew. Chem., Int. Ed.* **2011**, *50*, 10327–10329.
- (214) Manjare, S. T.; Kim, J.; Lee, Y.; Churchill, D. G. Facile meso-Bodipy Annulation and Selective Sensing of Hypochlorite in Water. *Org. Lett.* **2014**, *16*, 520–523.
- (215) Suzuki, I.; Ui, M.; Yamauchi, A. Supramolecular Probe for Bicarbonate Exhibiting Anomalous Pyrene Fluorescence in Aqueous Media. *J. Am. Chem. Soc.* **2006**, *128*, 4498–4499.
- (216) Niu, L. Y.; Guan, Y. S.; Chen, Y. Z.; Wu, L. Z.; Tung, C. H.; Yang, Q. Z. Bodipy-Based Ratiometric Fluorescent Sensor for Highly Selective Detection of Glutathione over Cysteine and Homocysteine. *J. Am. Chem. Soc.* **2012**, *134*, 18928–18931.
- (217) Reyheller, C.; Kubik, S. Selective Sensing of Sulfate in Aqueous Solution Using a Fluorescent Bis(Cyclopeptide). *Org. Lett.* **2007**, *9*, 5271–5274.
- (218) Bromfield, S. M.; Barnard, A.; Posocco, P.; Fermeglia, M.; Prich, S.; Smith, D. K. Mallard Blue: A High-Affinity Selective Heparin Sensor That Operates in Highly Competitive Media. *J. Am. Chem. Soc.* **2013**, *135*, 2911–2914.
- (219) Pu, K. Y.; Liu, B. Conjugated Polyelectrolytes as Light-up Macromolecular Probes for Heparin Sensing. *Adv. Funct. Mater.* **2009**, *19*, 277–284.
- (220) Shi, H.; Sun, H.; Yang, H.; Liu, S.; Jenkins, G.; Feng, W.; Li, F.; Zhao, Q.; Liu, B.; Huang, W. Cationic Polyfluorenes with Phosphorescent Iridium(III) Complexes for Time-Resolved Luminescent Biosensing and Fluorescence Lifetime Imaging. *Adv. Funct. Mater.* **2013**, *23*, 3268–3276.
- (221) Shi, H.; Xiujie, C.; Liu, S.; Xu, H.; An, Z.; Ouyang, L.; Tu, Z.; Zhao, Q.; Fan, Q.; Wang, L.; Huang, W. Hyper-Branched Phosphorescent Conjugated Polyelectrolytes for Time-Resolved Heparin Sensing. *ACS Appl. Mater. Interfaces* **2013**, *5*, 4562–4568.
- (222) Bromfield, S. M.; Wilde, E.; Smith, D. K. Heparin Sensing and Binding-Taking Supramolecular Chemistry Towards Clinical Applications. *Chem. Soc. Rev.* **2013**, *42*, 9184–9195.
- (223) Wiskur, S. L.; Ait-Haddou, H.; Lavigne, J. J.; Anslyn, E. V. Teaching Old Indicators New Tricks. *Acc. Chem. Res.* **2001**, *34*, 963–972.
- (224) Metzger, A.; Anslyn, E. V. A Chemosensor for Citrate in Beverages. *Angew. Chem., Int. Ed.* **1998**, *37*, 649–652.
- (225) Zhang, T.; Anslyn, E. V. A Colorimetric Boronic Acid Based Sensing Ensemble for Carboxy and Phospho Sugars. *Org. Lett.* **2006**, *8*, 1649–1652.
- (226) Piña, M. N.; Soberats, B.; Rotger, C.; Ballester, P.; Deyà, P. M.; Costa, A. Selective Sensing of Competitive Anions by Non-Selective Hosts: The Case of Sulfate and Phosphate in Water. *New J. Chem.* **2008**, *32*, 1919–1923.
- (227) Sokkaligam, P.; Kim, D. S.; Hwang, H.; Sessler, J. L.; Lee, C. H. A Dicationic Calix[4]pyrrole Derivative and Its Use for the Selective Recognition and Displacement-Based Sensing of Pyrophosphate. *Chem. Sci.* **2012**, *3*, 1819–1824.
- (228) Yuen, K. K. Y.; Jolliffe, K. A. Bis[Zinc(II)Dipicolylamino]-Functionalised Peptides as High Affinity Receptors for Pyrophosphate Ions in Water. *Chem. Commun.* **2013**, *49*, 4824–4826.
- (229) Mateus, P.; Delgado, R.; Brandão, P.; Carvalho, S.; Félix, V. Selective Recognition of Tetrahedral Dianions by a Hexaaza Cryptand Receptor. *Org. Biomol. Chem.* **2009**, *7*, 4661–4673.
- (230) Jose, D. A.; Elstner, M.; Schiller, A. Allosteric Indicator Displacement Enzyme Assay for a Cyanogenic Glycoside. *Chem.—Eur. J.* **2013**, *19*, 14451–14457.
- (231) Minami, T.; Liu, Y.; Akdeniz, A.; Koutnik, P.; Esipenko, N. A.; Nishiyabu, R.; Kubo, Y.; Anzenbacher, P. Intramolecular Indicator Displacement Assay for Anions: Supramolecular Sensor for Glycophosphate. *J. Am. Chem. Soc.* **2014**, *136*, 11396–11401.

- (232) Calero, P.; Hecht, M.; Martínez-Máñez, R.; Sancenón, F.; Soto, J.; Vivancos, J. L.; Rurack, K. Silica Nanoparticles Functionalised with Cation Coordination Sites and Fluorophores for the Differential Sensing of Anions in a Quencher Displacement Assay (QDA). *Chem. Commun.* **2011**, *47*, 10599–10601.
- (233) Leonard, J. P.; dos Santos, C. M. G.; Plush, S. E.; McCabe, T.; Gunnlaugsson, T. pH Driven Self-Assembly of a Ternary Lanthanide Luminescence Complex: the Sensing of Anions Using a β -Diketonate-Eu(III) Displacement Assay. *Chem. Commun.* **2007**, *129*–131.
- (234) Lavigne, J. J.; Anslyn, E. V. Sensing a Paradigm Shift in the Field of Molecular Recognition: From Selective to Differential Receptors. *Angew. Chem., Int. Ed.* **2001**, *40*, 3119–3130.
- (235) Umali, A. P.; Anslyn, E. V. A General Approach to Differential Sensing Using Synthetic Molecular Receptors. *Curr. Opin. Chem. Biol.* **2010**, *14*, 685–692.
- (236) Diehl, K. L.; Anslyn, E. V. Array Sensing Using Optical Methods for Detection of Chemical and Biological Hazards. *Chem. Soc. Rev.* **2013**, *42*, 8596–8611.
- (237) Stewart, S.; Ivy, M. A.; Anslyn, E. V. The Use of Principal Component Analysis and Discriminant Analysis in Differential Sensing Routines. *Chem. Soc. Rev.* **2014**, *43*, 70–84.
- (238) Zamora-Olivares, D.; Kaoud, T. S.; Dalby, K. N.; Anslyn, E. V. In-Situ Generation of Differential Sensors That Fingerprint Kinases and the Cellular Response to Their Expression. *J. Am. Chem. Soc.* **2013**, *135*, 14814–14820.
- (239) Ivy, M. A.; Gallagher, L. T.; Ellington, A. D.; Anslyn, E. V. Exploration of Plasticizer and Plastic Explosive Detection and Differentiation with Serum Albumin Cross-Reactive Arrays. *Chem. Sci.* **2012**, *3*, 1773–1779.
- (240) Palacios, M. A.; Nishiyabu, R.; Marquez, M.; Anzenbacher, P., Jr. Supramolecular Chemistry Approach to the Design of a High-Resolution Sensor Array for Multianion Detection in Water. *J. Am. Chem. Soc.* **2007**, *129*, 7538–7544.
- (241) Zyryanov, G. V.; Palacios, M. A.; Anzenbacher, P., Jr. Rational Design of a Fluorescence-Turn-on Sensor Array for Phosphates in Blood Serum. *Angew. Chem., Int. Ed.* **2007**, *46*, 7849–7852.
- (242) Esipenko, N. A.; Koutnik, P.; Minami, T.; Mosca, L.; Lynch, V. M.; Zyryanov, G. V.; Anzenbacher, P., Jr. First Supramolecular Sensors for Phosphonate Anions. *Chem. Sci.* **2013**, *4*, 3617–3623.
- (243) Cametti, M.; Nissinen, M.; Cort, A. D.; Mandolini, L.; Rissanen, K. Uranyl-Salophen Based Ditopic Receptors for the Recognition of Quaternary Ammonium Halides. *Chem. Commun.* **2003**, 2420–2421.
- (244) Cametti, M.; Cort, A. D.; Bartik, K. Fluoride Binding in Water: A New Environment for a Known Receptor. *ChemPhysChem* **2008**, *9*, 2168–2171.
- (245) Ábalos, T.; Royo, S.; Martínez-Máñez, R.; Sancenón, F.; Soto, J.; Costero, A. M.; Gil, S.; Parra, M. Surfactant-Assisted Chromogenic Sensing of Cyanide in Water. *New J. Chem.* **2009**, *33*, 1641–1645.
- (246) Amilan Jose, D.; Stadibauer, S.; König, B. Polydiacetylene-Based Colorimetric Self-Assembled Vesicular Receptors for Biological Phosphate Ion Recognition. *Chem.—Eur. J.* **2009**, *15*, 7404–7412.
- (247) Banerjee, S.; Bhuyan, M.; König, B. Tb(III) Functionalized Vesicles for Phosphate Sensing: Membrane Fluidity Controls the Sensitivity. *Chem. Commun.* **2013**, *49*, 5681–5683.
- (248) Caballero, A.; Zapata, F.; Beer, P. D. Interlocked Host Molecules for Anion Recognition and Sensing. *Coord. Chem. Rev.* **2013**, *257*, 2434–2455.
- (249) Langton, M. J.; Beer, P. D. Rotaxane and Catenane Host Structures for Sensing Charged Guest Species. *Acc. Chem. Res.* **2014**, *47*, 1935–1949.
- (250) Langton, M. J.; Beer, P. D. Sulfate-Selective Binding and Sensing of a Fluorescent [3]Rotaxane Host System. *Chem.—Eur. J.* **2012**, *18*, 14406–14412.
- (251) Caballero, A.; Zapata, F.; White, N. G.; Costa, P. J.; Félix, V.; Beer, P. D. A Halogen-Bonding Catenane for Anion Recognition and Sensing. *Angew. Chem., Int. Ed.* **2012**, *51*, 1876–1880.
- (252) Gassensmith, J. J.; Barr, L.; Baumes, J. M.; Paek, A.; Nguyen, A.; Smith, B. D. Synthesis and Photophysical Investigation of Squaraine Rotaxanes by “Clicked Capping”. *Org. Lett.* **2008**, *10*, 3343–3346.
- (253) Collins, C. G.; Peck, E. M.; Kramer, P. J.; Smith, B. D. Squaraine Rotaxane Shuttle as a Ratiometric Deep-Red Optical Chloride Sensor. *Chem. Sci.* **2013**, *4*, 2557–2563.
- (254) Massue, J.; Quinn, S. J.; Gunnlaugsson, T. Lanthanide Luminescent Displacement Assays: The Sensing of Phosphate Anions Using Eu(III)-Cyclen-Conjugated Gold Nanoparticles in Aqueous Solution. *J. Am. Chem. Soc.* **2008**, *130*, 6900–6901.
- (255) Shang, L.; Jin, L.; Dong, S. Sensitive Turn-on Fluorescent Detection of Cyanide Based on the Dissolution of Fluorophore Functionalized Gold Nanoparticles. *Chem. Commun.* **2009**, 3077–3079.
- (256) Tian, D.; Qian, Z.; Xia, Y.; Zhu, C. Gold Nanocluster-Based Fluorescent Probes for near-Infrared and Turn-on Sensing of Glutathione in Living Cells. *Langmuir* **2012**, *28*, 3945–3951.
- (257) Hu, X.; Huang, J.; Zhang, W.; Li, M.; Tao, C.; Li, G. Photonic Ionic Liquids Polymer for Naked-Eye Detection of Anions. *Adv. Mater.* **2008**, *20*, 4074–4078.
- (258) Gui, R.; Jin, H.; Liu, X.; Wang, Z.; Zhang, F.; Xia, J.; Yang, M.; Bi, S. Upconversion Luminescent Logic Gates and Turn-on Sensing of Glutathione Based on Two-Photon Excited Quantum Dots Conjugated with Dopamine. *Chem. Commun.* **2014**, *50*, 14847–14850.
- (259) Shang, L.; Zhang, L.; Dong, S. Turn-on Fluorescent Cyanide Sensor Based on Copper Ion-Modified CdTe Quantum Dots. *Analyst* **2009**, *134*, 107–113.
- (260) Zhang, M.; Ye, B. C. A Reversible Fluorescent DNA Logic Gate Based on Graphene Oxide and Its Application for Iodide Sensing. *Chem. Commun.* **2012**, *48*, 3647–3649.
- (261) Kumar, A.; Chhatra, R. K.; Pandey, P. S. Synthesis of Click Bile Acid Polymers and Their Application in Stabilization of Silver Nanoparticles Showing Iodide Sensing Property. *Org. Lett.* **2010**, *12*, 24–27.
- (262) Kresge, C. T.; Leonowicz, M. E.; Roth, W. J.; Vartuli, J. C.; Beck, J. S. Ordered Mesoporous Molecular Sieves Synthesized by a Liquid-Crystal Template Mechanism. *Nature* **1992**, *359*, 710–712.
- (263) Comes, M.; Aznar, E.; Moragues, M.; Marcos, M. D.; Martínez-Máñez, R.; Sancenón, F.; Soto, J.; Villaescusa, L. A.; Gil, L.; Amorós, P. Mesoporous Hybrid Materials Containing Nanoscopic “Binding Pockets” for Colorimetric Anion Signaling in Water by Using Displacement Assays. *Chem.—Eur. J.* **2009**, *15*, 9024–9033.
- (264) Delgado-Pinar, E.; Rotger, C.; Costa, A.; Piña, M. N.; Jiménez, H. R.; Alarcón, J.; García-España, E. Grafted Squaramide Monoamine Nanoparticles as Simple Systems for Sulfate Recognition in Pure Water. *Chem. Commun.* **2012**, *48*, 2609–2611.
- (265) Sun, H.; Scharff-Poulsen, A. M.; Gu, H.; Jakobsen, I.; Kossmann, J. M.; Frommer, W. B.; Almdal, K. Phosphate Sensing by Fluorescent Reporter Proteins Embedded in Polyacrylamide Nanoparticles. *ACS Nano* **2008**, *2*, 19–24.
- (266) Beer, P. D.; Gale, P. A.; Chen, G. Z. Mechanisms of Electrochemical Recognition of Cations, Anions and Neutral Guest Species by Redox-Active Receptor Molecules. *Coord. Chem. Rev.* **1999**, *185*–186, 3–36.
- (267) Evans, N. H.; Beer, P. D. A Ferrocene Functionalized Rotaxane Host System Capable of the Electrochemical Recognition of Chloride. *Org. Biomol. Chem.* **2011**, *9*, 92–100.
- (268) Evans, N. H.; Serpell, C. J.; Beer, P. D. A Redox-Active [3]Rotaxane Capable of Binding and Electrochemically Sensing Chloride and Sulfate Anions. *Chem. Commun.* **2011**, *47*, 8775–8777.
- (269) Evans, N. H.; Serpell, C. J.; White, N. G.; Beer, P. D. A 1,2,3,4,5-Pentaphenylferrocene-Stoppered Rotaxane Capable of Electrochemical Anion Recognition. *Chem.—Eur. J.* **2011**, *17*, 12347–12354.
- (270) Lim, J. Y. C.; Cunningham, M. J.; Davis, J. J.; Beer, P. D. Neutral Redox-Active Hydrogen- and Halogen-Bonding [2]Rotaxanes for the Electrochemical Sensing of Chloride. *Dalton Trans.* **2014**, *43*, 17274–17282.
- (271) Caballero, A.; White, N. G.; Beer, P. D. A Ferrocene Imidazolium-Based Macrocycle as an Electrochemical Chemosensor for Halide Anions. *CrystEngComm* **2014**, *16*, 3694–3698.
- (272) Willener, Y.; Joly, K. M.; Moody, C. J.; Tucker, J. H. R. An Exploration of Ferrocenyl Ureas as Enantioselective Electrochemical

- Sensors for Chiral Carboxylate Anions. *J. Org. Chem.* **2008**, *73*, 1225–1233.
- (273) Clare, J. P.; Statnikov, A.; Lynch, V.; Sargent, A. L.; Sibert, J. W. “Wurster-Type” Ureas as Redox-Active Receptors for Anions. *J. Org. Chem.* **2009**, *74*, 6637–6646.
- (274) Cao, Q. Y.; Pradhan, T.; Kim, S.; Kim, J. S. Ferrocene-Appended Aryl Triazole for Electrochemical Recognition of Phosphate Ions. *Org. Lett.* **2011**, *13*, 4386–4389.
- (275) Lotfi Zadeh Zhad, H. R.; Lai, R. Y. A Hg(II)-Mediated “Signal-on” Electrochemical Glutathione Sensor. *Chem. Commun.* **2014**, *50*, 8385–8387.
- (276) Bakker, E.; Qin, Y. Electrochemical Sensors. *Anal. Chem.* **2006**, *78*, 3965–3983.
- (277) Antonisse, M. M. G.; Snellink-Ruel, B. H. M.; Ion, A. C. C.; Engbersen, J. F. J.; Reinhoudt, D. N. Synthesis of Novel Uranyl Salophene Derivatives and Evaluation as Sensing Molecules in Chemically Modified Field Effect Transistors (Chemfets). *J. Chem. Soc., Perkin Trans. 2* **1999**, 1211–1218.
- (278) *Anion Coordination Chemistry*; Wiley-VCH: Weinheim, 2011.
- (279) Kimmel, D. W.; LeBlanc, G.; Meschievitz, M. E.; Cliffel, D. E. Electrochemical Sensors and Biosensors. *Anal. Chem.* **2011**, *84*, 685–707.
- (280) Górski, L.; Saniewska, A.; Parzuchowski, P.; Meyerhoff, M. E.; Malinowska, E. Zirconium(IV)-Salophens as Fluoride-Selective Ionophores in Polymeric Membrane Electrodes. *Anal. Chim. Acta* **2005**, *551*, 37–44.
- (281) Górski, T.; Matusevich, A.; Parzuchowski, P.; Łuciuk, I.; Malinowska, E. Fluoride-Selective Polymeric Membrane Electrodes Based on Zr(IV)- and Al(III)-Salen Ionophores of Various Structures. *Anal. Chim. Acta* **2010**, *665*, 39–46.
- (282) Hattori, H.; Hoshino, M.; Wakii, T.; Yuchi, A. Effects of Two-Phase Reactions on Composition and Potential Response of Zirconium(IV)-Tetraphenylporphyrin Complexes as Carrier for Citrate-Selective Electrode. *Anal. Chem.* **2004**, *76*, 5056–5062.
- (283) Qin, Y.; Bakker, E. Elimination of Dimer Formation in Iniiiporphyrin-Based Anion-Selective Membranes by Covalent Attachment of the Ionophore. *Anal. Chem.* **2004**, *76*, 4379–4386.
- (284) Le Goff, T.; Braven, J.; Ebdon, L.; Scholefield, D. Phosphate-Selective Electrodes Containing Immobilised Ionophores. *Anal. Chim. Acta* **2004**, *510*, 175–182.
- (285) Ortúñ, J. A.; Expósito, R.; Sánchez-Pedreño, C.; Albero, M. I.; Espinosa, A. A Nitrate-Selective Electrode Based on a Tris(2-Aminoethyl)Amine Triamide Derivative Receptor. *Anal. Chim. Acta* **2004**, *525*, 231–237.
- (286) Schazmann, B.; Diamond, D. Improved Nitrate Sensing Using Ion Selective Electrodes Based on Urea-Calixarene Ionophores. *New J. Chem.* **2007**, *31*, 587–592.
- (287) Cuartero, M.; Más-Montoya, M.; Soledad García, M.; Curiel, D.; Ortúñ, J. A. New Carbazolo[1,2-a]Carbazole Derivative as Ionophore for Anion-Selective Electrodes: Remarkable Recognition Towards Dicarboxylate Anions. *Talanta* **2014**, *123*, 200–206.
- (288) Steed, J. W. Anion-Tuned Supramolecular Gels: A Natural Evolution from Urea Supramolecular Chemistry. *Chem. Soc. Rev.* **2010**, *39*, 3686–3699.
- (289) Džolić, Z.; Cametti, M.; Dalla Cort, A.; Mandolini, L.; Žinić, M. Fluoride-Responsive Organogelator Based on Oxalamide-Derived Anthraquinone. *Chem. Commun.* **2007**, 3535–3537.
- (290) (a) Piepenbrock, M. O. M.; Lloyd, G. O.; Clarke, N.; Steed, J. W. Gelation Is Crucially Dependent on Functional Group Orientation and May Be Tuned by Anion Binding. *Chem. Commun.* **2008**, 2644–2646. (b) Valero, J.; Escuder, B.; Miravet, J. F.; de Mendoza, J. Anion-Responsive Diguanidinium-Based Chiral Organogelators. *Chem.—Eur. J.* **2012**, *18*, 13038–13047.
- (291) Lin, Q.; Zhu, X.; Fu, Y. P.; Zhang, Y. M.; Fang, R.; Yang, L. Z.; Wei, T. B. Rationally Designed Anion-Responsive-Organogels: Sensing F⁻ via Reversible Color Changes in Gel-Gel States with Specific Selectivity. *Soft Matter* **2014**, *10*, 5715–5723.
- (292) Kishimura, A.; Yamashita, T.; Aida, T. Phosphorescent Organogels via “Metallophilic” Interactions for Reversible RGB-Color Switching. *J. Am. Chem. Soc.* **2005**, *127*, 179–183.
- (293) Kim, H. J.; Lee, J. H.; Lee, M. Stimuli-Responsive Gels from Reversible Coordination Polymers. *Angew. Chem., Int. Ed.* **2005**, *44*, 5811–5814.
- (294) Shen, J. S.; Li, D. H.; Cai, Q. G.; Jiang, Y. B. Highly Selective Iodide-Responsive Gel-Sol State Transition in Supramolecular Hydrogels. *J. Mater. Chem.* **2009**, *19*, 6219–6224.
- (295) Piepenbrock, M. O. M.; Clarke, N.; Steed, J. W. Shear Induced Gelation in a Copper(II) Metallogel: New Aspects of Ion-Tunable Rheology and Gel-Reformation by External Chemical Stimuli. *Soft Matter* **2010**, *6*, 3441–3457.
- (296) Zapata, F.; Caballero, A.; Tárraga, A.; Molina, P. Ferrocene-Substituted Nitrogen-Rich Ring Systems as Multichannel Molecular Chemosensors for Anions in Aqueous Environment. *J. Org. Chem.* **2010**, *75*, 162–169.
- (297) Alfonso, M.; Espinosa, A.; Tárraga, A.; Molina, P. Multichannel HSO₄⁻ Recognition Promoted by a Bound Cation within a Ferrocene-Based Ion Pair Receptor. *Chem. Commun.* **2012**, *48*, 6848–6850.
- (298) Liu, J. W.; Yang, Y.; Chen, C. F.; Ma, J. T. Novel Anion-Tuning Supramolecular Gels with Dual-Channel Response: Reversible Sol-Gel Transition and Color Changes. *Langmuir* **2010**, *26*, 9040–9044.
- (299) Zhang, Y.; Jiang, S. Fluoride-Responsive Gelator and Colorimetric Sensor Based on Simple and Easy-to-Prepare Cyano-Substituted Amide. *Org. Biomol. Chem.* **2012**, *10*, 6973–6979.
- (300) Zhang, Y. M.; Lin, Q.; Wei, T. B.; Qin, X. P.; Li, Y. A Novel Smart Organogel Which Could Allow a Two Channel Anion Response by Proton Controlled Reversible Sol-Gel Transition and Color Changes. *Chem. Commun.* **2009**, 6074–6076.
- (301) Choi, K.; Hamilton, A. D. A Dual Channel Fluorescence Chemosensor for Anions Involving Intermolecular Excited State Proton Transfer. *Angew. Chem., Int. Ed.* **2001**, *40*, 3912–3915.
- (302) Liu, J.; Sun, Y. Q.; Huo, Y.; Zhang, H.; Wang, L.; Zhang, P.; Song, D.; Shi, Y.; Guo, W. Simultaneous Fluorescence Sensing of Cys and GSH from Different Emission Channels. *J. Am. Chem. Soc.* **2014**, *136*, 574–577.
- (303) Schindler, D. W. Eutrophication and Recovery in Experimental Lakes: Implications for Lake Management. *Science* **1974**, *184*, 897–899.
- (304) Wildung, R. E.; McFadden, K. M.; Garland, T. R. Technetium Sources and Behavior in the Environment. *J. Environ. Qual.* **1979**, *8*, 156–161.
- (305) Corradini, M.; Campbell, D.; Draye, M.; Drummond, C., III; Hayward, P.; Hobbs, L.; Lahoda, E.; Rogers, R.; Sternberg, B.; Zebroski, E. *Research Needs for High-Level Waste Stored in Tanks and Bins at US Department of Energy Sites*; National Academy Press: Washington, DC, 2001.
- (306) Wilson, A. M.; Bailey, P. J.; Tasker, P. A.; Turkington, J. R.; Grant, R. A.; Love, J. B. Solvent Extraction: The Coordination Chemistry Behind Extractive Metallurgy. *Chem. Soc. Rev.* **2014**, *43*, 123–134.
- (307) Hofmeister, F. Zur Lehre Von Der Wirkung Der Salze. *Arch. Exp. Pathol. Pharmakol.* **1888**, *24*, 247–260.
- (308) Kunz, W.; Henle, J.; Ninham, B. W. ‘Zur Lehre Von Der Wirkung Der Salze’ (About the Science of the Effect of Salts): Franz Hofmeister’s Historical Papers. *Curr. Opin. Colloid Interface Sci.* **2004**, *9*, 19–37.
- (309) *Ion Exchange and Solvent Extraction; Volume 21, Supramolecular Aspects of Solvent Extraction*. Moyer, B. A., Ed.; CRC Press: Boca Raton, 2013.
- (310) Wichmann, K.; Antonioli, B.; Söhnle, T.; Wenzel, M.; Gloe, K.; Gloe, K.; Price, J. R.; Lindoy, L. F.; Blake, A. J.; Schröder, M. Polyamine-Based Anion Receptors: Extraction and Structural Studies. *Coord. Chem. Rev.* **2006**, *250*, 2987–3003.
- (311) Teresa Albelda, M.; Frias, J. C.; García-España, E.; Schneider, H.-J. Supramolecular Complexation for Environmental Control. *Chem. Soc. Rev.* **2012**, *41*, 3859–3877.

- (312) Gloe, K.; Antonelli, B.; Gloe, K.; Lindoy, L. F. In *Encyclopedia of Supramolecular Chemistry*; Atwood, J. L., Steed, J. W., Wallace, K. J., Eds.; Taylor & Francis: 2007.
- (313) Gloe, K.; Stephan, H.; Grotjahn, M. Where Is the Anion Extraction Going? *Chem. Eng. Technol.* **2003**, *26*, 1107–1117.
- (314) Levitskaia, T. G.; Maya, L.; Van Berkem, G. J.; Moyer, B. A. Anion Partitioning and Ion-Pairing Behavior of Anions in the Extraction of Cesium Salts by 4,5''-Bis(*tert*-Octylbenzo)Dibenzo-24-Crown-8 in 1,2-Dichloroethane. *Inorg. Chem.* **2006**, *46*, 261–272.
- (315) Borman, C. J.; Bonnesen, P. V.; Moyer, B. A. Selectivity Control in Synergistic Liquid–Liquid Anion Exchange of Univalent Anions Via Structure-Specific Cooperativity between Quaternary Ammonium Cations and Anion Receptors. *Anal. Chem.* **2012**, *84*, 8214–8221.
- (316) Wintergerst, M. P.; Levitskaia, T. G.; Moyer, B. A.; Sessler, J. L.; Delmau, L. H. Calix[4]pyrrole: A New Ion-Pair Receptor as Demonstrated by Liquid–Liquid Extraction. *J. Am. Chem. Soc.* **2008**, *130*, 4129–4139.
- (317) Custelcean, R.; Delmau, L. H.; Moyer, B. A.; Sessler, J. L.; Cho, W.-S.; Gross, D.; Bates, G. W.; Brooks, S. J.; Light, M. E.; Gale, P. A. Calix[4]pyrrole: An Old yet New Ion-Pair Receptor. *Angew. Chem., Int. Ed.* **2005**, *44*, 2537–2542.
- (318) Kim, S. K.; Lynch, V. M.; Young, N. J.; Hay, B. P.; Lee, C.-H.; Kim, J. S.; Moyer, B. A.; Sessler, J. L. KF and CsF Recognition and Extraction by a Calix[4]crown-5 Strapped Calix[4]Pyrrole Multitopic Receptor. *J. Am. Chem. Soc.* **2012**, *134*, 20837–20843.
- (319) Aydogan, A.; Coady, D. J.; Lynch, V. M.; Akar, A.; Marquez, M.; Bielawski, C. W.; Sessler, J. L. Poly(Methyl Methacrylate)s with Pendant Calixpyrroles: Polymeric Extractants for Halide Anion Salts. *Chem. Commun.* **2008**, 1455–1457.
- (320) Aydogan, A.; Akar, A. Tri- and Pentacalix[4]pyrroles: Synthesis, Characterization and Their Use in the Extraction of Halide Salts. *Chem.—Eur. J.* **2012**, *18*, 1999–2005.
- (321) Aydogan, A.; Coady, D. J.; Kim, S. K.; Akar, A.; Bielawski, C. W.; Marquez, M.; Sessler, J. L. Poly(Methyl Methacrylate)s with Pendant Calixpyrroles and Crown Ethers: Polymeric Extractants for Potassium Halides. *Angew. Chem., Int. Ed.* **2008**, *120*, 9794–9798.
- (322) Sokkalingam, P.; Hong, S.-J.; Aydogan, A.; Sessler, J. L.; Lee, C.-H. Decoration of Gold Nanoparticles by a Double-Armed Calix[4]pyrrole: A Receptor-Decorated Nanoensemble for Anion Sensing and Extraction. *Chem.—Eur. J.* **2013**, *19*, 5860–5867.
- (323) McDonald, K. P.; Qiao, B.; Twum, E. B.; Lee, S.; Gamache, P. J.; Chen, C.-H.; Yi, Y.; Flood, A. H. Quantifying Chloride Binding and Salt Extraction with Poly(Methyl Methacrylate) Copolymers Bearing Aryl-Triazoles as Anion Receptor Side Chains. *Chem. Commun.* **2014**, *50*, 13285–13288.
- (324) Clare, J. P.; Ayling, A. J.; Joos, J.-B.; Sisson, A. L.; Magro, G.; Pérez-Payán, M. N.; Lambert, T. N.; Shukla, R.; Smith, B. D.; Davis, A. P. Substrate Discrimination by Cholapod Anion Receptors: Geometric Effects and the “Affinity–Selectivity Principle”. *J. Am. Chem. Soc.* **2005**, *127*, 10739–10746.
- (325) Sisson, A. L.; Clare, J. P.; Davis, A. P. Contra-Hofmeister Anion Extraction by Cyclosteroidal Receptors. *Chem. Commun.* **2005**, *5263–5265*.
- (326) (a) Galbraith, S. G.; Lindoy, L. F.; Tasker, P. A.; Plieger, P. G. Simple Procedures for Assessing and Exploiting the Selectivity of Anion Extraction and Transport. *Dalton Trans.* **2006**, 1134–1136. (b) Galbraith, S. G.; Wang, Q.; Li, L.; Blake, A. J.; Wilson, C.; Collinson, S. R.; Lindoy, L. F.; Plieger, P. G.; Schröder, M.; Tasker, P. A. Anion Selectivity in Zwitterionic Amide-Functionalised Metal Salt Extractants. *Chem.—Eur. J.* **2007**, *13*, 6091–6107.
- (327) Gattuso, G.; Pappalardo, A.; Parisi, M. F.; Pisagatti, I.; Crea, F.; Liantonio, R.; Metrangolo, P.; Navarrini, W.; Resnati, G.; Pilati, T.; Pappalardo, S. Dipyridinocalixcrown/diodoperfluorocarbon binary host systems for CsI: structural studies and fluorous phase extraction of caesium. *Tetrahedron* **2007**, *63*, 4951–4958.
- (328) Das, P.; Mandal, A. K.; Kesharwani, M. K.; Suresh, E.; Ganguly, B.; Das, A. Receptor Design and Extraction of Inorganic Fluoride Ion from Aqueous Medium. *Chem. Commun.* **2011**, *47*, 7398–7400.
- (329) Chiu, C.-W.; Gabbaï, F. P. Fluoride Ion Capture from Water with a Cationic Borane. *J. Am. Chem. Soc.* **2006**, *128*, 14248–14249.
- (330) Ravikumar, I.; Ghosh, P. Recognition and Separation of Sulfate Anions. *Chem. Soc. Rev.* **2012**, *41*, 3077–3098.
- (331) Moyer, B. A.; Custelcean, R.; Hay, B. P.; Sessler, J. L.; Bowman-James, K.; Day, V. W.; Kang, S.-O. A Case for Molecular Recognition in Nuclear Separations: Sulfate Separation from Nuclear Wastes. *Inorg. Chem.* **2012**, *52*, 3473–3490.
- (332) Ojovan, M. I.; Lee, W. E. *An Introduction to Nuclear Waste Immobilisation*, 2nd ed.; Elsevier: Oxford, 2013.
- (333) Eller, L. R.; Stępień, M.; Fowler, C. J.; Lee, J. T.; Sessler, J. L.; Moyer, B. A. Octamethyl-Octaundecyclo[8]pyrrole: A Promising Sulfate Anion Extractant. *J. Am. Chem. Soc.* **2007**, *129*, 11020–11021.
- (334) Fowler, C. J.; Haverlock, T. J.; Moyer, B. A.; Shriner, J. A.; Gross, D. E.; Marquez, M.; Sessler, J. L.; Hossain, M. A.; Bowman-James, K. Enhanced Anion Exchange for Selective Sulfate Extraction: Overcoming the Hofmeister Bias. *J. Am. Chem. Soc.* **2008**, *130*, 14386–14387.
- (335) Moyer, B. A.; Sloop, F. V.; Fowler, C. J.; Haverlock, T. J.; Kang, H.-A.; Delmau, L. H.; Bau, D. M.; Hossain, M. A.; Bowman-James, K.; Shriner, J. A.; Bill, N. L.; Gross, D. E.; Marquez, M.; Lynch, V. M.; Sessler, J. L. Enhanced Liquid–Liquid Anion Exchange Using Macroyclic Anion Receptors: Effect of Receptor Structure on Sulphate–Nitrate Exchange Selectivity. *Supramol. Chem.* **2010**, *22*, 653–671.
- (336) Borman, C. J.; Custelcean, R.; Hay, B. P.; Bill, N. L.; Sessler, J. L.; Moyer, B. A. Supramolecular Organization of Calix[4]pyrrole with a Methyl-Trialkylammonium Anion Exchanger Leads to Remarkable Reversal of Selectivity for Sulfate Extraction vs. Nitrate. *Chem. Commun.* **2011**, *47*, 7611–7613.
- (337) Kim, S. K.; Lee, J.; Williams, N. J.; Lynch, V. M.; Hay, B. P.; Moyer, B. A.; Sessler, J. L. Bipyrrole-Strapped Calix[4]Pyrroles: Strong Anion Receptors That Extract the Sulfate Anion. *J. Am. Chem. Soc.* **2014**, *136*, 15079–15085.
- (338) Jia, C.; Wu, B.; Li, S.; Huang, X.; Zhao, Q.; Li, Q.-S.; Yang, X.-J. Highly Efficient Extraction of Sulfate Ions with a Tripodal Hexaurea Receptor. *Angew. Chem., Int. Ed.* **2011**, *50*, 486–490.
- (339) Hay, B. P.; Firman, T. K.; Moyer, B. A. Structural Design Criteria for Anion Hosts: Strategies for Achieving Anion Shape Recognition through the Complementary Placement of Urea Donor Groups. *J. Am. Chem. Soc.* **2005**, *127*, 1810–1819.
- (340) Fernando, I. R.; Surmann, S. A.; Urech, A. A.; Poulsen, A. M.; Mezei, G. Selective Total Encapsulation of the Sulfate Anion by Neutral Nano-Jars. *Chem. Commun.* **2012**, *48*, 6860–6862.
- (341) Wenzel, M.; Knapp, Q. W.; Plieger, P. G. A Bis-Salicylaldoximato-Copper(II) Receptor for Selective Sulfate Uptake. *Chem. Commun.* **2011**, *47*, 499–501.
- (342) Wenzel, M.; Jameson, G. B.; Ferguson, L. A.; Knapp, Q. W.; Forgan, R. S.; White, F. J.; Parsons, S.; Tasker, P. A.; Plieger, P. G. Anion-Induced Contraction of Helical Receptors. *Chem. Commun.* **2009**, 3606–3608.
- (343) Bates, G. W.; Davidson, J. E.; Forgan, R. S.; Gale, P. A.; Henderson, D. K.; King, M. G.; Light, M. E.; Moore, S. J.; Tasker, P. A.; Tong, C. C. A Dual Host Approach to NiSO_4 Extraction. *Supramol. Chem.* **2011**, *24*, 117–126.
- (344) Wenzel, M.; Gloe, K.; Gloe, K.; Bernhard, G.; Clegg, J. K.; Ji, X.-K.; Lindoy, L. F. A New 34-Membered N_6O_4 -Donor Macrocycle: Synthetic, X-Ray and Solvent Extraction Studies. *New J. Chem.* **2008**, *32*, 132–137.
- (345) Cohen, M. D.; Kargacin, B.; Klein, C. B.; Costa, M. Mechanisms of Chromium Carcinogenicity and Toxicity. *Crit. Rev. Toxicol.* **1993**, *23*, 255–281.
- (346) Roundhill, D. M.; Koch, H. F. Methods and Techniques for the Selective Extraction and Recovery of Oxoanions. *Chem. Soc. Rev.* **2002**, *31*, 60–67.
- (347) Bozkurt, S.; Karakucuk, A.; Sirit, A.; Yilmaz, M. Synthesis of Two Calix[4]arene Diamide Derivatives for Extraction of Chromium(VI). *Tetrahedron* **2005**, *61*, 10443–10448.
- (348) Tabakci, M.; Memon, S.; Yilmaz, M. Synthesis and Extraction Properties of New ‘Proton-Switchable’ Tri- and Tetra-Substituted

- Calix[4]arene Derivatives Bearing Pyridinium Units. *Tetrahedron* **2007**, *63*, 6861–6865.
- (349) Yilmaz, A.; Tabakci, B.; Akceylan, E.; Yilmaz, M. Synthesis and Dichromate Anion Extraction Ability of *p*-*tert*-Butylcalix[4]arene Diamide Derivatives with Different Binding Sites. *Tetrahedron* **2007**, *63*, 5000–5005.
- (350) Bayrakci, M.; Ertul, S.; Sahin, O.; Yilmaz, M. Synthesis of Two New *p*-*tert*-Butylcalix[4]arene β -Ketoimin Derivatives for Extraction of Dichromate Anion. *J. Inclusion Phenom. Macrocyclic Chem.* **2009**, *63*, 241–247.
- (351) Ertul, S.; Bayrakci, M.; Yilmaz, M. Removal of Chromate and Phosphate Anion from Aqueous Solutions Using Calix[4]arene Receptors Containing Proton Switchable Units. *J. Hazard. Mater.* **2010**, *181*, 1059–1065.
- (352) Sap, A.; Tabakci, B.; Yilmaz, A. Calix[4]arene-Based Mannich and Schiff Bases as Versatile Receptors for Dichromate Anion Extraction: Synthesis and Comparative Studies. *Tetrahedron* **2012**, *68*, 8739–8745.
- (353) Jurisson, S. S.; Lydon, J. D. Potential Technetium Small Molecule Radiopharmaceuticals. *Chem. Rev.* **1999**, *99*, 2205–2218.
- (354) Volkert, W. A.; Hoffman, T. J. Therapeutic Radiopharmaceuticals. *Chem. Rev.* **1999**, *99*, 2269–2292.
- (355) Katayev, E. A.; Kolesnikov, G. V.; Sessler, J. L. Molecular Recognition of Pertechnetate and Perrhenate. *Chem. Soc. Rev.* **2009**, *38*, 1572–1586.
- (356) Alberto, R.; Bergamaschi, G.; Braband, H.; Fox, T.; Amendola, V. $^{99}\text{TcO}_4^-$: Selective Recognition and Trapping in Aqueous Solution. *Angew. Chem., Int. Ed.* **2012**, *51*, 9772–9776.
- (357) Amendola, V.; Alberti, G.; Bergamaschi, G.; Biesuz, R.; Boiocchi, M.; Ferrito, S.; Schmidtchen, F.-P. Cavity Effect on Perrhenate Recognition by Polyammonium Cages. *Eur. J. Inorg. Chem.* **2012**, *2012*, 3410–3417.
- (358) Kolesnikov, G. V.; German, K. E.; Kirakosyan, G.; Tananaev, I. G.; Ustyryuk, Y. A.; Khrustalev, V. N.; Katayev, E. A. Macroyclic Receptor for Pertechnetate and Perrhenate Anions. *Org. Biomol. Chem.* **2011**, *9*, 7358–7364.
- (359) Veverkova, L.; Zaruba, K.; Koukolova, J.; Kral, V. Oxoanion Binding: A Change of Selectivity for Porphyrin-Alkaloid Conjugates as a Result of Substitution Pattern. *New J. Chem.* **2010**, *34*, 117–122.
- (360) Ali, M. C.; Kawasaki, T.; Nogami, M.; Saeki, M.; Sasaki, Y.; Ikeda, Y. Selective Extraction of Perrehnate Anion in Nitric Acid Solution Using 2,2'-(Methylimino)Bis(N,N'-Diethylacetamide) as an Extractant. *Prog. Nuclear Energy* **2011**, *53*, 1005–1008.
- (361) Sasaki, Y.; Kitatsui, Y.; Kimura, T. Highly Selective Extraction of TCO_4^- , ReO_4^- , and MoO_4^{2-} by the New Ligand, 2,2'-(Methylimino)-Bis(N,N-Diethylacetamide) (Midoa). *Chem. Lett.* **2007**, *36*, 1394–1395.
- (362) Turkington, J. R.; Bailey, P. J.; Love, J. B.; Wilson, A. M.; Tasker, P. A. Exploiting Outer-Sphere Interactions to Enhance Metal Recovery by Solvent Extraction. *Chem. Commun.* **2013**, *49*, 1891–1899.
- (363) Bell, K. J.; Westra, A. N.; Warr, R. J.; Chartres, J.; Ellis, R.; Tong, C. C.; Blake, A. J.; Tasker, P. A.; Schröder, M. Outer-Sphere Coordination Chemistry: Selective Extraction and Transport of the $[\text{PtCl}_6]^{2-}$ Anion. *Angew. Chem., Int. Ed.* **2008**, *47*, 1745–1748.
- (364) Warr, R. J.; Westra, A. N.; Bell, K. J.; Chartres, J.; Ellis, R.; Tong, C.; Simmance, T. G.; Gadzhieva, A.; Blake, A. J.; Tasker, P. A.; Schröder, M. Selective Extraction and Transport of the $[\text{PtCl}_6]^{2-}$ Anion through Outer-Sphere Coordination Chemistry. *Chem.—Eur. J.* **2009**, *15*, 4836–4850.
- (365) Ellis, R. J.; Chartres, J.; Sole, K. C.; Simmance, T. G.; Tong, C. C.; White, F. J.; Schröder, M.; Tasker, P. A. Outer-Sphere Amidopyridyl Extractants for Zinc(II) and Cobalt(II) Chlorometallates. *Chem. Commun.* **2009**, 583–585.
- (366) Ellis, R. J.; Chartres, J.; Henderson, D. K.; Cabot, R.; Richardson, P. R.; White, F. J.; Schröder, M.; Turkington, J. R.; Tasker, P. A.; Sole, K. C. Design and Function of Pre-Organised Outer-Sphere Amidopyridyl Extractants for Zinc(II) and Cobalt(II) Chlorometallates: The Role of C–H Hydrogen Bonds. *Chem.—Eur. J.* **2012**, *18*, 7715–7728.
- (367) Turkington, J. R.; Cocalia, V.; Kendall, K.; Morrison, C. A.; Richardson, P.; Sassi, T.; Tasker, P. A.; Bailey, P. J.; Sole, K. C. Outer-Sphere Coordination Chemistry: Amido-Ammonium Ligands as Highly Selective Tetrachloridozinc(II)ate Extractants. *Inorg. Chem.* **2012**, *51*, 12805–12819.
- (368) Coxall, R. A.; Lindoy, L. F.; Miller, H. A.; Parkin, A.; Parsons, S.; Tasker, P. A.; White, D. J. Solvent Extraction of Metal Sulfates by Zwitterionic Forms of Ditopic Ligands. *Dalton Trans.* **2003**, 55–64.
- (369) Lin, T.; Gasperov, V.; Smith, K. J.; Tong, C. C.; Tasker, P. A. Double Loading of ZnCl_2 by Polytopic Ligands Which Co-Extract Zn^{2+} and Tetrachloridozincate. *Dalton Trans.* **2010**, *39*, 9760–9762.
- (370) Mahoney, J. M.; Beatty, A. M.; Smith, B. D. Selective Solid-Liquid Extraction of Lithium Halide Salts Using a Ditopic Macroyclic Receptor. *Inorg. Chem.* **2004**, *43*, 7617–7621.
- (371) Eckelmann, J.; Saggiomo, V.; Sonnichsen, F. D.; Luning, U. The First Supramolecular Ion Triplet Complex. *New J. Chem.* **2010**, *34*, 1247–1250.
- (372) Khlobystov, A. N.; Champness, N. R.; Roberts, C. J.; Tendler, S. J. B.; Thompson, C.; Schröder, M. Anion Exchange in Coordination Polymers: A Solid-State or a Solvent-Mediated Process? *CrystEngComm* **2002**, *4*, 426–431.
- (373) Thompson, C.; Champness, N. R.; Khlobystov, A. N.; Roberts, C. J.; Schröder, M.; Tendler, S. J. B.; Wilkinson, M. J. Using Microscopic Techniques to Reveal the Mechanism of Anion Exchange in Crystalline Co-ordination Polymers. *J. Microsc.* **2004**, *214*, 261–271.
- (374) Custelcean, R.; Moyer, B. A. Anion Separation with Metal-Organic Frameworks. *Eur. J. Inorg. Chem.* **2007**, *2007*, 1321–1340.
- (375) Fan, J.; Gan, L.; Kawaguchi, H.; Sun, W.-Y.; Yu, K.-B.; Tang, W.-X. Reversible Anion Exchanges between the Layered Organic-Inorganic Hybridized Architectures: Syntheses and Structures of Manganese(II) and Copper(II) Complexes Containing Novel Tripodal Ligands. *Chem.—Eur. J.* **2003**, *9*, 3965–3973.
- (376) Zhao, W.; Fan, J.; Okamura, T.-a.; Sun, W.-Y.; Ueyama, N. Syntheses, Crystal Structures and Anion-Exchange Properties of Copper(II) and Cadmium(II) Complexes Containing a Novel Tripodal Ligand. *New J. Chem.* **2004**, *28*, 1142–1150.
- (377) Wan, S.-Y.; Huang, Y.-T.; Li, Y.-Z.; Sun, W.-Y. Synthesis, Structure and Anion-Exchange Property of the First Example of Self-Penetrated Three-Dimensional Metal-Organic Framework with Flexible Three-Connecting Ligand and Nickel(II) Perchlorate. *Microporous Mesoporous Mater.* **2004**, *73*, 101–108.
- (378) Zhao, W.; Fan, J.; Song, Y.; Kawaguchi, H.; Okamura, T.-A.; Sun, W.-Y.; Ueyama, N. Syntheses, Crystal Structures and Properties of Novel Copper(II) Complexes Obtained by Reactions of Copper(II) Sulfate Pentahydrate with Tripodal Ligands. *Dalton Trans.* **2005**, 1509–1517.
- (379) Xu, G.-C.; Ding, Y.-J.; Huang, Y.-Q.; Liu, G.-X.; Sun, W.-Y. Structure Diversity and Anion Exchange Property of Zinc(II) Coordination Polymers with Flexible Tripodal Ligand 1,3,5-Tris-(Imidazol-1-ylmethyl)Benzene. *Microporous Mesoporous Mater.* **2008**, *113*, 511–522.
- (380) Xu, G.-C.; Ding, Y.-J.; Okamura, T.-a.; Huang, Y.-Q.; Liu, G.-X.; Sun, W.-Y.; Ueyama, N. Structure Diversity and Reversible Anion Exchange Properties of Cadmium(II) Complexes with 1,3,5-Tris-(Imidazol-1-ylmethyl)Benzene: Counteranion-Directed Flexible Ligand Conformational Variation. *CrystEngComm* **2008**, *10*, 1052–1062.
- (381) Xu, G.-C.; Hua, Q.; Okamura, T.-a.; Bai, Z.-S.; Ding, Y.-J.; Huang, Y.-Q.; Liu, G.-X.; Sun, W.-Y.; Ueyama, N. Cadmium(II) Coordination Polymers with Flexible Tetradentate Ligand 1,2,4,5-Tetrakis(Imidazol-1-ylmethyl)Benzene: Anion Effect and Reversible Anion Exchange Property. *CrystEngComm* **2009**, *11*, 261–270.
- (382) Fu, J.; Li, H.; Mu, Y.; Hou, H.; Fan, Y. Reversible Single Crystal to Single Crystal Transformation with Anion Exchange-Induced Weak Cu^{2+}I^- Interactions and Modification of the Structures and Properties of MOFs. *Chem. Commun.* **2011**, *47*, 5271–5273.
- (383) Hamilton, B. H.; Kelly, K. A.; Wagler, T. A.; Espe, M. P.; Ziegler, C. J. Lead Tetrakis(Imidazolyl)Borate Solids: Anion Exchange, Solvent Intercalation, and Self Assembly of an Organic Anion. *Inorg. Chem.* **2004**, *43*, 50–56.
- (384) Du, M.; Bu, X.-H.; Guo, Y.-M.; Liu, H.; Batten, S. R.; Ribas, J.; Mak, T. C. W. First Cu^{II} Diamondoid Net with 2-Fold Interpenetrating

- Frameworks. The Role of Anions in the Construction of the Supramolecular Arrays. *Inorg. Chem.* **2002**, *41*, 4904–4908.
- (385) Du, M.; Guo, Y.-M.; Chen, S.-T.; Bu, X.-H.; Batten, S. R.; Ribas, J.; Kitagawa, S. Preparation of Acentric Porous Coordination Frameworks from an Interpenetrated Diamondoid Array through Anion-Exchange Procedures: Crystal Structures and Properties. *Inorg. Chem.* **2004**, *43*, 1287–1293.
- (386) Du, M.; Zhao, X.-J.; Guo, J.-H.; Batten, S. R. Direction of Topological Isomers of Silver(I) Coordination Polymers Induced by Solvent, and Selective Anion-Exchange of a Class of PtS-Type Host Frameworks. *Chem. Commun.* **2005**, 4836–4838.
- (387) Chen, J.; Li, C.-P.; Shang, J.; Du, M. A 3-D Metal–Organic Framework of Cu^{II} Perchlorate and 2-(2-Pyridyl)-S-(4-Pyridyl)-1,3,4-Oxadiazole Showing the Exclusive Anion-Exchange Selectivity to Benzoate. *Inorg. Chem. Commun.* **2012**, *15*, 172–175.
- (388) Fei, H.; Paw U, L.; Rogow, D. L.; Bresler, M. R.; Abdollahian, Y. A.; Oliver, S. R. J. Synthesis, Characterization, and Catalytic Application of a Cationic Metal–Organic Framework: Ag₂(4,4'-Bi-py)₂(O₃SCH₂CH₂SO₃). *Chem. Mater.* **2010**, *22*, 2027–2032.
- (389) Fei, H.; Rogow, D. L.; Oliver, S. R. J. Reversible Anion Exchange and Catalytic Properties of Two Cationic Metal–Organic Frameworks Based on Cu(I) and Ag(I). *J. Am. Chem. Soc.* **2010**, *132*, 7202–7209.
- (390) Fei, H.; Bresler, M. R.; Oliver, S. R. J. A New Paradigm for Anion Trapping in High Capacity and Selectivity: Crystal-to-Crystal Transformation of Cationic Materials. *J. Am. Chem. Soc.* **2011**, *133*, 11110–11113.
- (391) Fei, H.; Han, C. S.; Robins, J. C.; Oliver, S. R. J. A Cationic Metal–Organic Solid Solution Based on Co(II) and Zn(II) for Chromate Trapping. *Chem. Mater.* **2013**, *25*, 647–652.
- (392) Wang, S.; Alekseev, E. V.; Diwu, J.; Casey, W. H.; Phillips, B. L.; Depmeier, W.; Albrecht-Schmitt, T. E. NdTb-1: A Supertetrahedral Cationic Framework That Removes TcO₄⁻ from Solution. *Angew. Chem., Int. Ed.* **2010**, *49*, 1057–1060.
- (393) Cao, R.; McCarthy, B. D.; Lippard, S. J. Immobilization, Trapping, and Anion Exchange of Perrhenate Ion Using Copper-Based Tripodal Complexes. *Inorg. Chem.* **2011**, *50*, 9499–9507.
- (394) Adarsh, N. N.; Gréard, A.; Dufourc, E. J.; Dastidar, P. Sequestering Hydrated Fluoride in a Three-Dimensional Non-Interpenetrated Octahedral Coordination Polymer Via a Single-Crystal-to-Single-Crystal Fashion. *Cryst. Growth Des.* **2012**, *12*, 3369–3373.
- (395) Sarkar, M.; Biradha, K. Interplay of Hydrogen Bonds in Assembling (4,4)-Coordination Networks: Transformations from Open to Interpenetrated Networks Via Anion Exchange. *Cryst. Growth Des.* **2006**, *6*, 1742–1745.
- (396) Ma, J.-P.; Yu, Y.; Dong, Y.-B. Fluorene-Based Cu(II)-MOF: A Visual Colorimetric Anion Sensor and Separator Based on an Anion-Exchange Approach. *Chem. Commun.* **2012**, *48*, 2946–2948.
- (397) Fang, C.; Liu, Q.-K.; Ma, J.-P.; Dong, Y.-B. Independent 1D Nanosized Metal–Organic Tube: Anion Exchange, Separation, and Anion-Responsive Luminescence. *Inorg. Chem.* **2012**, *51*, 3923–3925.
- (398) Hou, S.; Liu, Q.-K.; Ma, J.-P.; Dong, Y.-B. Cd(II)-Coordination Framework: Synthesis, Anion-Induced Structural Transformation, Anion-Responsive Luminescence, and Anion Separation. *Inorg. Chem.* **2013**, *52*, 3225–3235.
- (399) Shi, P.-F.; Zhao, B.; Xiong, G.; Hou, Y.-L.; Cheng, P. Fast Capture and Separation of, and Luminescent Probe for, Pollutant Chromate Using a Multi-Functional Cationic Heterometal-Organic Framework. *Chem. Commun.* **2012**, *48*, 8231–8233.
- (400) Yang, Q.-Y.; Li, K.; Luo, J.; Pan, M.; Su, C.-Y. A Simple Topological Identification Method for Highly (3,12)-Connected 3D MOFs Showing Anion Exchange and Luminescent Properties. *Chem. Commun.* **2011**, *47*, 4234–4236.
- (401) Zhao, X.; Bu, X.; Wu, T.; Zheng, S.-T.; Wang, L.; Feng, P. Selective Anion Exchange with Nanogated Isoreticular Positive Metal-Organic Frameworks. *Nat. Commun.* **2013**, *4*, 2344.
- (402) Yang, G.; Raptis, R. G. A Robust, Porous, Cationic Silver(I) 3,5-Diphenyl-1,2,4-Triazolate Framework with a Uninodal 4⁹.6⁶ Net. *Chem. Commun.* **2004**, 2058–2059.
- (403) Qiu, Y.; Liu, Z.; Li, Y.; Deng, H.; Zeng, R.; Zeller, M. Reversible Anion Exchange and Sensing in Large Porous Materials Built from 4,4'-Bipyridine via π···π and H-Bonding Interactions. *Inorg. Chem.* **2008**, *47*, 5122–5128.
- (404) Phuenphai, P.; Massera, C.; Reedijk, J.; Youngme, S.; Gamez, P. Anion Exchange in Coordination-Network Materials. *Eur. J. Inorg. Chem.* **2013**, *2013*, 4812–4822.
- (405) Ajaz, A.; Lama, P.; Bharadwaj, P. K. Two-Dimensional Coordination Polymer with a Non-Interpenetrated (4,4) Net Showing Anion Exchange and Structural Transformation in Single-Crystal-to-Single-Crystal Fashion. *Inorg. Chem.* **2010**, *49*, 5883–5889.
- (406) Tzeng, B.-C.; Chiu, T.-H.; Chen, B.-S.; Lee, G.-H. Novel Single-Crystal-to-Single-Crystal Anion Exchange and Self-Assembly of Luminescent d¹⁰ Metal (Cd^{II}, Zn^{II}, and Cu^{II}) Complexes Containing C₃-Symmetrical Ligands. *Chem.—Eur. J.* **2008**, *14*, 5237–5245.
- (407) Wei, W.; Yu, H.; Jiang, F.; Liu, B.; Ma, J.; Hong, M. Anion-Controlled Conformational Variation: Structural Modulation and Anion Exchange of Ag(I) Coordination Networks. *CrystEngComm* **2012**, *14*, 1693–1700.
- (408) Liu, J.-Y.; Wang, Q.; Zhang, L.-J.; Yuan, B.; Xu, Y.-Y.; Zhang, X.; Zhao, C.-Y.; Wang, D.; Yuan, Y.; Wang, Y.; Ding, B.; Zhao, X.-J.; Yue, M. M. Anion-Exchange and Anthracene-Encapsulation within Copper(II) and Manganese(II)-Triazole Metal–Organic Confined Space in a Single Crystal-to-Single Crystal Transformation Fashion. *Inorg. Chem.* **2014**, *53*, 5972–5985.
- (409) Halper, S. R.; Do, L.; Stork, J. R.; Cohen, S. M. Topological Control in Heterometallic Metal–Organic Frameworks by Anion Templating and Metallocligand Design. *J. Am. Chem. Soc.* **2006**, *128*, 15255–15268.
- (410) Ma, J.-x.; Huang, X.-f.; Song, Y.; Song, X.-q.; Liu, W.-s. From Metallocligand to Interpenetrating Channels: Synthesis, Characterization, and Properties of a 2p-3d-4f Heterometallic Coordination Polymer {[Na₅Cu₈Sm₄(NTA)₈(ClO₄)₈(H₂O)₂₂]·ClO₄·8H₂O}N. *Inorg. Chem.* **2009**, *48*, 6326–6328.
- (411) Michaelides, A.; Skoulika, S. Anion-Induced Formation of Lanthanide-Organic Chains from 3D Framework Solids. Anion Exchange in a Crystal-to-Crystal Manner. *Cryst. Growth Des.* **2009**, *9*, 2039–2042.
- (412) Wong, K. L.; Law, G. L.; Yang, Y. Y.; Wong, W. T. A Highly Porous Luminescent Terbium–Organic Framework for Reversible Anion Sensing. *Adv. Mater.* **2006**, *18*, 1051–1054.
- (413) Goulding, H. V.; Hulse, S. E.; Clegg, W.; Harrington, R. W.; Playford, H. Y.; Walton, R. I.; Fogg, A. M. Yb₃O(OH)₆Cl·2H₂O: An Anion-Exchangeable Hydroxide with a Cationic Inorganic Framework Structure. *J. Am. Chem. Soc.* **2010**, *132*, 13618–13620.
- (414) Oliver, S. R. J. Cationic Inorganic Materials for Anionic Pollutant Trapping and Catalysis. *Chem. Soc. Rev.* **2009**, *38*, 1868–1881.
- (415) Danil de Namor, A. F.; Shehab, M.; Khalife, R.; Abbas, I. Modified Calix[4]pyrrole Receptor: Solution Thermodynamics of Anion Complexation and a Preliminary Account on the Phosphate Extraction Ability of Its Oligomer. *J. Phys. Chem. B* **2007**, *111*, 12177–12184.
- (416) Danil de Namor, A. F.; Khalife, R. Calix[4]pyrrole Derivative: Recognition of Fluoride and Mercury Ions and Extracting Properties of the Receptor-Based New Material. *J. Phys. Chem. B* **2008**, *112*, 15766–15774.
- (417) Harland, C. E. *Ion Exchange: Theory and Practice*, 2nd ed.; Royal Society of Chemistry: Cambridge, 1994.
- (418) Kokufuta, E.; Sodeyama, T.; Takeda, S. Oxochloromolybdenum(V)Tetraphenylporphyrin Complex-Containing Polymer as a Phosphate Ion Exchanger. *Polym. Bull.* **1986**, *15*, 479–484.
- (419) Kibbey, C. E.; Meyerhoff, M. E. Preparation and Characterization of Covalently Bound Tetraphenylporphyrin-Silica Gel Stationary Phases for Reversed-Phase and Anion-Exchange Chromatography. *Anal. Chem.* **1993**, *65*, 2189–2196.
- (420) Sessler, J. L.; Gale, P. A.; Genge, J. W. Calix[4]pyrroles: New Solid-Phase HPLC Supports for the Separation of Anions. *Chem.—Eur. J.* **1998**, *4*, 1095–1099.

- (421) Kalędkowski, A.; Trochimczuk, A. W. Novel Chelating Resins Containing Calix[4]Pyrroles: Synthesis and Sorptive Properties. *React. Funct. Polym.* **2006**, *66*, 740–746.
- (422) Kalędkowski, A.; Trochimczuk, A. W. Performance of Chelating Resins Containing Calixpyrroles in Sorption of Anions. *Sep. Sci. Technol.* **2006**, *41*, 3431–3447.
- (423) Aydogan, A.; Akar, A. Siloxane-Functionalized Calix[4]pyrrole: Synthesis, Characterization and Modification of Silica-Based Solid Supports. *Tetrahedron Lett.* **2011**, *52*, 2790–2793.
- (424) Bozkurt, S.; Kocabas, E.; Durmaz, M.; Yilmaz, M.; Sirit, A. Synthesis and Dichromate Anion Sorption of Silica Gel-Immobilized Calix[4]arenes. *J. Hazard. Mater.* **2009**, *165*, 974–979.
- (425) Tabakci, M.; Ersoz, M.; Yilmaz, M. A Calix[4]arene-Containing Polysiloxane Resin for Removal of Heavy Metals and Dichromate Anion. *J. Macromol. Sci., Part A* **2006**, *43*, 57–69.
- (426) Qureshi, I.; Memon, S.; Yilmaz, M. Estimation of Chromium(VI) Sorption Efficiency of Novel Regenerable *p*-tert-Butylcalix[8]-Areneoctamide Impregnated Amberlite Resin. *J. Hazard. Mater.* **2009**, *164*, 675–682.
- (427) Karakucük, A.; Kocabas, E.; Sirit, A.; Memon, S.; Yilmaz, M.; Roundhill, D. M. Polymer Supported Calix[4]arene Schiff Bases: A Novel Chelating Resin for Hg^{2+} and Dichromate Anions. *J. Macromol. Sci., A* **2005**, *42*, 691–704.
- (428) Akceylan, E.; Yilmaz, M.; Bartsch, R. A. Immobilization of Cyclic Alkylamine Calix[4]Arene Derivatives on Merrifield Resin: Evaluation of Extraction Ability toward Dichromate. *J. Macromol. Sci., A* **2006**, *43*, 477–486.
- (429) Ozcan, F.; Ersoz, M.; Yilmaz, M. Preparation and Application of Calix[4]arene-Grafted Magnetite Nanoparticles for Removal of Dichromate Anions. *Mater. Sci. Eng.: C* **2009**, *29*, 2378–2383.
- (430) Sayin, S.; Ozcan, F.; Yilmaz, M. Synthesis and Evaluation of Chromate and Arsenate Anions Extraction Ability of a N-Methylglucamine Derivative of Calix[4]arene Immobilized onto Magnetic Nanoparticles. *J. Hazard. Mater.* **2010**, *178*, 312–319.
- (431) Wang, J.; Harrison, R. G.; Lamb, J. D. Anion Separation and Preconcentration with Cyclen and Cyclen-Resorcinarene Derivatives. *J. Chromatogr. Sci.* **2009**, *47*, 510–515.
- (432) Gardner, J. S.; Peterson, Q. P.; Walker, J. O.; Jensen, B. D.; Adhikary, B.; Harrison, R. G.; Lamb, J. D. Anion Transport through Polymer Inclusion Membranes Facilitated by Transition Metal Containing Carriers. *J. Membr. Sci.* **2006**, *277*, 165–176.
- (433) Mahoney, J. M.; Nawaratna, G. U.; Beatty, A. M.; Duggan, P. J.; Smith, B. D. Transport of Alkali Halides through a Liquid Organic Membrane Containing a Ditopic Salt-Binding Receptor. *Inorg. Chem.* **2004**, *43*, 5902–5907.
- (434) Custelcean, R. Ion Separation by Selective Crystallization of Organic Frameworks. *Curr. Opin. Solid State Mater. Sci.* **2009**, *13*, 68–75.
- (435) Custelcean, R. Anions in Crystal Engineering. *Chem. Soc. Rev.* **2010**, *39*, 3675–3685.
- (436) Custelcean, R. Urea-Functionalized Crystalline Capsules for Recognition and Separation of Tetrahedral Oxoanions. *Chem. Commun.* **2013**, *49*, 2173–2182.
- (437) Custelcean, R.; Gorbunova, M. G. A Metal–Organic Framework Functionalized with Free Carboxylic Acid Sites and Its Selective Binding of a $Cl(H_2O)_4^-$ Cluster. *J. Am. Chem. Soc.* **2005**, *127*, 16362–16363.
- (438) Custelcean, R.; Haverlock, T. J.; Moyer, B. A. Anion Separation by Selective Crystallization of Metal–Organic Frameworks. *Inorg. Chem.* **2006**, *45*, 6446–6452.
- (439) Custelcean, R.; Moyer, B. A.; Bryantsev, V. S.; Hay, B. P. Anion Coordination in Metal–Organic Frameworks Functionalized with Urea Hydrogen-Bonding Groups. *Cryst. Growth Des.* **2005**, *6*, 555–563.
- (440) Custelcean, R.; Jiang, D.-e.; Hay, B. P.; Luo, W.; Gu, B. Hydrogen-Bonded Helices for Anion Binding and Separation. *Cryst. Growth Des.* **2008**, *8*, 1909–1915.
- (441) Banerjee, S.; Adarsh, N. N.; Dastidar, P. Selective Separation of the Sulfate Anion by *in Situ* Crystallization of Cd^{II} Coordination Compounds Derived from Bis(Pyridyl) Ligands Equipped with a Urea/Amide Hydrogen-Bonding Backbone. *Eur. J. Inorg. Chem.* **2010**, *2010*, 3770–3779.
- (442) Banerjee, S.; Dastidar, P. Studying Fluorous Interactions in a Series of Coordination Compounds Derived from Mono-Pyridyl Ligands Equipped with Hydrogen Bonding Functionality: Exploiting Anion- π F Interaction in Separating ClO_4^- Anion from a Competing Mixture of Anions. *CrystEngComm* **2013**, *15*, 9415–9428.
- (443) Akhuli, B.; Ghosh, P. Selective Recognition of Sulphate in a Cu^{II} Assisted 1D Polymer of a Simple Pentafluorophenyl Substituted Pyridyl-Urea Via Second Sphere Coordination. *Dalton Trans.* **2013**, *42*, 5818–5825.
- (444) Akhuli, B.; Ghosh, T. K.; Ghosh, P. Effect of Coordinating (-CN) Vs. Non-Coordinating (-F) Substituents in 3-Pyridyl Urea Receptors toward Second Sphere Sulfate Recognition: Selective Crystallisation of $CuSO_4$ from Mixtures of Competing Anions/Cations. *CrystEngComm* **2013**, *15*, 9472–9482.
- (445) Wu, B.; Huang, X.; Xia, Y.; Yang, X.-J.; Janiak, C. Oxo-Anion Binding by Protonated (Dimethylphenyl)(Pyridyl)Ureas. *CrystEngComm* **2007**, *9*, 676–685.
- (446) Custelcean, R.; Sellin, V.; Moyer, B. A. Sulfate Separation by Selective Crystallization of a Urea-Functionalized Metal-Organic Framework. *Chem. Commun.* **2007**, *1541*–1543.
- (447) Adarsh, N. N.; Kumar, D. K.; Dastidar, P. Zn^{II} Metal-Organic Frameworks (MOFs) Derived from a Bis-Pyridyl-Bis-Urea Ligand: Effects of Crystallization Solvents on the Structures and Anion Binding Properties. *CrystEngComm* **2008**, *10*, 1565–1573.
- (448) Wu, B.; Liang, J.; Zhao, Y.; Li, M.; Li, S.; Liu, Y.; Zhang, Y.; Yang, X.-J. Sulfate Encapsulation in Three-Fold Interpenetrated Metal-Organic Frameworks with Bis(Pyridylurea) Ligands. *CrystEngComm* **2010**, *12*, 2129–2134.
- (449) Xia, Y.; Wu, B.; Liu, Y.; Yang, Z.; Huang, X.; He, L.; Yang, X.-J. A Flexible Bis(Pyridylcarbamate) Anion Receptor: Binding of Infinite Double-Stranded Phosphate, $[-\text{Sulfate}-(H_2O)_2]_n$, and Hydrogen-Bridged Helical Perchlorate Chain. *CrystEngComm* **2009**, *11*, 1849–1856.
- (450) Užarević, K.; Đilović, I.; Matković-Čalogović, D.; Šišak, D.; Cindrić, M. Anion-Directed Self-Assembly of Flexible Ligands into Anion-Specific and Highly Symmetrical Organic Solids. *Angew. Chem., Int. Ed.* **2008**, *47*, 7022–7025.
- (451) Adarsh, N. N.; Dastidar, P. A Borromean Weave Coordination Polymer Sustained by Urea–Sulfate Hydrogen Bonding and Its Selective Anion Separation Properties. *Cryst. Growth Des.* **2009**, *10*, 483–487.
- (452) Paul, M.; Adarsh, N. N.; Dastidar, P. Cu^{II} Coordination Polymers Capable of Gelation and Selective SO_4^{2-} Separation. *Cryst. Growth Des.* **2012**, *12*, 4135–4143.
- (453) Custelcean, R.; Remy, P.; Bonnesen, P. V.; Jiang, D.-e.; Moyer, B. A. Sulfate Recognition by Persistent Crystalline Capsules with Rigidified Hydrogen-Bonding Cavities. *Angew. Chem., Int. Ed.* **2008**, *47*, 1866–1870.
- (454) Custelcean, R.; Bock, A.; Moyer, B. A. Selectivity Principles in Anion Separation by Crystallization of Hydrogen-Bonding Capsules. *J. Am. Chem. Soc.* **2010**, *132*, 7177–7185.
- (455) Wu, B.; Liang, J.; Yang, J.; Jia, C.; Yang, X.-J.; Zhang, H.; Tang, N.; Janiak, C. Sulfate Ion Encapsulation in Caged Supramolecular Structures Assembled by Second-Sphere Coordination. *Chem. Commun.* **2008**, *1762*–1764.
- (456) Custelcean, R.; Remy, P. Selective Crystallization of Urea-Functionalized Capsules with Tunable Anion-Binding Cavities. *Cryst. Growth Des.* **2009**, *9*, 1985–1989.
- (457) Rajbanshi, A.; Custelcean, R. Structure and Selectivity Trends in Crystalline Urea-Functionalised Anion-Binding Capsules. *Supramol. Chem.* **2011**, *24*, 65–71.
- (458) Rajbanshi, A.; Moyer, B. A.; Custelcean, R. Sulfate Separation from Aqueous Alkaline Solutions by Selective Crystallization of Alkali Metal Coordination Capsules. *Cryst. Growth Des.* **2011**, *11*, 2702–2706.
- (459) Rajbanshi, A.; Moyer, B. A.; Custelcean, R. Sulfate Separation from Hanford Waste Simulants by Selective Crystallization of Urea-Functionalized Capsules. *Sep. Sci. Technol.* **2012**, *47*, 2145–2150.
- (460) Zhuge, F.; Wu, B.; Liang, J.; Yang, J.; Liu, Y.; Jia, C.; Janiak, C.; Tang, N.; Yang, X.-J. Full- or Half-Encapsulation of Sulfate Anion by a

- Tris(3-Pyridylurea) Receptor: Effect of the Secondary Coordination Sphere[†]. *Inorg. Chem.* **2009**, *48*, 10249–10256.
- (461) Liu, Z.; Frasconi, M.; Lei, J.; Brown, Z. J.; Zhu, Z.; Cao, D.; Iehl, J.; Liu, G.; Fahrenbach, A. C.; Botros, Y. Y.; Farha, O. K.; Hupp, J. T.; Mirkin, C. A.; Fraser Stoddart, J. Selective Isolation of Gold Facilitated by Second-Sphere Coordination with α -Cyclodextrin. *Nat. Commun.* **2013**, *4*, 1855.
- (462) Welsh, M. J.; Smith, A. E. Molecular Mechanisms of CFTR Chloride Channel Dysfunction in Cystic Fibrosis. *Cell* **1993**, *73*, 1251–1254.
- (463) Lloyd, S. E.; Pearce, S. H. S.; Fisher, S. E.; Steinmeyer, K.; Schwappach, B.; Scheinman, S. J.; Harding, B.; Bolino, A.; Devoto, M.; Goodyer, P.; Rigden, S. P. A.; Wrong, O.; Jentsch, T. J.; Craig, I. W.; Thakker, R. V. A Common Molecular Basis for Three Inherited Kidney Stone Diseases. *Nature* **1996**, *379*, 445–449.
- (464) Simon, D. B.; Bindra, R. S.; Mansfield, T. A.; Nelson-Williams, C.; Mendonca, E.; Stone, R.; Schurman, S.; Nayir, A.; Alpay, H.; Bakkaloglu, A.; Rodriguez-Soriano, J.; Morales, J. M.; Sanjad, S. A.; Taylor, C. M.; Pilz, D.; Brem, A.; Trachtman, H.; Griswold, W.; Richard, G. A.; John, E.; Lifton, R. P. Mutations in the Chloride Channel Gene, CICNK8, Cause Bartter's Syndrome Type III. *Nat. Genet.* **1997**, *17*, 171–178.
- (465) Simon, D. B.; Karet, F. E.; Hamdan, J. M.; Pietro, A. D.; Sanjad, S. A.; Lifton, R. P. Bartter's Syndrome, Hypokalaemic Alkalosis with Hypercalcioria, Is Caused by Mutations in the Na-K-2Cl Cotransporter NKCC2. *Nat. Genet.* **1996**, *13*, 183–188.
- (466) Scott, D. A.; Wang, R.; Kreman, T. M.; Sheffield, V. C.; Karniski, L. P. The Pendred Syndrome Gene Encodes a Chloride-Iodide Transport Protein. *Nat. Genet.* **1999**, *21*, 440–443.
- (467) Moseley, R. H.; Höglund, P.; Wu, G. D.; Silberg, D. G.; Haila, S.; De La Chapelle, A.; Holmberg, C.; Kere, J. Downregulated in Adenoma Gene Encodes a Chloride Transporter Defective in Congenital Chloride Diarrhea. *Am. J. Physiol., Gastrointest. Liver Physiol.* **1999**, *276*, G185–G192.
- (468) Ashcroft, F. M. *Ion Channels and Disease*; Academic Press: San Diego and London, 2000.
- (469) Gokel, G. W.; Barkey, N. Transport of Chloride Ion through Phospholipid Bilayers Mediated by Synthetic Ionophores. *New J. Chem.* **2009**, *33*, 947–963.
- (470) Matile, S.; Vargas Jentzsch, A.; Montenegro, J.; Fin, A. Recent Synthetic Transport Systems. *Chem. Soc. Rev.* **2011**, *40*, 2453–2474.
- (471) Davis, A. P.; Sheppard, D. N.; Smith, B. D. Development of Synthetic Membrane Transporters for Anions. *Chem. Soc. Rev.* **2007**, *36*, 348–357.
- (472) Davis, A. P. Anion Binding and Transport by Steroid-Based Receptors. *Coord. Chem. Rev.* **2006**, *250*, 2939–2951.
- (473) Davis, J. T.; Okunola, O.; Quesada, R. Recent Advances in the Transmembrane Transport of Anions. *Chem. Soc. Rev.* **2010**, *39*, 3843–3862.
- (474) Gale, P. A. From Anion Receptors to Transporters. *Acc. Chem. Res.* **2011**, *44*, 216–226.
- (475) Busschaert, N.; Gale, P. A. Small-Molecule Lipid-Bilayer Anion Transporters for Biological Applications. *Angew. Chem., Int. Ed.* **2013**, *52*, 1374–1382.
- (476) Reddy, G. L.; Iwamoto, T.; Tomich, J. M.; Montal, M. Synthetic Peptides and Four-Helix Bundle Proteins as Model Systems for the Pore-Forming Structure of Channel Proteins. II. Transmembrane Segment M2 of the Brain Glycine Receptor Is a Plausible Candidate for the Pore-Lining Structure. *J. Biol. Chem.* **1993**, *268*, 14608–14615.
- (477) Wallace, D. P.; Tomich, J. M.; Iwamoto, T.; Henderson, K.; Grantham, J. J.; Sullivan, L. P. A Synthetic Peptide Derived from Glycine-Gated Cl[−] Channel Induces Transepithelial Cl[−] and Fluid Secretion. *Am. J. Physiol. Cell Physiol.* **1997**, *272*, C1672–C1679.
- (478) Broughman, J. R.; Shank, L. P.; Prakash, O.; Schultz, B. D.; Iwamoto, T.; Tomich, J. M.; Mitchell, K. Structural Implications of Placing Cationic Residues at Either the NH₂- or COOH-Terminus in a Pore-Forming Synthetic Peptide. *J. Membr. Biol.* **2002**, *190*, 93–103.
- (479) Broughman, J. R.; Shank, L. P.; Takeguchi, W.; Schultz, B. D.; Iwamoto, T.; Mitchell, K. E.; Tomich, J. M. Distinct Structural Elements That Direct Solution Aggregation and Membrane Assembly in the Channel-Forming Peptide M2GLYR. *Biochemistry* **2002**, *41*, 7350–7358.
- (480) Cook, G. A.; Prakash, O.; Zhang, K.; Shank, L. P.; Takeguchi, W. A.; Robbins, A.; Gong, Y.-X.; Iwamoto, T.; Schultz, B. D.; Tomich, J. M. Activity and Structural Comparisons of Solution Associating and Monomeric Channel-Forming Peptides Derived from the Glycine Receptor M2 Segment. *Biophys. J.* **2004**, *86*, 1424–1435.
- (481) Bukovnik, U.; Gao, J.; Cook, G. A.; Shank, L. P.; Seabra, M. B.; Schultz, B. D.; Iwamoto, T.; Chen, J.; Tomich, J. M. Structural and Biophysical Properties of a Synthetic Channel-Forming Peptide: Designing a Clinically Relevant Anion Selective Pore. *Biochim. Biophys. Acta, Biomembr.* **2012**, *1818*, 1039–1048.
- (482) Oblatt-Montal, M.; Reddy, G. L.; Iwamoto, T.; Tomich, J. M.; Montal, M. Identification of an Ion Channel-Forming Motif in the Primary Structure of CFTR, the Cystic Fibrosis Chloride Channel. *Proc. Natl. Acad. Sci. U.S.A.* **1994**, *91*, 1495–1499.
- (483) Pajewski, R.; Ferdani, R.; Pajewska, J.; Li, R.; Gokel, G. W. Cation Dependence of Chloride Ion Complexation by Open-Chained Receptor Molecules in Chloroform Solution. *J. Am. Chem. Soc.* **2005**, *127*, 18281–18295.
- (484) Cook, G. A.; Pajewski, R.; Aburi, M.; Smith, P. E.; Prakash, O.; Tomich, J. M.; Gokel, G. W. NMR Structure and Dynamic Studies of an Anion-Binding, Channel-Forming Heptapeptide. *J. Am. Chem. Soc.* **2006**, *128*, 1633–1638.
- (485) Schlesinger, P. H.; Ferdani, R.; Liu, J.; Pajewska, J.; Pajewski, R.; Saito, M.; Shabany, H.; Gokel, G. W. SCMTM: A Chloride-Selective, Membrane-Anchored Peptide Channel That Exhibits Voltage Gating. *J. Am. Chem. Soc.* **2002**, *124*, 1848–1849.
- (486) Djedovic, N.; Ferdani, R.; Harder, E.; Pajewska, J.; Pajewski, R.; Weber, M. E.; Schlesinger, P. H.; Gokel, G. W. The C-and N-Terminal Residues of Synthetic Heptapeptide Ion Channels Influence Transport Efficacy through Phospholipid Bilayers. *New. J. Chem.* **2005**, *29*, 291–305.
- (487) Pajewski, R.; Ferdani, R.; Pajewska, J.; Djedovic, N.; Schlesinger, P. H.; Gokel, G. W. Evidence for Dimer Formation by an Amphiphilic Heptapeptide That Mediates Chloride and Carboxyfluorescein Release from Liposomes. *Org. Biomol. Chem.* **2005**, *3*, 619–625.
- (488) Pajewski, R.; Pajewski, R.; Pajewska, J.; Schlesinger, P. H.; Gokel, G. W. The Effect of Midpolar Regime Mimics on Anion Transport Mediated by Amphiphilic Heptapeptides. *New J. Chem.* **2007**, *31*, 1960–1972.
- (489) Ferdani, R.; Pajewski, R.; Pajewska, J.; Schlesinger, P. H.; Gokel, G. W. Glycine Position Permutations and Peptide Length Alterations Change the Aggregation State and Efficacy of Ion-Conducting, Pore-Forming Amphiphiles. *Chem. Commun.* **2006**, 439–441.
- (490) Schlesinger, P. H.; Ferdani, R.; Pajewska, J.; Pajewski, R.; Gokel, G. W. Replacing Proline at the Apex of Heptapeptide-Based Chloride Ion Transporters Alters Their Properties and Their Ionophoretic Efficacy. *New J. Chem.* **2003**, *27*, 60–67.
- (491) You, L.; Ferdani, R.; Li, R.; Kramer, J. P.; Winter, R. E. K.; Gokel, G. W. Carboxylate Anion Diminishes Chloride Transport through a Synthetic, Self-Assembled Transmembrane Pore. *Chem.—Eur. J.* **2008**, *14*, 382–396.
- (492) Daschbach, M. M.; Negin, S.; You, L.; Walsh, M.; Gokel, G. W. Aggregation and Supramolecular Membrane Interactions That Influence Anion Transport in Tryptophan-Containing Synthetic Peptides. *Chem.—Eur. J.* **2012**, *18*, 7608–7623.
- (493) Sakai, N.; Brennan, K. C.; Weiss, L. A.; Matile, S. Toward Biomimetic Ion Channels Formed by Rigid-Rod Molecules: Length-Dependent Ion-Transport Activity of Substituted Oligo(p-Phenylene)s. *J. Am. Chem. Soc.* **1997**, *119*, 8726–8727.
- (494) Weiss, L. A.; Sakai, N.; Ghebremariam, B.; Ni, C.; Matile, S. Rigid Rod-Shaped Polyols: Functional Nonpeptide Models for Transmembrane Proton Channels. *J. Am. Chem. Soc.* **1997**, *119*, 12142–12149.
- (495) Vargas Jentzsch, A.; Matile, S. Transmembrane Halogen-Bonding Cascades. *J. Am. Chem. Soc.* **2013**, *135*, 5302–5303.

- (496) Talukdar, P.; Bollot, G.; Mareda, J.; Sakai, N.; Matile, S. Synthetic Ion Channels with Rigid-Rod π -Stack Architecture That Open in Response to Charge-Transfer Complex Formation. *J. Am. Chem. Soc.* **2005**, *127*, 6528–6529.
- (497) Gorteau, V.; Bollot, G.; Mareda, J.; Perez-Velasco, A.; Matile, S. Rigid Oligonaphthalenediimide Rods as Transmembrane Anion- π Slides. *J. Am. Chem. Soc.* **2006**, *128*, 14788–14789.
- (498) Gorteau, V.; Bollot, G.; Mareda, J.; Matile, S. Rigid-Rod Anion- π Slides for Multi-ion Hopping across Lipid Bilayers. *Org. Biomol. Chem.* **2007**, *5*, 3000–3012.
- (499) Dawson, R. E.; Hennig, A.; Weimann, D. P.; Emery, D.; Ravikumar, V.; Montenegro, J.; Takeuchi, T.; Gabutti, S.; Mayor, M.; Mareda, J.; Schalley, C. A.; Matile, S. Experimental Evidence for the Functional Relevance of Anion- π Interactions. *Nat. Chem.* **2010**, *2*, 533–538.
- (500) Mareda, J.; Matile, S. Anion- π Slides for Transmembrane Transport. *Chem.—Eur. J.* **2009**, *15*, 28–37.
- (501) Gorteau, V.; Julliard, M. D.; Matile, S. Hydrophilic Anchors for Transmembrane Anion- π Slides. *J. Membr. Sci.* **2008**, *321*, 37–42.
- (502) Perez-Velasco, A.; Gorteau, V.; Matile, S. Rigid Oligoperylene diimide Rods: Anion- π Slides with Photosynthetic Activity. *Angew. Chem., Int. Ed.* **2008**, *47*, 921–923.
- (503) Doval, D. A.; Fin, A.; Takahashi-Umebayashi, M.; Riezman, H.; Roux, A.; Sakai, N.; Matile, S. Amphiphilic Dynamic NDI and PDI Probes: Imaging Microdomains in Giant Unilamellar Vesicles. *Org. Biomol. Chem.* **2012**, *10*, 6087–6093.
- (504) Elie, C.-R.; Noujeim, N.; Pardin, C.; Schmitzer, A. R. Uncovering New Properties of Imidazolium Salts: Cl⁻ Transport and Supramolecular Regulation of Their Transmembrane Activity. *Chem. Commun.* **2011**, *47*, 1788–1790.
- (505) Elie, C.-R.; Hebert, A.; Charbonneau, M.; Haiun, A.; Schmitzer, A. R. Benzimidazolium-Based Synthetic Chloride and Calcium Transporters in Bacterial Membranes. *Org. Biomol. Chem.* **2013**, *11*, 923–928.
- (506) Elie, C.-R.; Charbonneau, M.; Schmitzer, A. R. An Anion Structure-Activity Relationship of Imidazolium-Based Synthetic Transporters. *MedChemComm* **2012**, *3*, 1231–1234.
- (507) Kempf, J.; Noujeim, N.; Schmitzer, A. R. 2,4,7-Triphenylbenzimidazole: The Monomeric Unit of Supramolecular Helical Rod-Like Transmembrane Transporters. *RSC Adv.* **2014**, *4*, 42293–42298.
- (508) Vidal, M.; Elie, C.-R.; Campbell, S.; Claing, A.; Schmitzer, A. R. Biologically Active Binaphthol-Scaffolded Imidazolium Salts. *MedChemComm* **2014**, *5*, 436–440.
- (509) Vidal, M.; Schmitzer, A. Molecular Parameters and Transmembrane Transport Mechanism of Imidazolium-Functionalized Binols. *Chem.—Eur. J.* **2014**, *20*, 9998–10004.
- (510) Madhavan, N.; Robert, E. C.; Gin, M. S. A Highly Active Anion-Selective Aminocyclodextrin Ion Channel. *Angew. Chem., Int. Ed.* **2005**, *44*, 7584–7587.
- (511) Jog, P. V.; Gin, M. S. A Light-Gated Synthetic Ion Channel. *Org. Lett.* **2008**, *10*, 3693–3696.
- (512) Licen, S.; Coppola, C.; D’Onofrio, J.; Montesarchio, D.; Tecilla, P. Cyplos: A New Family of Synthetic Ionophores. *Org. Biomol. Chem.* **2009**, *7*, 1060–1063.
- (513) De Riccardis, F.; Izzo, I.; Montesarchio, D.; Tecilla, P. Ion Transport through Lipid Bilayers by Synthetic Ionophores: Modulation of Activity and Selectivity. *Acc. Chem. Res.* **2013**, *46*, 2781–2790.
- (514) Montesarchio, D.; Coppola, C.; Boccalon, M.; Tecilla, P. Carbohydrate-Based Synthetic Ion Transporters. *Carbohydr. Res.* **2012**, *356*, 62–74.
- (515) Coppola, C.; Paciello, A.; Mangiapia, G.; Licen, S.; Boccalon, M.; De Napoli, L.; Paduano, L.; Tecilla, P.; Montesarchio, D. Design, Synthesis and Characterisation of a Fluorescently Labelled CyPLOS Ionophore. *Chem.—Eur. J.* **2010**, *16*, 13757–13772.
- (516) Simeone, L.; Milano, D.; De Napoli, L.; Irace, C.; Di Pascale, A.; Boccalon, M.; Tecilla, P.; Montesarchio, D. Design, Synthesis and Characterisation of Guanosine-Based Amphiphiles. *Chem.—Eur. J.* **2011**, *17*, 13854–13865.
- (517) Boccalon, M.; Iengo, E.; Tecilla, P. Metal–Organic Transmembrane Nanopores. *J. Am. Chem. Soc.* **2012**, *134*, 20310–20313.
- (518) Izzo, I.; Licen, S.; Maulucci, N.; Autore, G.; Marzocco, S.; Tecilla, P.; De Riccardis, F. Cationic Calix[4]arenes as Anion-Selective Ionophores. *Chem. Commun.* **2008**, 2986–2988.
- (519) Sidorov, V.; Kotch, F. W.; Abdrakhmanova, G.; Mizani, R.; Fettinger, J. C.; Davis, J. T. Ion Channel Formation from a Calix[4]arene Amide That Binds HCl. *J. Am. Chem. Soc.* **2002**, *124*, 2267–2278.
- (520) Okunola, O. A.; Seganish, J. L.; Salimian, K. J.; Zavalij, P. Y.; Davis, J. T. Membrane-Active Calixarenes: Toward ‘Gating’ Transmembrane Anion Transport. *Tetrahedron* **2007**, *63*, 10743–10750.
- (521) Seganish, J. L.; Santacroce, P. V.; Salimian, K. J.; Fettinger, J. C.; Zavalij, P.; Davis, J. T. Regulating Supramolecular Function in Membranes: Calixarenes That Enable or Inhibit Transmembrane Cl⁻ Transport. *Angew. Chem., Int. Ed.* **2006**, *45*, 3334–3338.
- (522) Seganish, J. L.; Fettinger, J. C.; Davis, J. T. Facilitated Chloride Transport across Phosphatidylcholine Bilayers by an Acyclic Calixarene Derivative: Structure-Function Relationships. *Supramol. Chem.* **2006**, *18*, 257–264.
- (523) Li, X.; Shen, B.; Yao, X.-Q.; Yang, D. A Small Synthetic Molecule Forms Chloride Channels to Mediate Chloride Transport across Cell Membranes. *J. Am. Chem. Soc.* **2007**, *129*, 7264–7265.
- (524) Ma, B.; Zha, H.; Li, N.; Yang, D.; Lin, G. Effect of Structural Modification of α -Aminoxy Peptides on Their Intestinal Absorption and Transport Mechanism. *Mol. Pharmaceutics* **2011**, *8*, 1073–1082.
- (525) Shen, B.; Li, X.; Wang, F.; Yao, X.; Yang, D. A Synthetic Chloride Channel Restores Chloride Conductance in Human Cystic Fibrosis Epithelial Cells. *PLoS One* **2012**, *7*, e34694.
- (526) Ma, B.; Yin, C.; Yang, D.; Lin, G. Effect of Structural Modification on the Gastrointestinal Stability and Hepatic Metabolism of α -Aminoxy Peptides. *Amino Acids* **2012**, *43*, 2073–2085.
- (527) Yamnitz, C. R.; Negin, S.; Carasel, I. A.; Winter, R. K.; Gokel, G. W. Dianilides of Dipicolinic Acid Function as Synthetic Chloride Channels. *Chem. Commun.* **2010**, *46*, 2838–2840.
- (528) Atkins, J. L.; Patel, M. B.; Daschbach, M. M.; Meisel, J. W.; Gokel, G. W. Anion Complexation and Transport by Isophthalamide and Dipicolinamide Derivatives: DNA Plasmid Transformation in *E. Coli*. *J. Am. Chem. Soc.* **2012**, *134*, 13546–13549.
- (529) Fürstner, A. Chemistry and Biology of Roseophilin and the Prodigiosin Alkaloids: A Survey of the Last 2500 Years. *Angew. Chem., Int. Ed.* **2003**, *42*, 3582–3603.
- (530) Davis, J. T. In *Topics in Heterocyclic Chemistry*; Gale, P. A., Dehaen, W., Eds.; Springer: New York, 2010; Vol. 24.
- (531) Perez-Tomas, R.; Montaner, B.; Llagostera, E.; Soto-Cerrato, V. The Prodigiosins, Proapoptotic Drugs with Anticancer Properties. *Biochem. Pharmacol.* **2003**, *66*, 1447–1452.
- (532) Castro, A. J. Antimalarial Activity of Prodigiosin. *Nature* **1967**, *213*, 903–904.
- (533) Williamson, N. R.; Fineran, P. C.; Gristwood, T.; Chawrai, S. R.; Leeper, F. J.; Salmon, G. P. Anticancer and Immunosuppressive Properties of Bacterial Prodiginines. *Future Microbiol.* **2007**, *2*, 605–618.
- (534) Sato, T.; Konno, H.; Tanaka, Y.; Kataoka, T.; Nagai, K.; Wasserman, H. H.; Ohkuma, S. Prodigiosins as a New Group of H⁺/Cl⁻ Symporters That Uncouple Proton Translocators. *J. Biol. Chem.* **1998**, *273*, 21455–21462.
- (535) Ohkuma, S.; Sato, T.; Okamoto, M.; Matsuya, H.; Arai, K.; Kataoka, T.; Nagai, K.; Wasserman, H. H. Prodigiosins Uncouple Lysosomal Vacuolar-Type ATPase through Promotion of H⁺/Cl⁻ Symport. *Biochem. J.* **1998**, *334*, 731–741.
- (536) Seganish, J. L.; Davis, J. T. Prodigiosin Is a Chloride Carrier That Can Function as an Anion Exchanger. *Chem. Commun.* **2005**, 5781–5783.
- (537) Davis, J. T.; Gale, P. A.; Okunola, O. A.; Prados, P.; Iglesias-Sánchez, J. C.; Torroba, T.; Quesada, R. Using Small Molecules to Facilitate Exchange of Bicarbonate and Chloride Anions across Liposomal Membranes. *Nat. Chem.* **2009**, *1*, 138–144.
- (538) Joudeh, J.; Claxton, D. Obatoclax Mesylate: Pharmacology and Potential for Therapy of Hematological Neoplasms. *Expert Opin. Invest. Drugs* **2012**, *21*, 363–373.

- (539) Goard, C. A.; Schimmer, A. D. An Evidence-Based Review of Obatoclax Mesylate in the Treatment of Hematological Malignancies. *Core Evidence* **2013**, *8*, 15–26.
- (540) Díaz de Greñu, B.; Hernández, P. I.; Espina, M.; Quiñonero, D.; Light, M. E.; Torroba, T.; Pérez-Tomás, R.; Quesada, R. Synthetic Prodiginine Obatoclax (GX15-070) and Related Analogues: Anion Binding, Transmembrane Transport, and Cytotoxicity Properties. *Chem.—Eur. J.* **2011**, *17*, 14074–14083.
- (541) Sessler, J. L.; Eller, L. R.; Cho, W.-S.; Nicolaou, S.; Aguilar, A.; Lee, J. T.; Lynch, V. M.; Magda, D. J. Synthesis, Anion-Binding Properties, and *in vitro* Anticancer Activity of Prodigiosin Analogue. *Angew. Chem., Int. Ed.* **2005**, *44*, 5989–5992.
- (542) Rastogi, S.; Marchal, E.; Uddin, I.; Groves, B.; Colpitts, J.; McFarland, S. A.; Davis, J. T.; Thompson, A. Synthetic Prodigiosenes and the Influence of C-Ring Substitution on DNA Cleavage, Transmembrane Chloride Transport and Basicity. *Org. Biomol. Chem.* **2013**, *11*, 3834–3845.
- (543) Marchal, E.; Rastogi, S.; Thompson, A.; Davis, J. T. Influence of B-Ring Modifications on Proton Affinity, Transmembrane Anion Transport and Anti-Cancer Properties of Synthetic Prodigiosenes. *Org. Biomol. Chem.* **2014**, *12*, 7515–7522.
- (544) Hernandez, P. I.; Moreno, D.; Javier, A. A.; Torroba, T.; Perez-Tomas, R.; Quesada, R. Tambjamine Alkaloids and Related Synthetic Analogs: Efficient Transmembrane Anion Transporters. *Chem. Commun.* **2012**, *48*, 1556–1558.
- (545) Saggiomo, V.; Otto, S.; Marques, I.; Felix, V.; Torroba, T.; Quesada, R. The Role of Lipophilicity in Transmembrane Anion Transport. *Chem. Commun.* **2012**, *48*, 5274–5276.
- (546) Hernando, E.; Soto-Cerrato, V.; Cortes-Arroyo, S.; Perez-Tomas, R.; Quesada, R. Transmembrane Anion Transport and Cytotoxicity of Synthetic Tambjamine Analogs. *Org. Biomol. Chem.* **2014**, *12*, 1771–1778.
- (547) Valkenier, H.; Davis, A. P. Making a Match for Valinomycin: Steroidal Scaffolds in the Design of Electroneutral, Electrogenic Anion Carriers. *Acc. Chem. Res.* **2013**, *46*, 2898–2909.
- (548) Brotherhood, P. R.; Davis, A. P. Steroid-Based Anion Receptors and Transporters. *Chem. Soc. Rev.* **2010**, *39*, 3633–3647.
- (549) Koulov, A. V.; Lambert, T. N.; Shukla, R.; Jain, M.; Boon, J. M.; Smith, B. D.; Li, H.; Sheppard, D. N.; Joos, J.-B.; Clare, J. P.; Davis, A. P. Chloride Transport across Vesicle and Cell Membranes by Steroid-Based Receptors. *Angew. Chem., Int. Ed.* **2003**, *42*, 4931–4933.
- (550) McNally, B. A.; Koulov, A. V.; Smith, B. D.; Joos, J.-B.; Davis, A. P. A Fluorescent Assay for Chloride Transport; Identification of a Synthetic Anionophore with Improved Activity. *Chem. Commun.* **2005**, 1087–1089.
- (551) McNally, B. A.; Koulov, A. V.; Lambert, T. N.; Smith, B. D.; Joos, J.-B.; Sisson, A. L.; Clare, J. P.; Sgarlata, V.; Judd, L. W.; Magro, G.; Davis, A. P. Structure–Activity Relationships in Cholapod Anion Carriers: Enhanced Transmembrane Chloride Transport through Substituent Tuning. *Chem.—Eur. J.* **2008**, *14*, 9599–9606.
- (552) Valkenier, H.; Judd, L. W.; Li, H.; Hussain, S.; Sheppard, D. N.; Davis, A. P. Preorganized Bis-Thioureas as Powerful Anion Carriers: Chloride Transport by Single Molecules in Large Unilamellar Vesicles. *J. Am. Chem. Soc.* **2014**, *136*, 12507–12512.
- (553) Judd, L. W.; Davis, A. P. From Cholapod to Cholaphane Transmembrane Anion Carriers: Accelerated Transport through Binding Site Enclosure. *Chem. Commun.* **2010**, *46*, 2227–2229.
- (554) Cooper, J. A.; Street, S. T. G.; Davis, A. P. A Flexible Solution to Anion Transport: Powerful Anionophores Based on a Cyclohexane Scaffold. *Angew. Chem., Int. Ed.* **2014**, *53*, 5609–5613.
- (555) Andrews, N. J.; Haynes, C. J. E.; Light, M. E.; Moore, S. J.; Tong, C. C.; Davis, J. T.; Harrell, W. A. Jr.; Gale, P. A. Structurally Simple Lipid Bilayer Transport Agents for Chloride and Bicarbonate. *Chem. Sci.* **2011**, *2*, 256–260.
- (556) Busschaert, N.; Gale, P. A.; Haynes, C. J. E.; Light, M. E.; Moore, S. J.; Tong, C. C.; Davis, J. T.; Harrell, J. W. A. Tripodal Transmembrane Transporters for Bicarbonate. *Chem. Commun.* **2010**, *46*, 6252–6254.
- (557) Busschaert, N.; Wenzel, M.; Light, M. E.; Iglesias-Hernández, P.; Pérez-Tomás, R.; Gale, P. A. Structure–Activity Relationships in Tripodal Transmembrane Anion Transporters: The Effect of Fluorination. *J. Am. Chem. Soc.* **2011**, *133*, 14136–14148.
- (558) Karagiannidis, L. E.; Hiscock, J. R.; Gale, P. A. The Influence of Stereochemistry on Anion Binding and Transport. *Supramol. Chem.* **2013**, *25*, 626–630.
- (559) Moore, S. J.; Wenzel, M.; Light, M. E.; Morley, R.; Bradberry, S. J.; Gomez-Iglesias, P.; Soto-Cerrato, V.; Perez-Tomas, R.; Gale, P. A. Towards “Drug-Like” Indole-Based Transmembrane Anion Transporters. *Chem. Sci.* **2012**, *3*, 2501–2509.
- (560) Karagiannidis, L. E.; Haynes, C. J. E.; Holder, K. J.; Kirby, I. L.; Moore, S. J.; Wells, N. J.; Gale, P. A. Highly Effective yet Simple Transmembrane Anion Transporters Based Upon Ortho-Phenylenediamine Bis-Ureas. *Chem. Commun.* **2014**, *50*, 12050–12053.
- (561) Busschaert, N.; Bradberry, S. J.; Wenzel, M.; Haynes, C. J. E.; Hiscock, J. R.; Kirby, I. L.; Karagiannidis, L. E.; Moore, S. J.; Wells, N. J.; Herniman, J.; Langley, G. J.; Horton, P. N.; Light, M. E.; Marques, I.; Costa, P. J.; Felix, V.; Frey, J. G.; Gale, P. A. Towards Predictable Transmembrane Transport: QSAR Analysis of Anion Binding and Transport. *Chem. Sci.* **2013**, *4*, 3036–3045.
- (562) Valkenier, H.; Haynes, C. J. E.; Herniman, J.; Gale, P. A.; Davis, A. P. Lipophilic Balance — A New Design Principle for Transmembrane Anion Carriers. *Chem. Sci.* **2014**, *5*, 1128–1134.
- (563) Svarovsky, S. A.; Simoyi, R. H.; Makarov, S. V. A Possible Mechanism for Thiourea-Based Toxicities; Kinetics and Mechanism of Decomposition of Thiourea Dioxides in Alkaline Solutions. *J. Phys. Chem. B* **2001**, *105*, 12634–12643.
- (564) Wenzel, M.; Light, M. E.; Davis, A. P.; Gale, P. A. Thiourea Isosteres as Anion Receptors and Transmembrane Transporters. *Chem. Commun.* **2011**, *47*, 7641–7643.
- (565) Cranwell, P. B.; Hiscock, J. R.; Haynes, C. J. E.; Light, M. E.; Wells, N. J.; Gale, P. A. Anion Recognition and Transport Properties of Sulfamide-, Phosphoric Triamide- and Thiophosphoric Triamide-Based Receptors. *Chem. Commun.* **2013**, *49*, 874–876.
- (566) Haynes, C. J. E.; Busschaert, N.; Kirby, I. L.; Herniman, J.; Light, M. E.; Wells, N. J.; Marques, I.; Felix, V.; Gale, P. A. Acylthioureas as Anion Transporters: The Effect of Intramolecular Hydrogen Bonding. *Org. Biomol. Chem.* **2014**, *12*, 62–72.
- (567) Busschaert, N.; Kirby, I. L.; Young, S.; Coles, S. J.; Horton, P. N.; Light, M. E.; Gale, P. A. Squaramides as Potent Transmembrane Anion Transporters. *Angew. Chem., Int. Ed.* **2012**, *51*, 4426–4430.
- (568) Deng, L.-Q.; Lu, Y.-M.; Zhou, C.-Q.; Chen, J.-X.; Wang, B.; Chen, W.-H. Synthesis and Potent Ionophoric Activity of a Squaramide-Linked Bis(Choloyl) Conjugate. *Bioorg. Med. Chem. Lett.* **2014**, *24*, 2859–2862.
- (569) Busschaert, N.; Elmes, R. B. P.; Czech, D. D.; Wu, X.; Kirby, I. L.; Peck, E. M.; Hendzel, K. D.; Shaw, S. K.; Chan, B.; Smith, B. D.; Jolliffe, K. A.; Gale, P. A. Thiosquaramides: pH Switchable Anion Transporters. *Chem. Sci.* **2014**, *5*, 3617–3626.
- (570) Santacroce, P. V.; Davis, J. T.; Light, M. E.; Gale, P. A.; Iglesias-Sánchez, J. C.; Prados, P.; Quesada, R. Conformational Control of Transmembrane Cl⁻ Transport. *J. Am. Chem. Soc.* **2007**, *129*, 1886–1887.
- (571) Koulov, A. V.; Mahoney, J. M.; Smith, B. D. Facilitated Transport of Sodium or Potassium Chloride across Vesicle Membranes Using a Ditetra Salt-Binding Macrocyclic. *Org. Biomol. Chem.* **2003**, *1*, 27–29.
- (572) Gale, P. A.; Garric, J.; Light, M. E.; McNally, B. A.; Smith, B. D. Conformational Control of HCl Co-Transporter: Imidazole Functionaliised Isophthalamide vs. 2,6-Dicarboxamidopyridine. *Chem. Commun.* **2007**, 1736–1738.
- (573) Gale, P. A.; Light, M. E.; McNally, B.; Navakhun, K.; Sliwinski, K. E.; Smith, B. D. Co-Transport of H⁺/Cl⁻ by a Synthetic Prodigiosin Mimic. *Chem. Commun.* **2005**, 3773–3775.
- (574) Kim, D. S.; Sessler, J. L. Calix[4]pyrroles: Versatile Molecular Containers with Ion Transport, Recognition, and Molecular Switching Functions. *Chem. Soc. Rev.* **2015**, *44*, 532–546.
- (575) Tong, C. C.; Quesada, R.; Sessler, J. L.; Gale, P. A. Meso-Octamethylcalix[4]pyrrole: An Old yet New Transmembrane Ion-Pair Transporter. *Chem. Commun.* **2008**, 6321–6323.

- (576) Gale, P. A.; Tong, C. C.; Haynes, C. J. E.; Adeosun, O.; Gross, D. E.; Karnas, E.; Sedenberg, E. M.; Quesada, R.; Sessler, J. L. Octafluorocalix[4]pyrrole: A Chloride/Bicarbonate Antiport Agent. *J. Am. Chem. Soc.* **2010**, *132*, 3240–3241.
- (577) Fisher, M. G.; Gale, P. A.; Hiscock, J. R.; Hursthouse, M. B.; Light, M. E.; Schmidtchen, F. P.; Tong, C. C. 1,2,3-Triazole-Strapped Calix[4]pyrrole: A New Membrane Transporter for Chloride. *Chem. Commun.* **2009**, 3017–3019.
- (578) Yano, M.; Tong, C. C.; Light, M. E.; Schmidtchen, F. P.; Gale, P. A. Calix[4]pyrrole-Based Anion Transporters with Tunable Transport Properties. *Org. Biomol. Chem.* **2010**, *8*, 4356–4363.
- (579) Ko, S.-K.; Kim, S. K.; Share, A.; Lynch, V. M.; Park, J.; Namkung, W.; Van Rossom, W.; Busschaert, N.; Gale, P. A.; Sessler, J. L.; Shin, I. Synthetic Ion Transporters Can Induce Apoptosis by Facilitating Chloride Anion Transport into Cells. *Nat. Chem.* **2014**, *6*, 885–892.
- (580) Li, Y.; Flood, A. H. Strong, Size-Selective, and Electronically Tunable C–H···Halide Binding with Steric Control over Aggregation from Synthetically Modular, Shape-Persistent [3₄]Triazolophanes. *J. Am. Chem. Soc.* **2008**, *130*, 12111–12122.
- (581) Shang, J.; Si, W.; Zhao, W.; Che, Y.; Hou, J.-L.; Jiang, H. Preorganized Aryltriazole Foldamers as Effective Transmembrane Transporters for Chloride Anion. *Org. Lett.* **2014**, *16*, 4008–4011.
- (582) Berezin, S. K.; Davis, J. T. Catechols as Membrane Anion Transporters. *J. Am. Chem. Soc.* **2009**, *131*, 2458–2459.
- (583) Harrell, W. A., Jr; Bergmeyer, M. L.; Zavalij, P. Y.; Davis, J. T. Ceramide-Mediated Transport of Chloride and Bicarbonate across Phospholipid Membranes. *Chem. Commun.* **2010**, *46*, 3950–3952.
- (584) Siskind, L. J.; Kolesnick, R. N.; Colombini, M. Ceramide Forms Channels in Mitochondrial Outer Membranes at Physiologically Relevant Concentrations. *Mitochondrion* **2006**, *6*, 118–125.
- (585) Bahmanjah, S.; Zhang, N.; Davis, J. T. Monoacylglycerols as Transmembrane Cl⁻ Anion Transporters. *Chem. Commun.* **2012**, *48*, 4432–4434.
- (586) Choi, Y. R.; Chae, M. K.; Kim, D.; Lah, M. S.; Jeong, K.-S. Synthetic Chloride Transporters with the Binding Mode Observed in a CLC Chloride Channel. *Chem. Commun.* **2012**, *48*, 10346–10348.
- (587) Lee, J. H.; Lee, J. H.; Choi, Y. R.; Kang, P.; Choi, M.-G.; Jeong, K.-S. Synthetic K⁺/Cl⁻-Selective Symporter across a Phospholipid Membrane. *J. Org. Chem.* **2014**, *79*, 6403–6409.
- (588) Whitmarsh, S. D.; Redmond, A. P.; Sgarlata, V.; Davis, A. P. Cationic Cycloholamides; Toroidal Facial Amphiphiles with Potential for Anion Transport. *Chem. Commun.* **2008**, 3669–3671.
- (589) Licen, S.; Bagnacani, V.; Baldini, L.; Casnati, A.; Sansone, F.; Giannetto, M.; Pengo, P.; Tecilla, P. Anion Transport across Phospholipid Bilayers Promoted by a Guanidinium Calix[4]arene Conjugate. *Supramol. Chem.* **2013**, *25*, 631–640.
- (590) Vargas Jentzsch, A.; Emery, D.; Mareda, J.; Metrangolo, P.; Resnati, G.; Matile, S. Ditopic Ion Transport Systems: Anion-π Interactions and Halogen Bonds at Work. *Angew. Chem., Int. Ed.* **2011**, *50*, 11675–11678.
- (591) Jentzsch, A. V.; Emery, D.; Mareda, J.; Nayak, S. K.; Metrangolo, P.; Resnati, G.; Sakai, N.; Matile, S. Transmembrane Anion Transport Mediated by Halogen-Bond Donors. *Nat. Commun.* **2012**, *3*, 905.
- (592) Milano, D.; Benedetti, B.; Boccalon, M.; Brugnara, A.; Iengo, E.; Tecilla, P. Anion Transport across Phospholipid Membranes Mediated by a Diphosphine-Pd(II) Complex. *Chem. Commun.* **2014**, *50*, 9157–9160.
- (593) Wang, W.; Li, W.; Ma, N.; Steinhoff, G. Non-Viral Gene Delivery Methods. *Curr. Pharm. Biotechnol.* **2013**, *14*, 46–60.
- (594) Busschaert, N.; Karagiannidis, L. E.; Wenzel, M.; Haynes, C. J. E.; Wells, N. J.; Young, P. G.; Makuc, D.; Plavec, J.; Jolliffe, K. A.; Gale, P. A. Synthetic Transporters for Sulfate: A New Method for the Direct Detection of Lipid Bilayer Sulfate Transport. *Chem. Sci.* **2014**, *5*, 1118–1127.
- (595) Moore, S. J.; Haynes, C. J. E.; Gonzalez, J.; Sutton, J. L.; Brooks, S. J.; Light, M. E.; Herniman, J.; Langley, G. J.; Soto-Cerrato, V.; Perez-Tomas, R.; Marques, I.; Costa, P. J.; Felix, V.; Gale, P. A. Chloride, Carboxylate and Carbonate Transport by Ortho-Phenylenediamine-Based Bisureas. *Chem. Sci.* **2013**, *4*, 103–117.
- (596) Haynes, C. J. E.; Berry, S. N.; Garric, J.; Herniman, J.; Hiscock, J. R.; Kirby, I. L.; Light, M. E.; Perkes, G.; Gale, P. A. Small Neutral Molecular Carriers for Selective Carboxylate Transport. *Chem. Commun.* **2013**, *49*, 246–248.
- (597) Wu, X.; Busschaert, N.; Wells, N. J.; Jiang, Y.-B.; Gale, P. A. Dynamic Covalent Transport of Amino Acids across Lipid Bilayers. *J. Am. Chem. Soc.* **2015**, *137*, 1476–1484.
- (598) McNally, B. A.; O’Neil, E. J.; Nguyen, A.; Smith, B. D. Membrane Transporters for Anions That Use a Relay Mechanism. *J. Am. Chem. Soc.* **2008**, *130*, 17274–17275.
- (599) Janout, V.; Regen, S. L. Bioconjugate-Based Molecular Umbrellas. *Bioconjugate Chem.* **2009**, *20*, 183–192.
- (600) Janout, V.; Jing, B.; Regen, S. L. Molecular Umbrella-Assisted Transport of Thiolated AMP and ATP across Phospholipid Bilayers. *Bioconjugate Chem.* **2002**, *13*, 351–356.
- (601) Janout, V.; Jing, B.; Staina, I. V.; Regen, S. L. Selective Transport of ATP across a Phospholipid Bilayer by a Molecular Umbrella. *J. Am. Chem. Soc.* **2003**, *125*, 4436–4437.
- (602) Chhun, C.; Schmitzer, A. R. A Pseudorotaxane Umbrella Thread with Chloride Transmembrane Transport Properties. *MedChemComm* **2011**, *2*, 987–990.
- (603) Hennig, A.; Fischer, L.; Guichard, G.; Matile, S. Anion–Macrodipole Interactions: Self-Assembling Oligoureia/Amide Macrocycles as Anion Transporters That Respond to Membrane Polarization. *J. Am. Chem. Soc.* **2009**, *131*, 16889–16895.
- (604) Fischer, L.; Decossas, M.; Briand, J.-P.; Didierjean, C.; Guichard, G. Control of Duplex Formation and Columnar Self-Assembly with Heterogeneous Amide/Urea Macrocycles. *Angew. Chem., Int. Ed.* **2009**, *48*, 1625–1628.
- (605) Verkleij, A. J.; Post, J. A. Membrane Phospholipid Asymmetry and Signal Transduction. *J. Membr. Biol.* **2000**, *178*, 1–10.
- (606) Boon, J. M.; Smith, B. D. Facilitated Phospholipid Translocation across Vesicle Membranes Using Low-Molecular-Weight Synthetic Flippases. *J. Am. Chem. Soc.* **1999**, *121*, 11924–11925.
- (607) Boon, J. M.; Smith, B. D. Facilitated Phosphatidylcholine Flip-Flop across Erythrocyte Membranes Using Low Molecular Weight Synthetic Translocases. *J. Am. Chem. Soc.* **2001**, *123*, 6221–6226.
- (608) Boon, J. M.; Lambert, T. N.; Smith, B. D.; Beatty, A. M.; Ugrinova, V.; Brown, S. N. Structure/Activity Study of Tris(2-Aminoethyl)Amine-Derived Translocases for Phosphatidylcholine. *J. Org. Chem.* **2002**, *67*, 2168–2174.
- (609) Sasaki, Y.; Shukla, R.; Smith, B. D. Facilitated Phosphatidylserine Flip-Flop across Vesicle and Cell Membranes Using Urea-Derived Synthetic Translocases. *Org. Biomol. Chem.* **2004**, *2*, 214–219.
- (610) DiVittorio, K. M.; Hofmann, F. T.; Johnson, J. R.; Abu-Esba, L.; Smith, B. D. Facilitated Phospholipid Translocation in Vesicles and Nucleated Cells Using Synthetic Small Molecule Scramblases. *Bioorg. Med. Chem.* **2009**, *17*, 141–148.
- (611) Lambert, T. N.; Boon, J. M.; Smith, B. D.; Pérez-Payán, M. N.; Davis, A. P. Facilitated Phospholipid Flip-Flop Using Synthetic Steroid-Derived Translocases. *J. Am. Chem. Soc.* **2002**, *124*, 5276–5277.
- (612) Boon, J. M.; Lambert, T. N.; Sisson, A. L.; Davis, A. P.; Smith, B. D. Facilitated Phosphatidylserine (PS) Flip-Flop and Thrombin Activation Using a Synthetic PS Scramblase. *J. Am. Chem. Soc.* **2003**, *125*, 8195–8201.
- (613) DiVittorio, K. M.; Leevy, W. M.; O’Neil, E. J.; Johnson, J. R.; Vakulenko, S.; Morris, J. D.; Rosek, K. D.; Serazin, N.; Hilkert, S.; Hurley, S.; Marquez, M.; Smith, B. D. Zinc(II) Coordination Complexes as Membrane-Active Fluorescent Probes and Antibiotics. *ChemBioChem* **2008**, *9*, 286–293.
- (614) Moore, S. J.; Fisher, M. G.; Yano, M.; Tong, C. C.; Gale, P. A. A Dual Host Approach to Transmembrane Transport of Salts. *Chem. Commun.* **2011**, *47*, 689–691.
- (615) Moore, S. J.; Fisher, M. G.; Yano, M.; Tong, C. C.; Gale, P. A. A Synergistic Approach to Anion Antiport. *Dalton Trans.* **2011**, *40*, 12017–12020.
- (616) Alberts, B.; Bray, D.; Lewis, J.; Raff, M.; Roberts, K.; Watson, J. D.; Grimstone, A. Molecular Biology of the Cell (3rd Edn). *Trends Biochem. Sci.* **1995**, *20*, 210–210.

- (617) Lodish, H. F.; Berk, A.; Zipursky, S. L.; Matsudaira, P.; Baltimore, D.; Darnell, J. *Molecular and Cellular Biology*; W.H. Freeman: New York, 2000.
- (618) Safont-Sempere, M. M.; Fernández, G.; Würthner, F. Self-Sorting Phenomena in Complex Supramolecular Systems. *Chem. Rev.* **2011**, *111*, 5784–5814.
- (619) Stupp, S. I.; Palmer, L. C. Supramolecular Chemistry and Self-Assembly in Organic Materials Design. *Chem. Mater.* **2014**, *26*, 507–518.
- (620) Fukuzumi, S.; Ohkubo, K.; D’Souza, F.; Sessler, J. L. Supramolecular Electron Transfer by Anion Binding. *Chem. Commun.* **2012**, *48*, 9801–9815.
- (621) Vilar, R. Anion-Templated Synthesis. *Angew. Chem., Int. Ed.* **2003**, *42*, 1460–1477.
- (622) Gimeno, N.; Vilar, R. Anions as Templates in Coordination and Supramolecular Chemistry. *Coord. Chem. Rev.* **2006**, *250*, 3161–3189.
- (623) Yang, X.; Knobler, C. B.; Hawthorne, M. F. Representative of a New Class of Rigid Macroyclic Electrophiles: The Chloride Ion Complex of a Charge-Reversed Analogue of [12]Crown-4. *Angew. Chem. Int. Ed.* **1991**, *30*, 1507–1508.
- (624) Zheng, Z.; Knobler, C. B.; Hawthorne, M. F. Stereoselective Anion Template Effects: Syntheses and Molecular Structures of Tetraphenyl [12]Mercuracarborand-4 Complexes of Halide Ions. *J. Am. Chem. Soc.* **1995**, *117*, 5105–5113.
- (625) Hasenkopf, B.; Lehn, J.-M.; Kneisel, B. O.; Baum, G.; Fenske, D. Self-Assembly of a Circular Double Helicate. *Angew. Chem., Int. Ed.* **1996**, *35*, 1838–1840.
- (626) Hasenkopf, B.; Lehn, J.-M.; Boumediene, N.; Dupont-Gervais, A.; Van Dorsselaer, A.; Kneisel, B.; Fenske, D. Self-Assembly of Tetra- and Hexanuclear Circular Helicates. *J. Am. Chem. Soc.* **1997**, *119*, 10956–10962.
- (627) Ayme, J.-F.; Beves, J. E.; Leigh, D. A.; McBurney, R. T.; Rissanen, K.; Schultz, D. A Synthetic Molecular Pentafoil Knot. *Nat. Chem.* **2012**, *4*, 15–20.
- (628) Riddell, I. A.; Smulders, M. M. J.; Clegg, J. K.; Hristova, Y. R.; Breiner, B.; Thoburn, J. D.; Nitschke, J. R. Anion-Induced Reconstitution of a Self-Assembling System to Express a Chloride-Binding $\text{Co}_{10}\text{L}_{15}$ Pentagonal Prism. *Nat. Chem.* **2012**, *4*, 751–756.
- (629) Chifotides, H. T.; Dunbar, K. R. Anion- π Interactions in Supramolecular Architectures. *Acc. Chem. Res.* **2013**, *46*, 894–906.
- (630) Custelcean, R. Anion Encapsulation and Dynamics in Self-Assembled Coordination Cages. *Chem. Soc. Rev.* **2014**, *43*, 1813–1824.
- (631) Young, M. C.; Holloway, L. R.; Johnson, A. M.; Hooley, R. J. A Supramolecular Sorting Hat: Stereocontrol in Metal-Ligand Self-Assembly by Complementary Hydrogen Bonding. *Angew. Chem., Int. Ed.* **2014**, *53*, 9832–9836.
- (632) Wu, B.; Cui, F.; Lei, Y.; Li, S.; Amadeu, N. D. S.; Janiak, C.; Lin, Y.-J.; Weng, L.-H.; Wang, Y.-Y.; Yang, X.-J. Tetrahedral Anion Cage: Self-Assembly of a $(\text{PO}_4)_4\text{L}_4$ Complex from a Tris(Bisurea) Ligand. *Angew. Chem. Int. Ed.* **2013**, *52*, 5096–5100.
- (633) Sessler, J. L.; Andrievsky, A.; Gale, P. A.; Lynch, V. Anion Binding: Self-Assembly of Polypyrrolic Macrocycles. *Angew. Chem. Int. Ed.* **1996**, *35*, 2782–2785.
- (634) Caltagirone, C.; Bill, N. L.; Gross, D. E.; Light, M. E.; Sessler, J. L.; Gale, P. A. Bis-Cation Salt Complexation by Meso-Octamethylcalix[4]pyrrole: Linking Complexes in Solution and in the Solid State. *Org. Biomol. Chem.* **2010**, *8*, 96–99.
- (635) Aydogan, A.; Sessler, J. L. An Imidazolium-Functionalized Self-Assembling Calix[4]pyrrole. *Chem. Commun.* **2014**, *50*, 13600–13603.
- (636) Sánchez-Quesada, J.; Seel, C.; Prados, P.; de Mendoza, J. Anion Helicates: Double Strand Helical Self-Assembly of Chiral Bicyclic Guanidinium Dimers and Tetramers around Sulfate Templates Synthetic Molecules Possessing Helicity Derived from Their Primary or Secondary Structures Could Be Related to Polypeptides. *J. Am. Chem. Soc.* **1996**, *118*, 277–278.
- (637) Král, V.; Schmidtchen, F. P.; Lang, K.; Berger, M. Anion-Controlled Assembly of Porphyrin-Bicyclic Guanidine Conjugates. *Org. Lett.* **2001**, *4*, 51–54.
- (638) Li, Y.; Wang, Y.; Huang, G.; Ma, X.; Zhou, K.; Gao, J. Chaotropic-Anion-Induced Supramolecular Self-Assembly of Ionic Polymeric Micelles. *Angew. Chem., Int. Ed.* **2014**, *53*, 8074–8078.
- (639) García, F.; Aragó, J.; Viruela, R.; Ortí, E.; Sánchez, L. A Bis(Triazole)Benzamide Receptor for the Complexation of Halide Anions and Neutral Carboxylic Acid Guests. Guest-Controlled Topicity and Self-Assembly. *Org. Biomol. Chem.* **2013**, *11*, 765–772.
- (640) Lee, S.; Chen, C.-H.; Flood, A. H. A Pentagonal Cyanostar Macrocycle with Cyanostilbene CH Donors Binds Anions and Forms Dialkylphosphate [3]Rotaxanes. *Nat. Chem.* **2013**, *5*, 704–710.
- (641) Hirsch, B. E.; Lee, S.; Qiao, B.; Chen, C.-H.; McDonald, K. P.; Tait, S. L.; Flood, A. H. Anion-Induced Dimerization of 5-Fold Symmetric Cyanostars in 3D Crystalline Solids and 2D Self-Assembled Crystals. *Chem. Commun.* **2014**, *50*, 9827–9830.
- (642) Evans, N. H.; Beer, P. D. Progress in the Synthesis and Exploitation of Catenanes since the Millennium. *Chem. Soc. Rev.* **2014**, *43*, 4658–4683.
- (643) White, N. G.; Serpell, C. J.; Beer, P. D. Structural Study of Triazole and Amide Containing Anion-Templated Pseudorotaxanes. *Cryst. Growth Des.* **2014**, *14*, 3472–3479.
- (644) White, N. G.; Lovett, H. G.; Beer, P. D. Bis-Triazolium Containing Macrocycles, Pseudorotaxanes and Interlocked Structures for Anion Recognition. *RSC Adv.* **2014**, *4*, 12133–12147.
- (645) Metrangolo, P.; Resnati, G. Halogen Bonding: A Paradigm in Supramolecular Chemistry. *Chem.—Eur. J.* **2001**, *7*, 2511–2519.
- (646) Metrangolo, P.; Meyer, F.; Pilati, T.; Resnati, G.; Terraneo, G. Halogen Bonding in Supramolecular Chemistry. *Angew. Chem., Int. Ed.* **2008**, *47*, 6114–6127.
- (647) Caballero, A.; Bennett, S.; Serpell, C. J.; Beer, P. D. Iodo-Imidazolium Salts: Halogen Bonding in Crystals and Anion-Templated Pseudorotaxanes. *CrystEngComm* **2013**, *15*, 3076–3081.
- (648) Langton, M. J.; Duckworth, L. C.; Beer, P. D. Nitrate Anion Templated Assembly of a [2]Rotaxane for Selective Nitrate Recognition in Aqueous Solvent Mixtures. *Chem. Commun.* **2013**, *49*, 8608–8610.
- (649) White, N. G.; Beer, P. D. A Rotaxane Host System Containing Integrated Triazole C-H Hydrogen Bond Donors for Anion Recognition. *Org. Biomol. Chem.* **2013**, *11*, 1326–1333.
- (650) White, N. G.; Costa, P. J.; Carvalho, S.; Félix, V.; Beer, P. D. Increased Halide Recognition Strength by Enhanced Intercomponent Preorganisation in Triazolium Containing [2]Rotaxanes. *Chem.—Eur. J.* **2013**, *19*, 17751–17765.
- (651) White, N. G.; Colaço, A. R.; Marques, I.; Félix, V.; Beer, P. D. Halide Selective Anion Recognition by an Amide-Triazolium Axle Containing [2]Rotaxane. *Org. Biomol. Chem.* **2014**, *12*, 4924–4931.
- (652) Langton, M. J.; Beer, P. D. Nitrate Anion Templated Synthesis of a [2]Catenane for Nitrate Recognition in Organic-Aqueous Solvent Media. *Chem. Commun.* **2014**, *50*, 8124–8127.
- (653) Gilday, L. C.; Beer, P. D. Halogen- and Hydrogen-Bonding Catenanes for Halide-Anion Recognition. *Chem.—Eur. J.* **2014**, *20*, 8379–8385.
- (654) Steed, J. W. Supramolecular Gel Chemistry: Developments over the Last Decade. *Chem. Commun.* **2011**, *47*, 1379–1383.
- (655) Yu, G.; Yan, X.; Han, C.; Huang, F. Characterization of Supramolecular Gels. *Chem. Soc. Rev.* **2013**, *42*, 6697–6722.
- (656) Foster, J. A.; Piepenbrock, M.-O. M.; Lloyd, G. O.; Clarke, N.; Howard, J. A. K.; Steed, J. W. Anion-Switchable Supramolecular Gels for Controlling Pharmaceutical Crystal Growth. *Nat. Chem.* **2010**, *2*, 1037–1043.
- (657) Roy, S.; Javid, N.; Frederix, P. W. J. M.; Lamprou, D. a.; Urquhart, A. J.; Hunt, N. T.; Halling, P. J.; Ulijn, R. V. Dramatic Specific-Ion Effect in Supramolecular Hydrogels. *Chem.—Eur. J.* **2012**, *18*, 11723–11731.
- (658) Becker, T.; Yong Goh, C.; Jones, F.; McIldowie, M. J.; Mocerino, M.; Ogden, M. I. Proline-Functionalised Calix[4]arene: An Anion-Triggered Hydrogelator. *Chem. Commun.* **2008**, 3900–3902.
- (659) Shen, J.-S.; Cai, Q.-G.; Jiang, Y.-B.; Zhang, H.-W. Anion-Triggered Melamine Based Self-Assembly and Hydrogel. *Chem. Commun.* **2010**, *46*, 6786–6788.

- (660) Liu, S. Q.; Joshi, S. C.; Lam, Y. C. Effects of Salts in the Hofmeister Series and Solvent Isotopes on the Gelation Mechanisms for Hydroxypropylmethylcellulose Hydrogels. *J. Appl. Polym. Sci.* **2008**, *109*, 363–372.
- (661) Tripathi, A.; Pandey, P. S. Hydrogen Sulfate-Induced Organogelation of a Bile Acid Based Anion-Receptor. *Tetrahedron Lett.* **2011**, *52*, 3558–3560.
- (662) Oda, R.; Huc, I.; Candau, S. J. Gemini Surfactants as New, Low Molecular Weight Gelators of Organic Solvents and Water. *Angew. Chem., Int. Ed.* **1998**, *37*, 2689–2691.
- (663) Haketa, Y.; Sasaki, S.; Ohta, N.; Masunaga, H.; Ogawa, H.; Mizuno, N.; Araoka, F.; Takezoe, H.; Maeda, H. Oriented Salts: Dimension-Controlled Charge-by-Charge Assemblies from Planar Receptor-Anion Complexes. *Angew. Chem., Int. Ed.* **2010**, *49*, 10079–10083.
- (664) Maeda, H.; Terashima, Y.; Haketa, Y.; Asano, A.; Honsho, Y.; Seki, S.; Shimizu, M.; Mukai, H.; Ohta, K. Discotic Columnar Mesophases Derived from 'Rod-Like' π -Conjugated Anion-Responsive Acyclic Oligopyrroles. *Chem. Commun.* **2010**, *46*, 4559–4561.
- (665) Maeda, H.; Haketa, Y.; Nakanishi, T. Aryl-Substituted C₃-Bridged Oligopyrroles as Anion Receptors for Formation of Supramolecular Organogels. *J. Am. Chem. Soc.* **2007**, *129*, 13661–13674.
- (666) Terashima, Y.; Takayama, M.; Isozaki, K.; Maeda, H. Ion-Based Materials of Boron-Modified Dipyrrolyldiketones as Anion Receptors. *Chem. Commun.* **2013**, *49*, 2506–2508.
- (667) Maeda, H.; Naritani, K.; Honsho, Y.; Seki, S. Anion Modules: Building Blocks of Supramolecular Assemblies by Combination with π -Conjugated Anion Receptors. *J. Am. Chem. Soc.* **2011**, *133*, 8896–8899.
- (668) Haketa, Y.; Sakamoto, S.; Chigusa, K.; Nakanishi, T.; Maeda, H. Synthesis, Crystal Structures, and Supramolecular Assemblies of Pyrrole-Based Anion Receptors Bearing Modified Pyrrole β -Substituents. *J. Org. Chem.* **2011**, *76*, 5177–5184.
- (669) Haketa, Y.; Honsho, Y.; Seki, S.; Maeda, H. Ion Materials Comprising Planar Charged Species. *Chem.—Eur. J.* **2012**, *18*, 7016–7020.
- (670) Dong, B.; Sakurai, T.; Bando, Y.; Seki, S.; Takaishi, K.; Uchiyama, M.; Muranaka, A.; Maeda, H. Ion-Based Materials Derived from Positively and Negatively Charged Chloride Complexes of π -Conjugated Molecules. *J. Am. Chem. Soc.* **2013**, *135*, 14797–14805.
- (671) Dong, B.; Sakurai, T.; Honsho, Y.; Seki, S.; Maeda, H. Cation Modules as Building Blocks Forming Supramolecular Assemblies with Planar Receptor–Anion Complexes. *J. Am. Chem. Soc.* **2013**, *135*, 1284–1287.
- (672) Sekiya, R.; Tsutsui, Y.; Choi, W.; Sakurai, T.; Seki, S. Ion-Based Assemblies of Planar Anion Complexes and Cationic Pt^{II} Complexes. *Chem. Commun.* **2014**, *50*, 10615–10618.
- (673) Breslow, R. Centenary Lecture. Biomimetic Chemistry. *Chem. Soc. Rev.* **1972**, *1*, 553–580.
- (674) Breslow, R. Artificial Enzymes. *Science* **1982**, *218*, 532–537.
- (675) Mangani, S.; Ferraroni, M. In *Supramolecular Chemistry of Anions*; Bianchi, A., Bowman-James, K., García-España, E., Eds.; Wiley-VCH: New York, 1997; Vol. 62.
- (676) Zhang, Z.; Schreiner, P. R. Thio-Urea Organocatalysis—What Can Be Learnt from Anion Recognition? *Chem. Soc. Rev.* **2009**, *38*, 1187–1198.
- (677) Beckendorf, S.; Asmus, S.; Mancheño, O. G. H-Donor Anion Acceptor Organocatalysis—the Ionic Electrophile Activation Approach. *ChemCatChem* **2012**, *4*, 926–936.
- (678) Connon, S. J. The Design of Novel, Synthetically Useful (Thio)Urea-Based Organocatalysts. *Synlett* **2009**, 354–376.
- (679) Connon, S. J. Asymmetric Catalysis with Bifunctional Cinchona Alkaloid-Based Urea and Thiourea Organocatalysts. *Chem. Commun.* **2008**, 2499–2510.
- (680) Van Rossom, W.; Caers, J.; Robeysns, K.; Van Meervelt, L.; Maes, W.; Dehaen, W. Thio)Ureido Anion Receptors Based on a 1,3-Alternate Oxacalix[2]Arene[2]Pyrimidine Scaffold. *J. Org. Chem.* **2012**, *77*, 2791–2797.
- (681) Thomas, J.; Van Rossom, W.; Hecke, K. V.; Van Meervelt, L.; Smet, M.; Maes, W.; Dehaen, W. Selenacalix[3]Triazines: Synthesis and Host-Guest Chemistry. *Chem. Commun.* **2012**, *48*, 43–45.
- (682) Merckx, T.; Verwilst, P.; Dehaen, W. Preorganization in Bistriazolyl Anion Receptors. *Tetrahedron Lett.* **2013**, *54*, 4237–4240.
- (683) Taylor, M. S.; Jacobsen, E. N. Highly Enantioselective Catalytic Acyl-Pictet-Spengler Reactions. *J. Am. Chem. Soc.* **2004**, *126*, 10558–10559.
- (684) Taylor, M. S.; Tokunaga, N.; Jacobsen, E. N. Enantioselective Thiourea-Catalyzed Acyl-Mannich Reactions of Isoquinolines. *Angew. Chem., Int. Ed.* **2005**, *44*, 6700–6704.
- (685) Raheem, I. T.; Thiara, P. S.; Peterson, E. A.; Jacobsen, E. N. Enantioselective Pictet-Spengler-Type Cyclizations of Hydroxylactams: H-Bond Donor Catalysis by Anion Binding. *J. Am. Chem. Soc.* **2007**, *129*, 13404–13405.
- (686) Raheem, I. T.; Thiara, P. S.; Jacobsen, E. N. Regio- and Enantioselective Catalytic Cyclization of Pyrroles onto N-Acyliminium Ions. *Org. Lett.* **2008**, *10*, 1577–1580.
- (687) Reisman, S. E.; Doyle, A. G.; Jacobsen, E. N. Enantioselective Thiourea-Catalyzed Additions to Oxocarbenium Ions. *J. Am. Chem. Soc.* **2008**, *130*, 7198–7199.
- (688) Peterson, E. A.; Jacobsen, E. N. Enantioselective, Thiourea-Catalyzed Intermolecular Addition of Indoles to Cyclic N-Acyl Iminium Ions. *Angew. Chem., Int. Ed.* **2009**, *48*, 6328–6331.
- (689) Knowles, R. R.; Lin, S.; Jacobsen, E. N. Enantioselective Thiourea-Catalyzed Cationic Polycyclizations. *J. Am. Chem. Soc.* **2010**, *132*, 5030–5032.
- (690) Yamaoka, Y.; Miyabe, H.; Takemoto, Y. Catalytic Enantioselective Petasis-Type Reaction of Quinolines Catalyzed by a Newly Designed Thiourea Catalyst. *J. Am. Chem. Soc.* **2007**, *129*, 6686–6687.
- (691) Bergonzini, G.; Schindler, C. S.; Wallentin, C.-J.; Jacobsen, N.; Stephenson, C. R. J. Chemical Science Photoredox Activation and Anion Binding Catalysis in the Dual Catalytic Enantioselective Synthesis of β -Amino Esters†. *Chem. Sci.* **2014**, *5*, 112–116.
- (692) McDonald, K.; Hua, Y.; Flood, A. In *Anion Recognition in Supramolecular Chemistry*; Gale, P. A., Dehaen, W., Eds.; Springer: Berlin Heidelberg, 2010; Vol. 24.
- (693) Beckendorf, S.; Asmus, S.; Mück-Lichtenfeld, C.; García Mancheño, O. "Click" Bis-Triazoles as Neutral C-H···Anion-Acceptor Organocatalysts. *Chem.—Eur. J.* **2013**, *19*, 1581–1585.
- (694) Van Rossom, W.; Matsushita, Y.; Ariga, K.; Hill, J. P. New Synthesis of Unsymmetrically-Substituted 2,S-Diarylpyrroles from Homopropargyl Sulfonamides. *RSC Adv.* **2014**, *4*, 4897–4900.
- (695) Van Rossom, W.; Terentyeva, T. G.; Sodeyama, K.; Matsushita, Y.; Tateyama, Y.; Ariga, K.; Hill, J. P. Arylpyprole Oligomers as Tunable Anion Receptors. *Org. Biomol. Chem.* **2014**, *12*, 5492–5499.
- (696) Schafer, A. G.; Wieting, J. M.; Fisher, T. J.; Mattson, A. E. Chiral Silanediols in Anion-Binding Catalysis. *Angew. Chem. Int. Ed.* **2013**, *52*, 11321–11324.
- (697) Brown, A. R.; Kuo, W.-H.; Jacobsen, E. N. Enantioselective Catalytic Alpha-Alkylation of Aldehydes Via an S_N1 Pathway. *J. Am. Chem. Soc.* **2010**, *132*, 9286–9288.
- (698) Birrell, J. A.; Desrosiers, J.-N.; Jacobsen, E. N. Enantioselective Acylation of Silyl Ketene Acetals through Fluoride-Anion Binding Catalysis. *J. Am. Chem. Soc.* **2011**, *133*, 13872–13875.
- (699) Damrauer, R.; Crowell, A. J.; Craig, C. F. Electron, Hydride, and Fluoride Affinities of Silicon-Containing Species: Computational Studies. *J. Am. Chem. Soc.* **2003**, *125*, 10759–10766.
- (700) Kniep, F.; Rout, L.; Walter, S. M.; Bensch, H. K. V.; Jungbauer, S. H.; Herdtweck, E.; Huber, S. M. S-Iodo-1,2,3-Triazolium-Based Multidentate Halogen-Bond Donors as Activating Reagents. *Chem. Commun.* **2012**, *48*, 9299–9301.
- (701) Kniep, F.; Walter, S. M.; Herdtweck, E.; Huber, S. M. 4,4'-Azobis(Halopyridinium) Derivatives: Strong Multidentate Halogen-Bond Donors with a Redox-Active Core. *Chem.—Eur. J.* **2012**, *18*, 1306–1310.
- (702) Walter, S. M.; Kniep, F.; Herdtweck, E.; Huber, S. M. Halogen-Bond-Induced Activation of a Carbon–Heteroatom Bond. *Angew. Chem., Int. Ed.* **2011**, *50*, 7187–7191.

- (703) Jungbauer, S. H.; Walter, S. M.; Schindler, S.; Rout, L.; Kniep, F.; Huber, S. M. Activation of a Carbonyl Compound by Halogen Bonding. *Chem. Commun.* **2014**, *50*, 6281–6284.
- (704) Sigman, M. S.; Jacobsen, E. N. Schiff Base Catalysts for the Asymmetric Strecker Reaction Identified and Optimized from Parallel Synthetic Libraries. *J. Am. Chem. Soc.* **1998**, *120*, 4901–4902.
- (705) Vachal, P.; Jacobsen, E. N. Structure-Based Analysis and Optimization of a Highly Enantioselective Catalyst for the Strecker Reaction. *J. Am. Chem. Soc.* **2002**, *124*, 10012–10014.
- (706) Joseph Harriman, D.; Deleavy, G. F.; Lambropoulos, A.; Deslongchamps, G. Reverse-Docking Study of the Organocatalyzed Asymmetric Strecker Hydrocyanation of Aldimines and Ketimines. *Tetrahedron* **2007**, *63*, 13032–13038.
- (707) Corey, E. J.; Grogan, M. J. Enantioselective Synthesis of Alpha-Amino Nitriles from N-Benzhydryl Imines and HCN with a Chiral Bicyclic Guanidine as Catalyst. *Org. Lett.* **1999**, *1*, 157–160.
- (708) Pan, S. C.; Zhou, J.; List, B. Catalytic Asymmetric Acylcyanation of Imines. *Angew. Chem., Int. Ed.* **2007**, *46*, 612–614.
- (709) Pan, S. C.; List, B. The Catalytic Acylcyanation of Imines. *Chem. Asian J.* **2008**, *3*, 430–437.
- (710) Zuend, S. J.; Jacobsen, E. N. Mechanism of Amido-Thiourea Catalyzed Enantioselective Imine Hydrocyanation: Transition State Stabilization Via Multiple Non-Covalent Interactions. *J. Am. Chem. Soc.* **2009**, *131*, 15358–15374.
- (711) Zuend, S. J.; Coughlin, M. P.; Lalonde, M. P.; Jacobsen, E. N. Scaleable Catalytic Asymmetric Strecker Syntheses of Unnatural Alpha-Amino Acids. *Nature* **2009**, *461*, 968–970.
- (712) De, C. K.; Klauber, E. G.; Seidel, D. Merging Nucleophilic and Hydrogen Bonding Catalysis: An Anion Binding Approach to the Kinetic Resolution of Amines. *J. Am. Chem. Soc.* **2009**, *131*, 17060–17061.
- (713) Seidel, D. The Anion-Binding Approach to Catalytic Enantioselective Acyl Transfer. *Synlett* **2014**, *25*, 783–794.
- (714) Klauber, E. G.; De, C. K.; Shah, T. K.; Seidel, D. Merging Nucleophilic and Hydrogen Bonding Catalysis: An Anion Binding Approach to the Kinetic Resolution of Propargylic Amines. *J. Am. Chem. Soc.* **2010**, *132*, 13624–13626.
- (715) De, C. K.; Seidel, D. Catalytic Enantioselective Desymmetrization of Meso-Diamines: A Dual Small-Molecule Catalysis Approach. *J. Am. Chem. Soc.* **2011**, *133*, 14538–14541.
- (716) Klauber, E. G.; Mittal, N.; Shah, T. K.; Seidel, D. A Dual-Catalysis/Anion-Binding Approach to the Kinetic Resolution of Allylic Amines. *Org. Lett.* **2011**, *13*, 2464–2467.
- (717) Mittal, N.; Sun, D. X.; Seidel, D. Kinetic Resolution of Amines Via Dual Catalysis: Remarkable Dependence of Selectivity on the Achiral Cocatalyst. *Org. Lett.* **2012**, *14*, 3084–3087.
- (718) Min, C.; Mittal, N.; De, C. K.; Seidel, D. A Dual-Catalysis Approach to the Kinetic Resolution of 1,2-Diaryl-1,2-Diaminoethanes. *Chem. Commun.* **2012**, *48*, 10853–10855.
- (719) De, C. K.; Mittal, N.; Seidel, D. A Dual-Catalysis Approach to the Asymmetric Steglich Rearrangement and Catalytic Enantioselective Addition of O-Acylated Azlactones to Isoquinolines. *J. Am. Chem. Soc.* **2011**, *133*, 16802–16805.
- (720) Klausen, R. S.; Jacobsen, E. N. Weak Brønsted Acid-Thiourea Co-Catalysis: Enantioselective, Catalytic Protio-Pictet-Spengler Reactions. *Org. Lett.* **2009**, *11*, 887–890.
- (721) Lee, Y.; Klausen, R. S.; Jacobsen, E. N. Thiourea-Catalyzed Enantioselective Iso-Pictet-Spengler Reactions. *Org. Lett.* **2011**, *13*, 5564–5567.
- (722) Lalonde, M. P.; McGowan, M. A.; Rajapaksa, N. S.; Jacobsen, E. N. Enantioselective Formal Aza-Diels-Alder Reactions of Enones with Cyclic Imines Catalyzed by Primary Aminothioureas. *J. Am. Chem. Soc.* **2013**, *135*, 1891–1894.
- (723) Burns, N. Z.; Witten, M. R.; Jacobsen, E. N. Dual Catalysis in Enantioselective Oxidopyrylium-Based [5 + 2] Cycloadditions. *J. Am. Chem. Soc.* **2011**, *133*, 14578–14581.
- (724) Witten, M. R.; Jacobsen, E. N. Catalytic Asymmetric Synthesis of 8-Oxabicyclooctanes by Intermolecular [5 + 2] Pyrylium Cycloadditions. *Angew. Chem., Int. Ed.* **2014**, *53*, 5912–5916.
- (725) Weil, T.; Kotke, M.; Kleiner, C. M.; Schreiner, P. R. Cooperative Brønsted Acid-Type Organocatalysis: Alcoholysis of Styrene Oxides. *Org. Lett.* **2008**, *10*, 1513–1516.
- (726) Couch, E. D.; Auvin, T. J.; Mattson, A. E. Urea-Induced Acid Amplification: A New Approach for Metal-Free Insertion Chemistry. *Chem.—Eur. J.* **2014**, *20*, 8283–8287.
- (727) Zhao, Y.; Domoto, Y.; Orentas, E.; Beuchat, C.; Emery, D.; Mareda, J.; Sakai, N.; Matile, S. Catalysis with Anion-π Interactions. *Angew. Chem., Int. Ed.* **2013**, *52*, 9940–9943.
- (728) Zhao, Y.; Beuchat, C.; Domoto, Y.; Gajewy, J.; Wilson, A.; Mareda, J.; Sakai, N.; Matile, S. Anion-π Catalysis. *J. Am. Chem. Soc.* **2014**, *136*, 2101–2111.
- (729) Lu, T.; Wheeler, S. E. Quantifying the Role of Anion-π Interactions in Anion-π Catalysis. *Org. Lett.* **2014**, *16*, 3268–3271.
- (730) Ihmels, H.; Luo, J. Effects of Anion Complexation on the Photoreactivity of Bisureido- and Bisthioureido-Substituted Dibenzobarrelene Derivatives. *Beilstein J. Org. Chem.* **2011**, *7*, 278–289.
- (731) Boyle, P. H.; Convery, M. A.; Davis, A. P.; Hosken, G. D.; Murray, B. A. Deprotonation of Nitroalkanes by Bicyclic Amidine and Guanidine Bases; Evidence for Molecular Recognition within a Catalytic Cycle for C-C Bond Formation. *J. Chem. Soc., Chem. Commun.* **1992**, 239–242.
- (732) Aitken, L.; Arezki, N.; Dell’Isola, A.; Cobb, A. Asymmetric Organocatalysis and the Nitro Group Functionality. *Synthesis* **2013**, *45*, 2627–2648.
- (733) Breugst, M.; Houk, K. N. Computational Analysis of Cyclophane-Based Bisthioureia-Catalyzed Henry Reactions. *J. Org. Chem.* **2014**, *79*, 6302–6309.
- (734) Kitagaki, S.; Ueda, T.; Mukai, C. Planar Chiral [2.2]-Paracyclophane-Based Bis(Thiourea) Catalyst: Application to Asymmetric Henry Reaction. *Chem. Commun.* **2013**, *49*, 4030–4032.
- (735) So, S. S.; Oottikkal, S.; Badjić, J. D.; Hadad, C. M.; Mattson, A. E. Urea-Catalyzed N-H Insertion-Arylation Reactions of Nitrodiazoesters. *J. Org. Chem.* **2014**, *79*, 4832–4842.
- (736) Kotke, M.; Schreiner, P. R. Acid-Free, Organocatalytic Acetalization. *Tetrahedron* **2006**, *62*, 434–439.
- (737) Xu, H.; Zuend, S. J.; Woll, M. G.; Tao, Y.; Jacobsen, E. N. Asymmetric Cooperative Catalysis of Strong Brønsted Acid-Promoted Reactions Using Chiral Ureas. *Science* **2010**, *327*, 986–990.
- (738) Lin, S.; Jacobsen, E. N. Thiourea-Catalysed Ring Opening of Episulfonium Ions with Indole Derivatives by Means of Stabilizing Non-Covalent Interactions. *Nat. Chem.* **2012**, *4*, 817–824.
- (739) Diosdado, S.; López, R.; Palomo, C. Ureidopeptide-Based Brønsted Bases: Design, Synthesis and Application to the Catalytic Enantioselective Synthesis of β-Amino Nitriles from (Arylsulfonyl)-Acetonitriles. *Chem.—Eur. J.* **2014**, *20*, 6526–6531.
- (740) Kinsella, M.; Duggan, P. G.; Muldoon, J.; Eccles, K. S.; Lawrence, S. E.; Lennon, C. M. Synthesis and NMR Binding Studies Towards Rational Design of a Series of Electron-Withdrawing Diamide Receptors/Organocatalysts. *Eur. J. Org. Chem.* **2011**, *2011*, 1125–1132.
- (741) Borovika, A.; Tang, P.-I.; Klapman, S.; Nagorny, P. Thiophosphoramido-Based Cooperative Catalysts for Brønsted Acid Promoted Ionic Diels-Alder Reactions. *Angew. Chem., Int. Ed.* **2013**, *52*, 13424–13428.
- (742) Kótai, B.; Kardos, G.; Hamza, A.; Farkas, V.; Pápai, I.; Soós, T. On the Mechanism of Bifunctional Squaramide-Catalyzed Organocatalytic Michael Addition: A Protonated Catalyst as an Oxyanion Hole. *Chem.—Eur. J.* **2014**, *20*, 5631–5639.
- (743) Phipps, R. J.; Hamilton, G. L.; Toste, F. D. The Progression of Chiral Anions from Concepts to Applications in Asymmetric Catalysis. *Nat. Chem.* **2012**, *4*, 603–614.
- (744) Mahlau, M.; List, B. Asymmetric Counteranion-Directed Catalysis: Concept, Definition, and Applications. *Angew. Chem., Int. Ed.* **2013**, *52*, 518–533.
- (745) Shunatona, H. P.; Früh, N.; Wang, Y.-M.; Rauniyar, V.; Toste, F. D. Enantioselective Fluoroamination: 1,4-Addition to Conjugated Dienes Using Anionic Phase-Transfer Catalysis. *Angew. Chem., Int. Ed.* **2013**, *52*, 7724–7727.

- (746) Yang, X.; Phipps, R. J.; Toste, F. D. Asymmetric Fluorination of α -Branched Cyclohexanones Enabled by a Combination of Chiral Anion Phase-Transfer Catalysis and Enamine Catalysis Using Protected Amino Acids. *J. Am. Chem. Soc.* **2014**, *136*, 5225–5228.
- (747) Wu, J.; Wang, Y.-M.; Drljevic, A.; Rauniar, V.; Phipps, R. J.; Toste, F. D. A Combination of Directing Groups and Chiral Anion Phase-Transfer Catalysis for Enantioselective Fluorination of Alkenes. *Proc. Natl. Acad. Sci. U.S.A.* **2013**, *110*, 13729–13733.
- (748) Yawer, M. A.; Havel, V.; Sindelar, V. A Bambusuril Macrocycle That Binds Anions in Water with High Affinity and Selectivity. *Angew. Chem., Int. Ed.* **2015**, *54*, 276–279.
- (749) Hirsch, B. E.; Lee, S.; Qiao, B.; Chen, C.-H.; McDonald, K. P.; Tait, S. L.; Flood, A. H. Anion-Induced Dimerization of 5-Fold Symmetric Cyanostars in 3D Crystalline Solids and 2D Self-Assembled Crystals. *Chem. Commun.* **2014**, *50*, 9827–9830.
- (750) Blazek, V.; Molcanov, K.; Mlinaric-Majerski, K.; Kojic-Prodic, B.; Basaric, N. Adamantane Bisurea Derivatives: Anion Binding in the Solution and in the Solid State. *Tetrahedron* **2013**, *69*, 517–526.
- (751) Pandurangan, K.; Kitchen, J. A.; Blasco, S.; Boyle, E. M.; Fitzpatrick, B.; Feeney, M.; Kruger, P. E.; Gunnlaugsson, T. Unexpected Self-Sorting Self-Assembly Formation of a [4:4] Sulfate:Ligand Cage from a Preorganized Tripodal Urea Ligand. *Angew. Chem., Int. Ed.* **2015**, *54*, 4566–4570.